PACIFIC SLEEPER SHARKS IN THE NORTHEAST PACIFIC OCEAN: RELATIVE ABUNDANCE, PLAUSIBLE INCIDENTAL EXPLOITATION RATES, TROPHIC ECOLOGY, AND HABITAT USE

By

Dean L. Courtney, B.A., M.S.

A Dissertation Submitted in Partial Fulfillment of the Requirements

for the Degree of

Doctor of Philosophy

in

Fisheries

University of Alaska Fairbanks

December 2017

APPROVED:

Dr. Milo D. Adkison, Committee Chair

Dr. Robert Foy, Committee Member

Dr. Mike Sigler, Committee Member

Dr. Keith R. Criddle, Committee Member

Dr. Gerard DiNardo, Committee Member

Dr. Milo D. Adkison, Chair

Department of Fisheries

Dr. S. Bradley Moran, Dean

College of Fisheries and Ocean Sciences

Dr. Michael Castellini,

Dean of Graduate School

Abstract

Pacific sleeper shark relative abundance indices in the eastern Bering Sea and Gulf of Alaska were developed from sablefish longline surveys and the sustainability of a plausible range in Pacific sleeper shark incidental exploitation rates in the Gulf of Alaska was evaluated with a risk analysis using Monte Carlo simulation for use in fisheries management. A significant increase in Pacific sleeper shark relative abundance was identified in the Gulf of Alaska during the years 1989–2003. The aggregate risk of ending in an overfished condition in the Gulf of Alaska increased from 0% under a low exploitation rate scenario to 59% under a high exploitation rate scenario. Baseline information about Pacific sleeper shark trophic ecology and habitat utilization in the eastern Bering Sea and Gulf of Alaska was developed for use in ecosystem-based fishery management. Analysis of stable isotope ratios of nitrogen ($\delta^{15}N$) and lipid normalized carbon ($\delta^{13}C'$) identified significant geographic and ontogenetic variability in the trophic ecology of Pacific sleeper sharks in the eastern Bering Sea and Gulf of Alaska and revealed wider variability in the feeding ecology of Pacific sleeper sharks than previously obtained from diet data based on stomach contents alone. Time series analysis of Pacific sleeper shark electronic tag data from the Gulf of Alaska identified a simple autoregressive relationship governing short-term movements (hours) throughout the time series which included substantial variation in longer time period movement patterns (months) and demonstrated that statistical inference about habitat utilization could be drawn from simultaneous analysis of an entire time series depth profile (six months of data) stored on an electronic archival tag.

Table of Contents

List of Figures

Page

List of Tables

Acknowledgements

This research was conceptualized during a National Oceanic and Atmospheric Administration (NOAA) Advanced Studies Program (D. L. C.) in collaboration with the NMFS Alaska Fisheries Science Center (AFSC; M. S. and R. F.), the NMFS Pacific Island Fisheries Science Center (PIFSC; G. D.), and the University of Alaska Fairbanks College of Fisheries and Ocean Sciences (M. D. A.; K. R. C.). Funding (D. L. C.) was provided by the NMFS Auke Bay Laboratory (ABL), the NMFS Pacific Islands Fisheries Science Center (PIFSC), and the NMFS Southeast Fisheries Science Center (SEFSC) Panama City Laboratory.

Special thanks to my mom for her inspiration, to my family for their patience, and to the Olmstead and Schlosser families, and to Herb and Janie Freer, for their support.

Introduction

Three large bodied (> 4 m) sleeper shark species (*Somniosus spp.*) have been described in the scientific literature: the Pacific sleeper shark (*S. pacificus*), the Greenland shark (*S. microcephalus*), and the Antarctic sleeper shark (*S. antarcticus*) (Compagno 1984; Yano et al. 2004, 2007). The Pacific sleeper shark is thought to occur primarily in the North Pacific Ocean, the Greenland shark is common in both the North Atlantic and Arctic oceans, and the Antarctic sleeper shark is thought to occur primarily in the southern hemisphere (Compagno 1984; Yano et al. 2004, 2007). However, it is difficult to identify large bodied sleeper sharks to species based on their morphometric characteristics alone, which overlap (Benz et al. 2004). The genetic structure of large bodied sleeper shark species is also uncertain.

The Greenland shark and the Pacific sleeper shark have been identified as genetically distinct species (Walter et al. 2017), with speciation of the Greenland shark occurring 1 – 2.34 Ma, possibly associated with periods of repeated glaciations during the Pleistocene geological epoch (Walter et al. 2017). Pacific sleeper shark and Greenland shark genetic hybridization also occurs (Hussey et al. 2015; Walter et al. 2017), possibly in association with inter-glacial periods after genetic isolation (Walter et al. 2017). These results are consistent with previous genetic analysis of Pacific sleeper sharks collected from the North Pacific Ocean and the Bering Sea, which identified several frequently occurring haplotypes within two distinct clades consistent with geologically recent population expansion and with genetic mixing after separation (O'Brien et al. 2013).

Walter et al. (2017) also hypothesized an ancestral sleeper shark with a possibly pan-deep-ocean distribution prior to the Miocene, which is consistent with a lack of evidence of genetic differences among sleeper shark specimens obtained from the North Pacific (Alaska and Taiwan) and the southern hemisphere (Murray et al. 2008). Murray et al. (2008) hypothesized either a pan-Pacific stock or geologically recent deep-ocean connectivity among *S. pacificus* and *S. antarcticus*, and noted that increased sample size or alternative genetic techniques would be required to evaluate genetic structure resulting from recent genetic isolation.

In the high-latitude North Pacific Ocean and the Bering Sea, Pacific sleeper sharks are commonly encountered at bottom depths of 200 to 700 m as well as pelagic depths of 100 to 200 m associated with the continental shelfs and upper continental slopes (Compagno 1984; Ebert et al. 1987; Orlov 1999; Orlov and Moiseev 1999a, b; Mecklenburg et al. 2002; Yano et al. 2004, 2007; Ebert and Winton 2010; Orlov and Baitalyuk 2014). Pacific sleeper sharks have also been encountered more rarely in both the Arctic (Benz et al. 2004) and in relatively deep-water (~1000 m and deeper) of the temperate and subtropical North Pacific Ocean associated with sea mounts (Borets 1986), the Hawaiian archipelago (Yeh and Drazen 2009), and the continental shelf east of Taiwan (Wang and Yang 2004).

Within U.S. federally managed waters (>5.56 km [3 nautical miles] from shore to 370.4 km [200 nautical miles]) Pacific sleeper sharks are captured incidentally in commercial fisheries targeting pelagic species (walleye Pollock *Gadus chalcogrammus*) and demersal fish species (groundfish) in the eastern Bering Sea (EBS), Aleutian Islands (AI) and Gulf of Alaska (GOA) (Courtney et al. 2006a, b). Pacific sleeper shark incidental catch within U.S. federally managed waters off of Alaska is managed by the North Pacific Fishery Management Council (NPFMC) under separate Fishery Management Plans (FMPs) established for the eastern Bearing Sea and Aleutian Islands (BSAI) and the Gulf of Alaska (GOA). The Magnuson–Stevens Reauthorization Act of 2006 (MSRA 2006) established new requirements to end and prevent overfishing through the use of annual catch limits and mandated that such limits be established for all stocks included within U.S. federally managed fishery management plans by 2011. However, only limited data are available to assess the Pacific sleeper shark stock status within the BSAI and GOA FMPs because there are no directed fisheries for sharks in these regions, and most incidentally captured sharks are not retained (Tribuzio et al. 2011, 2012). Despite these data limitations, elasmobranchs may be relatively more vulnerable to overfishing than the teleost target species with which they are captured (Smith et al. 1998; Forrest and Walters 2009; Kyne and Simpfendorfer 2010). For example, in the GOA, time series data available for both Pacific sleeper shark incidental catch and fishery-independent CPUE have shown an increasing trend followed by a decreasing trend (Tribuzio et al. 2011). These trends are worrisome because they indicate that incidental catch levels, or other unknown factors, may be affecting Pacific sleeper shark relative abundance in the region, which could be a fisheries conservation concern for the species under the MSRA.

Additionally, ecosystem-based fishery management (EBFM) requires the collection of data on species interactions in order to minimize the risk of irreversible changes to natural assemblages of species and ecosystem processes from the effects of fishing (Pikitch et al. 2004). For example, sharks may function as keystone predators and therefore would be essential to the maintenance and stability of food webs (Myers et al. 2007). Changes in elasmobranch abundance over time may also be indicative of, or in response to, ecosystem-level restructuring, for example following the effects of fishing (e.g., Kitchell et al. 2002; Myers et al. 2007; Baum and Worm 2009) or following the effects of a decadal-scale climatic regime shift which occurred in the region (e.g., Hollowed and Wooster 1995). As a cold-water adapted elasmobranch, the Pacific sleeper shark may also be relatively more vulnerable to the effects of contemporary climate change than other sharks (O'Brien et al. 2013).

Pacific sleeper sharks are large predators capable of consuming fast swimming prey including large teleosts and marine mammals, and their diet varies ontogenetically as well as by season, geographic region, and capture depth likely in response to prey availability (Bright 1959; Gotshall and Jow 1965; Ebert et al. 1987; Orlov 1999; Orlov and Moiseev 1999a, 1999b; Yang and Page 1999; Smith and Baco

2003; Wang and Yang 2004; Sigler et al. 2006; Yano et al. 2007). Pacific sleeper sharks have also been implicated as predators of an endangered Steller sea lion subpopulation in the eastern North Pacific Ocean west of 144° W (Horning and Mellish 2014) and of a declining harbor seal subpopulation in Glacier Bay, Southeast Alaska (Taggart et al. 2005). However, a directed diet study of Pacific sleeper sharks sampled near four large rookeries of the endangered Gulf of Alaska Steller sea lion subpopulation concluded that although the species ranges overlapped (Hulbert et al. 2006, their Figure 1), predation on Steller sea lions was unlikely, at least near rookeries where pups first enter the water (August) or occur during weaning (May) (Sigler et al. 2006). Instead, diet was dominated by cephalopods in May and teleosts in August (Sigler et al. 2006). Marine mammal tissues were identified in 15% of stomachs examined, but no Steller sea lion tissue was detected. Marine mammal tissue was primarily cetacean (probably scavenged), but also included harbor seal (possibly consumed alive) (Sigler et al. 2006).

However, even when direct predation events are rare, long-lived species such as marine mammals are predicted to engage in antipredator behavior in response to predation risk (Heithaus et al. 2008). For example, in Prince William Sound, Alaska, both harbor seals and Steller sea lions are predicted to change their foraging behavior in response to predation risk from large predators including Pacific sleeper sharks and Killer whales, and to reverse their foraging preferences in response to simulated removals of large predators, leading to increased seal predation on some teleost taxa and relaxed predation on others (Frid et al. 2007, 2008, 2009; Heithaus et al. 2010).

This dissertation addressed single species stock assessment and ecosystem based fisheries management of Pacific sleeper sharks in the eastern North Pacific Ocean. Chapter 1 developed Pacific sleeper shark relative abundance indices from sablefish longline surveys in the eastern Bering Sea, Aleutian Islands, and Gulf of Alaska. Chapter 2 conducted a risk analysis to determine if recent (status quo) incidental exploitation rates in the Gulf of Alaska are likely to be sustainable. Chapter 3 developed baseline information about Pacific sleeper shark feeding ecology in the eastern Bering Sea and Gulf of Alaska from stable isotope ratios of lipid normalized carbon ($\delta^{13}C'$) and nitrogen ($\delta^{15}N$) to determine food web and relative trophic position, respectively. Chapter 4 developed baseline information about Pacific sleeper shark habitat utilization in the Gulf of Alaska based on times series analysis combined with linear regression models of electronic archived tag depth and environmental data. A brief summary of each chapter is provided below.

Summary of Chapter 1

An accurate index of relative abundance is a necessary component for stock assessment. Chapter 1 developed trends in Pacific sleeper shark relative abundance in the northeast Pacific Ocean from sablefish longline surveys conducted annually from 1979 – 2003. Pacific sleeper shark area-weighted

catch per unit effort (CPUE) was calculated using standard methods previously applied to sablefish longline surveys. Annual trends in CPUE were tested for statistical significance by comparing 95% confidence intervals obtained from bootstrap resampling (Sigler and Fujioka 1988).

Within the GOA, Pacific sleeper shark area-weighted CPUE was significantly higher ($P < 0.05$) during the years 1993, 1994, 1996, 1998, and 2000–2003 than during the years 1989–1992. The increase in GOA area-weighted CPUE was driven largely by incidental catch in one sablefish longline survey region (Shelikof Trough, 13,000 km^2, 201–300 m depth, n = 850 sharks). In comparison, a separate study also found that the CPUE of Pacific sleeper sharks captured incidentally in fishery independent bottom trawl surveys had increased significantly between the years 1984 and 1996 in this region (Mueter and Norcross 2002), as well as in another adjacent GOA bottom trawl survey region. Within the EBS, Pacific sleeper shark area-weighted CPUE was significantly higher ($P < 0.05$) during the year 1994 compared to the years 1988 and 1992.

However, the number of Pacific sleeper sharks captured in the sablefish longline survey from 1979 – 2003 was very low (n = 1,565). Sample sizes were too low to test for significant differences among survey years with bootstrap resampling prior to 1989 within the GOA and during most years within the EBS and AI. There was also significant inter-annual variability in the GOA in the year 1997, a significant decrease followed by a significant increase. High inter-annual variability in relative abundance (e.g., as in 1997) is not consistent with the long life, low fecundity, and slow population growth rate assumed for Pacific sleeper sharks. Consequently high inter-annual variability (e.g., as in 1997) may have been caused by factors other than abundance, such as hook competition and correlation of catch rates among non-target species captured on sablefish longline survey gear (Rodgveller et al. 2008) or changes in Pacific sleeper shark distribution over time, for example, in response to changes in prey availability.

A priority for future research of Pacific sleeper shark relative abundance in the northeast Pacific Ocean is to develop abundance indices with less inter-annual variability. Fishery-independent surveys conducted by the International Pacific Halibut Commission (IPHC) incidentally capture Pacific sleeper sharks in the northeast Pacific Ocean (Menon 2004; Menon et al. 2005; Tribuzio et al. 2011), and may be useful for developing an index of Pacific sleeper shark relative abundance. Additionally, it may be possible to develop relative abundance indices using techniques adapted from commercial catch and effort data standardization (Maunder and Punt 2004).

Summary of Chapter 2

Fisheries management under the MSRA requires an estimate of stock status relative to overfishing and overfished benchmarks. Because of high inter-annual variability in relative abundance indices and a lack of life history information for Pacific sleeper sharks in the northeast Pacific Ocean, a

risk analysis approach was developed in Chapter 2 to provide management advice. The risk analysis was based on Monte Carlo simulation of a generic long-lived shark population with characteristics similar to those assumed for the Pacific sleeper shark population in the GOA. The risk analysis was implemented over a plausible range of exploitation rates (low versus high) obtained from available catch and bottom trawl survey data in the GOA. The exploitation rate was calculated as an annual average rate in order to be robust to the inter-annual variability observed in both estimates of incidental catch obtained from the commercial fishery and estimates of exploitable biomass obtained from the bottom trawl survey. The risk analysis included a range in length based selectivity (asymptotic versus dome-shaped) derived from the observed size range of Pacific sleeper sharks captured incidentally in the GOA relative to their assumed maximum size (~7 m). The risk analysis also included a range in the productivity of the stock based on a plausible range in the steepness (h) of the assumed Beverton-Holt stock-recruitment relationship (0.25 and 0.39), and included a range in the assumed life history characteristics of the stock based on a plausible range in maximum age (30, 50, and 100 years).

The risk analysis results were summarized as the fraction of 1,000 simulation runs ending in an overfished condition after 100 years of incidental exploitation. The risk analysis results were most sensitive to the range of uncertainty identified for the incidental exploitation rate. The aggregate risk of ending in an overfished condition increased from 0.0% under low exploitation rate scenario to 59% under the high exploitation rate scenario. This result is informative for management advice under the MSRA. On the one hand, the low exploitation rate scenario was based on the current official Pacific sleeper shark incidental catch statistics in the GOA and suggests that the officially reported annual incidental catches of Pacific sleeper sharks in the GOA are sustainable under a plausible range of simulated conditions. On the other hand, the high exploitation rate scenario included preliminary annual estimates of previously unreported incidental catches from the GOA, that were not included in the officially reported annual incidental catches of Pacific sleeper sharks. Given that the high exploitation rate scenario is at least plausible, the risk of ending in an overfished condition under status quo management may be fairly high (59% after 100 years of exploitation) when unreported incidental catch is included in the plausible range of simulated conditions. This result indicates that a priority for management is to reduce the uncertainty in unreported Pacific sleeper shark incidental catch estimates in the GOA. An observer program is now in place to monitor the historically unobserved Pacific halibut fishery in the GOA, which incidentally catches Pacific sleeper sharks; hence, this major uncertainty will be reduced.

Risk analysis results were also sensitive to the assumed shape of the length-based selectivity curve. The percentage of simulations that ended in an overfished condition was very low (0.0%) for alternative model configurations evaluated under the low exploitation rate scenario, regardless of whether the length-based selectivity curve was assumed to be asymptotic or dome-shaped. However, the aggregate

percentage of simulations resulting in an overfished condition was very high (100.0%) for alternative model configurations evaluated under the combination of a high exploitation rate and asymptotic selectivity. The dome-shaped selectivity scenario was most consistent with the observed size range of Pacific sleeper sharks captured incidentally in the GOA and was based on the assumption that the largest sharks were either not available to the fishing gear or were not vulnerable to capture when in contact with the fishing gear. In contrast, a combination of high exploitation and asymptotic selectivity could also plausibly explain the observed size range of Pacific sleeper sharks, based on the assumption that the largest sharks were removed from the population by fishing mortality. Additional research on the selectivity of fishing gear relative to the true size range of Pacific sleeper sharks in the northeast Pacific Ocean is necessary in order to discriminate among these selectivity assumptions.

Overall, the risk analysis results were less sensitive to the plausible ranges assumed for stock recruitment steepness and maximum age than they were to those assumed for exploitation rate and selectivity. However, for alternative model configurations evaluated under the combination of relatively low stock productivity (h = 0.25), dome-shaped selectivity, and high exploitation, the percentage of simulations resulting in an overfished condition increased (0.1, 6.3, and 99.8%) with increasing maximum age (30, 50, and 100 years, respectively). This result is important for management, because it suggests that under some plausible scenario combinations, reducing the current uncertainty in Pacific sleeper shark life history will be important for providing accurate management advice.

The utility of the simulation approach developed here is that it can be periodically updated as new data become available. For example, it will be informative to re-evaluate the risk analysis once official incidental bycatch estimates of Pacific sleeper sharks become available for the previously unobserved Pacific halibut fishery. It may also be informative to re-examine assumptions about life history as new life history research (e.g., Nielsen et al. 2016) and meta-analyses (Then et al. 2015) become available. It may also be informative to evaluate alternative structural model assumptions, for example use of a stock recruit relationship developed for low-fecundity sharks (Taylor et al. 2013).

Summary of Chapter 3

Pacific sleeper shark trophic interactions in the northeast Pacific Ocean have previously only been investigated based on stomach content analysis (Yang and Page 1999; Sigler et al. 2006; Yano et al. 2007). However, reliance on stomach contents alone to quantify the diet of elasmobranchs has limitations (e.g., Wetherbee and Cortés 2004). Chapter 3 evaluated stable-isotope analysis of nitrogen ($\delta^{15}N$) and carbon ($\delta^{13}C$) (DeNiro and Epstein 1978, 1981; Minagawa and Wada 1984) as a predictor of Pacific sleeper shark trophic relationships in the northeast Pacific Ocean (Vander Zanden et al. 1997; Post 2002; Martínez del Rio et al. 2009; e.g., Marsh et al. 2012). The nitrogen stable-isotope is useful for predicting

trophic position based on empirical evidence that during the ingestion of food and the excretion of wastes, there is an enrichment fractionation of the heavier nitrogen isotope, ^{15}N, in animal tissues relative to the lighter nitrogen isotope, ^{14}N. In contrast, $\delta^{13}C$, which is on average enriched less than $\delta^{15}N$, is more useful for the prediction of feeding in different food webs based on differences in $\delta^{13}C$ sources of primary productivity among benthic or nearshore food webs compared to pelagic food webs.

Chapter 3 identified mathematically significant differences in lipid-normalized carbon stable-isotope ratios ($\delta^{13}C'$) and $\delta^{15}N$ of Pacific sleeper shark muscle tissue, as well as in Pacific sleeper shark trophic position determined from $\delta^{15}N$ (T_{PN}) among geographic strata in the EBS, GOA, and northern Southeast Alaska (NSE). These results suggest that there may be important regional differences in the feeding behavior of Pacific sleeper sharks between the EBS and the GOA-NSE. The major results of the study are summarized below.

δThe $^{13}C'$ of Pacific sleeper shark muscle tissue obtained from the GOA-NSE was significantly enriched (less negative) relative to that of the EBS. A probable explanation is that enrichment in $\delta^{13}C'$ may have resulted from feeding in different food webs. Benthic or nearshore prey may have been relatively more important in the diet of Pacific sleeper sharks in the GOA-NSE and pelagic prey may have been relatively more important in the EBS. There may also be individual specialization in Pacific sleeper shark diet. For example, Pacific sleeper sharks captured incidentally in the EBS may have been consuming the pelagic prey targeted, or discarded, by the commercial fishery in the EBS (walleye pollock) compared to the demersal prey (groundfish) targeted, or discarded, by the bottom trawl survey in the GOA-NSE. In either case, the observed difference in the feeding ecology of Pacific sleeper sharks between the EBS and the GOA-NSE based on stable-isotope ratios is consistent with previous results from electronic tagging studies which suggest that there is relatively little annual interchange of individual Pacific sleeper sharks between the EBS and the GOA. In particular, 76% of electronically tagged Pacific sleeper sharks in the GOA were recovered within 100 km of their release location up to c. 1 year after release (Hulbert et al. 2006). Isotopic differences would be expected to be minimal if there were higher annual mixing rates between the regions because of the slow isotopic turnover of $\delta^{13}C$ in elasmobranch muscle tissue (95% turnover in elasmobranch white muscle $\delta^{13}C$ occurs between *c.* 555 and 786 days; Logan and Lutcavage 2010a, 2010b). In contrast, some numerically tagged Greenland sharks at liberty for up to 8 years exhibited much longer distance movements (> 1000 km; Hansen 1963).

Muscle tissue $\delta^{15}N$ was modelled as a function of shark total length (L_T) and geographic strata of capture (Z) with linear regression: $\delta^{15}N = L_T + Z + L_T \times Z + \varepsilon$, where ε was assumed normally distributed error. The best linear model based on the Akaike information criterion (AIC) was the full model. Geographic strata that did not have significantly different coefficients were pooled. The rate of linear increase in $\delta^{15}N$ with increasing length differed significantly among some geographic strata, which may

reflect regional differences in feeding patterns similar to those hypothesized above for $\delta^{13}C'$. Increasing $\delta^{15}N$ with increasing length is also consistent with previous Pacific sleeper shark diet studies based on stomach content analysis, which found evidence of an ontogenetic shift in diet in both the eastern and the western North Pacific Ocean.

The linear model was used to predict $\delta^{15}N$ along with a 95% prediction interval for selected geographic strata at a standard shark length of 201.5 cm L_T. The shark length used for prediction was the approximate mean length of northeast Pacific Ocean Pacific sleeper sharks previously examined for diet based on stomach contents (Yang and Page 1999; Sigler et al. 2006; Yano et al. 2007).

Trophic position determined from $\delta^{15}N$ (T_{PN}) was obtained for each point forecast of $\delta^{15}N$ along with its 95% prediction interval: $T_{PN} = T_{Pbaseline} + (\delta^{15}N_{consumer} - \delta^{15}N_{baseline})(\Delta_n)^{-1}$, where $T_{Pbaseline}$ was the baseline trophic position assumed for copepods (2.3), and Δ_n was the assumed mean consumer to diet discrimination factor ($\Delta^{15}N = \delta^{15}N_{consumer} - \delta^{15}N_{diet}$) for an unknown number (n) of trophic links between Pacific sleeper sharks and copepods in the eastern North Pacific Ocean. Uncertainty in Δ_n was incorporated by including four different point estimates of $\Delta^{15}N$ obtained from the scientific literature. Two were obtained from ecosystem level meta-analyses of consumer to diet discrimination factors: 3.4 ‰ (Minagawa and Wada 1984; Vander Zanden and Rasmussen 2001; Post 2002) and 2.7 ‰ (Vanderklift and Ponsard 2003; Dale et al. 2011). Two were obtained from muscle tissue to diet discrimination factors specifically estimated for large carnivorous sharks: 2.3 ‰ (Hussey et al. 2010a; e.g., Hussey et al. 2010b, 2011, 2012) and 4.0 ‰ (McMeans et al. 2010).

For comparison with T_{PN} obtained in this study, the trophic position determined from diet (T_{PD}) was calculated for Pacific sleeper sharks in the eastern North Pacific Ocean from three previously published diet studies based on stomach contents (Yang and Page 1999; Sigler et al. 2006; Yano et al. 2007) following standard methods (Cortés 1999). Most Pacific sleeper sharks previously examined for diet (n = 211) were obtained during summer months in the National Marine Fisheries Service (NMFS) central GOA regulatory area (Yang and Page 1999; Sigler et al. 2006). In comparison, stable isotope samples from the GOA were obtained from primarily the same geographic region but also included some samples from the Western GOA and NSE.

Pacific sleeper shark $\delta^{15}N$ values obtained in this study were compared to those obtained from previously published scientific literature for other aquatic organisms in the eastern North Pacific Ocean separately for the EBS and the GOA. The expected range in consumer to diet discrimination factor enrichment of Pacific sleeper shark muscle tissue $\delta^{15}N$, $\Delta^{15}N$, was 2.3 – 4.0‰, as described above. However, Pacific sleeper shark muscle tissue $\Delta^{15}N$ was lower than expected relative to those of fish and squid in both the EBS and GOA. Available stomach-content data suggest that fishes and squid are

important prey of Pacific sleeper sharks in the eastern North Pacific Ocean and that, consequently, Pacific sleeper shark muscle tissue $\delta^{15}N$ values should be enriched (2.3 – 4.0 ‰ higher) relative to those of fish and squid. Similarly, Pacific sleeper shark muscle tissue $\Delta^{15}N$ was lower than expected relative to humpback whales in both the EBS and GOA. Available stomach-content data, along with fatty acid composition, suggest that filter feeding whale carrion may be an energetically important component of Pacific sleeper shark diet in the eastern North Pacific Ocean. In the central GOA, cetaceans comprised about one-third of Pacific sleeper shark stomach contents by mass (at least 70%, probably scavenged) and, as a result, appeared to be energetically important (Sigler et al. 2006). Preliminary analysis of the fatty acid composition of Pacific sleeper shark liver and muscle obtained from the GOA also revealed nutritional dependence on planktivores, which was consistent with scavenging on filter feeding whales (Schaufler et al. 2005).

One explanation for the lower than expected Pacific sleeper shark muscle tissue $\delta^{15}N$ values relative to their putative prey (fishes, squid, and filter feeding whales) in the eastern North Pacific Ocean is a possible negative bias in $\delta^{15}N$ resulting from the retention of urea in elasmobranch muscle tissue (*c.* 2.0 ‰; Kim and Koch 2012). Additionally, Pacific sleeper shark muscle tissue $\Delta^{15}N$ values at the lower end of the range used in this study, *c.* 2.3 ‰ (Hussey et al. 2010a) or *c.* 2.7 ‰ (Vanderklift and Ponsard 2003; Caut et al. 2009; Dale et al. 2011), would be most consistent with the observed Pacific sleeper shark $\delta^{15}N$ values relative to those of their putative prey (fishes, squid, and filter feeding whales) in both the EBS and GOA.

Future research of Pacific sleeper shark trophic ecology could benefit from the evaluation of compound-specific stable-isotope analysis (e.g., Dale et al. 2011). An advantage of compound-specific stable-isotope analysis is that both baseline $\delta^{15}N$ values and the tissue specific trophic enrichment, $\Delta^{15}N$, can be determined from individual amino acids of consumer tissues (Chikaraishi et al. 2009; Martínez del Rio et al. 2009; Wolf et al. 2009; Dale et al. 2011). Another advantage is that compound-specific stable-isotope analysis integrates the effects of variable consumer to diet discrimination factors at lower trophic levels of a consumer's diet.

Summary of Chapter 4

Chapter 4 characterized Pacific sleeper shark vertical movement patterns of habitat use in the Gulf of Alaska, which is important for improving commercial fisheries bycatch estimates and identifying potential ecological interactions with an endangered subpopulation of Steller sea lions. A structural model relating habitat use to environmental data was combined with an iterative time series error correction procedure. A strong autoregressive process at a lag of one hourly time step was identified in the average hourly depth profile obtained from one shark during June – November, 2002. None of the environmental

factors explored as predictors for observed structural changes in the depth profile over time were included in the most parsimonious model identified by AIC. However, implementation of the iterative approach required a structural explanatory variable (in this case month of the year) to achieve stationary residuals for time series analysis. This result indicated that Pacific sleeper shark movement behavior over relatively long time periods could be explained largely by a change in average depth each month. Our results have important implications for future research because they demonstrate that statistical inference about habitat utilization can be drawn from an entire time series depth profile stored on electronic archival tags. Specifically, we found a simple autoregressive relationship governing short-term movements throughout the time series which included substantial variation in longer time period movement patterns.

1. Chapter 1 Pacific Sleeper Shark Relative Abundance Trends[1]

1.1. Abstract

The deep-water Pacific sleeper shark *Somniosus pacificus* is an opportunistic predator in the northeast Pacific Ocean. Pacific sleeper shark life history and distribution are poorly understood, and changes in Pacific sleeper shark relative abundance or distribution could have direct and indirect effects on the ecosystem. There are no directed fisheries or surveys for Pacific sleeper sharks in Alaskan marine waters; consequently, abundance estimation is limited to indirect methods. We analyzed Pacific sleeper shark incidental catch (bycatch) from sablefish longline surveys conducted on the upper continental slope of the eastern Bering Sea, Aleutian Islands, and Gulf of Alaska during the years 1979 to 2003. Our objectives were to estimate trends in Pacific sleeper shark relative abundance and their statistical significance. A total of 1,565 Pacific sleeper sharks were captured by sablefish longline surveys during the years 1979 to 2003 with a sample effort of 19.7 million hooks. Area (km^2) weighted catch per unit effort (CPUE) of Pacific sleeper sharks was analyzed from standardized sablefish longline surveys during the years 1982 to 2003 with bootstrap 95% confidence intervals as an index of relative abundance in numbers. Within the limited time series available for hypothesis testing, area-weighted CPUE of Pacific sleeper sharks increased significantly in the eastern Bering Sea during the years 1988 to 1994 and in the Gulf of Alaska during the years 1989 to 2003, but also decreased significantly in the Gulf of Alaska in 1997. The increasing trend in the Gulf of Alaska was driven entirely by one region, Shelikof Trough, where most (54%) Pacific sleeper sharks were captured. Increasing trends in area-weighted CPUE of Pacific sleeper sharks in the eastern Bering Sea and Shelikof Trough are consistent with previous analyses of fishery-dependent and fishery-independent data from the northeast Pacific Ocean and with evidence of a climatic regime shift that began in 1976 and 1977. Whether increasing trends in area-weighted CPUE of Pacific sleeper sharks from sablefish longline surveys represent an increase in the absolute abundance of Pacific sleeper sharks at the population level or just reflect changes in local densities is unknown because of caveats associated with computing area-weighted CPUE of Pacific sleeper sharks from sablefish longline surveys and because of a lack of information on the life history and distribution of Pacific sleeper sharks.

[1] Courtney, D. L., and M. F. Sigler. 2007. Trends in area-weighted CPUE of Pacific sleeper sharks (*Somniosus pacificus*) in the northeast Pacific Ocean determined from sablefish longline surveys. Alaska Fishery Research Bulletin 12:291–315.

1.2. Introduction

Pacific sleeper sharks (*Somniosus pacificus*), spiny dogfish (*Squalus acanthias*), and salmon sharks (*Lamna ditropis*) are the three most abundant shark species in Alaskan marine waters (Mecklenburg et al. 2002). Of these, Pacific sleeper sharks are the least understood (e.g., Yano et al. 2004, 2007). Pacific sleeper sharks range in the North Pacific from Japan along the Siberian coast to the Bering Sea, and southward to southern California USA and Baja California, Mexico (Compagno 1984). Pacific sleeper sharks have also been identified on seamounts in the North Pacific (Borets 1986) and along the Pacific coasts as far south as Taiwan (Wang and Yang 2004) and Chile (Crovetto et al. 1992), although Yano et al. (2004) suggest that the range of Pacific sleeper sharks is limited to the northern hemisphere. In Alaskan marine waters, Pacific sleeper sharks occur on the continental shelf and slope of the Chukchi Sea, Bering Sea, Aleutian Islands, and Gulf of Alaska (Hart 1973; Mecklenburg et al. 2002; Benz et al. 2004; Courtney et al. 2006a, 2006b). Published observations suggest that mature female Pacific sleeper sharks are in excess of 365 cm TL (total length), mature male Pacific sleeper sharks are in excess of 397 cm TL, and size at birth is approximately 40 cm TL (Gotshall and Jow 1965; Yano et al. 2007). Pacific sleeper sharks are assumed to bear live young, although little is known about their reproduction or other aspects of their life history including age (Ebert et al. 1987; Yano et al. 2007). Virtually nothing is known about the space utilization or geographic movements of Pacific sleeper sharks within Alaskan marine waters. Tagging studies in Alaska have shown that at least some Pacific sleeper sharks reside in the Gulf of Alaska and Prince William Sound, where most tagged sharks exhibited relatively limited geographic movement (< 100 km) throughout the year (Hulbert et al. 2006).

Pacific sleeper sharks appear to be opportunistic predators, and changes in their relative abundance or distribution could have direct and indirect effects on the ecosystem. Pacific sleeper sharks are known to feed directly on a wide variety of mid-water and benthic prey and to consume whales as carrion (Bigelow and Schroeder 1948; Bright 1959; Hart 1973; Compagno 1984; Smith and Baco 2003; Sigler et al. 2006; Yano et al. 2007). Prey items found in Pacific sleeper shark stomachs include flatfishes *Pleuronectiformes*, Pacific salmon *Oncorhynchus* spp., rockfishes *Sebastes* spp., walleye pollock *Theragra chalcogramma*, and invertebrate species including Tanner crab *Chionoecetes bairdi*, cephalopods, gastropods, and occasionally even sponges (Compagno 1984; Orlov 1999; Yang and Page 1999; Sigler et al. 2006). Harbor seals *Phoca vitulina* have also been documented in the stomach contents of Pacific sleeper sharks; however, whether harbor seals are consumed as living prey or as carrion is not known (Bright 1959; Sigler et al. 2006). Frid et al. (2006, 2007a, 2007b, 2008) modeled predation risk of harbor seals from Pacific sleeper sharks and predicted indirect effects of the removal of Pacific sleeper

sharks on two species consumed by harbor seals, Pacific herring *Clupea pallasii* and walleye pollock, mediated by changes in harbor seal behavior in response to predation risk.

Although the trophic relationships of Pacific sleeper sharks in the ecosystem are still uncertain (e.g., McMeans et al. 2007), Pacific sleeper sharks have been implicated in the decline of Steller sea lions *Eumetopias jubatus* in western Alaska (NRC 2003) and in the decline of harbor seals in Glacier Bay, Alaska (Taggart et al. 2005). The NRC (2003) recommended research into potential predator feeding habits and population size, including 1) collection of sleeper shark incidental catch (bycatch) data from longline fisheries to assess shark abundance and 2) examination of shark stomach contents to determine diet. A subsequent study of Pacific sleeper shark predation on sea lions found no sea lion remains in the stomachs of nearly 200 sleeper sharks (130–284 cm TL) captured near sea lion rookeries (Sigler et al. 2006). Directed studies of Pacific sleeper shark predation on harbor seals have not been conducted. This study responds to the NRC (2003) recommendation to assess trends in sleeper shark abundance in the northeast Pacific Ocean.

There are no directed fisheries for Pacific sleeper sharks in Alaskan marine waters, length compositions are not available, and age determination is not currently possible (Courtney et al. 2006a, 2006b). Consequently, abundance estimation is limited to indirect methods. Pacific sleeper sharks are occasionally captured in longline surveys for sablefish *Anoplopoma fimbria* conducted by the National Marine Fisheries Service (NMFS) on the upper continental slope and deep-water gullies of the continental shelf of the eastern Bering Sea-Aleutian Islands (BSAI) and Gulf of Alaska (GOA) within NMFS regulatory areas (Figure 1.1). Shark bycatch from sablefish longline surveys has not previously been analyzed.

For this report, historic data from sablefish longline surveys were tabulated, and area-(km^2) weighted CPUE of Pacific sleeper sharks was calculated with statistical methods previously implemented for the sablefish longline surveys (Gulland 1969; Quinn et al. 1982; Sasaki 1985; Sigler and Fujioka 1988; Sigler and Zenger 1989; Zenger and Sigler 1992). Trends in area-weighted catch per unit effort (CPUE) of Pacific sleeper sharks were tested for statistical significance by comparing 95% confidence intervals obtained from bootstrap resampling (Efron 1982; Efron and Tibshirani 1986). Bootstrap resampling has been implemented for the sablefish longline surveys (Sigler and Fujioka 1988) and for sablefish pot surveys (Kimura and Balsiger 1985), and is reviewed for use in survey sampling of marine fishes by Gunderson (1993) and Kimura and Somerton (2006). This is the first time that area-weighted CPUE and bootstrap resampling have been applied to shark bycatch from sablefish longline surveys.

1.3. Materials and Methods

1.3.1. Survey Methods

Since 1979, annual sablefish longline surveys have sampled the 201–1,000 m depths of the upper continental slope and shelf break in the eastern Bering Sea, Aleutian Islands, and Gulf of Alaska including some deep-water gullies (>200 m) in the Gulf of Alaska. The time series includes two surveys, the Japan-U.S. cooperative longline survey from 1979 to 1994 (cooperative survey) and the NMFS domestic longline survey from 1988 to present (domestic survey; Sasaki 1985; Sigler and Fujioka 1988; Sigler and Zenger 1989; and Zenger and Sigler 1992).

Surveys were conducted each year from May to September. Survey station locations were fixed, and the same station locations were fished each year. Survey stations were distributed as uniformly as possible within NMFS regulatory areas (Figure 1.1). The eastern Bering Sea slope stations sampled five geographic regions: Bering-V, Bering-IV, Bering-III, Bering-II, and Bering-I (Sasaki 1985). The Aleutian Islands slope stations sampled four geographic regions: Northwest (NW) Aleutians, southwest (SW) Aleutians, northeast (NE) Aleutians, and southeast (SE) Aleutians (Sasaki 1985). The Gulf of Alaska slope stations sampled six geographic regions: Shumagin, Chirikof, Kodiak, West Yakutat, East Yakutat, and Southeast Outside (Sasaki 1985; Sigler and Fujioka 1988; Sigler and Zenger 1989; Zenger and Sigler 1992). Gulf of Alaska gully stations were added in 1989 to index pre-recruit sablefish (Sasaki 1985), but were not included in sablefish assessments (Sigler and Fujioka 1988; Sigler and Zenger 1989; Zenger and Sigler 1992). The Gulf of Alaska gully stations sampled fourteen geographic regions: Shumagin Gully, West Semidi, Shelikof Trough, Chiniak Gully, Amatuli Gully, Western Grounds, Yakutat Valley, Alsek Strath, Spencer Gully, Southeastern Shelf, Southeastern, Omany Trench, Iphigenia Trench, and Dixon Entrance.

One station was fished per day, except in Gulf of Alaska gullies where two adjacent stations were fished per day. Each slope station in the Aleutian Islands and Gulf of Alaska fished 160 hachis (the Japanese word for "skate" or length of longline). Each slope station in the Bering Sea fished 180 hachis. Each gully station in the Gulf of Alaska fished 80 hachis. A standard longline survey hachi consisted of a 100 m groundline with 45 hooks spaced 2 m apart on 1.2 m gangions with 5 meters of groundline left bare on each end of the hachi. The hook was a type of J-hook called a Tara hook or a circle hook. Ring-cut short-finned squid were used as bait. At slope stations, the longline was set at right angles to the isobaths in a manner to cover the depth range of 201–1,000 m. However, the distance between 201 and 1,000 m varied at each station, and the complete depth range could not be covered at stations where this distance exceeded the length of the longline gear—16 km at slope stations in the Gulf of Alaska and Aleutian Islands, and 18 km at slope stations in the eastern Bering Sea. The longline was usually set from

shallow to deep waters and was retrieved in the same direction. At gully stations in the Gulf of Alaska, the longline was set along the bottom of the gully where the maximum depth was generally between 300–400 m. Although some hooks landed in shallower (<200 m) and deeper (>1,000 m) depths, only depths between 201–1,000 m received full coverage with the sablefish longline survey gear.

Hauling the longline started two hours after the set was completed. The soak time averaged five to six hours, but varied by section of the longline. For the first section of the longline hauled, the soaking time was about three hours, but for the last section hauled it was about seven to nine hours. The depth at which fish were caught was estimated by measuring the depth of water under the vessel with an echo sounder for every fifth hachi. The catch in numbers was recorded by species or species group for each hachi. Large non-target species such as Pacific sleeper sharks were counted and released at the rail. As a result, length, weight, and sex were not recorded for Pacific sleeper sharks captured in sablefish longline surveys.

The domestic survey (1988–2003) was similar to the cooperative survey (1979 –1994) with some exceptions: the domestic survey sampling design was expanded in 1989 to include more deep-water gullies (>200 m depth) of the Gulf of Alaska continental shelf; the domestic survey sampling design did not include the western Aleutians; the domestic survey sampling design did not include the eastern Bering Sea and eastern Aleutian Islands in all years; the domestic survey gear used stronger beckets and gangions than the cooperative survey; the domestic survey gear used circle hooks (Eagle Claw No. 7), whereas the cooperative survey used a J-hook 74 mm in length and 21 mm in width; the domestic survey chartered U.S. commercial longline vessels of 37–45 m, whereas cooperative survey chartered Japanese commercial longline vessels of approximately 500 gross tons, but otherwise with essentially the same structural characteristics.

1.3.2. Statistical Methods

First, the CPUE of Pacific sleeper sharks was tabulated from the combined cooperative survey (1979–1994) and domestic survey (1988–2003) to identify trends over time (1979–2003) and to identify the distribution of CPUE by survey region and depth (Figure 1.1). The CPUE was tabulated for all stations fished, during all years, in all depths where hooks landed (0–1,200 m or greater), and in all survey regions. The CPUE was calculated as the number of Pacific sleeper sharks captured per hachi from each region (r), station (j), and depth (k) as:

$$\mathrm{CPUE}_{rjk} = \frac{\mathrm{sleeper\ sharks}_{rjk}}{\mathrm{hachi}_{rjk}}. \tag{1.1}$$

Second, area-weighted CPUE of Pacific sleeper sharks was calculated from sablefish longline surveys as an index of relative abundance in numbers. An attempt was made to control for factors unrelated to abundance by limiting the calculation of area-weighted CPUE to standard survey years, standard survey regions, standard survey stations, standard survey depths, and effective hachis, following methods in Sasaki (1985), Sigler and Zenger (1989), and Zenger and Sigler (1992). Standard survey years were defined as years with the same survey design each year: 1982–1994 for the cooperative survey, and 1989–2003 for the domestic survey. Standard survey regions were defined as geographically stratified regions within each regulatory area that were designed to be sampled by one or more fixed station locations each year (Figure 1.1). Standard survey stations were defined as fixed station locations designed to be fished each year and spread as uniformly as possible within standard survey regions along the upper continental slope, continental shelf break, and deep-water gullies (>200 m depth). Standard survey depths were defined as the following stratified depth ranges (depth strata) between 201–1,000 m designed to have full coverage by the longline gear: 201–300 m, 301– 400 m, 401– 600 m, 601–800 m, 801–1,000 m. Effective hachis were defined as hachis with five or fewer ineffective hooks. Ineffective hooks were identified during gear retrieval and generally included hooks tangled in a snarl, missing hooks or hooks straightened with bait removed, and hooks on a hachi associated with a parted ground line. Standard survey stations were also excluded from calculation of standardized area-weighted CPUE if they experienced whale predation on the gear, competition with other fishing vessels, or excessive loss of gear.

Trends in area-weighted CPUE were calculated separately for the standardized cooperative survey (1982–1994) and the standardized domestic survey (1989–2003). The standardized surveys differed in the design of their station locations and regions. In particular, the standardized domestic survey design included several deep-water gullies (>200 m depth) on the Gulf of Alaska continental shelf, including Shelikof Trough, where Pacific sleeper shark appeared to be relatively abundant. The standardized cooperative survey design had more limited sampling of deep-water gullies and did not include Shelikof Trough. The types of hooks and gangions also differed between the standardized cooperative and domestic surveys, which may have affected the catchability of sleeper sharks.

Standardizing CPUE of Pacific sleeper sharks between the two sablefish surveys was not attempted here because of low Pacific sleeper shark sample sizes within geographic regions sampled by both surveys in the same years. The cooperative and domestic longline surveys have been standardized for sablefish CPUE (Kimura and Zenger 1997; Zenger 1997).

Area-weighted CPUE of Pacific sleeper sharks in sablefish longline surveys was calculated following methods previously implemented for sablefish longline surveys (Sasaki 1985; Sigler and Fujioka 1988; Sigler and Zenger 1989; Zenger and Sigler 1992). The CPUE at each station was multiplied by the estimated bottom area (A_{rk}; km^2) within each standard survey region and depth stratum

combination (Table 19 in Sasaki 1985; Table 2 in Sigler and Fujioka 1988; M. Sigler, unpublished data). Results for each station were summed across depth strata to obtain an independent estimate of Pacific sleeper shark relative population numbers (RPNs) for the standard survey region sampled by the station as:

$$\mathrm{RPN}_{rj} = \sum_{k} A_{rk} * \mathrm{CPUE}_{rjk} . \tag{1.2}$$

Station RPNs were averaged within standard survey regions to obtain regional RPNs as:

$$\mathrm{RPN}_{r} = \frac{\sum_{j} \mathrm{RPN}_{rj}}{j} . \tag{1.3}$$

Regional RPNs were summed within regulatory areas to obtain regulatory area RPNs as:

$$\mathrm{RPN} = \sum_{r} \mathrm{RPN}_{r} . \tag{1.4}$$

Following Gulland (1969) and Quinn et al. (1982), regional RPNs obtained from Equation (1.3) were divided by the total bottom area (A_r; km^2) surveyed within each standard survey region to obtain area-weighted CPUEs for standard survey regions as:

$$\text{Area-weighted CPUE}_{r} = \frac{\mathrm{RPN}_{r}}{A_{r}} . \tag{1.5}$$

Similarly, area RPNs obtained from Equation (1.4) were divided by the total bottom area (A; km^2) surveyed within each regulatory area (Eastern Bering Sea, Aleutian Islands, Western Gulf of Alaska, Central Gulf of Alaska, Eastern Gulf of Alaska, and Gulf of Alaska total) to obtain area-weighted CPUEs for regulatory areas as:

$$\text{Area-weighted CPUE} = \frac{\mathrm{RPN}}{A} . \tag{1.6}$$

Third, bootstrap 95% confidence intervals were calculated for area-weighted CPUE of Pacific sleeper sharks from sablefish longline surveys with bootstrap resampling to determine if trends in Pacific sleeper shark area-weighted CPUE over time were statistically significant. Following Sigler and Fujioka

(1988), each station was treated as an independent estimator of area-weighted CPUE for the standard survey region it sampled. Stations within each standard survey region were randomly resampled with replacement. A new RPN estimate was calculated for each standard survey region as the average of the randomly resampled station RPNs using Equation (1.3) and termed the bootstrap replicate (RPN_r^*). Bootstrap replicates of RPNs for regulatory areas (RPN*) were computed using Equation (1.4). Bootstrap replicates of area-weighted CPUE for standard survey regions (Area-weighted $CPUE_r^*$) were computed using Equation (1.5). Bootstrap replicates of area-weighted CPUE for regulatory areas (Area-weighted CPUE*) were computed using Equation (1.6). The bootstrap procedure was repeated 1,000 times. A bootstrap 95% confidence interval was obtained from the 1,000 bootstrap replicates of area-weighted CPUE by the percentile method (Efron and Tibshirani 1986).

There were insufficient data to conduct hypothesis testing for all survey regions during all survey years. The percentile method (Efron and Tibshirani 1986) requires approximately normally distributed bootstrap replicates. Histograms of bootstrap replicate distributions of area-weighted CPUE were graphed and visually inspected for selected standard survey regions and regulatory areas by year. Bootstrap 95% confidence intervals were computed for time series of area-weighted CPUE from standard survey regions and regulatory areas with approximately normally distributed bootstrap replicates.

Finally, an additional bootstrap resampling step was used to test the null hypothesis that the difference (Area-weighted $CPUE_{i'}$) – (Area-weighted $CPUE_i$) = 0, where i = year and i' = any subsequent year (Sigler and Fujioka 1988). Hypothesis testing was limited to selected time series of area-weighted CPUE from standard survey regions and regulatory areas with non-zero catches and approximately normally distributed bootstrap replicates. A difference was computed from each pair of 1,000 bootstrap replicates (Area-weighted $CPUE_{i'}^*$) – (Area-weighted $CPUE_i^*$), producing a bootstrap distribution of 1,000 differences. The percentile method was used to compute bootstrap 95% confidence intervals for the difference (Efron and Tibshirani 1986). The statistical significance of the difference (Area-weighted $CPUE_{i'}$) – (Area-weighted $CPUE_i$) was evaluated by the following criteria. If the 95% confidence interval for the difference did not include zero, then the null hypothesis was rejected, and the annual change in the area-weighted CPUE was considered statistically significant. However, because of multiple testing, approximate P-values for any individual year to year combination may be greater than 0.05.

1.4. Results

1.4.1. CPUE of Pacific Sleeper Sharks

The CPUE of Pacific sleeper sharks was tabulated from the combined cooperative survey (1979–1994) and domestic survey (1988–2003) for all survey years (1979–2003), regions, stations, depths, and hachis fished. Pacific sleeper shark bycatch was distributed along the entire upper continental slope and shelf break sampled by the sablefish surveys, except for the western Aleutian Islands (Figures 1.1 and 1.2). Sleeper shark catches occurred at 419 of 3,100 stations fished, and sleeper shark catch per station from stations with sleeper shark catch ranged from 1 to 44 (Figure 1.3). A total of 1,565 Pacific sleeper sharks were captured during sablefish longline surveys from 1979 to 2003 (Table 1.1). Pacific sleeper shark bycatch increased almost every year of the sablefish longline surveys and ranged from a low of 0 in 1979 and 1983 to a high of 176 in 2001 (Table 1.1). Similarly, Pacific sleeper shark CPUE increased almost every year of the sablefish longline surveys and ranged from 0.0 in 1979 and 1983 to a high of 1.4 in 2002 (Table 1.1). Most (67%) of Pacific sleeper sharks were captured in the 201–300 m depth stratum (Table 1.2); 54% of Pacific sleeper sharks were captured in Shelikof Trough, another 11% were captured in Amatuli Gully and Yakutat Valley combined, and another 21% were captured in the eastern Bering Sea (Table 1.3; Figures 1.1 and 1.2).

1.4.2. Area-weighted CPUE of Pacific Sleeper sharks

Analysis of area-weighted CPUE of Pacific sleeper sharks was conducted separately for the standardized cooperative survey (1982–1994) and the standardized domestic survey (1989–2003). The cooperative and domestic surveys differed in the design of their standard station locations (Table 1.4). Analysis of area-weighted CPUE within each survey was limited to standard survey regions, standard survey stations, standard survey depths, and effective hachis. The number of standardized fixed station locations fished successfully varied from year to year for each survey (Tables 1.5 and 1.6). Limiting the analysis to standardized surveys and to stations fished successfully reduced the sample size of Pacific sleeper shark bycatch to 147 in the cooperative survey and to 1,052 in the domestic survey (Tables 1.5 and 1.6). Total bottom area (km^2) surveyed within each standard survey region and depth stratum combination was used to weight Pacific sleeper shark CPUE from the cooperative and domestic surveys (Table 1.7). Weighting CPUE by the total bottom area (km^2) surveyed resulted in area-weighted CPUE with units of Pacific sleeper sharks captured per hachi. Area-weighted CPUEs were multiplied by 100 and reported as Pacific sleeper sharks captured per 100 hachis because of low sample sizes (Tables 1.8 and 1.9; Figures 1.4 – 1.6).

Area-weighted CPUE of Pacific sleeper sharks was higher in the Gulf of Alaska than in the eastern Bering Sea or the Aleutian Islands, and within the Gulf of Alaska was higher in the domestic survey than in the cooperative survey (Tables 1.8 and 1.9; Figure 1.4). In the eastern Bering Sea, area-weighted CPUE increased in 1993, 1994, and 1997, and then decreased. Area-weighted CPUE increased within each standard survey region of the Bering Sea between the years 1992 and 1994, with the largest increase in Bering IV in 1994 (Table 1.8; Figure 1.5). In the Aleutian Islands, area-weighted CPUE increased in the 1980s and decreased by 1990. In the Gulf of Alaska, there was no trend in the cooperative survey, but area-weighted CPUE in the domestic survey increased in 1993 and again in 2001. The increasing trend in area-weighted CPUE in the Gulf of Alaska was driven entirely by one standard survey region, Shelikof Trough (Table 1.9; Figure 1.6).

1.4.3. Bootstrapped 95% Confidence Intervals

Analysis of bootstrapped 95% confidence intervals for area-weighted CPUE was also limited to standard survey years (1982–2003), standard survey regions, standard survey stations, standard survey depths, and effective hachis. Bootstrapped 95% confidence intervals were also analyzed separately for the standardized cooperative survey (1982–1994) and the standardized domestic survey (1989–2003). There were insufficient data to calculate bootstrapped 95% confidence intervals for all standard survey regions and regulatory areas each survey year. As a result, analysis of bootstrapped 95% confidence intervals was further limited to the following standard survey regions and regulatory areas with non-zero catches and approximately normally distributed bootstrap replicates (Appendix 1.A): Eastern Bering Sea cooperative survey 1988, 1992–1994 (Figure 1.A.1); Gulf of Alaska total domestic survey 1989–2003 (Figure 1.A.2); Gulf of Alaska domestic survey Shelikof Trough 1992–2003 (Figure 1.A.3); and Gulf of Alaska total domestic survey without Shelikof Trough 1989, 1991, 1995, 1997–2000 (Figure 1.A.4). Results are provided in Tables 1.8 and 1.9 and Figures 1.4 – 1.6. There were insufficient data to calculate bootstrapped 95% confidence intervals for the domestic survey in the eastern Bering Sea during the years 1999, 2001, and 2003; for the cooperative and domestic surveys in the Aleutian Islands from 1982 to 2002; and for the cooperative survey in the Gulf of Alaska from 1982 to 1994 (Tables 1.8 and 1.9; Figures 1.4 – 1.6).

Within the limited time series available to conduct hypothesis testing in the eastern Bering Sea, area-weighted CPUE of Pacific sleeper sharks increased significantly in the cooperative survey between the years 1998 and 1994 (Table 1.10A; Figure 1.4). There were insufficient data to conduct hypothesis testing for the cooperative survey within individual survey regions of the Bering Sea (Table 1.8; Figure 1.5).

Within the limited time series available to conduct hypothesis testing in the Gulf of Alaska, area-weighted CPUE of Pacific sleeper sharks increased significantly in the domestic survey between the years 1989 and 2003, but also decreased significantly between the years 1996 and 1997 (Table 1.10B; Figure 1.4). The largest increases occurred between the years 1992 and 1993 and between the years 2000 and 2001 (Figure 1.4C). As before, the increasing trend in the Gulf of Alaska was driven entirely by one standard survey region, Shelikof Trough. Area-weighted CPUE of Pacific sleeper sharks increased significantly in Shelikof Trough between the years 1992 and 2003, but also decreased significantly in 1997 and again in 2003 (Table 1.10C; Figure 1.6A). There was no trend in area-weighted CPUE of Pacific sleeper sharks in the Gulf of Alaska after Shelikof Trough was removed (Figure 1.6B). Area-weighted CPUE of Pacific sleeper sharks in the Gulf of Alaska after Shelikof Trough was removed increased significantly between the years 1989 and 2000 but also decreased significantly in 1999 (Table 1.10D).

1.5. Discussion

Within the limited time series available for hypothesis testing, area-weighted CPUE of Pacific sleeper sharks increased significantly in the eastern Bering Sea between the years 1988 and 1994 and in the Gulf of Alaska between the years 1989 and 2003, but also decreased significantly in the Gulf of Alaska in 1997. The increasing trend in the Gulf of Alaska was driven entirely by one region, Shelikof Trough, where most (54%) Pacific sleeper sharks were captured.

The main obstacle to conducting hypothesis testing of trends in area-weighted CPUE was the small sample size of Pacific sleeper shark bycatch in sablefish longline surveys. The percentile method (Efron and Tibshirani 1986) requires approximately normally distributed bootstrap replicates. Therefore, we assumed that time series of area-weighted CPUE with approximately normally distributed bootstrap replicates had sufficient data to conduct hypothesis testing of differences in Area-weighted CPUE from bootstrap 95% confidence intervals. Insufficient data existed to compute bootstrap 95% confidence intervals in some standard survey regions and regulatory areas, so hypothesis testing was limited to time series of area-weighted CPUE from selected standard survey regions and regulatory areas with non-zero catches and approximately normally distributed bootstrap replicates (Appendix 1.A).

Increasing trends in area-weighted CPUE of Pacific sleeper sharks in the eastern Bering Sea and Shelikof Trough are consistent with previous analyses of fishery-dependent and fishery-independent data from the northeast Pacific Ocean. These analyses indicate that bycatch of Pacific sleeper sharks in commercial fisheries for groundfish and in fishery-independent bottom trawl surveys have been increasing in the Bering Sea and Gulf of Alaska (Courtney et al. 2006a, 2006b). Mueter and Norcross (2002) conducted a separate analysis of NMFS fishery-independent bottom trawl survey data from the

Gulf of Alaska continental shelf and upper slope from 100 to 500 m depth. The CPUE of Pacific sleeper sharks in bottom trawl surveys increased significantly between the years 1984 and 1996 in two NMFS statistical areas, Chirikof (200–300 m depth), and Kodiak (100–200 m depth; Mueter and Norcross 2002). The Chirikof statistical area includes Shelikof Trough (Figure 1.1). Increasing trends in area-weighted CPUE of Pacific sleeper sharks in the eastern Bering Sea and Shelikof Trough are also consistent with evidence of oceanographic fluctuations or a change in prey composition that began with a climatic regime shift in 1976 and 1977. This regime shift triggered a substantial change in the northeast Pacific Ocean fish community (Hollowed and Wooster 1995). Sleeper shark abundance changes may have taken longer to become apparent than the abundance changes of other species due to sleeper shark's assumed long life, low fecundity, and slow growth rates.

Increasing trends in area-weighted CPUE of Pacific sleeper sharks from sablefish longline surveys may also simply reflect changes in local densities resulting from a shift in distribution. Assumptions required for area-weighted CPUE to represent trends in relative abundance at the population level are that survey effort and the relative area occupied by Pacific sleeper sharks are proportional to the bottom area (km^2) surveyed, that catchability of Pacific sleeper sharks in sablefish longline surveys is constant, and that the area inhabited by Pacific sleeper sharks is constant (Gulland 1969; Quinn et al. 1982). However, the distribution of Pacific sleeper sharks in the eastern Bering Sea, Aleutian Islands, and Gulf of Alaska relative to the area sampled by NMFS sablefish longline surveys is unknown. The catchability of Pacific sleeper sharks with sablefish longline gear is also unknown and may vary depending on factors not accounted for in this study. In particular, the sablefish longline survey is not designed to capture Pacific sleeper sharks, and they have not been captured in large numbers during the history of the survey (Table 1.1). Pacific sleeper sharks are large animals and can be stripped from the gear before being tallied at the surface if the weather is rough or if the gear is hauled too fast. Pacific sleeper sharks may also interact with other species captured on sablefish longline gear through predation or competition for bait. These caveats may explain some of the between-year variability in area-weighted CPUE of Pacific sleeper sharks estimated from Shelikof Trough (Figure 1.6) and the Gulf of Alaska (Figure 1.4C).

Length compositions, age determination, and size and age at maturity of Pacific sleeper sharks are needed to determine if increasing trends in area-weighted CPUE of Pacific sleeper sharks from sablefish longline surveys represent a change in abundance of Pacific sleeper sharks associated with recruitment of a strong year-class. Pacific sleeper sharks are large animals and cannot easily be brought on board commercial fishing and survey vessels for length measurements and specimen collections. As a result, length measurements and collections for age and maturity were not available from sablefish longline surveys. Length of Pacific sleeper sharks from a directed study in the Gulf of Alaska with longline gear

similar to that used in sablefish longline surveys ranged from 130 to 284 cm TL (n = 198; 40% female; years 2001 and 2002; Sigler et al. 2006). Maturity was not reported, but based on the observations from Yano et al. (2007), Pacific sleeper sharks less than 300 cm TL are probably immature. We recommend collection of basic life history information on Pacific sleeper sharks captured in commercial fisheries and longline surveys in the northeast Pacific Ocean to determine if trends in CPUE reflect trends in relative abundance of Pacific sleeper shark at the population level.

Despite these caveats, development of Pacific sleeper shark relative abundance time series along with estimates of uncertainty will foster the determination of sustainable bycatch limits for sharks in the northeast Pacific Ocean. The NMFS Alaska Fisheries Science Center has formed a non-target species working group to improve assessment of non-target species including sharks within NMFS regulatory areas of the BSAI and GOA. The determination of sustainable bycatch limits for non-target species such as sharks is a priority for the non-target species working group (Courtney et al. 2006a, 2006b). Additionally, this study responds to calls for the incorporation of ecosystem considerations into stock assessments of commercial fisheries managed by the NMFS (NRC 1999; Witherell 1999; Witherell et al. 2000; Pikitch et al. 2004). Time series of Pacific sleeper shark relative abundance may prove useful as an ecosystem indicator of predator relative abundance within the BSAI and GOA (Courtney and Sigler 2002; 2003).

1.6. Literature Cited

Benz, G. W., R. Hocking, A. Kowunna Sr., S. A. Bullard, and J. C. George. 2004. A second species of Arctic Shark: Pacific sleeper shark *Somniosus pacificus* from Point Hope, Alaska. Polar Biology 27:250–252.

Bigelow, H. B., and W. C. Schroeder. 1948. Sharks. Pages 59–546 *in* Fishes of the Western North Atlantic. Part 1, Lancelets, Cyclostomes and Sharks. Memorial Sears Foundation for Marine Research, Yale University, New Haven, Connecticut.

Borets, L. A. 1986. Ichthyofauna of the Northwestern and Hawaiian Submarine Ranges. Journal of Ichthyology 26:1–13. Translation UDC 597.591.9 of Voprosy Ikhtiologii 26:208–220.

Bright, H. B. 1959. The occurrence and food of the sleeper shark, *Somniosus pacificus*, in a central Alaska bay. Copeia 1:76–77.

Compagno, L. J. V. 1984. FAO species catalogue. Vol. 4. Sharks of the world. An annotated and illustrated catalogue of shark species known to date. Part 1- Hexanchiformes to Lamniformes. FAO Fisheries Synopsis 125. United Nations Development Programme. Food and Agriculture Organization of the United Nations, Rome, Italy.

Courtney, D., and M. F. Sigler. 2002. A new analysis of Pacific sleeper shark (*Somniosus pacificus*) abundance trends. Pages 98–108 *in* Stock assessment and fishery evaluation report, ecosystem considerations for 2003. North Pacific Fishery Management Council, 605 W 4th Ave, Suite 306, Anchorage, AK 99501.

Courtney, D., and M. F. Sigler. 2003. Analysis of Pacific sleeper shark (*Somniosus pacificus*) abundance trends from sablefish longline surveys 1979 – 2003. Pages 155–169 *in* Stock assessment and fishery evaluation report, ecosystem considerations for 2004. North Pacific Fishery Management Council, 605 W 4th Ave, Suite 306, Anchorage, AK 99501.

Courtney, D., C. Tribuzio, and K. J. Goldman. 2006a. BSAI Sharks. Pages 1,083–1,132 *in* Stock assessment and fishery evaluation report for the groundfish resources of the Bering Sea and Aleutian Islands for 2007. North Pacific Fishery Management Council, 605 W 4th Ave, Suite 306, Anchorage, AK 99501.

Courtney, D., C. Tribuzio, K. J. Goldman, and J. Rice. 2006b. GOA Sharks. Pages 481–561 *in* Stock assessment and fishery evaluation report for the groundfish resources of the Gulf of Alaska for 2007. North Pacific Fishery Management Council, 605 W 4th Ave, Suite 306, Anchorage, AK 99501.

Crovetto, A., J. Lamilla, and G. Pequeno. 1992. *Lissodelphis peronii*, Lacepede 1804 (Delphinidae Cetacea) within the stomach contents of a sleeping shark *Somniosus* cf. *pacificus* Bigelow and Schroeder 1944, in Chilean waters. Marine Mammal Science 8:312–314.

Ebert, D. A., L. J. V. Compagno, and L. J. Natanson. 1987. Biological notes on the Pacific sleeper shark, *Somniosus pacificus* (Chondrichthyes: Squalidae). California Fish and Game 73:117–123.

Efron, B. 1982. The jacknife, the bootstrap, and other resampling plans. Society for Industrial and Applied Mathematics, Applied Mathematics 38.

Efron, B., and R. Tibshirani. 1986. Bootstrap methods for standard errors, confidence intervals, and other measures of statistical accuracy. Statistical Science 1:54–75.

Frid, A., G. G. Baker, and L. M. Dill. 2006. Do resource declines increase predation rates on North Pacific harbor seals? A behavior-based plausibility model. Marine Ecology Progress Series 312:265–275.

Frid, A., G. G. Baker, and L. M. Dill. 2008. Do shark declines create fear-released systems? Oikos.

Frid, A., L. M. Dill, R. E. Thorne, and G. M. Blundell. 2007a. Inferring prey perception of relative danger in large-scale marine systems. Evolutionary Ecology Research 9:635–649.

Frid, A., M. R. Heithaus, and L. M. Dill. 2007b. Dangerous dive cycles and the proverbial ostrich. Oikos 116:893–902.

Gotshall, D. W., and T. Jow. 1965. Sleeper sharks (*Somniosus pacificus*) off Trinidad, California, with life history notes. California Fish and Game 51:294–298.

Gulland, J. A. 1969. Manual of methods for fish stock assessment. Part 1. Fish population analysis. St. Paul's Press Ltd., Malta, Italy.

Gunderson, D. R.1993. Surveys of fisheries resources. John Wiley and Sons, New York, New York.

Hart J. L. 1973. Pacific fishes of Canada. Bulletin of the Fisheries Research Board of Canada 180.

Hollowed, A. B., and W. S. Wooster. 1995. Decadal-scale variations in the eastern subarctic Pacific: II. Response of Northeast Pacific fish stocks. Pages 373–385 *in* R. J. Beamish, editor. Climate change and northern fish populations. Canadian Special Publication in Fisheries and Aquatic Science 121.

Hulbert, L. B., M. F. Sigler, and C. R. Lunsford. 2006. Depth and movement behavior of the Pacific sleeper shark in the north-east Pacific Ocean. Journal of Fish Biology 69:406–425.

Kimura, D. K., and J. W. Balsiger. 1985. Bootstrap methods for evaluating sablefish pot index surveys. North American Journal of Fisheries Management 5:47–56.

Kimura, D. K., and D. A. Somerton. 2006. Review of statistical aspects of survey sampling for marine fisheries. Reviews in Fisheries Science 14:245–283.

Kimura, D. K., and H. H. Zenger, Jr. 1997. Standardizing sablefish (*Anoplopoma fimbria*) long-line survey indices by modeling the log-ratio of paired comparative fishing CPUEs. ICES Journal of Marine Science 54:48–59.

McMeans, B. C., K. Borga, W. R. Bechtol, D. Higginbotham, and A. T. Fisk. 2007. Essential and non-essential element concentrations in two sleeper shark species collected in arctic waters. Environmental Pollution 148:281–290.

Mecklenburg, C. W., T. A. Mecklenburg, and L. K. Thorsteinson. 2002. Fishes of Alaska. American Fisheries Society. Bethesda, Maryland.

Mueter, F. J., and B. L. Norcross. 2002. Spatial and temporal patterns in the demersal fish community on the shelf and upper slope regions of the Gulf of Alaska. Fishery Bulletin 100:559–581.

National Research Council (NRC). 1999. Sustaining marine fisheries. National Academy Press, Washing, D.C.

National Research Council (NRC). 2003. The decline of Steller sea lions in Alaskan waters: Untangling food webs and fishing nets. National Academy Press, Washington, D.C.

Orlov, A. M. 1999. Capture of especially large sleeper shark *Somniosus pacificus* (Squalidae) with some notes on its ecology in the northwestern Pacific. Journal of Ichthyology 39:548–553.

Pikitch, E. K. and 16 coauthors. 2004. Ecosystem-based fishery management. Science 305:346–347.

Quinn, T. J. II, S. H. Hoag, and G. M. Southward. 1982. Comparison of two methods of combining catch-per-unit-effort data from geographic regions. Canadian Journal of Fisheries and Aquatic Sciences 39:837–846.

Sasaki, T. 1985. Studies on the sablefish resources in the North Pacific Ocean. Far Seas Fisheries Research Laboratory Bulletin 22:1–108. Fishery Agency of Japan, Shimizu.

Sigler, M. F., and J. T. Fujioka. 1988. Evaluation of variability in sablefish, *Anoplopoma fimbria,* abundance indices in the Gulf of Alaska using the bootstrap method. Fishery Bulletin 86:445–452.

Sigler, M. F., L. B. Hulbert, C. R. Lunsford, N. H. Thompson, K. Burek, G. O'Corry-Crowe, and A. C. Hirons. 2006. Diet of Pacific sleeper sharks, a potential Steller sea lion predator, in the northeast Pacific Ocean. Journal of Fish Biology 69:392–405.

Sigler, M. F., and H. H. Zenger, Jr. 1989. Assessment of Gulf of Alaska sablefish and other groundfish based on the domestic longline survey, 1987. U.S. Department of Commerce NOAA Technical Memorandum NMFS F/NWC-169.

Smith, C. R., and A. R. Baco. 2003. Ecology of whale falls at the deep-sea floor. Oceanography and Marine Biology: an Annual Review 41:311–354.

Taggart, S. J., A. G. Andrews, J. Mondragon, and E. A. Mathews. 2005. Co-occurrence of Pacific sleeper sharks *Somniosus pacificus* and harbor seals *Phoca vitulina* in Glacier Bay. Alaska Fishery Research Bulletin 11:113–117.

Wang, J. W., and S.-C. Yang. 2004. First records of Pacific sleeper sharks (*Somniosus pacificus* Bigelow and Schroeder, 1944) in the subtropical waters of Eastern Taiwan. Bulletin of Marine Science. 74:229–235.

Witherell, D. 1999. Incorporating ecosystem considerations into management of Bering Sea groundfish stocks. Pages 315–328 *in* Ecosystem approaches for fisheries management. University of Alaska Sea Grant, AK-SG-99-01, Fairbanks.

Witherell, D., C. Pautzke, and D. Fluharty. 2000. An ecosystem-based approach for Alaska groundfish fisheries. ICES Journal of Marine Science 57:771–777.

Yang, M.-S., and B. N. Page. 1999. Diet of Pacific sleeper shark, *Somniosus pacificus,* in the Gulf of Alaska. Fishery Bulletin 97:406–409.

Yano, K., J. D. Stevens, and L. J. V. Compagno. 2004. A review of the systematics of the sleeper shark genus *Somniosus* with redescriptions of *Somniosus* (*Somniosus*) *antarcticus* and *Somniosus* (*Rhinoscymnus*) *longus* (Squaliformes: Somniosidae). Ichthyological Research 51:360–373.

Yano, K., J. D. Stevens, and L. J. V. Compagno. 2007. Distribution, reproduction and feeding of the Greenland shark *Somniosus* (*Somniosus*) *microcephalus*, with notes on two other sleeper sharks, *Somniosus* (*Somniosus*) *pacificus* and *Somniosus* (*Somniosus*) *antarcticus.* Journal of Fish Biology 70:374–390.

Zenger, Jr. H. H. 1997. Comparisons of sablefish, *Anoplopoma fimbria*, abundance indices estimated from two longline surveys. Pages 215–228 *in* M. Saunders and M. Wilkins, editors. Biology and Management of sablefish, *Anoplopoma fimbria*. U.S. Department of Commerce NOAA Technical Report NMFS 130.

Zenger, Jr. H. H., and M. F. Sigler. 1992. Relative abundance of Gulf of Alaska sablefish and other groundfish based on National Marine Fisheries Service longline surveys, 1988–90. U.S. Department of Commerce NOAA Technical Memorandum NMFS F/NWC-216.

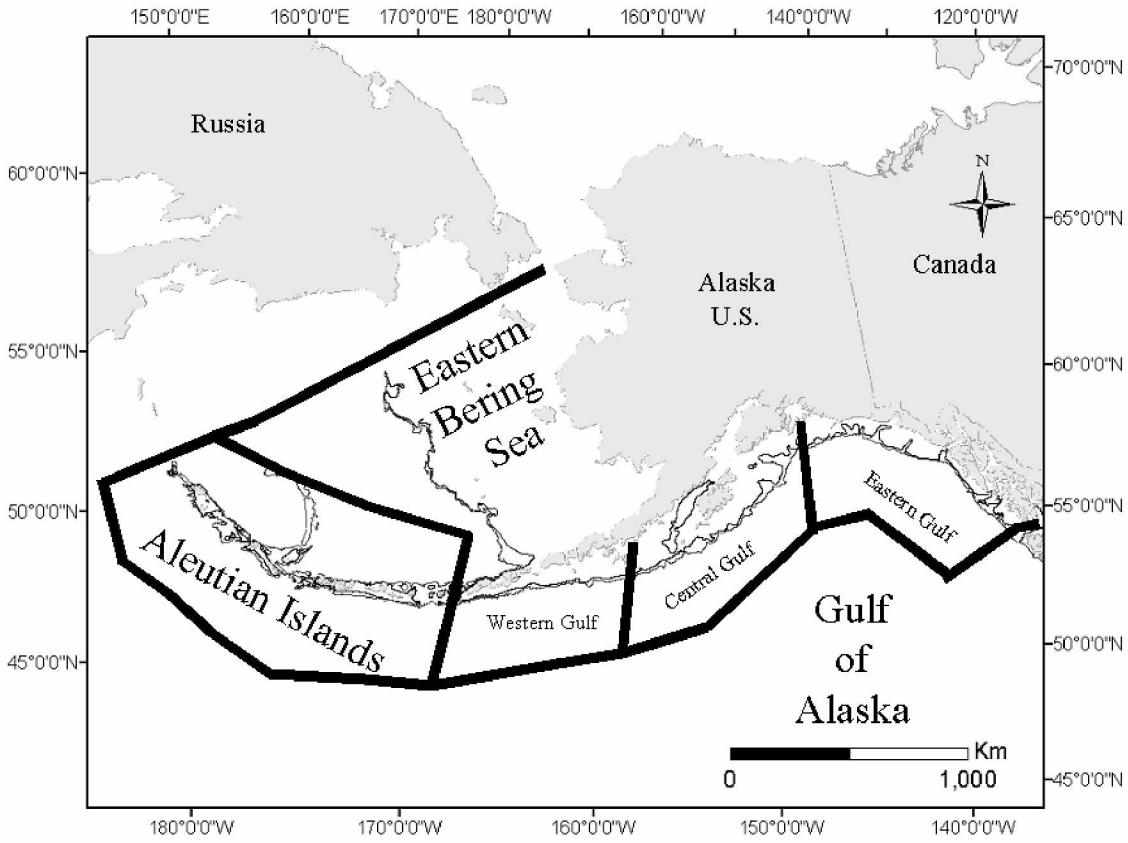

Figure 1.1: Map of the study location.
Sablefish longline surveys sampled the continental shelf break and upper continental slope of Alaskan marine waters in the northeast Pacific Ocean between the 200 and 1,000 m contour intervals outlined in black.

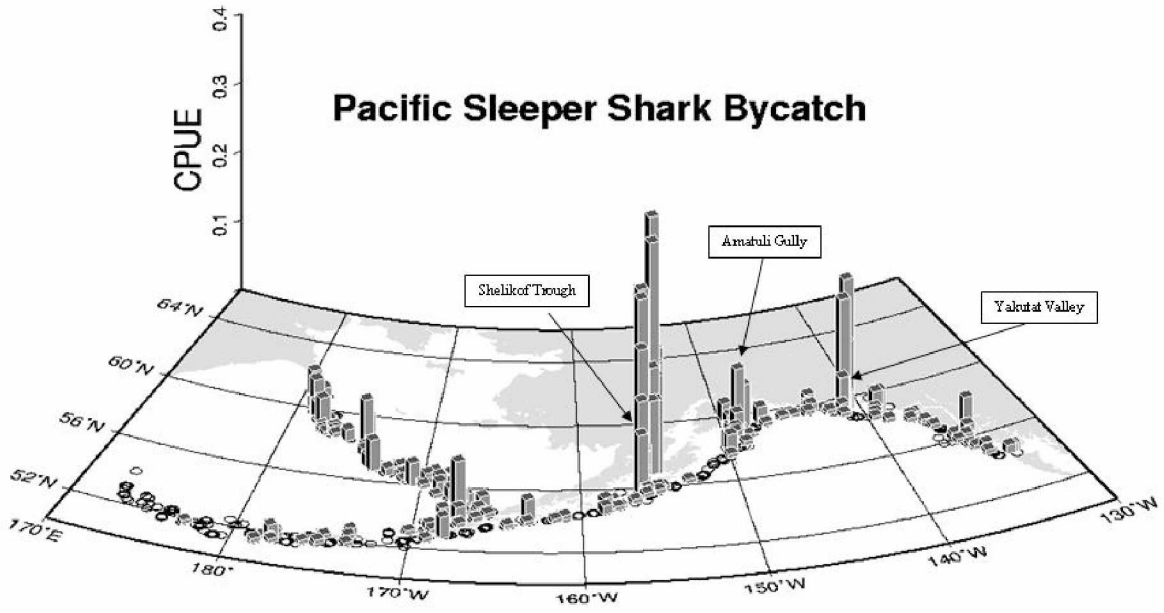

Figure 1.2: Map of Pacific sleeper shark CPUE from sablefish longline surveys.
CPUE of Pacific sleeper sharks from sablefish longline surveys in the northeast Pacific Ocean during the years 1979–2003; Empty circles represent stations fished where no sharks were caught.

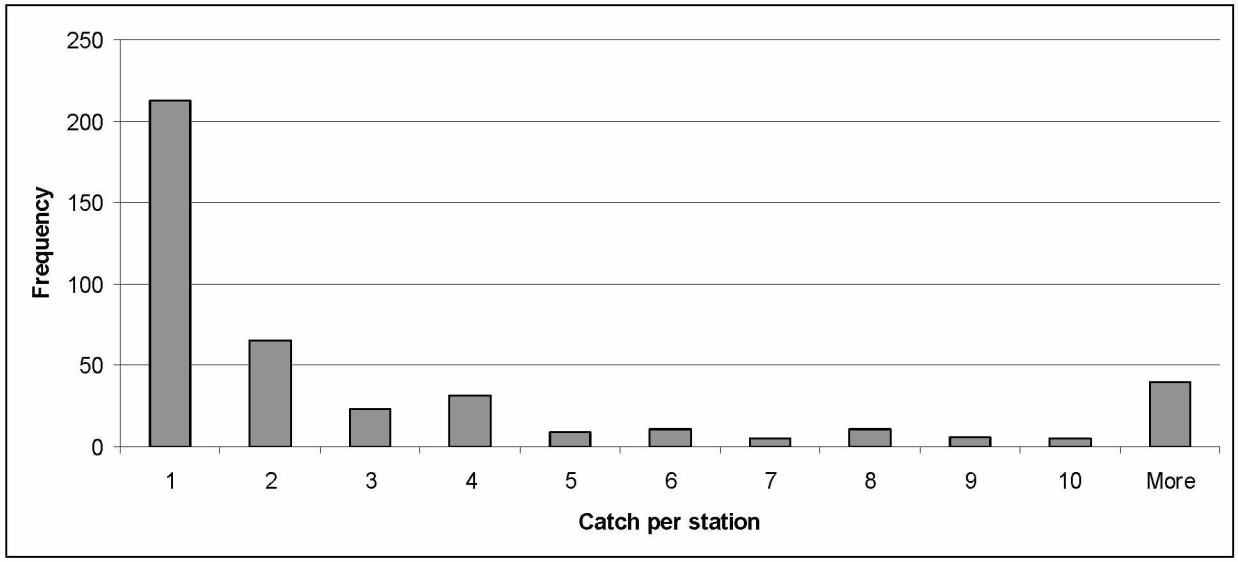

Figure 1.3: Pacific sleeper shark positive catch per station.
Pacific sleeper shark positive catch per station in sablefish longline surveys in the northeast Pacific Ocean during the years 1979–2003 from 419 stations with sleeper shark catches out of 3,001 stations fished.

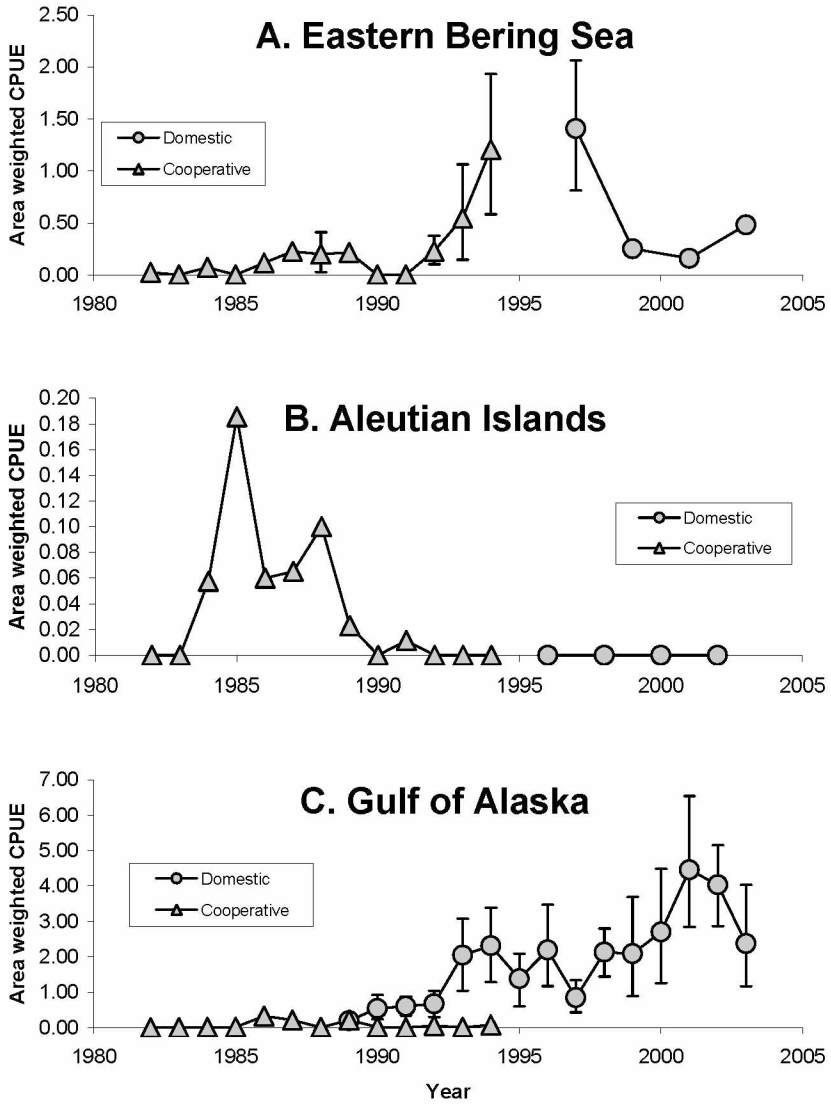

Figure 1.4: Area-weighted CPUE of Pacific sleeper sharks from sablefish longline surveys.
Area-weighted CPUE of Pacific sleeper sharks from standardized sablefish longline surveys (cooperative survey 1982–1994, and domestic survey 1989–2003) in the eastern Bering Sea (A), Aleutian Islands (B), and Gulf of Alaska (C) with bootstrap 95% confidence intervals for time series with sufficient data.

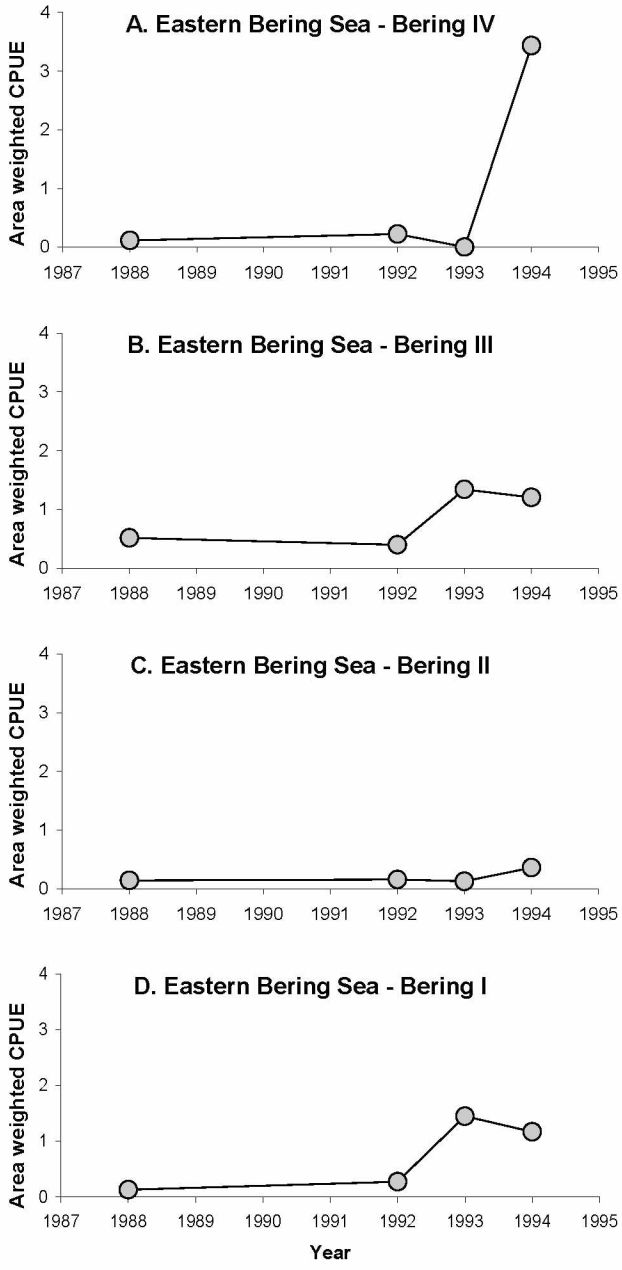

Figure 1.5: Area-weighted CPUE in the eastern Bering Sea.
Area-weighted CPUE of Pacific sleeper sharks from the standardized cooperative sablefish longline survey (1988, 1992–1994) in the eastern Bering Sea by standard survey region; Bering IV (A), Bering III (B), Bering II (C), and Bering I (D).

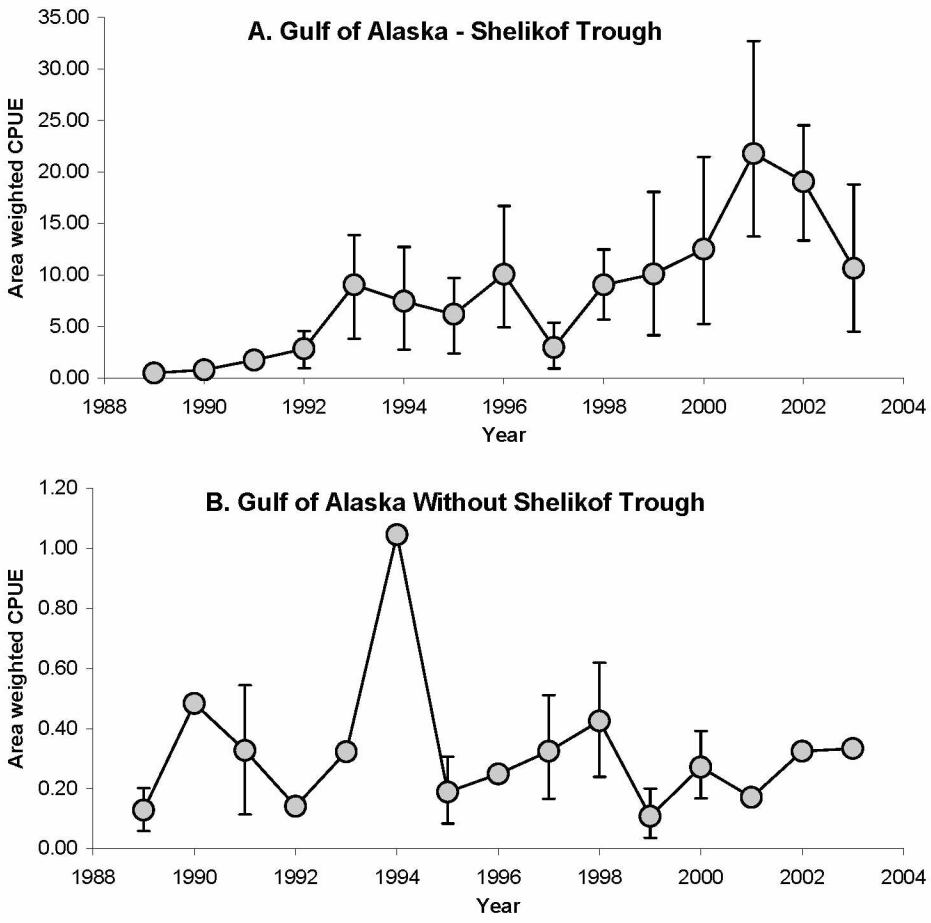

Figure 1.6: Area-weighted CPUE in the Gulf of Alaska.
Area-weighted CPUE of Pacific sleeper sharks from the standardized domestic sablefish longline survey (1989–2003) in Shelikof Trough (A) and in the combined Gulf of Alaska (Western, Central, and Eastern) with Shelikof Trough removed (B) with bootstrap 95% confidence intervals for time series with sufficient data.

Table 1.1: CPUE of Pacific sleeper sharks from sablefish longline surveys by year.
CPUE of Pacific sleeper sharks from sablefish longline surveys by year (1979–2003) for all survey stations, all survey regions, all survey depths, and all hachis fished.

Year [a]	Number of sleeper sharks	Number of stations fished	Number of hachis [b] fished	Number of hooks fished	Catch per hachi (CPUE)×100
1979	0	57	8,069	363,105	0.00
1980	1	75	11,153	501,885	0.01
1981	1	75	11,469	516,105	0.01
1982	1	108	16,950	762,750	0.01
1983	0	104	16,344	735,480	0.00
1984	5	108	17,139	771,255	0.03
1985	10	107	17,062	767,790	0.06
1986	9	107	16,959	763,155	0.05
1987	27	107	16,844	757,980	0.16
1988	21	165	25,909	1,165,905	0.08
1989	45	184	26,980	1,214,100	0.17
1990	33	195	28,572	1,285,740	0.12
1991	34	190	28,192	1,268,640	0.12
1992	74	194	28,728	1,292,760	0.26
1993	110	195	28,749	1,293,705	0.38
1994	175	190	29,415	1,323,675	0.59
1995	61	81	11,176	502,920	0.55
1996	86	94	12,281	552,645	0.70
1997	103	137	13,920	626,400	0.74
1998	91	87	12,030	541,350	0.76
1999	93	89	12,475	561,375	0.75
2000	111	87	11,895	535,275	0.93
2001	176	89	12,423	559,035	1.42
2002	169	87	11,761	529,245	1.44
2003	129	89	12,403	558,135	1.04
Total	1,565	3,001	438,898	19,750,410	

[a] Sablefish longline survey time-line:
1979—First year of Japan-U.S. cooperative sablefish longline survey;
1982— First year of Japan-U.S. cooperative survey in the eastern Bering Sea;
1982— First year of standardized Japan-U.S. cooperative survey in the eastern Bering Sea, Aleutian Islands, and Gulf of Alaska;
1987—Experimental domestic sablefish longline survey in the Gulf of Alaska (using herring as bait);
1988—First year of experimental domestic sablefish longline survey in the Gulf of Alaska (using squid as bait);
1989—First year of standardized domestic sablefish longline survey. Also, first year of additional gully stations in the Gulf of Alaska;
1994—Last year of standardized Japan-U.S. cooperative sablefish longline survey in the Gulf of Alaska;
1996—First year of standardized domestic sablefish longline survey in the Aleutian Islands (Aleutians sampled every other year thereafter);
1997—First year of standardized domestic sablefish longline survey in the eastern Bering Sea (eastern Bering Sea sampled every other year thereafter); also, experimental fishing alongside a submersible in the Gulf of Alaska;
[b] a hachi is a standardized 100 m section of longline containing 45 hooks spaced 2 m apart with 5 m between each end of the line and the nearest hook; 160 hachis were tied together and deployed at each station on the Gulf of Alaska slope and Aleutian Island slope; 180 hachis were deployed per station on the eastern Bering Sea slope and 80 hachis were deployed per station on Gulf of Alaska gullies; upon retrieval of the gear, catch was recorded per hachi; the number of hooks listed here is extrapolated as 45 times the number of hachis retrieved.

Table 1.2: CPUE of Pacific sleeper sharks by depth strata.
CPUE of Pacific sleeper sharks from sablefish longline surveys by depth strata for all survey years (1979–2003), all survey stations, all survey regions, all survey depths, and all hachis fished.

Depth Strata[a]	Depth (meters)		Number of sleeper sharks	Percent of total number	Number of stations fished	Number of hachis fished	Number of hooks fished	Catch per hachi (CPUE) *100
	Min	Max						
Unknown	NA	NA	3	0.19%	NA	NA	NA	NA
1	0	100	0	0.00%	126	1,550	69,750	0.00
2	101	200	115	7.35%	1,835	84,704	3,811,680	0.14
3	201	300	1,042	66.58%	2,604	80,313	3,614,085	1.30
4	301	400	89	5.69%	2,354	50,833	2,287,485	0.18
5	401	600	152	9.71%	2,320	103,353	4,650,885	0.15
6	601	800	133	8.50%	2,059	90,053	4,052,385	0.15
7	801	1,000	31	1.98%	1,304	26,604	1,197,180	0.12
8	1,001	1,200	0	0.00%	144	1,429	64,305	0.00
9	1,200	Greater	0	0.00%	4	59	2,655	0.00
Total			1,565	100%	3,001[b]	438,898	19,750,410	

[a] Depth strata 1, 2, 8 and 9 are not effectively sampled by the sablefish longline surveys and are not included in standardized sablefish longline survey CPUE; the sablefish longline surveys (both cooperative and domestic) set gear from shallow to deep to cover the 201 to 1,000 m depths along the continental shelf break and upper continental slope of the northeast Pacific Ocean as well as some deep-water gullies (> 200 m) on the shelf break of the Gulf of Alaska. Some hooks landed in shallower and deeper depths (0 – 200 m, and > 1,000 m);
[b] a total of 3,001 stations were fished, but all depth strata were not fished in at each station because of differences in the bottom contour.

Table 1.3: CPUE of Pacific sleeper sharks by survey region.
CPUE of Pacific sleeper sharks from sablefish longline surveys by survey region for all survey years (1979–2003), all survey stations, all survey regions, all survey depths, and all hachis fished.

Survey region **Regulatory area** - Slope stations - Gully stations	Number of sleeper sharks	Percent of total number	Number of stations fished	Number of hachis fished	Number of hooks fished	Catch per hachi (CPUE)×100
- NA	1	0.1%	NA	640	28,800	0.16
Eastern Bering Sea						
- Bering V [a]	51	3.3%	45	7,400	333,000	0.69
- Bering IV	77	4.9%	94	15,468	696,060	0.50
- Bering III	61	3.9%	137	22,454	1,010,430	0.27
- Bering II	75	4.8%	200	32,333	1,454,985	0.23
- Bering I	62	4.0%	87	13,963	628,335	0.44
Aleutian Islands						
- NW Aleutians	0	0.0%	61	9,687	435,915	0.00
- SW Aleutians	1	0.1%	89	13,901	625,545	0.01
- NE Aleutians	11	0.7%	142	20,941	942,345	0.05
- SE Aleutians	12	0.8%	169	25,828	1,162,260	0.05
Western Gulf of Alaska						
- Shumagin	35	2.2%	321	50,562	2,275,290	0.07
- Shumagin Gully [a]	2	0.1%	16	1,453	65,385	0.14
Central Gulf of Alaska						
- Chirikof	44	2.8%	222	35,551	1,599,795	0.12
- West Semidi [a]	0	0.0%	1	160	7,200	0.00
- Shelikof Trough	850	54%	124	10,313	464,085	8.24
Kodiak	6	0.4%	288	45,985	2,069,325	0.01
- Chiniak Gully [a]	0	0.0%	1	159	7,155	0.00
- Amatuli Gully	71	4.5%	116	11,994	539,730	0.59
Eastern Gulf of Alaska						
West Yakutat	13	0.8%	259	41,209	1,854,405	0.03
- Western Grounds	5	0.3%	30	2,418	108,810	0.21
- Yakutat Valley	104	6.6%	30	2,416	108,720	4.30
East Yakutat	20	1.3%	94	14,841	667,845	0.13
- Alsek Strath [a]	13	0.8%	12	960	43,200	1.35
Southeast Alaska	19	1.2%	280	43,535	1,959,075	0.04
- Spencer Gully	1	0.1%	31	2,578	116,010	0.04
- Southeastern Shelf [a]	1	0.1%	32	4,910	220,950	0.02
- Southeastern [a]	0	0.0%	48	1,440	64,800	0.00
- Ommaney Trench	21	1.3%	30	2,417	108,765	0.87
- Iphigenia Gully [a]	0	0.0%	12	966	43,470	0.00
- Dixon Entrance	9	0.6%	30	2,416	108,720	0.37
Gulf of Alaska sub-total, slope stations	137	8.8%	1,464	231,683	10,425,735	0.06
Gulf of Alaska sub-total, gully stations	1,077	69%	513	44,600	2,007,000	2.41
Gulf of Alaska sub-total	1,214	78%	1,977	276,283	12,432,735	0.44
Grand total	1,565	100%	3,001	438,898	19,750,410	

[a] Experimental or discontinued survey regions.

Table 1.4: Cooperative and domestic survey fixed station locations.
Number of fixed station locations in the survey designs of the standardized cooperative sablefish longline survey (1982–1994) and the standardized domestic sablefish longline survey (1989–2003).

Survey region	Number of standard survey stations		Longitude	
Regulatory area				
- Slope stations	Cooperative survey	Domestic survey		
- Gully stations	1982–1994	1989–2003	Maximum	Minimum
Eastern Bering Sea				
- Bering V [a]	-	-	178° 51.3' W	177° 22.8' W
- Bering IV	6	4	177° 34.9' W	174° 18.0' W
- Bering III	8	5	174° 13.9' W	170° 34.3' W
- Bering II	12	4	169° 57.0' W	166° 1.8' W
- Bering I	5	3	169° 15.0' W	165° 40.0' W
Aleutian Islands				
- NW Aleutians	4	-	179° 55.0' E	172° 43.0' E
- SW Aleutians	6	-	179° 34.0' E	172° 57.4' E
- NE Aleutians	8	6	177° 35.0' W	170° 8.5' W
- SE Aleutians	9	8	178° 36.6' W	173° 30.3' W
Western Gulf of Alaska				
- Shumagin	10	10	169° 5.9' W	159° 52.7' W
- Shumagin Gully [a]	-	-	158° 30.4' W	158° 0.4' W
Central Gulf of Alaska				
- Chirikof	7	7	158° 33.4' W	154° 47.8' W
- West Semidi [a]	-	-	157° 30.3' W	157° 30.3' W
- Shelikof Trough	-	8	156° 13.7' W	155° 2.4' W
- Kodiak	9	9	153° 4.9' W	148° 20.4' W
- Chiniak Gully [a]	-	-	151° 41.9' W	151° 41.9' W
- Amatuli Gully	1	9	149° 54.7' W	146° 58.6' W
Eastern Gulf of Alaska				
- West Yakutat	8	8	146° 51.3' W	141° 20.0' W
- Western Grounds	-	2	143° 35.7' W	143° 23.3' W
- Yakutat Valley	-	2	141° 16.2' W	140° 56.2' W
- East Yakutat	3	3	139° 29.0' W	137° 22.4' W
Alsek Strath [a]	-	-	139° 20.1' W	139° 5.0' W
- Southeast Outside	8	8	136° 32.4' W	133° 55.1' W
- Spencer Gully	-	2	137° 5.32' W	137° 5.3' W
- Southeastern Shelf [a]	-	-	135° 24.0' W	135° 24.0' W
- Southeastern [a]	-	-	136° 17.8' W	136° 6.6' W
- Ommaney Trench	-	2	134° 58.6' W	134° 54.2' W
- Iphigenia Gully [a]	-	-	134° 40.2' W	134° 24.4' W
- Dixon Entrance	-	2	133° 9.2' W	132° 50.6' W

[a] Experimental or discontinued survey regions.

Table 1.5: Cooperative survey station locations fished successfully by region.
Number of fixed station locations fished successfully (number of stations with sleeper shark catches; and number of sleeper sharks captured) during the standardized cooperative sablefish longline survey (1982–1994). Stations were excluded from computation of area-weighted CPUE for the standardized sablefish longline surveys if they had whale predation on the gear, competition with other fishing vessels, or excessive loss of gear.

Survey region	Year													
Regulatory area														
- Slope stations														
- Gully stations	1982	1983	1984	1985	1986	1987	1988	1989	1990	1991	1992	1993	1994	Total
Bering Sea														
- Bering IV	6(0;0)	4(0;0)	4(0;0)	6(0;0)	6(0;0)	5(1;1)	5(1;1)	4(1;1)	4(0;0)	4(0;0)	4(2;2)	4(0;0)	4(4;24)	60(9;29)
- Bering III	8(0;0)	7(0;0)	5(0;0)	8(0;0)	7(0;0)	7(2;3)	7(1;2)	7(2;2)	3(0;0)	4(0;0)	6(4;5)	6(3;7)	6(4;15)	81(16;34)
- Bering II	12(0;0)	8(0;0)	9(1;1)	10(0;0)	10(1;1)	11(2;5)	12(2;3)	12(0;0)	9(0;0)	6(0;0)	12(3;3)	12(2;4)	12(3;7)	135(14;24)
- Bering I	5(1;1)	5(0;0)	5(1;1)	5(0;0)	5(0;0)	5(0;0)	5(1;1)	5(1;1)	5(0;0)	4(0;0)	5(2;2)	5(2;6)	5(2;2)	64(10;14)
Aleutian Islands														
- NW Aleutians	4(0;0)	4(0;0)	4(0;0)	4(0;0)	4(0;0)	4(0;0)	4(0;0)	4(0;0)	4(0;0)	4(0;0)	4(0;0)	4(0;0)	4(0;0)	52(0;0)
- SW Aleutians	6(0;0)	5(0;0)	6(0;0)	6(1;1)	6(0;0)	6(0;0)	6(0;0)	6(0;0)	6(0;0)	6(0;0)	6(0;0)	6(0;0)	6(0;0)	77(1;1)
- NE Aleutians	8(0;0)	7(0;0)	8(1;1)	8(1;1)	8(1;2)	8(1;1)	8(2;2)	6(1;1)	7(0;0)	8(0;0)	8(0;0)	8(0;0)	8(0;0)	100(7;8)
- SE Aleutians	9(0;0)	8(0;0)	9(1;1)	9(1;3)	8(0;0)	8(1;1)	9(2;2)	9(0;0)	9(0;0)	9(1;1)	9(0;0)	9(0;0)	9(0;0)	114(6;8)
Western Gulf of Alaska														
- Shumagin	10(0;0)	10(0;0)	10(0;0)	10(1;1)	10(1;1)	10(3;8)	10(0;0)	9(0;0)	10(0;0)	10(0;0)	10(0;0)	10(0;0)	10(0;0)	129(5;10)
Central Gulf of Alaska														
- Chirikof	7(0;0)	7(0;0)	7(1;1)	7(0;0)	7(0;0)	7(1;2)	7(1;1)	7(0;0)	7(0;0)	7(0;0)	7(1;1)	7(0;0)	7(1;1)	91(5;6)
- Kodiak	9(0;0)	9(0;0)	9(0;0)	8(0;0)	9(0;0)	9(0;0)	9(0;0)	9(0;0)	9(0;0)	9(0;0)	9(0;0)	9(0;0)	9(0;0)	116(0;0)
- Amatuli Gully	1(0;0)	1(0;0)	1(0;0)	1(0;0)	1(1;1)	1(0;0)	1(0;0)	1(1;1)	1(0;0)	1(0;0)	1(0;0)	1(0;0)	1(0;0)	13(2;2)
Eastern Gulf of Alaska														
- West Yakutat	8(0;0)	8(0;0)	8(0;0)	8(0;0)	8(0;0)	8(2;2)	8(0;0)	8(1;1)	8(0;0)	8(0;0)	8(1;1)	8(0;0)	8(0;0)	104(4;4)
- East Yakutat	3(0;0)	3(0;0)	3(0;0)	3(0;0)	3(0;0)	3(2;2)	3(0;0)	3(1;1)	3(1;1)	3(0;0)	3(0;0)	3(2;2)	3(1;1)	39(7;7)
- Southeast Outside	8(0;0)	8(0;0)	8(0;0)	8(0;0)	8(0;0)	8(0;0)	8(0;0)	8(0;0)	8(0;0)	8(0;0)	8(0;0)	8(0;0)	8(0;0)	104(0;0)
	104	94	96	101	100	100	102	98	93	91	100	100	100	1,279
Grand total	(1;1)	(0;0)	(5;5)	(4;6)	(4;5)	(15;25)	(10;12)	(8;8)	(1;1)	(1;1)	(13;14)	(9;19)	(15;50)	(86;147)

Table 1.6: Domestic survey station locations fished successfully by region.
Number of fixed station locations fished successfully (number of stations with sleeper shark catches; and number of sleeper sharks captured) during the standardized domestic sablefish longline survey (1989 – 2003). Stations were excluded from computation of area-weighted CPUE for the standardized sablefish longline surveys if they had whale predation on the gear, competition with other fishing vessels, or excessive loss of gear.

Survey region	Year															
Regulatory area																
- Slope stations																
- Gully stations	1989	1990	1991	1992	1993	1994	1995	1996	1997	1998	1999	2000	2001	2002	2003	Total
Bering Sea																
- Bering IV									4(4;12)		4(1;6)		2(1;1)		3(1;1)	13(7;20)
- Bering III									5(4;9)		3(1;1)		3(1;1)		3(1;1)	14(7;12)
- Bering III									4(4;11)		3(1;1)		4(0;0)		3(1;2)	14(6;14)
- Bering I									3(3;17)		2(1;1)		3(1;2)		2(1;5)	10(6;25)
Aleutian Islands																
- NE Aleutians										6(0;0)		6(0;0)		6(0;0)		18(0;0)
- SE Aleutians								8(0;0)		8(0;0)		8(0;0)		8(0;0)		32(0;0)
Western Gulf of Alaska																
- Shumagin	10(0;0)	10(1;6)	10(1;4)	10(0;0)	10(3;4)	10(1;1)	10(0;0)	10(0;0)	10(0;0)	10(2;2)	10(0;0)	10(0;0)	10(0;0)	8(0;0)	7(0;0)	145(8;17)
Central Gulf of Alaska																
- Chirikof	7(1;2)	7(0;0)	7(1;1)	7(0;0)	7(0;0)	7(1;1)	7(0;0)	7(1;1)	7(1;1)	7(1;2)	7(1;1)	7(1;1)	7(1;3)	7(2;4)	7(0;0)	105(11;17)
- Shelikof Trough	8(3;3)	8(1;5)	8(6;11)	8(5;17)	8(7;53)	8(6;43)	8(7;40)	8(7;64)	8(5;18)	8(8;53)	8(8;61)	8(7;77)	8(8;125)	8(8;101)	8(8;49)	120(94;720)
- Kodiak	9(0;0)	9(0;0)	9(0;0)	9(0;0)	9(0;0)	9(0;0)	9(1;1)	9(0;0)	9(0;0)	9(0;0)	9(0;0)	9(2;2)	9(2;2)	9(0;0)	9(0;0)	135(5;5)
- Amatuli Gully	3(0;0)	3(3;5)	3(2;3)	3(1;2)	3(1;4)	3(3;18)	9(4;7)	9(0;0)	9(3;4)	9(6;10)	9(3;4)	9(1;1)	9(0;0)	9(0;0)	9(0;0)	99(27;58)
Eastern Gulf of Alaska																
- West Yakutat	8(2;2)	8(0;0)	8(1;1)	8(0;0)	8(0;0)	8(0;0)	8(1;1)	8(1;1)	8(1;1)	8(0;0)	8(0;0)	8(2;2)	8(0;0)	8(0;0)	8(0;0)	120(8;8)
- Western Grounds	2(0;0)	2(0;0)	2(0;0)	2(1;1)	2(1;1)	2(0;0)	2(0;0)	2(0;0)	2(0;0)	2(0;0)	2(0;0)	2(1;1)	2(0;0)	2(0;0)	2(0;0)	30(3;3)
- Yakutat Valley	2(2;6)	2(1;8)	2(1;4)	2(1;1)	2(1;2)	2(0;0)	2(2;2)	2(1;16)	2(2;12)	2(2;6)	2(1;1)	2(2;7)	2(1;7)	2(2;10)	2(2;14)	30(21;96)
- East Yakutat	3(0;0)	3(0;0)	3(1;2)	3(1;1)	3(1;1)	3(0;0)	3(0;0)	3(0;0)	3(1;1)	3(1;1)	3(0;0)	3(2;5)	3(0;0)	3(1;1)	3(0;0)	45(8;12)
- Southeast Outside	8(1;1)	8(0;0)	8(0;0)	8(0;0)	8(0;0)	8(1;1)	8(0;0)	8(0;0)	8(1;1)	8(2;2)	8(0;0)	8(0;0)	8(0;0)	8(0;0)	8(4;11)	120(9;16)
- Spencer Gully	2(0;0)	2(0;0)	2(0;0)	2(0;0)	2(0;0)	2(0;0)	2(1;1)	2(0;0)	2(0;0)	2(0;0)	2(0;0)	2(0;0)	2(0;0)	2(0;0)	2(0;0)	30(1;1)
- Ommaney Trench	2(0;0)	2(0;0)	2(0;0)	2(0;0)	2(0;0)	2(1;1)	2(0;0)	2(0;0)	2(0;0)	2(1;2)	2(1;2)	2(2;6)	2(1;1)	2(2;3)	2(1;6)	30(9;21)
- Dixon Entrance	2(0;0)	2(0;0)	2(0;0)	2(0;0)	2(0;0)	2(0;0)	2(1;1)	2(1;1)	2(1;1)	2(1;1)	2(0;0)	2(1;1)	2(0;0)	2(1;1)	2(1;1)	30(7;7)
	66	66	66	66	66	66	72	80	88	86	84	86	84	84	80	1,140
Grand total	(9;14)	(6;24)	(13;6)	(9;22)	(14;65)	(13;65)	(17;53)	(11;83)	(30;88)	(24;79)	(18;78)	(21;103)	(16;142)	(16;120)	(20;90)	(237;1,052)

Table 1.7: Area (km^2) of each standard survey region.
Area (km^2) of each standard survey region and depth stratum combination used to weight Pacific sleeper shark CPUE from standardized sablefish longline surveys (1982 – 2003).

Survey region	Depth strata				
Regulatory area					
- Slope stations					
- Gully stations	201 – 300 m	301 – 400 m	401 – 600 m	601 – 800 m	801 – 1,000 m
Eastern Bering Sea					
- Bering IV [a]	1,030	840	960	920	1,050
- Bering III [a]	600	520	890	1,160	900
- Bering II [a]	2,440	2,090	3,010	3,150	1,700
- Bering I [a]	770	730	1,270	1,160	1,130
Aleutian Islands					
- NW Aleutians [a]	1,130	1,300	3,100	2,640	2,210
- SW Aleutians [a]	1,440	1,570	3,480	2,820	2,130
- NE Aleutians [b]	2,141	2,085	3,800	3,250	2,786
- SE Aleutians [b]	2,530	2,096	2,396	1,978	1,570
Western Gulf of Alaska					
- Shumagin [c]	2,737	1,264	2,269	1,629	1,248
Central Gulf of Alaska					
- Chirikof [c]	1,533	817	1,766	1,955	2,012
- Shelikof Trough [c]	13,076				
- Kodiak [c]	1,626	1,480	2,255	1,923	2,296
- Amatuli Gully [c]	6,346				
Eastern Gulf of Alaska					
- West Yakutat [c]	992	992	1,271	1,245	1,282
- Western Grounds [c]	1,008	302			
- Yakutat Valley [c]	1,268	768			
- East Yakutat [c]	502	502	395	225	207
- Southeast Outside [c]	891	891	822	1,006	1,165
- Spencer Gully [c]	189	189	301	50	
- Ommaney Trench [c]	521	610	122		
- Dixon Entrance [c]	1,130	793	58		

[a] Sasaki (1985);
[b] M. Sigler, unpublished;
[c] Zenger and Sigler (1992).

Table 1.8: Cooperative survey area-weighted CPUE by regulatory area.
Area-weighted CPUE and bootstrap 95% confidence intervals (lower; and upper)[a] of Pacific sleeper sharks from the standardized cooperative sablefish longline survey during 1982–1994.

Survey region	Year												
Regulatory area													
- Slope stations													
- Gully stations	1982	1983	1984	1985	1986	1987	1988	1989	1990	1991	1992	1993	1994
Eastern Bering Sea													
- Slope	0.02	0.00	0.07	0.00	0.11	0.22	0.20[a] (0.0; 0.41)	0.21	0.00	0.00	0.23[a] (0.1; 0.38)	0.55[a] (0.14; 1.06)	1.2[a] (0.58; 1.93)
Aleutian Islands													
- Slope	0.00	0.00	0.06	0.19	0.06	0.07	0.10	0.02	0.00	0.01	0.00	0.00	0.00
Western Gulf of Alaska													
- Slope	0.00	0.00	0.00	0.07	0.08	0.64	0.00	0.00	0.00	0.00	0.00	0.00	0.00
Central Gulf of Alaska													
- Slope	0.00	0.00	0.01	0.00	0.00	0.08	0.02	0.00	0.00	0.00	0.03	0.00	0.01
- Gully[b]	0.00	0.00	0.00	0.00	2.22	0.00	0.00	1.47	0.00	0.00	0.00	0.00	0.00
Eastern Gulf of Alaska													
- Slope	0.00	0.00	0.00	0.00	0.00	0.20	0.00	0.04	0.04	0.00	0.17	0.04	0.27
Gulf of Alaska sub totals													
- Slope	0.00	0.00	0.00	0.02	0.02	0.25	0.01	0.01	0.01	0.00	0.06	0.01	0.09
- Slope and gully[b]	0.00	0.00	0.00	0.01	0.33	0.21	0.01	0.21	0.01	0.00	0.06	0.01	0.08

[a] Bootstrap 95% confidence intervals from the percentile method for selected time series with sufficient sample size to produce approximately normally distributed bootstrap replicates (Appendix 1.A.);
[b] Amatuli Gully.

Table 1.9: Domestic survey area-weighted CPUE by regulatory area.
Area-weighted CPUE and bootstrap 95% confidence intervals (lower; and upper)[a] of Pacific sleeper sharks from the standardized domestic sablefish longline survey during 1989–2003.

Survey region	Year														
Regulatory area															
- Slope stations															
- Gully stations	1989	1990	1991	1992	1993	1994	1995	1996	1997	1998	1999	2000	2001	2002	2003
Eastern Bering Sea															
- Slope									1.41[a] (0.81; 2.06)		0.25		0.16		0.48
Eastern Aleutian Islands															
- Slope								0.00		0.00		0.00		0.00	
Western Gulf of Alaska															
- Slope	0.00	0.37	0.42	0.00	0.19	0.06	0.00	0.00	0.00	0.19	0.00	0.00	0.00	0.00	0.00
Central Gulf of Alaska															
- Slope	0.05	0.00	0.03	0.00	0.00	0.03	0.03	0.03	0.01	0.02	0.01	0.17	0.16	0.10	0.00
- Gullies [b]	0.32	1.33	1.58	2.18	6.72	7.75	4.52	6.76	2.18	6.63	7.01	8.50	14.66	12.82	7.16
- Shelikof Trough				2.84[a] (0.94;	9.04[a] (3.79;	7.44[a] (2.76;	6.19[a] (2.38;	10.05[a] (4.91;	2.96[a] (0.92;	9.0[a] (5.66;	10.09[a] (4.13;	12.51[a] (5.23;	21.78[a] (13.7;	19.04[a] (13.3;	10.64[a] (4.52;
	0.47	0.78	1.74	4.57)	13.9)	12.7)	9.73)	16.7)	5.36)	12.5)	18.0)	21.4)	32.7)	24.5)	18.8)
Eastern Gulf of Alaska															
- Slope	0.14	0.00	0.12	0.01	0.01	0.02	0.02	0.04	0.54	0.04	0.00	0.17	0.00	0.01	0.24
- Gullies [c]	0.59	0.89	0.48	0.28	0.38	0.09	0.30	1.66	0.90	1.26	0.17	1.05	0.85	2.09	2.00
Gulf of Alaska sub totals															
- Slope	0.06	0.09	0.15	0.00	0.05	0.04	0.02	0.03	0.18	0.07	0.01	0.13	0.07	0.05	0.08
- Gullies [b,c]	0.39	1.21	1.28	1.66	4.99	5.65	3.37	5.37	1.83	5.16	5.14	6.46	10.89	9.88	5.75
Gulf of Alaska grand total															
- Slope and gullies [b,c]	0.20[a] (0.10; 0.30)	0.54[a] (0.24; 0.92)	0.61[a] (0.34; 0.87)	0.68[a] (0.3; 1.04)	2.05[a] (1.04; 3.07)	2.31[a] (1.28; 3.39)	1.38[a] (0.6; 2.09)	2.19[a] (1.17; 3.47)	0.85[a] (0.43; 1.34)	2.13[a] (1.44; 2.8)	2.09[a] (0.89; 3.68)	2.7[a] (1.25; 4.49)	4.46[a] (2.84; 6.54)	4.04[a] (2.87; 5.16)	2.38[a] (1.17; 4.03)
Gulf of Alaska grand total without Shelikof Trough															
- Slope and gullies [d]	0.13[a] (0.06; 0.20)	0.48	0.33[a] (0.11; 0.54)	0.14	0.32	1.05	0.19[a] (0.08; 0.31)	0.25	0.32[a] (0.17; 0.51)	0.43[a] (0.24; 0.62)	0.11[a] (0.04; 0.2)	0.27[a] (0.17; 0.39)	0.17	0.32	0.33

[a] Bootstrap 95% confidence intervals from the percentile method for selected time series with sufficient sample size to produce approximately normally distributed bootstrap replicates (Appendix 1. A);
[b] Shelikof Trough and Amatuli Gully;
[c] Western Grounds, Yakutat Valley, Spencer Gully, Omany Trench, and Dixon Entrance;
[d] Amatuli Gully, Western Grounds, Yakutat Valley, Spencer Gully, Omany Trench, and Dixon Entrance.

Table 1.10: Statistical significance of annual changes in area-weighted CPUE.
Statistical significance of annual changes in area-weighted CPUE of Pacific sleeper sharks from standardized sablefish longline surveys (1982–2003) for the eastern Bering Sea (A), Gulf of Alaska total (B), Shelikof Trough (C) and Gulf of Alaska total without Shelikof Trough (D). The symbols used are defined as follows: "+" indicates a significant increase (95%): "-" indicates a significant decrease (95%): "o" indicates no significant change.

A. Eastern Bering Sea

Year	1992	1993	1994
1988	o	o	+
1992		o	+
1993			o

B. Gulf of Alaska Total

Year	1990	1991	1992	1993	1994	1995	1996	1997	1998	1999	2000	2001	2002	2003
1989	+	+	+	+	+	+	+	+	+	+	+	+	+	+
1990		o	o	+	+	o	+	o	+	+	+	+	+	+
1991			o	+	+	+	+	o	+	+	+	+	+	+
1992				+	+	o	+	o	+	+	+	+	+	+
1993					o	o	o	-	o	o	o	+	+	o
1994						o	o	-	o	o	o	+	+	o
1995							o	o	o	o	o	+	+	o
1996								-	o	o	o	+	+	o
1997									+	o	+	+	+	+
1998										o	o	+	+	o
1999											o	+	o	o
2000												o	o	o
2001													o	o
2002														o

C. Shelikof Trough

Year	1993	1994	1995	1996	1997	1998	1999	2000	2001	2002	2003
1992	+	o	o	+	o	+	+	+	+	+	+
1993		o	o	o	-	o	o	o	+	+	o
1994			o	o	o	o	o	o	+	+	o
1995				o	o	o	o	o	+	+	o
1996					-	o	o	o	+	+	o
1997						+	+	+	+	+	+
1998							o	o	+	+	o
1999								o	o	o	o
2000									o	o	o
2001										o	-
2002											o

D. Gulf of Alaska without Shelikof Trough

Year	1991	1995	1997	1998	1999	2000
1989	o	o	+	+	o	+
1991		o	o	o	o	o
1995			o	o	o	o
1997				o	-	o
1998					-	o
1999						o

1.7. Appendix 1.A. Bootstrap Replicates.

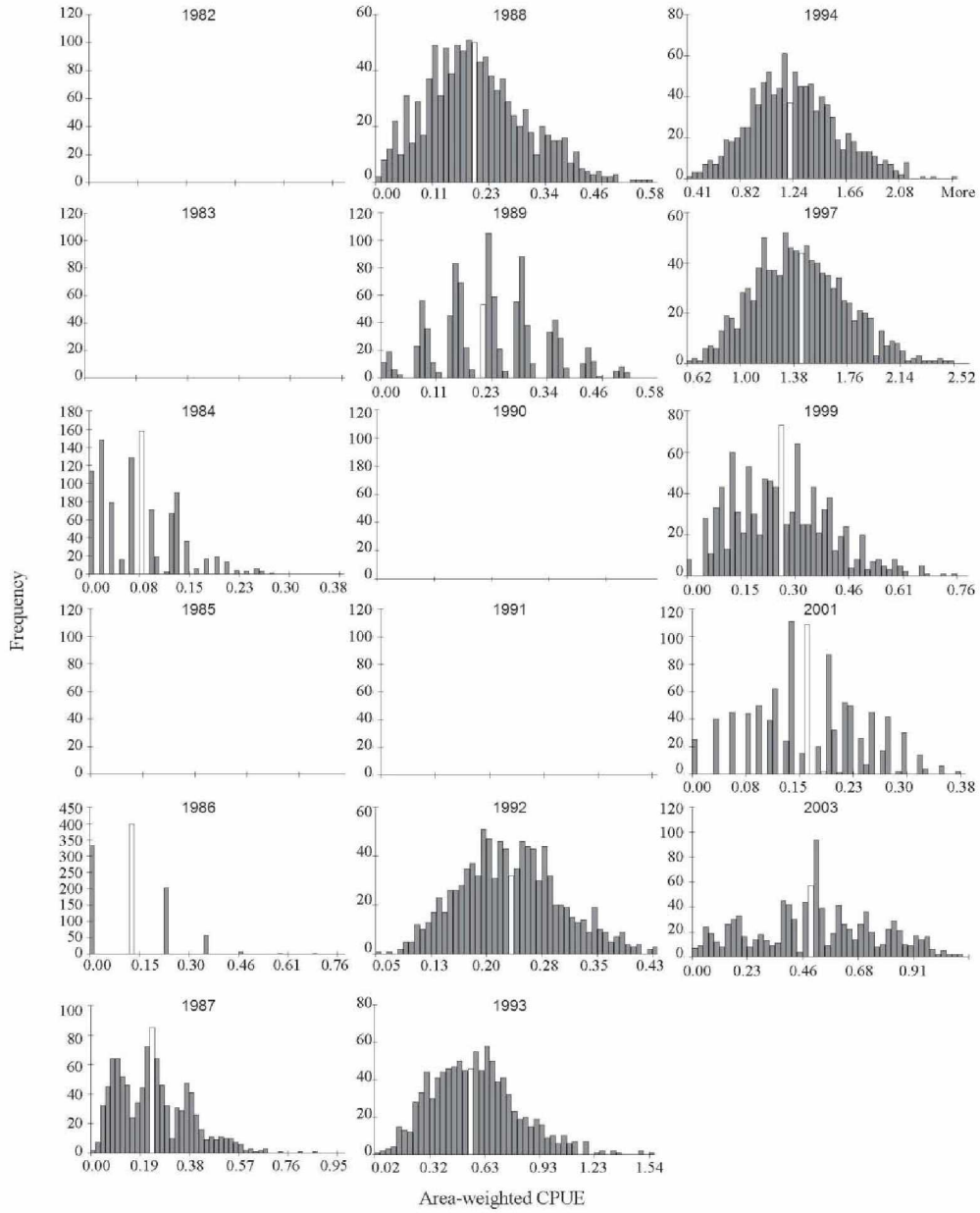

Figure 1.A.1: Bootstrap replicates for the eastern Bering Sea.
Eastern Bering Sea total Pacific sleeper shark area-weighted CPUE estimates 1982–2003 from 1,000 bootstrap replicates; unshaded bars indicate original CPUE estimate.

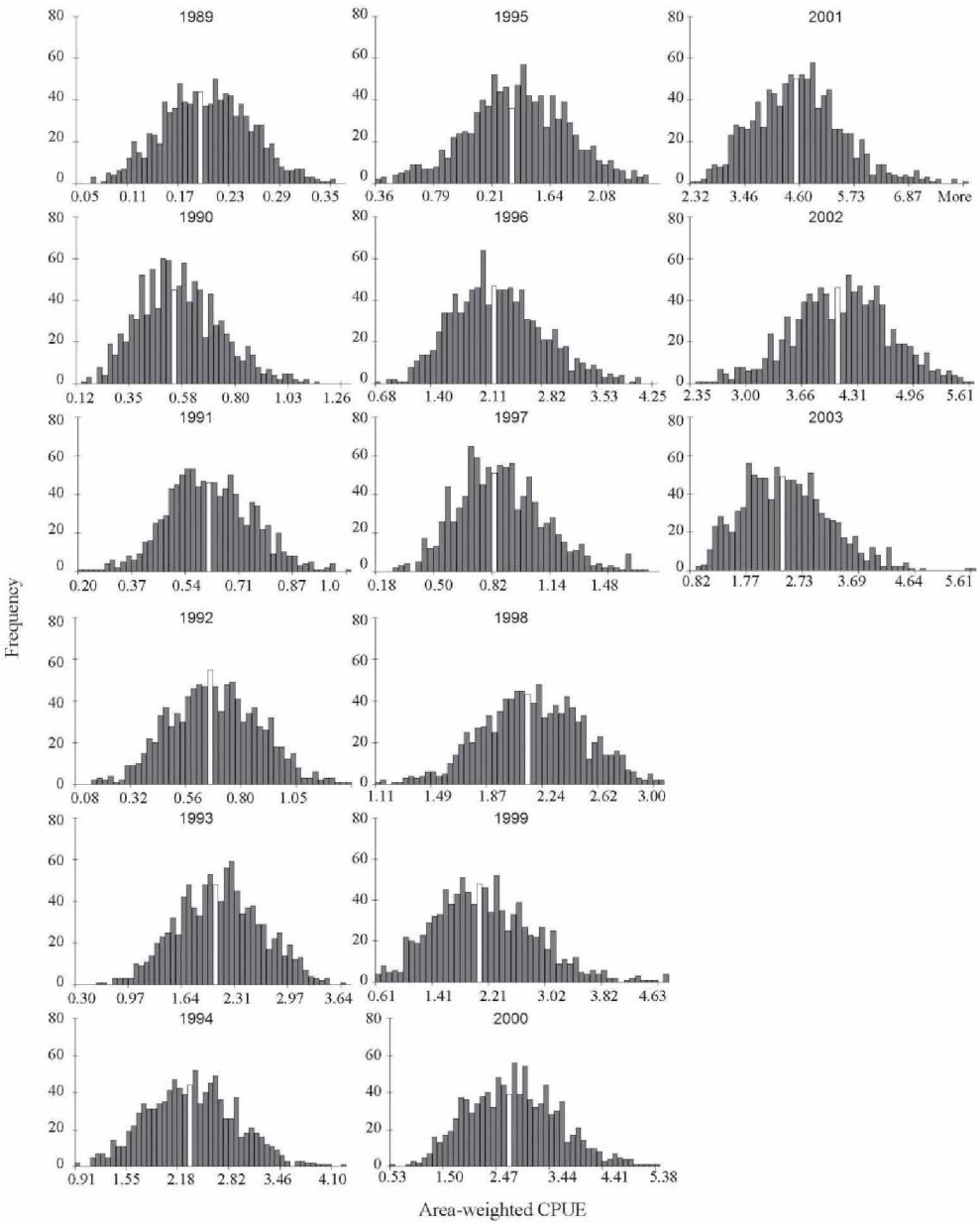

Figure 1.A.2: Bootstrap replicates for the Gulf of Alaska.
Gulf of Alaska total Pacific sleeper shark area-weighted CPUE estimates 1989–2003 from 1,000 bootstrap replicates; unshaded bars indicate original CPUE estimate.

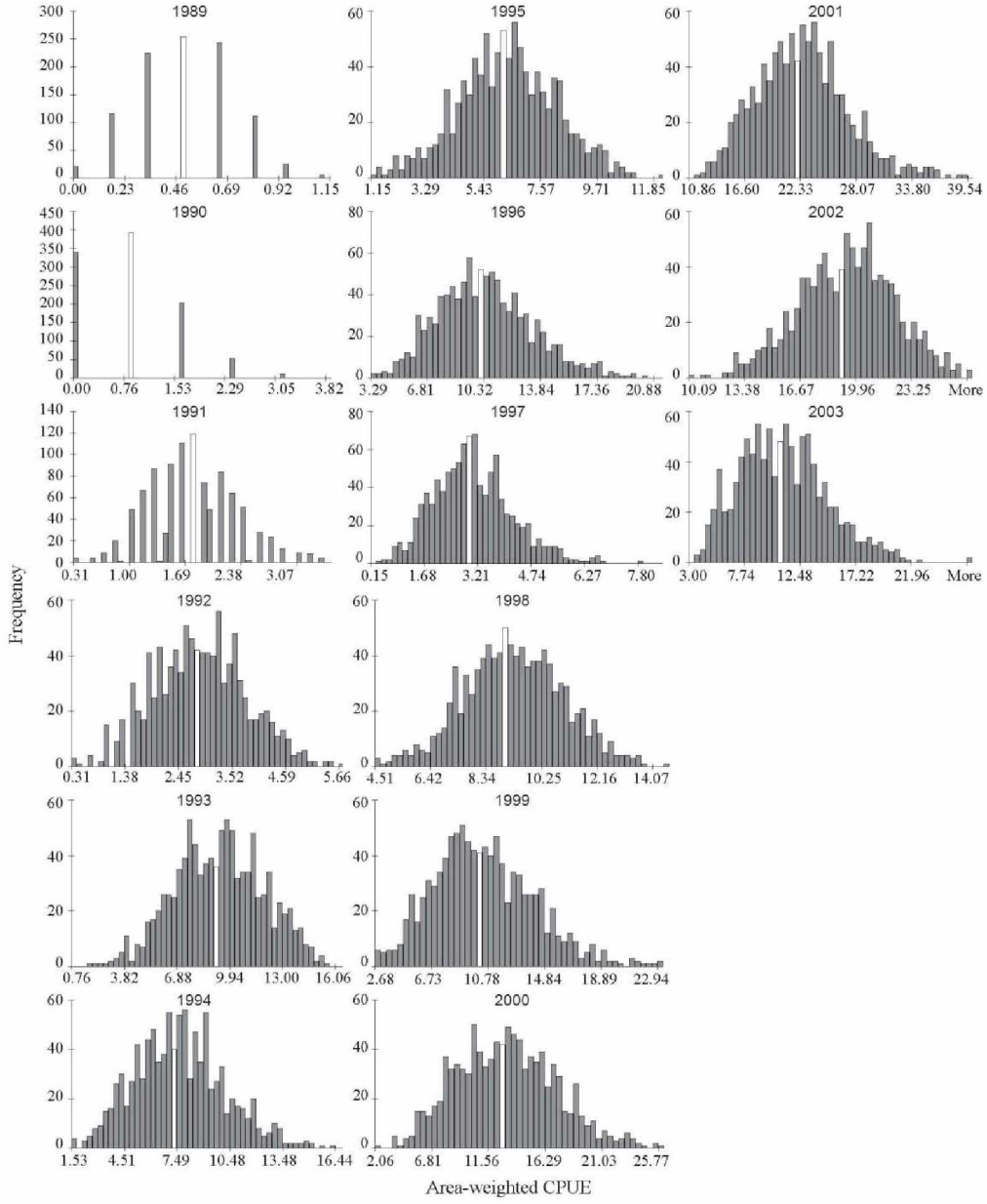

Figure 1.A.3: Bootstrap replicates for the Shelikof Trough.
Shelikof Trough total Pacific sleeper shark area-weighted CPUE estimates 1989–2003 from 1,000 bootstrap replicates; unshaded bars indicate original CPUE estimate.

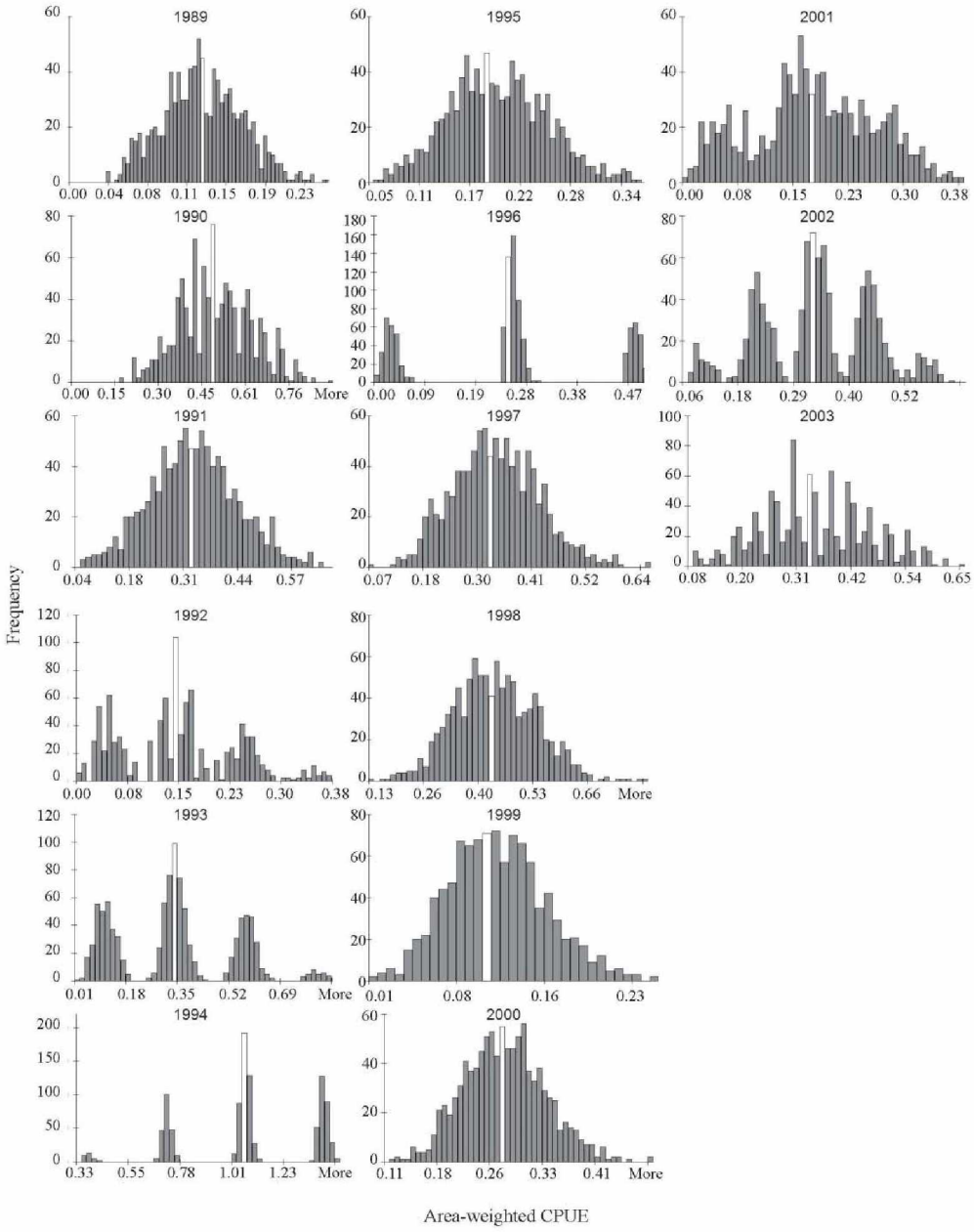

Figure 1.A.4: Bootstrap replicates for the Gulf of Alaska without Shelikof Trough.
Gulf of Alaska without Shelikof Trough Pacific sleeper shark area-weighted CPUE estimates 1989–2003 from 1,000 bootstrap replicates; unshaded bars indicate original CPUE estimate.

2. Chapter 2 - Pacific Sleeper Shark Incidental Exploitation Rates[2]

2.1. Abstract

Monte Carlo simulation was used to investigate the sustainability of incidental exploitation rates (U) for Pacific Sleeper Sharks *Somniosus pacificus* in the Gulf of Alaska (GOA) under status quo management. Monte Carlo simulations were implemented with a standard, length-based, age-structured model that was evaluated with forward projection. Given the paucity of relevant data, we investigated the sensitivity of simulation results to a range of assumptions about key model parameters by using 24 alternative model configurations, each simulated 1,000 times. The risk analysis results were most sensitive to Pacific Sleeper Shark U-values. The aggregate fraction of simulations ending in an overfished condition increased from 0% under the low-U scenario to 59% under the high-U scenario. Risk analysis results were also sensitive to the assumed shape of the length-based selectivity curve (asymptotic or dome shaped) but were less sensitive to the range of assumptions about other key model parameters, including maximum age and stock productivity. These results indicate that a priority for Pacific Sleeper Shark management is to reduce the uncertainty in U. This major uncertainty will be decreased by an observer program that is now in place to monitor the historically unobserved GOA Pacific Halibut *Hippoglossus stenolepis* fishery, which incidentally catches Pacific Sleeper Sharks.

[2]Courtney, D. L., Adkison, M. D., and M. F. Sigler. 2016. Risk analysis of plausible incidental exploitation rates for the Pacific sleeper shark, a data-poor species in the Gulf of Alaska. North American Journal of Fisheries Management 36:523–548.

2.2. Introduction

The Magnuson–Stevens Reauthorization Act of 2006 (MSRA 2006) established new requirements to end and prevent overfishing through the use of annual catch limits and mandated that such limits be established for all stocks included within U.S. federally managed fishery management plans by 2011. The U.S. National Standard 1 guidelines (U.S. Office of the Federal Register 2009) provide guidance on implementing annual catch limits and recommend (1) determining acceptable biological catch by reducing the overfishing limit to account for scientific uncertainty and (2) setting the annual catch limit at a value less than or equal to the acceptable biological catch.

Within U.S. federally managed waters (>5.56 km [3 nautical miles] from shore to 370.4 km [200 nautical miles]) of the Gulf of Alaska (GOA), eastern Bering Sea, and Aleutian Islands region (Figure 2.1), only limited data are available to assess the stock status of shark populations because most sharks are captured incidentally in commercial fisheries targeting other demersal fish species (groundfish) and are not retained (Gaichas et al. 1999; Gaichas 2002; Courtney et al. 2006a, 2006b; Tribuzio et al. 2011, 2012; NMFS 2013). Within the GOA, incidental shark catch is composed primarily of Pacific Spiny Dogfish *Squalus suckleyi*, Pacific Sleeper Sharks *Somniosus pacificus*, and Salmon Sharks *Lamna ditropis*, which on average accounted for 54, 30, and 7%, respectively, of the total incidental shark catch in weight during 1990–2011 (Tribuzio et al. 2011). Accurate incidental catch data and fishery-independent survey data, which are necessary for stock assessment, are lacking for all shark species within the GOA (Tribuzio et al. 2011). Life history information that is necessary for stock assessment has been investigated for Pacific Spiny Dogfish (Fordham 2005; Tribuzio et al. 2010; Tribuzio and Kruse 2011, 2012) and Salmon Sharks (Goldman 2002; Goldman and Human 2005; Goldman and Musick 2006, 2008) but is generally lacking for Pacific Sleeper Sharks, as detailed below.

Pacific Sleeper Sharks can attain a large size (~7 m TL) and are commonly encountered by commercial fishing gear and fishery-independent surveys on the continental shelves and the upper continental slopes of the high-latitude North Pacific Ocean (Compagno 1984; Ebert et al. 1987; Orlov 1999; Orlov and Moiseev 1999a, 1999b; Mecklenburg et al. 2002; Yano et al. 2004, 2007; Murray et al. 2008; Ebert and Winton 2010; Kyne and Simpfendorfer 2010; O'Brien et al. 2013; Orlov and Baitalyuk 2014). However, Pacific Sleeper Sharks also occur in both the Arctic (Benz et al. 2004) and the lower latitude North Pacific Ocean (Borets 1986; Wang and Yang 2004; Yeh and Drazen 2009). In the northeast Pacific Ocean, Pacific Sleeper Sharks appear to be opportunistic consumers of the available prey and carrion (Yang and Page 1999; Smith and Baco 2003; Hulbert et al. 2006; Sigler et al. 2006; Yano et al. 2007; Courtney and Foy 2012; Horning and Mellish 2012, 2014). In the GOA, satellite-tagged Pacific Sleeper Sharks primarily occupied depths between 250 and 450 m (61% of observations), but they made

regular ascents to depths less than 100 m (58% of days observed; Hulbert et al. 2006). Most (76%) of the satellite-tagged Pacific Sleeper Sharks in the GOA were relocated within 100 km of their release locations up to 1 year after release (Hulbert et al. 2006).

In the GOA, time series describing the incidental catch and fishery-independent CPUE of Pacific Sleeper Sharks have both shown an increasing trend followed by a decreasing trend during recent years (Mueter and Norcross 2002; Courtney and Sigler 2007; Tribuzio et al. 2011). The recent declines in incidental catch and CPUE of GOA Pacific Sleeper Sharks are worrisome because the Greenland Shark *Somniosus microcephalus*—a similar large-bodied sleeper shark occurring in the Atlantic Ocean—is assumed to be slow growing (Hansen 1963) and long lived (Fisk et al. 2002; Davis et al. 2013). The annual estimates of incidental catch and CPUE for Pacific Sleeper Sharks in the GOA are highly uncertain (Tribuzio et al. 2011), and catch statistics alone do not necessarily reflect trends in abundance (Pauly et al. 2013; Worm et al. 2013). However, the spatial distribution of Pacific Sleeper Sharks in the GOA overlaps with that of several commercial groundfish fisheries as well as that of several fishery-independent groundfish surveys (Mueter and Norcross 2002; Menon 2004; Menon et al. 2005; Courtney and Sigler 2007; Tribuzio et al. 2011; Orlov and Baitalyuk 2014). Consequently, recent trends in the annual estimates of Pacific Sleeper Shark incidental catch and CPUE within the GOA could be indicative of changes in this species' relative abundance in the region.

The objective of this study was to use Monte Carlo simulation to investigate the simulated stock status of a generic, long-lived shark population with characteristics similar to those of the Pacific Sleeper Shark population in the GOA. The intent of the simulation approach was to provide managers with a plausible range of scientific uncertainty in the current stock status of this data-poor population. The available time series of Pacific Sleeper Shark incidental catch during 2001–2009 and the available fishery-independent index of total biomass during the same period (Tables 2.1 and 2.2; Tribuzio et al. 2011) were used to develop a plausible range of incidental exploitation rates for GOA Pacific Sleeper Sharks under status quo management—namely, the limited retention of sharks and the monitoring of nontarget (incidental) shark catch, as described below. Monte Carlo simulations were implemented under the range of exploitation rates with a standard, length-based, age-structured model that was evaluated with forward projection (Punt and Walker 1998; Simpfendorfer et al. 2000). Given the paucity of relevant data, the sensitivity of simulation results to alternative assumptions about key model parameters was investigated. Simulations were conducted for 100 years in order to account for both the potential long life span of Pacific Sleeper Sharks and the potential historical duration of commercial groundfish fisheries in the GOA.

Simulated stock status was evaluated relative to equilibrium maximum sustainable yield (MSY; following the U.S. National Standard 1 guidelines; U.S. Office of the Federal Register 2009). The annual

exploitation rate (U) at equilibrium MSY (U_{MSY}) was used as the overfishing limit reference point. The risk of ending in an overfished condition was defined analogously to the North Pacific Fishery Management Council's (NPFMC) Tier 3 approach (NMFS 2013)—a relatively data-rich tier that is used to manage many Alaskan groundfish fisheries—except that here, a stock was defined as overfished if it was below half the spawning stock biomass (S) that would be obtained at MSY (S_{MSY}), as discussed in detail below.

2.3. Methods

2.3.1. Operating Model

Population dynamics were simulated with a standard, length-based, age-structured operating model.

Numbers at age.—Numbers at age were simulated with an age-structured approach (Punt and Walker 1998: their Equation A1.1) that utilized a generalization of Pope's approximation (Quinn and Deriso 1999), calculated here as

$$N_{t,a} = \begin{cases} N_{t,r} & a = 1 \\ \left(N_{t-1,a-1} e^{\left(-0.5M_{a-1}\right)} - C_{t-1,a-1}\right) e^{\left(-0.5M_{a-1}\right)} & 1 < a \leq a_{\max} - 1 \\ \left(N_{t-1,a_{\max}-1} e^{\left(-0.5M_{a_{\max}-1}\right)} - C_{t-1,a_{\max}-1}\right) e^{\left(-0.5M_{a_{\max}-1}\right)} + & a = a_{\max} \\ \left(N_{t-1,a_{\max}} e^{\left(-0.5M_{a_{\max}}\right)} - C_{t-1,a_{\max}}\right) e^{\left(-0.5M_{a_{\max}}\right)} & \end{cases}, \tag{2.1}$$

where $N_{t,a}$ is the number (thousands) at age a (years) at the start of year t; $C_{t,a}$ is the total annual catch in number at age a in year t; M_a is the natural mortality rate at age a; and a_{max} is the upper age bin used in the operating model.

Vulnerable biomass.—The biomass (B) that was vulnerable to the fishery (f) in the middle of year t was simulated (Punt and Walker 1998: their Equation A1.9; Simpfendorfer et al. 2000: their Equation 15) by using an age–length transition matrix (Hurtado-Ferro et al. 2014: their Equation A.11), calculated here as

$$B_{f,t}^{mid-year} = \sum_{l=1}^{l_{\max}} w_l \mathrm{sel}_{f,l} \sum_{a=1}^{a_{\max}} \phi_{a,l} \left(N_{t,a} e^{\left(-0.5M_a\right)}\right), \tag{2.2}$$

where w_l is the weight (kg) at the middle of each length bin l (cm TL), predicted from an allometric weight-at-length relationship (females and males combined) as described below; $\text{sel}_{f,l}$ is the selectivity of the fishery f at the middle of each length bin l and is calculated as described in Equation (2.9); and $\phi_{a,l}$ is the proportion of sharks from age a in each length bin l obtained from the age–length transition matrix (Equation 2.8).

Exploitation rate.—The U in year t was simulated from the ratio of yield (catch in weight) in year t (Y_t) to vulnerable biomass in the middle of year t (Punt and Walker 1998: their Equation A1.9; Simpfendorfer et al. 2000: their Equation 14; Methot and Wetzel 2013: their Equation A.5.19), calculated here as

$$U_t = Y_t \Big/ B_{f,t}^{mid-year} . \tag{2.3}$$

Catch at age and length.—Catch (thousands of sharks) in year t was simulated (Punt and Walker 1998: their Equation A1.8; Simpfendorfer et al. 2000: their Equation 13) by using an age–length transition matrix (Methot and Wetzel 2013: their Equation A.5.20; Hurtado-Ferro et al. 2014: their Equation A.12) to calculate catch in number at age a and length bin l simultaneously as

$$C_{t,a,l} = U_t \text{sel}_{f,l} \phi_{a,l} N_{t,a} e^{(-0.5M_a)} . \tag{2.4}$$

Catch (thousands) at age a in year t was then calculated from the results of Equation (2.4) as

$$C_{t,a} = \sum_{l=1}^{l\max} C_{t,a,l} . \tag{2.5}$$

Catch in weight (yield; metric tons [1,000 kg]) during year t was calculated from the results of Equation (2.4) and an allometric weight-at-length relationship for w_l (Hurtado-Ferro et al. 2014: their Equation A.13) as

$$Y_t = \sum_{a=1}^{a_{\max}} \sum_{l=1}^{l_{\max}} w_l C_{t,a,l} . \tag{2.6}$$

Length at age.—Length at age was simulated by using a von Bertalanffy growth model (VBGM; Quinn and Deriso 1999: their equation 4.9) as

$$L_a = L_\infty\left(1-e^{-\kappa(a-t_0)}\right)+\varepsilon_{L_a};\qquad \varepsilon_{L_a}\sim N\left(0;\sigma^2_{L_a}\right). \tag{2.7}$$

where L_∞ is the asymptotic (maximum) length; κ is the Brody growth parameter; t_0 is the age intercept (theoretical age at a length of zero); ε_{La} is the normally distributed error in length at age a; and σ_{L_a} is the SD of length at each age.

Age–length transition matrix.—The proportion of sharks from age a in each length bin l was modeled by using an age–length transition matrix (Wetzel and Punt 2011a: their Equation A.4; Hurtado-Ferro et al. 2014: their Equation A.23), calculated here as

$$\phi_{a,l}=\begin{cases}\Phi\left(\dfrac{L'_{\min}-L_a}{\sigma_{L_a}}\right); & l=1\\ \Phi\left(\dfrac{L'_{l+1}-L_a}{\sigma_{L_a}}\right)-\Phi\left(\dfrac{L'_{l}-L_a}{\sigma_{L_a}}\right); & l>1 \text{ to } l<l_{\max}\\ 1-\Phi\left(\dfrac{L'_{\max}-L_a}{\sigma_{L_a}}\right); & l=l_{\max}\end{cases}. \tag{2.8}$$

where Φ is the standard normal cumulative density function; L'_l is the lower limit of length bin l; $L'_{\min}$ is the lower limit of the smallest length bin; and $L'_{\max}$ is the lower limit of the largest length bin (l_{max}), which was fixed at 700 cm TL for all model configurations. The parameter L_a is the expected mean length of sharks at age a, as obtained from Equation (2.7), with normal error in length at age; the parameter σ_{L_a} is the SD in length of a shark at age a. The age–length transition matrix was parameterized by assuming a constant coefficient of variation (CV) in length at age for all ages, $\mathrm{CV}_{L_a}=\left(\sigma_{L_a}/L_a\right)=0.2$. The value 0.2 was determined by trial and error as a CV that allowed a small proportion of the distribution of simulated lengths (<1%) to attain 700 cm TL or larger (700+ cm TL) under each life history scenario, as described below.

Selectivity at length.—Selectivity at length (sel_L) was simulated by using an exponential-logistic equation (Thompson 1994: their Equation 1; Sigler 1999), calculated here as

$$\mathrm{sel}_L = \left(\frac{1}{1-\gamma}\right)\left(\frac{1-\gamma}{\gamma}\right)^{\gamma}\left(\frac{e^{\alpha\gamma(\beta-L)}}{1+e^{\alpha(\beta-L)}}\right), \tag{2.9}$$

where sel_L is the proportion selected at length L; and α, β, and γ are all positive constants with peak and inflection points as defined by Thompson (1994). The exponential-logistic equation automatically scales the maximum selectivity to 1.0 and reduces to asymptotic selectivity as γ approaches zero; when γ equals zero, the parameter β is the length at which 50% of the population is vulnerable and α is the slope of the function at 50% vulnerability (Sigler 1999). When γ is greater than zero, the parameters α and β lose their biological meaning because β no longer represents the length at 50% vulnerability (Sigler 1999).

The exponential-logistic equation was chosen for the simulations because it allowed for both (1) asymptotic selectivity, when selectivity was assumed to increase with length to an asymptote; and (2) dome-shaped selectivity, when selectivity was assumed to increase with length to a maximum and then decrease for older fish.

Maturity at length.—The proportion of sharks that were sexually mature at length was simulated by using a logistic equation (Quinn and Deriso 1999: their Equation 4.127), calculated here as

$$m_L = \frac{1}{1+e^{-k(L-L_{50})}}, \tag{2.10}$$

where m_L is the proportion mature at length L; k is the curvature; and L_{50} is the length at inflection (i.e., length at 50% maturity). The proportion of mature females in each length bin l (m_l) was then modeled with Equation (2.10) from the length L at the lower limit of each length bin l. The maximum proportion mature was assumed to equal 1.0 as length approached L_∞.

Recruitment at age.—Due to the lack of sex-specific life history information for Pacific Sleeper Sharks, a 1:1 sex ratio was assumed, and spawning stock biomass in year t (S_t) was assumed to be proportional to annual "egg" production (Quinn and Deriso 1999: their Equation 4.137). This corresponded to the assumptions that recruitment was limited by egg production rather than sperm production and that viable egg production per unit of spawning biomass was independent of spawner age or length (e.g., Gabriel et al. 1989). A distinction here was that "egg" production was assumed to represent the number of fertilized eggs that were carried to term and produced live pups at parturition.

Sharks were also assumed to recruit to the population and be vulnerable to the fishery and the survey at age 1 ($a_r = 1$). Simulated recruitment occurred on January 1 of the year after birth, regardless of the spawning season (e.g., Methot and Wetzel 2013). The annual number of sharks recruiting to the

population at the start of year $t + a_r$ (i.e., R_{t+a_r}) was then related to S_t by using a Beverton–Holt spawner–recruit curve (Quinn and Deriso 1999: their Equation 3.6; Brooks et al. 2010: their Equation 1), calculated here as

$$R_{t+a_r} = \frac{\alpha S_t}{1+\beta S_t} e^{\left(\varepsilon_t - 0.5\sigma_R^2\right)}; \quad \varepsilon_t \sim N\left(0;\sigma_R^2\right), \tag{2.11}$$

The parameter α controls productivity, and parameter β controls the level of density dependence (Quinn and Deriso 1999: their Equation 3.6). The parameterization $e^{\left(\varepsilon_t - 0.5\sigma_R^2\right)}$ is a bias correction to simulate the mean recruitment deviation (on the natural scale) from lognormally distributed recruitment error, where σ_R is the SD of normally distributed recruitment deviations in log space (Wetzel and Punt 2011a: their Equation A.7).

Stock–recruitment steepness.—The productivity and density dependent parameters of the Beverton–Holt stock–recruitment relationship (Equation 2.11) were parameterized in terms of the steepness parameter (h), defined as the proportion of recruitment relative to the recruitment at equilibrium with no fishing when the spawner abundance or biomass is reduced to 20% of the virgin level (Mace and Doonan 1988; Hilborn and Walters 1992; Myers et al. 1999; Brooks et al. 2010: their Equation 7; Haddon 2011: his Appendix 10.3). The stock– recruitment parameters are calculated as

$$\alpha = \frac{4hR_0}{S_0(1-h)}, \tag{2.12}$$

and

$$\beta = \frac{5h-1}{S_0(1-h)}, \tag{2.13}$$

where S_0 is the unexploited equilibrium spawning stock biomass of females (mature female biomass); and R_0 is the unexploited equilibrium recruitment (males and females combined), as defined below.

Two h-values (0.25 and 0.39) were evaluated with simulations. For Beverton–Holt stock recruitment, steepness is by definition mathematically limited to the range between 0.2 and 1.0 (e.g., z in Myers et al. 1999). However, a lower bound for h was assumed here to be 0.25 because values less than this are unlikely (Cope and Punt 2009; Cope 2013, citing He et al. 2006). By comparison, a lower bound

of 0.25 for h in Pacific Sleeper Sharks is also consistent with the use of a survival based stock–recruitment relationship (Taylor et al. 2013), which indicated that h-values greater than 0.28 led to unreasonably large estimates of pre-recruit survival (>1.0) for the Pacific Spiny Dogfish, a long-lived, low-fecundity, cold-water elasmobranch occurring in the northeast Pacific Ocean. An upper bound for h of cold-water Pacific Sleeper Sharks in the GOA was assumed to be 0.39. This upper h-value was the average calculated from an analytical relationship between h and the spawning potential ratio (SPR) at maximum excess recruitment (Brooks et al. 2010), which was applied to a range of relatively well-studied but primarily warm-water shark species (Brooks et al. 2010). The h-value of 0.39 is also consistent with the value obtained from a meta-analysis of long-lived teleosts (Scorpaenidae; Myers et al. 1999: their Table 1).

Spawning stock size.—Spawning stock biomass in year t (S_t) was parameterized here as mature female biomass at age a and year t (Hurtado-Ferro et al. 2014: their Equation A.26) from the numbers of females and males combined (per capita) as

$$S_t = \sum_{l=1}^{l_{\max}} w_l m_l \sum_{a=1}^{a_{\max}} \phi_{a,l}\, 0.5\left(N_{t,a} e^{(-M_a)(\tau_M)} - (\tau_U) C_{t,a}\right). \tag{2.14}$$

The value 0.5 represents the assumed proportion of females in the population numbers at age a in year t (after removing the catch); $\phi_{a,l}$ is the age–length transition matrix (Equation 2.8), representing the proportion of age-a sharks at the beginning of each length bin l; m_l is the proportion of mature females at the beginning of each length bin l; and w_l is the allometric weight of females and males (combined) at the middle of each length bin l. Due to a lack of information on the seasonality of pup production in Pacific Sleeper Sharks, parturition (pupping) was assumed to occur over a short period near the middle of each calendar year (~June 1). The fraction of natural mortality, M, that was expected to occur from the beginning of each calendar year (January 1) to the beginning of the pupping season (τ_M) and the fraction of annual U that was expected to occur from January 1 to the beginning of the pupping season (τ_U) were both fixed at 0.5.

2.3.2. Exploitation Rate Scenarios

Because of the historically limited amount of data available for assessing the status of shark populations within U.S. federally managed waters of the GOA (Figure 2.1), incidental shark catch before 2011 was managed under a total allowable catch established for a data-poor "other species" management unit that consisted of multiple nontarget species groups, including sharks (Gaichas et al. 1999; Courtney et al. 2006b; Tribuzio et al. 2011; NMFS 2013). Since 2011, nontarget incidental shark catch in the GOA

has been managed within a separate data-poor "shark" management unit (Tribuzio et al. 2011). In 2011, the overfishing limit for Pacific Spiny Dogfish was based on the NPFMC's data limited Tier 5 approach and was calculated from an estimate of exploitable biomass multiplied by an estimate of M (Tribuzio et al. 2011; NMFS 2013). In contrast, the overfishing limit for Pacific Sleeper Sharks, Salmon Sharks, and other (or unidentified) shark species in 2011 was based on a modification of the NPFMC's data-poor Tier 6 approach and was calculated as the average historical incidental catch for the period 1997–2007 (Tribuzio et al. 2011; NMFS 2013). In 2011, the acceptable biological catch for all shark species within the shark management unit was then calculated as 75% of the overfishing limit in accordance with the NPFMC control rule that was prescribed under both the Tier 5 and Tier 6 approaches (Tribuzio et al. 2011; NMFS 2013). However, due to the limited amount of data available for the data-poor other species management unit before 2011 and the data-poor shark management unit in 2011, the annual total allowable catch levels were combined for all species within each management unit. The annual total allowable catch levels established for the various management units that have included sharks have historically never been exceeded (Tribuzio et al. 2011: their Figure 20.15). Consequently, status quo management of incidental shark catch within the GOA has primarily involved the limited retention of sharks—as historically most of the incidentally captured sharks have not been retained—and the monitoring of nontarget incidental shark catch.

Incidental catch.—Incidental catch estimates for Pacific Sleeper Sharks in U.S. federal waters of the GOA (Figure 2.1) are variably incomplete. Catch estimates are available from the National Marine Fisheries Service (NMFS) for Pacific Sleeper Sharks that were captured incidentally in U.S. federally managed GOA commercial groundfish fisheries during 1990–2011 (Courtney et al. 2006b; Tribuzio et al. 2011), but only catch data from the period 1997–2011 are considered suitable for use in management (Tribuzio et al 2011). In addition, some GOA commercial fisheries for Pacific Halibut *Hippoglossus stenolepis* incidentally capture Pacific Sleeper Sharks, but those data have not historically been included in the NMFS incidental catch estimation procedure (Tribuzio et al. 2011, 2014).

For the purposes of this study, two time series of Pacific Sleeper Shark incidental catch in the GOA (Table 2.1) were obtained from the NMFS Alaska Fisheries Science Center (AFSC; Tribuzio et al. 2011). The first time series (1997–2011) represented the official annual estimates of Pacific Sleeper Shark incidental catch (metric tons) that were used to manage sharks in the GOA shark management unit (Tribuzio et al. 2011: their Table 20.4; updated data from the years 2010 and 2011 are used here, C. Tribuzio, NMFS, personal communication). The official estimates for 2003–2011 were obtained via the NMFS Alaska Regional Office's Catch Accounting System (CAS; hereafter, "CAS") estimation procedure; official estimates for 1997–2002 were obtained via similar methods by NMFS-AFSC staff (Gaichas et al. 1999; Gaichas 2002; Tribuzio et al. 2011: their Table 20.4). On average, Pacific Sleeper

Sharks accounted for 30% of the incidental shark catch within the GOA shark management unit during 1997–2011 but only 4% in 2009 (Tribuzio et al. 2011). Most of the incidentally captured Pacific Sleeper Sharks in the GOA shark management unit are discarded. Mortality rates of incidentally caught, discarded sharks are unknown but were conservatively estimated by NMFS-AFSC as 100% (Tribuzio et al. 2011).

The second time series (2001–2010) was obtained from a preliminary estimate of nontarget species catch, which was developed for historically unobserved Pacific Halibut fisheries prior to 2013 by the NMFS-AFSC Halibut Fishery Incidental Catch Estimation (HFICE) Working Group (hereafter, "HFICE"; Tribuzio et al. 2011: their Appendix 20A and Table 20A.3). The preliminary HFICE incidental catch estimates were still in development and may be subject to change (Tribuzio et al. 2014); there was also overlap between the HFICE incidental catch estimates and the CAS incidental catch estimates (Tribuzio et al. 2011: their Appendix 20A; Tribuzio et al. 2014). However, the HFICE incidental catch estimates were generally much larger than the CAS estimates (Table 1); during 2001–2010, the official CAS incidental catch estimates averaged only about 15% of the preliminary HFICE estimates.

Consequently, we used the official CAS incidental catch estimates together with the preliminary HFICE incidental catch estimates to develop a plausible range (low and high values) of Pacific Sleeper Shark incidental catch in the GOA for use in risk analyses (Table 2.2). The low-U scenario was developed from the official CAS incidental catch estimates. The high-U scenario was developed by combining the CAS estimates and the preliminary HFICE incidental catch estimates (Table 2.2). For unknown reasons, both time series of estimated catch declined dramatically beginning in 2008 (Table 2.1).

Exploitable biomass.—A minimum estimate of exploitable biomass for Pacific Sleeper Sharks in the GOA for use in risk analyses was developed from a NMFS-AFSC bottom trawl survey conducted in U.S. federal waters of the GOA ever 2–3 years during 1984–2011 (Table 2.1; Tribuzio et al. 2011: their Table 20.10). The NMFS-AFSC bottom trawl survey utilized a random stratified area-swept survey design to provide estimates of total exploitable biomass for many commercially important groundfish species in federal waters of the GOA (NMFS 2013). The survey also recorded incidentally captured species, including Pacific Sleeper Sharks. However, the NMFS-AFSC bottom trawl survey was not designed to capture Pacific Sleeper Sharks, and therefore very few individuals of this species were captured in the survey (Table 2.1). The efficiency of bottom trawl survey gear for sharks was also unknown; consequently, biomass estimates from the bottom trawl survey should be considered, at best, a relative index of minimum biomass for shark species in the GOA until more formal analyses of survey efficiencies can be conducted (Tribuzio et al. 2011). Furthermore, analysis of NMFS-AFSC bottom trawl exploitable biomass trends in the GOA is subject to the following caveats regarding the consistency of the survey time series. Survey efficiency may have increased for a variety of reasons between 1984 and 1990 but was likely stable after 1990 (Gaichas et al. 1999). Surveys in 1984, 1987, and 1999 included deeper

strata than the 1990–1996 surveys; therefore, biomass estimates for deeper-dwelling species may not be comparable across those years. The 2001 survey did not include all areas of the eastern GOA (Tribuzio et al. 2011: their Table 20.10). Bottom trawl survey estimates of Pacific Sleeper Shark biomass in the GOA increased from 1984 to 2005 and then declined from 2005 to 2011 (Table 2.1).

Exploitation rate scenarios.—A plausible range (low and high) of average annual exploitation rates ($\bar{U}$ = 0.006 and 0.145, respectively; Table 2.2) for GOA Pacific Sleeper Sharks was developed here for use in risk analyses from the available time series of Pacific Sleeper Shark incidental catch and bottom trawl survey biomass estimates for years with overlapping data (2001–2009; Table 2.2) as

$$\bar{U} = \sum_{t=1}^{n_s} \left(Y_t^{\text{obs}} / I_t^{\text{obs}} \right) \Big/ n_s , \tag{2.15}$$

where Y_t^{obs} is an annual estimate of incidental catch; I_t^{obs} is an annual estimate of bottom trawl survey biomass; and n_s is the number of years (5) with overlapping data (t = 2001, 2003, 2005, 2007, and 2009). The low-$\bar{U}$ scenario was developed from the official CAS incidental catch estimates. The high-$\bar{U}$ scenario was developed by combining the CAS and HFICE incidental catch estimates. The annual estimate of bottom trawl survey biomass was assumed to represent a minimum estimate of Pacific Sleeper Shark exploitable biomass in the GOA. Another assumption was that the vulnerability of Pacific Sleeper Sharks to the NMFS-AFSC bottom trawl survey was similar to their vulnerability to the GOA groundfish and Pacific Halibut fisheries, which capture Pacific Sleeper Sharks incidentally.

2.3.3. Life History Scenarios

Sources of life history information that were used to parameterize a plausible range of life history scenarios included the following, in order of preference: (1) the very limited life history data that were available for Pacific Sleeper Sharks in the northeast Pacific Ocean; (2) life history data that were available for large-bodied sleeper sharks *Somniosus* spp. in general; (3) independently estimated relationships among life history parameters that were available for sharks in general (Table 2.3); and (4) independently estimated relationships among life history parameters that were available for aquatic organisms in general (Table 2.3). Sex-specific differences in life history were accounted for when possible, but sex-specific numbers at age and at length were not included in the operating model (Equations 2.1–2.14).

Maximum age.—Age determination has not been feasible for Pacific Sleeper Sharks because their cartilage does not appear to calcify to the same degree as in many other shark species (Tribuzio et al. 2011). In the absence of available age data for this species in the northeast Pacific Ocean, the risk analysis

was implemented with three fixed parameter values for assumed maximum age (A_{max} = 30, 50, and 100 years) based on the range of maximum ages hypothesized for Greenland Sharks (Table 2.4; Hansen 1963; Fisk et al. 2002). Pacific Sleeper Sharks and Greenland Sharks occupy similar habitats and have similar life history characteristics; for example, female length at maturity is similar for Greenland Sharks (~450 cm TL) and Pacific Sleeper Sharks (~370–430 cm TL), and size at birth (~40 cm TL) is also similar between the two species (Ebert et al. 1987; Yano et al. 2007).

Tagging and chemical data (Hansen 1963; Fisk et al. 2002) indicate that Greenland Sharks may be slow growing and long lived. In particular, relative proportions of DDT metabolites in Greenland Sharks suggest that they have a low metabolic activity and a long life span (at least 30–50 years, n = 15; Fisk et al. 2002). Additionally, the relatively small mean FL of the Greenland Sharks examined by Fisk et al. (2002; mean ± SE = 283.6 ± 5.7 cm, n = 15) indicates that they were immature. The approximate sizes at maturity for female (~450 cm TL) and male (~300 cm TL) Greenland Sharks (Yano et al. 2007) were greater than the mean length of the individuals examined by Fisk et al. (2002). Fisk et al. (2002) also noted that the estimated growth rates of Greenland Sharks in Arctic waters were less than 1 cm/year (Hansen 1963), which could mean that a 300-cm Greenland Shark is over 100 years old.

The assumed range in A_{max} (30, 50, and 100 years) was used in the calculation of M, as described below; note that A_{max} differs from the upper age bin (a_{max}) used in the operating model (Equation 2.1). For these simulations, a_{max} was fixed at 150 years, a value that was determined from trial and error as the age bin at which only a small fraction (<1%) of the simulated numbers at age remained in the population under equilibrium conditions for all alternative life history scenarios (Table 2.4).

Natural mortality.—Instantaneous M was obtained analytically from the assumed A_{max} by using Hoenig's (1983) method. The risk analysis was implemented with three fixed values assumed for M (0.150, 0.091, and 0.046), which were obtained from the three A_{max} values (30, 50, and 100 years, respectively; Tables 2.3, 2.4; Hoenig 1983). Hoenig's (1983) method may provide a reasonable "rule of thumb" estimate of M, based on an empirical method, if the only available life history data are maximum age estimates (e.g., Hewitt and Hoenig 2005: their Equation 8). Annual survivorship in the operating model was obtained by fixing the simulated M at each age (M_a; Equation 2.1) equal to the constant M value assumed under each alternative life history scenario (M = 0.150, 0.091, or 0.046; Table 2.4).

Maximum length.—Pacific Sleeper Sharks can attain large sizes (~7 m TL) (Compagno 1984; Mecklenburg et al. 2002). However, few Pacific Sleeper sharks larger than approximately 440 cm TL have been documented (e.g., Compagno 1984; Ebert et al. 1987; Orlov 1999; Wang and Yang 2004; Yano et al. 2004, 2007; Orlov and Baitalyuk 2014). It is possible that the largest sharks are not captured by either fishery or survey gear (i.e., are not vulnerable to the fishing gear) or that the largest sharks occupy different habitat (i.e., are not available to the fishing gear), for example, due to ontogenetic migration

(Grubbs 2010). In contrast, incidental fishing mortality rates in the northeast Pacific region may be high enough to remove the largest sharks from the local population; alternatively, sharks in this region may be smaller because they belong to a distinct population.

Empirical data indicate that in both male and female sharks, length at first maturity (L_{mat}) typically corresponds to roughly 75% of the maximum observed length (L_{max}; Cortés 2000). Consequently, for these simulations, the L_{mat} of Pacific Sleeper Sharks in the GOA was approximated from the assumed L_{50} of female Pacific Sleeper Sharks in the GOA (L_{50} = 365 cm TL), obtained as described below. The value for L_{max} (500 cm TL) was then approximated from L_{mat} based on the independently estimated relationship among the parameters: $L_{max} = (4/3)L_{mat}$ (Tables 2.3, 2.4; Cortés 2000). To allow a small proportion of the simulated population to attain a size of 700 cm TL or larger under each life history scenario (Table 2.4), the age–length transition matrix (Equation 2.8) included normal error in length at age and a CV_{L_a} fixed at 0.2 for all ages (Table 2.4). The value of 0.2 was obtained by trial and error so that a small proportion (<1%) of the simulated population attained sizes of 700+ cm TL at A_{max} under each life history scenario.

Length at age.—Parameter values for the VBGM (Equation 2.7; Table 2.4; Figure 2.2) were developed as follows. First, L_∞ (473 cm TL), the average length that a shark would reach if it grew indefinitely, was obtained from L_{max} (~500 cm TL) by using a previously identified empirical relationship between L_∞ and L_{max} from 551 pairs of parameter values obtained from fish species (Table 3; Froese and Binohlan 2000: their Equation 5).

Second, empirical data indicate that in sharks, there is a significant negative correlation between longevity and the VBGM parameter κ (cm TL/year; Equation 2.7; Cortés 2000). Three fixed values for the assumed κ (0.221, 0.103, and 0.036; Table 2.4) were calculated from the three fixed values for assumed A_{max} (30, 50, and 100 years; Table 2.4) by using an independently estimated relationship (Pauly 1980) that was re-parameterized in terms of the natural logarithm (Table 2.3; Quinn and Deriso 1999: their Equation 8.91b; Tribuzio and Kruse 2012: their Table II). The required parameter value for water temperature (Table 2.4) was obtained as the median ambient water temperature that was occupied by satellite-tagged Pacific Sleeper Sharks in the GOA (5.9°C; range = 5.6–6.5°C, n = 3; Hulbert et al. 2006).

Third, the length at birth for Pacific Sleeper Sharks was assumed to be 40 cm TL (Yano et al. 2007). The VBGM parameter t_0 (Equation 2.7) was calculated analytically from the assumed size at birth (40 cm TL) and the assumed values of L_∞ and κ (Table 2.4; Figure 2.2A).

Weight at length.—An allometric weight-at-length relationship was assumed (Quinn and Deriso 1999). Parameter values were obtained from the combined-sex empirical observations for Pacific Sleeper Sharks (Table 2.3; Yano et al. 2007: their Table I).

Maturity at length.—Empirical data indicate that female sharks typically attain maturity at a larger size and older age than males and that females reach a larger maximum size and older age while growing at a slower rate than males (Cortés 2000). Based on the limited data available for Pacific Sleeper Sharks, mature females are likely to be larger than 365 cm TL, and mature males are likely to be larger than 397 cm TL (Yano et al. 2007). One mature female Pacific Sleeper Shark was apparently identified in the high-latitude northeast Pacific Ocean and was reported to be 430 cm TL (Yano et al. 2007). Those data are consistent with data obtained from (1) the Pacific Ocean off California, where female Pacific Sleeper Sharks may mature at about 370 cm TL (n = 15; Ebert et al. 1987); and (2) the GOA, where all Pacific Sleeper Sharks examined for diet (range = 130–284 cm TL; n = 199; Sigler et al. 2006) were found to be immature (M.F.S., unpublished data). Consequently, alternative parameter values for a logistic maturity-at-length relationship (Equation 2.10) were obtained here by solving numerically for curvature k (0.056; Table 2.4), which resulted in an L_{50} of 365 cm TL, a value of 0.025 for maturity at 280 cm TL, and a value of 0.975 for maturity at 430 cm TL.

2.3.4. Length-Based Selectivity

Size composition data for Pacific Sleeper Shark incidental catch in the GOA were limited because historically most sharks that have been captured incidentally in U.S. federally managed GOA commercial groundfish fisheries have not been measured (Courtney et al. 2006b; Tribuzio et al. 2011). Consequently, length composition of the Pacific Sleeper Shark incidental catch in the GOA was approximated here from available fishery-independent data, which were obtained separately from bottom trawl and bottom longline gear types (see Supplement 2.A).

Using the limited available length composition data, we developed two length-based selectivity scenarios: asymptotic and dome shaped. For each scenario, selectivity was calculated separately from the available length composition data for each gear type (bottom trawl and bottom longline; Supplement 2.A). Proportions at length were calculated from the available length composition data pooled by gear type:

$$P_{l,g}^{\text{obs}} = n_{l,g} \Big/ \sum_{l=1}^{l_{\max}} n_{l,g} \,, \tag{2.16}$$

where $n_{l,g}$ is the total number of sharks measured (observed) in length bin l for each gear type g during all years with available length composition data.

Asymptotic selectivity.—Asymptotic selectivity was calculated by fitting the ascending limb of the observed proportions at length separately for each gear type (bottom trawl and bottom longline) and assuming that lengths larger than the peak were fully selected. Parameter values for asymptotic selectivity

(β and α, Equation 2.9; Table 2.4) were obtained with the exponential-logistic equation by fixing γ (Equation 2.9; Table 2.4) at a value near zero (0.0001) and then minimizing the sum of squared deviations between $\text{sel}_{L,g}$ (Equation 2.9) and $P_{l,g}^{\text{obs}}$ (Equation 2.16) numerically in Microsoft Excel. Differences were minimized for lengths less than or equal to the peak in the observed proportions at length: 200 cm FL for bottom trawl gear and 210 cm FL for bottom longline gear.

Dome-shaped selectivity.—In contrast, for dome-shaped selectivity, the expected stable age distribution of the population per recruit was modeled as

$$P_{0,a}^{\text{exp}} = n_{0,a} \Big/ \sum_{a=1}^{a_{\max}} n_{0,a} \,, \tag{2.17}$$

where $n_{0,a}$ (Equation 2.21) is the equilibrium number at age per recruit in the absence of exploitation, as described below. The expected stable length distribution of the population was then modeled as

$$P_{0,l}^{\text{exp}} = \sum_{a=1}^{a_{\max}} \varphi_{a,l} P_{0,a}^{\text{exp}} \,. \tag{2.18}$$

The parameter $\phi_{a,l}$ was the assumed proportion of sharks from age-group a in length bin l as obtained from the age–length transition matrix (Equation 2.8).

The expected proportion of the population selected at length was then calculated separately for each gear type (bottom trawl and bottom longline) by comparing the proportion at length expected under constant recruitment to the observed proportion at length. Sharks were assumed to be fully selected at the maximum ratio of observed to expected proportions at length. The expected selectivity at each length bin was scaled to a maximum of 1.0 by calculating the ratio of observed to expected proportions at length and dividing by the maximum ratio for each gear type,

$$\text{sel}_{l,g}^{\text{exp}} = \frac{P_{l,g}^{\text{obs}}}{P_{0,l}^{\text{exp}}} \Bigg/ \max\left(\frac{P_{l,g}^{\text{obs}}}{P_{0,l}^{\text{exp}}} \right). \tag{2.19}$$

Parameter values for the dome-shaped selectivity scenario were obtained with the exponential-logistic equation (Equation 2.9) by minimizing the sum of squared deviations between $\text{sel}_{L,g}$ and $\text{sel}_{l,g}^{\text{exp}}$ numerically in Microsoft Excel.

The dome-shaped selectivity scenario was based on the lower bound for the total mortality schedule. Consequently, the expected stable length distribution of the population (Equation 2.17) was calculated with M fixed at 0.150 year^{-1} (alternative life history scenario 1; Table 2.4). The a_{max} (Table 2.4) was truncated from 150 years to 50 years in Equations (2.17) and (2.18) in order to simplify the dome-shaped selectivity calculations.

Length-based selectivity of incidental catch.—Length-based selectivity of the incidental Pacific Sleeper Shark catch in the GOA commercial groundfish fishery ($sel_{f,l}$; Equations 2.2 and 2.4) was approximated as the weighted average of the selectivity curves developed separately for bottom trawl and bottom longline data (Figure 2.3). Weights were the percentages of total incidental catch (metric tons) of Pacific Sleeper Sharks by commercial bottom trawls (43%) and commercial bottom longlines (57%) in GOA groundfish fisheries during 1990–2001 (adapted from Gaichas et al. 1999; Gaichas 2002; Courtney et al. 2006b).

2.3.5. Initial Conditions

Initial conditions were based on a common approach used in age–length-structured stock assessments, as described by Wetzel and Punt (2011a).

Equilibrium total spawning stock biomass per recruit.—Unexploited equilibrium female spawning stock biomass (mature female biomass) per recruit (males and females combined) was determined analytically (Brooks et al. 2010: their Equation 2) as

$$\varphi_0 \equiv \frac{S_0}{R_0} = \sum_{l=1}^{l_{\max}} w_l m_l \sum_{a=1}^{a_{\max}} \phi_{a,l}\, 0.5\left(n_{0,a} e^{(-\tau_M M_a)}\right), \tag{2.20}$$

where $n_{0,a}$ (Equation 2.21) is the equilibrium survival to age a per recruit; the value 0.5 represents the assumed proportion of female pups and is required to achieve the ratio of female spawners per average recruit (per capita); $\phi_{a,l}$ is the assumed proportion of sharks from age-group a in length bin l obtained from the age–length transition matrix (Equation 2.8); m_l is the proportion of females mature at the beginning of length bin l; w_l is the predicted weight at the middle of length bin l (Table 2.4); and τ_M is the fraction of M that is expected to occur from the beginning of the year (January 1) to the beginning of the pupping season. In the absence of data on the seasonality or periodicity of pup production in Pacific Sleeper Sharks, pupping was arbitrarily assumed to occur annually over a short period near the middle of each calendar year ($\tau_M = 0.5$), as described above.

The parameter $n_{0,a}$ was determined analytically from the assumed life history as the proportion of each age-class (i.e., average recruit) surviving to the beginning of age a and was modeled here as

$$n_{0,a} = \begin{cases} 1 & a = 1 \equiv r \\ e^{-\sum_{j=1}^{a-1} M_j} & 1 < a < a_{\max} \\ e^{-\sum_{j=1}^{\infty} M_j} = \left(e^{-\sum_{j=1}^{a_{\max}-1} M_j} \Big/ \left(1 - e^{-M a_{\max}}\right) \right) & a = a_{\max} \end{cases} . \quad (2.21)$$

For these simulations, the age-specific natural mortality rate M_j was fixed at the constant M value assumed under each alternative life history scenario (M = 0.150, 0.091, or 0.046; Table 2.4).

Unexploited equilibrium conditions.—The unfished equilibrium number at age ($N_{0,a}$; Equation 2.1) was obtained as $R_0 \times n_{0,a}$. The absolute size of the population was unknown. As a result, the value for the equilibrium recruitment parameter R_0 was assumed to be unknown and was set equal to 1.0 for all model configurations (with units defined as thousands of recruits). Assuming that the virgin population had a stable age distribution and given the arbitrary value used for R_0 as defined above, the corresponding value for S_0 was obtained from the unexploited spawning biomass per recruit as

$$S_0 = R_0 \phi_0 . \quad (2.22)$$

Annual recruitment deviations.—Preliminary risk analysis results were evaluated over a range of lognormal recruitment SDs (σ_R; the magnitude of process error, Equation 2.11) equal to 0.1, 0.2, and 0.4 (Punt and Walker 1998: their Table 2; Simpfendorfer et al. 2000: their section 2.5; Wiedenmann et al. 2013: their Table 2). However, results from preliminary operating model runs with 100 Monte Carlo simulations were not sensitive to the range of σ_R values. Consequently, the final risk analysis (n = 1,000 Monte Carlo simulations) was conducted with σ_R fixed at 0.4. This value was chosen in order to include the broadest range of process error in the risk analysis and was consistent with values evaluated in other simulation analyses for elasmobranchs (Pribac et al. 2005: their page 270).

Nonequilibrium initial conditions.—To allow simulated S to vary among simulations depending upon random recruitment deviations, a nonequilibrium starting population was created by applying the operating model without exploitation for an initialization period (Wetzel and Punt 2011a). To account for the potential longevity of Pacific Sleeper Sharks, the initialization period was fixed at 100 years for all simulations. The value of female spawning biomass at the end of the initial period ($\tilde{S}_{t=100}$) was defined as the nonequilibrium virgin spawning biomass for that simulation run. Exploitation was then implemented for years t = 101–200 (i.e., a period of 100 years). Simulations were summarized as the ratio of female

spawning biomass at the end of the exploitation period ($\tilde{S}_{t=200}$) relative to the nonequilibrium female spawning biomass prior to the start of exploitation (i.e., $\tilde{S}_{t=100}$), calculated here as $\tilde{S}_{t=200}/\tilde{S}_{t=100}$.

2.3.6. Simulations

The risk analysis was conducted using 1,000 Monte Carlo simulations of the operating model under recruitment variability (Equations 2.1–2.14) for 24 alternative model configurations, which resulted from all possible combinations of alternative assumptions about $\bar{U}$ (0.006 or 0.145; Equation 2.15; Table 2.2), life history (A_{max} = 30, 50, or 100 years), stock–recruitment steepness (h = 0.25 or 0.39), and length based selectivity (asymptotic or dome shaped; Table 2.4).

The approximate U_{MSY} and the S corresponding to U_{MSY} (S_{MSY}) were obtained for each model configuration by employing a grid search (Appendix 2.A). The grid search used the same operating model as the simulations (Equations 2.1–2.14) except that the grid search was conducted without recruitment variability over a range of trial values for equilibrium exploitation (U_{trial}) in increments of 0.001. For each alternative model configuration, the equilibrium stock size in the absence of exploitation (S_0) was obtained with U_{trial} fixed at zero (without recruitment variability). The equilibrium reference point for spawning stock biomass at MSY was then obtained as S_{MSY}/S_0.

Fraction of simulations ending in an overfished condition.—A simulation was defined to have ended in an overfished condition if the ratio $\tilde{S}_{t=200}/\tilde{S}_{t=100}$ was less than one-half the ratio S_{MSY}/S_0. Simulation results were then summarized as the fraction of simulations that ended in an overfished condition: $\tilde{S}_{t=200}/\tilde{S}_{t=100} < 0.5 \times (S_{\mathrm{MSY}}/S_0)$. Simulation results were also summarized for intermediate simulation years (t = 101–200) in order to determine how quickly the stock status ($\tilde{S}_t/\tilde{S}_{t=100}$) changed in relation to the overfished threshold ($0.5 \times [S_{\mathrm{MSY}}/S_0]$) under each alternative model configuration.

Fraction of model configurations in an overfishing condition.—A model configuration was defined as being in an overfishing condition if $\bar{U}$ exceeded U_{MSY}. The value of $\bar{U}$ was obtained with Equation (2.15), and the value of U_{MSY} was obtained based on the operating model implemented under equilibrium conditions without recruitment variability (Appendix 2.A) under each alternative model configuration.

Model sensitivity to assumptions about key model parameters.—Model sensitivity was evaluated from the aggregate number (and proportion) of simulations that ended in an overfished condition, $\tilde{S}_{t=200}/\tilde{S}_{t=100} < 0.5 \times (S_{\mathrm{MSY}}/S_0)$, and the aggregate number (and proportion) of model configurations that were in an overfishing condition, $\bar{U} > U_{\mathrm{MSY}}$, under each alternative $\bar{U}$ (0.006 or 0.145; Equation 2.15;

Table 2.2), life history (A_{max} = 30, 50, or 100 years), stock–recruitment steepness (h = 0.25 or 0.39), and length based selectivity (asymptotic or dome shaped; Table 2.4).

2.4. Results

2.4.1. Selectivity

The approach used here to model selectivity resulted in two length-based selectivity scenarios (asymptotic and dome shaped) for use in the risk analysis. The asymptotic selectivity scenario assumed that a relatively wide range of immature and mature shark lengths were selected by the fishery and by the survey gear types (bottom trawl and bottom longline; Figure 2.3A). In contrast, the dome-shaped selectivity scenario assumed that a relatively narrow range of immature shark lengths was selected by the fishery and by the two survey gear types (Figure 2.3B). Plots of the resulting length-based selectivity curves relative to the available length composition data are provided in Supplement 2.B.

2.4.2. Overfished Condition

The percentage of simulations (Equations 2.1–2.14) that ended in an overfished condition, $\tilde{S}_{t=200}/\tilde{S}_{t=100} < 0.5 \times (S_{MSY}/S_0)$, was very low (0.0%) for all alternative model configurations that were evaluated under the low $\bar{U}$ (0.006; Table 2.5, odd-numbered model configurations). In contrast, the percentage of simulations that resulted in an overfished condition was very high (100.0%) for all alternative model configurations that were evaluated under the combination of a high $\bar{U}$ (0.145) and asymptotic selectivity (Table 2.5, model configurations 4, 8, 12, 16, 20, and 24). The percentage of simulations resulting in an overfished condition also increased (0.1, 6.3, and 99.8%) with increasing A_{max} (30, 50, and 100 years, respectively) for alternative model configurations that were evaluated under the combination of a relatively low h (0.25), dome-shaped selectivity, and a high $\bar{U}$ (Table 2.5, model configurations 2, 10, and 18, respectively).

2.4.3. Intermediate-Year Overfished Results

Examples of overfished results for intermediate simulation years (t = 101–200) are provided for some of the alternative model configurations. For instance, model configurations 1 and 3 (Table 2.5) were typical of alternative model configurations evaluated under the low $\bar{U}$, which did not result in any simulations in an overfished condition after 100 years of exploitation (t = 200; Figures 2.4, 2.5A). Alternative model configuration 2 (Table 2.5; Figure 2.4B) was typical of alternative configurations that were evaluated under the combination of a relatively low h, dome-shaped selectivity, and a high $\bar{U}$

(model configurations 2, 10, and 18), which resulted in some simulations in an overfished condition after less than 100 years of exploitation ($t < 200$). Alternative model configuration 4 (Table 2.5; Figure 2.5B) was representative of alternative model configurations that were evaluated under the combination of a high $\bar{U}$ and asymptotic selectivity (model configurations 4, 8, 12, 16, 20, and 24), which resulted in a high fraction of simulations in an overfished condition after relatively few years of exploitation ($t < \sim 125$). Plots of intermediate-year overfished results ($t = 101–200$) for each alternative model configuration (Table 2.5) are provided separately in Supplement 2.B.

2.4.4. Overfishing Condition

The pattern of alternative model configurations that were determined to be in an overfishing condition ($\bar{U} > U_{\mathrm{MSY}}$; Appendix 2.A) was similar to the pattern of alternative model configurations that resulted in an overfished condition. For example, only one alternative model configuration that was evaluated under the low $\bar{U}$ (0.006) led to an overfishing condition under equilibrium conditions (Table 2.5, model configuration 19). In contrast, all of the alternative model configurations that were evaluated under the combination of a high $\bar{U}$ and asymptotic selectivity resulted in an overfishing condition under equilibrium conditions (Table 2.5, model configurations 4, 8, 12, 16, 20, and 24). Three alternative model configurations that were evaluated under the combination of a relatively low h (0.25), dome-shaped selectivity, and a high $\bar{U}$ also produced an overfishing condition under equilibrium conditions (Table 2.5, model configurations 2, 10, and 18). In addition, one alternative model configuration that was evaluated under the combination of a relatively high h (0.39), dome-shaped selectivity, and a high $\bar{U}$ resulted in an overfishing condition under equilibrium conditions (Table 2.5, model configuration 22).

2.4.5. Model Sensitivity to Overfished and Overfishing Determinations

The aggregate results for the overfished designation, $\tilde{S}_{t=200} / \tilde{S}_{t=100} < 0.5 \times (S_{\mathrm{MSY}}/S_0)$, were most sensitive to uncertainty in $\bar{U}$ (0.006 or 0.145; Equation 2.15; Table 2.6). The aggregate proportion of simulations ending in an overfished condition after 100 years of exploitation increased from 0.0% under the low-$\bar{U}$ scenario to 59% under the high-$\bar{U}$ scenario (Table 2.6). The aggregate results were also sensitive to the shape of the length-based selectivity curve (Table 2.6). The aggregate proportion of simulations that ended in an overfished condition increased from 9% under the domeshaped selectivity scenario to 50% under the asymptotic selectivity scenario (Table 2.6). The aggregate results for the overfished determination were less sensitive to the range of values evaluated for A_{max} (30, 50, and 100 years) and h (0.25 and 0.39). However, as expected, the aggregate proportion of simulations that ended in

an overfished condition increased with increasing A_{max} (30, 50, and 100 years) and with decreasing h (0.39 and 0.25; Table 2.6).

Similarly, the overfishing results obtained under equilibrium conditions ($\bar{U} > U_{\mathrm{MSY}}$; Appendix 2.A) were also most sensitive to uncertainty in $\bar{U}$ (0.006 or 0.145; Equation 2.15; Table 2.6). The aggregate number of model configurations determined to be in an overfishing condition increased from 1 of 12 (8.3%) under the low-$\bar{U}$ scenario to 10 of 12 (83%) under the high-$\bar{U}$ scenario (Table 2.6). The aggregate number of model configurations that produced an overfishing condition increased from 4 of 12 (33%) under the dome-shaped selectivity scenario to 7 of 12 (58%) under the asymptotic selectivity scenario (Table 2.6). The fraction of simulations ending in an overfishing condition also increased with increasing A_{max} (30, 50, and 100 years) and with decreasing h (0.39 and 0.25; Table 2.6).

2.5. Discussion

Determining the risk associated with the incidental exploitation of Pacific Sleeper Sharks in the GOA is important because elasmobranchs may be more vulnerable to overfishing than the teleost target species with which they are captured (Smith et al. 1998; Forrest and Walters 2009; Kyne and Simpfendorfer 2010). Changes in elasmobranch abundance may be indicative of or may in response to ecosystem-level restructuring after the effects of fishing (Kitchell et al. 2002; Myers et al. 2007; Baum and Worm 2009); sharks may function as keystone predators and therefore would be essential to the maintenance and stability of food webs (Myers et al. 2007). In the high-latitude northeast Pacific Ocean, changes in the relative abundance of Pacific Sleeper Sharks could have both direct trophic effects on the ecosystem (Yang and Page 1999; Hulbert et al. 2006; Sigler et al. 2006; Yano et al. 2007; Courtney and Foy 2012; Horning and Mellish 2012, 2014) and indirect effects on the ecosystem, mediated through the behavioral responses of potential prey (Frid et al. 2006, 2007a, 2007b, 2008, 2009; Heithaus et al. 2008, 2010; Wirsing et al. 2008; Kuker and Barrett-Lennard 2010).

The risk analysis results presented here (percentage of simulation runs ending in an overfished condition) were most sensitive to the range of uncertainty identified for the incidental exploitation rates of Pacific Sleeper Sharks in the GOA ($\bar{U}$ = 0.006 or 0.145; Equation 2.15; Tables 2.2, 2.5, 2.6). Depending upon which incidental catch data set was chosen for use in the plausible U calculation (Table 2.2), the aggregate risk of ending in an overfished condition increased from 0.0% under the low-$\bar{U}$ scenario to 59% under the high-$\bar{U}$ scenario (Table 2.6). This result is informative for management. On the one hand, the low-$\bar{U}$ scenario (Equation 2.15; Table 2.2) was based on the official CAS estimates of Pacific Sleeper Shark incidental catch in the GOA (Table 2.1). On the other hand, the high-$\bar{U}$ scenario (Equation 2.15; Table 2.2) was based on (1) preliminary HFICE estimates of Pacific Sleeper Shark incidental catch in

previously unobserved GOA Pacific Halibut fisheries plus (2) the official CAS estimates of Pacific Sleeper Shark incidental catch in the GOA (Table 2.1). Both of the exploitation rate scenarios assumed that the NMFS-AFSC bottom trawl survey represented a minimum estimate of Pacific Sleeper Shark exploitable biomass in the GOA.

Consequently, a priority for management is to reduce the uncertainty in U for GOA Pacific Sleeper Sharks. A restructured at-sea scientific observer program has been authorized (Amendment 76 to the Fishery Management Plan for Groundfish of the GOA; U.S. Office of the Federal Register 2012) to monitor the historically unobserved GOA Pacific Halibut fishery and is intended to provide estimates of nontarget species catch in the future. Methods for estimating the historical catch of nontarget species from previously unobserved Pacific Halibut fisheries are also under development (Tribuzio et al. 2014). The utility of the simulation approach developed here is that it can be periodically updated as new data become available. For example, it may be informative to re-evaluate the range of U-values assumed for Pacific Sleeper Sharks in the GOA once official catch estimates become available for the previously unobserved Pacific Halibut fishery.

However, historical values of U for Pacific Sleeper Sharks in the GOA are likely to remain uncertain. For example, a range of incidental groundfish catch estimates has been developed for the previously unobserved Pacific Halibut fishery prior to 2013 (Tribuzio et al. 2014), but the range in Pacific Sleeper Shark incidental catch estimates is very large (Tribuzio et al. 2014). In addition, reconstruction of the historical incidental catch of sharks in GOA commercial groundfish fisheries has not been attempted for years prior to 1990, although GOA catch statistics are available for commercial groundfish target species beginning in 1956 (NMFS 2013) and for Pacific Halibut beginning in 1929 (Thompson and Freeman 1930; Myhre et al. 1977; Clark and Hare 2006). Post-release survival rates of Pacific Sleeper Sharks captured by specific gear types have not been investigated (e.g., Morgan and Burgess 2007; Braccini et al. 2012) and are currently assumed to be negligible.

The assumption that data from the NMFS-AFSC bottom trawl survey represent a minimum estimate of Pacific Sleeper Shark exploitable biomass in the GOA has not been evaluated. As mentioned above, the NMFS-AFSC bottom trawl survey was not designed to capture Pacific Sleeper Sharks, and very few individuals of this species have been captured during the survey (Table 2.1; Tribuzio et al. 2011). Because Pacific Sleeper Sharks are large animals, they may be able to actively avoid bottom trawl survey gear. Pacific Sleeper Sharks also occur in the upper water column (Hulbert et al. 2006; Courtney and Hulbert 2007) as well as near the demersal zone. As mentioned above, both time series of estimated catch (CAS and HFICE) used in these simulations declined dramatically beginning in 2008 for unknown reasons (Table 2.1). By comparison, bottom trawl survey estimates of Pacific Sleeper Shark biomass in the GOA increased from 1984 to 2005 and then declined from 2005 to 2011 but at a more gradual rate

(Table 2.1). However, we attempted to limit the effects of interannual variability observed in the incidental catch estimates and the biomass estimates by calculating an average historical U under each scenario (Equation 2.15; Table 2.2).

Because of the aforementioned limitations in the available data necessary to accurately calculate historical U for Pacific Sleeper Sharks in the GOA, it may be informative to compare the results obtained via the simulation approach developed here with results that have been obtained by other data-limited methods for determining stock status (e.g., Carruthers et al. 2014; Berkson and Thorson 2015; Newman et al. 2015). For example, fishery-independent surveys conducted by the International Pacific Halibut Commission (IPHC) may capture a relatively large number of Pacific Sleeper Sharks annually over a larger geographic area in the GOA than other fishery independent surveys in the region (Tribuzio et al. 2011). Consequently, it may be informative to continue the development of Pacific Sleeper Shark relative abundance indices from fishery-independent IPHC surveys (e.g., Menon 2004; Menon et al. 2005; Tribuzio et al. 2011) for use as indicators of the relative stock status of Pacific Sleeper Sharks in the GOA, analogously to indices explored previously from other fishery independent surveys (Mueter and Norcross 2002; Courtney and Sigler 2007), while taking into consideration the effects of the survey sampling design on gear saturation and hook competition among different species captured in longline surveys (Rodgveller et al. 2008).

Our risk analysis results were sensitive to the assumed shape of the length-based selectivity curve (asymptotic versus dome shaped; Tables 2.5, 2.6). The percentage of simulations that ended in an overfished condition was very low (0.0%) for all alternative model configurations evaluated under a low $\bar{U}$ (0.006; Table 2.5, odd-numbered model configurations), regardless of whether the length-based selectivity curve was assumed to be asymptotic or dome shaped. However, the percentage of simulations resulting in an overfished condition was very high (100.0%) for all alternative model configurations that were evaluated under the combination of a high $\bar{U}$ (0.145) and asymptotic selectivity (Table 2.5, model configurations 4, 8, 12, 16, 20, and 24). The asymptotic selectivity scenario (Figure 2.3A) was based on the assumption that lengths larger than the peak in available length composition data were fully selected, as described above. In contrast, the domeshaped selectivity scenario (Figure 2.3B) was based on the assumption that the incidental exploitation rate was low enough to have had a negligible effect on the stable length distribution of the population.

The dome-shaped selectivity scenario was most consistent with the available length composition data. In particular, the relatively narrow range of lengths that were selected under the dome-shaped selectivity scenario was consistent with the relatively narrow range observed in the available fishery-independent length frequency data collected for this study (see Supplement 2.A). Consequently, the ontogenetic migration of larger-sized Pacific Sleeper Sharks from the GOA is a distinct possibility.

However, it is also possible that relatively large sharks are captured incidentally in the commercial fisheries but are not reported. For example, on large bottom trawl vessels, the sharks may be pre-sorted by the fishing crew and removed from the catch before they can be measured; on commercial longline fishing vessels, they may be removed from or may drop off the bottom longline gear before they can be observed or measured.

The hypothesis that Pacific Sleeper Sharks in the high latitude northeast Pacific Ocean are smaller because they belong to a distinct population was not investigated. However, the implications of this hypothesis for stock status results could be investigated within the current simulation framework—for instance, by systematically reducing the CV_{L_a} from the assumed value of 0.2 to a smaller value (Table 2.4).

The risk analysis results were less sensitive to the assumed range of A_{max} (30, 50, and 100 years) and stock productivity (h = 0.39 and 0.25) than to the assumed range in plausible $\bar{U}$-values or to length-based selectivity (Tables 2.5, 2.6). However, a critical assumption used in these simulations was that the A_{max} of Pacific Sleeper Sharks was similar to the A_{max} hypothesized for Greenland Sharks. Consequently, the parameter values we developed for Pacific Sleeper Shark M should be interpreted cautiously because they depended upon both an assumed A_{max} and an independently estimated analytical relationship between M and A_{max} that was obtained from the scientific literature (Hoenig 1983). Because Hoenig (1983) did not include data from shark species (e.g., Tribuzio and Kruse 2012), his method may result in higher estimates of M for sharks relative to other life-history-invariant methods (McAuley et al. 2007). Many other empirical relationships (Alverson and Carney 1975; Pauly 1980; Gunderson and Dygert 1988; Lorenzen 1996) and theoretical relationships (Peterson and Wroblewski 1984; Chen and Watanabe 1989; Charnov et al. 1993; Jensen 1996) that are commonly used to determine M analytically from life history invariants were not explored here because they require life history data that were not available for Pacific Sleeper Sharks.

An update of Hoenig's (1983) method is available from a recent study by Then et al. (2015), who focused on improving the point estimation of M for teleosts and elasmobranchs. Then et al. (2015) recommended the relationship $M_{estimated} = 4.899A_{\max}^{-0.916}$ when only an estimate of A_{max} is available. Applying the updated relationship from Then et al. (2015) to the current simulations would result in estimated M values of 0.217 for an A_{max} of 30 years, 0.136 for an A_{max} of 50 years, and 0.072 for an A_{max} of 100 years. The above M-estimates obtained with the updated relationship (Then et al. 2015) for A_{max} of 50 and 100 years are similar to those used in current simulations for A_{max} of 30 and 50 years (M = 0.150 and 0.091, respectively). Consequently, the expected outcome of applying the updated relationship

between M and A_{max} (Then et al. 2015) in this study would be a lower proportion of simulations ending in an overfished condition.

Similarly, individual growth rate was modeled from M and temperature by using Pauly's method (Pauly 1980; Quinn and Deriso 1999). Pauly's method was chosen because of the extremely cold temperatures occupied by Pacific Sleeper Sharks in the GOA (5.9°C; range = 5.6–6.5°C, n = 3; Hulbert et al. 2006). However, an update of Pauly's method is also available from Then et al. (2015), who recommended the relationship $M_{estimated} = 4.118\kappa^{0.73}L_{\infty}^{-0.33}$ when an estimate of A_{max} is unavailable. Then et al. (2015) reported that (1) the temperature coefficient changed substantially when estimated with their updated data set and (2) the inclusion or exclusion of temperature was not a useful predictor of M with the updated data set, perhaps because of species-specific differences in the response to temperature or because mean temperature was not well estimated. An updated relationship for allometric weight (kg) at a given body length (cm TL) is also available for Pacific Sleeper Sharks in the North Pacific Ocean (Orlov and Baitalyuk 2014: their Figure 11; e.g., for both sexes combined, $w_L = 6.03x10^{-5}L^{2.695}$, $R^2 = 0.701$, $n = 905$) but was not investigated here. Consequently, if uncertainty in Pacific Sleeper Shark $\bar{U}$ within the GOA can be reduced in the future, then it might be informative to re-evaluate the sensitivity of our simulation results to the recently updated, independently estimated relationships among life history parameters (e.g., Orlov and Baitalyuk 2014; Then et al. 2015).

It might also be informative to explore model sensitivity to intermediate $\bar{U}$-values so as to obtain the central tendency of a distribution of results. However, it would first be necessary to define probability distributions for the full range of uncertainty identified in each key model parameter ($\bar{U}$, A_{max}, h, and selectivity; Tables 2.2, 2.4). Furthermore, it would be important to identify potential biases in the assumed model processes, such as the stock–recruitment relationship and the independently estimated life history relationships (Table 2.3), since those biases would make it difficult to develop informative probability distributions for the uncertainty in key model parameters. In any case, the distribution of results obtained from such an exercise would be expected to fall somewhere within the range of the results obtained here.

The implementation of a constant U in these simulations (Equations 2.1–2.14) did not account for the possibility of historical changes in fishing effort for commercial groundfish target species (NMFS 2013) or for Pacific Halibut (Clark and Hare 2006). Similarly, these simulations did not specifically account for the possibility of historical changes in productivity, such as those resulting from regime shifts. There is evidence of increased groundfish recruitment success in the high-latitude northeast Pacific Ocean after a climatic regime shift in 1976 (Hollowed and Wooster 1992; Francis et al. 1998; Wooster and Zhang 2004). This regime shift triggered a substantial change in fish communities of the northeast Pacific

Ocean and Bering Sea (e.g., Hare and Mantua 2000; Aydin and Mueter 2007; Mueter et al. 2007). Due to the Pacific Sleeper Shark's assumed long life, low fecundity, and slow growth rates, significant changes in Pacific Sleeper Shark relative abundance (Mueter and Norcross 2002; Courtney and Sigler 2007) as a response to prey availability in the GOA may have taken longer to become apparent than the changes in groundfish abundances. Similarly, as opportunistic consumers of available prey and carrion, Pacific Sleeper Sharks in the northeast Pacific Ocean could also exhibit fluctuating relative abundance trends in response to the relative availability of carrion from diverse sources ranging from fishery waste (Orlov and Baitalyuk 2014) to whale falls (Smith and Baco 2003; Schaufler et al. 2005; Smith 2006).

Our simulations did not specifically account for uncertainty in Pacific Sleeper Shark reproductive biology. As noted above, the reproductive biology of this species in the northeast Pacific Ocean is largely unknown. Fecundity estimates for large-bodied sleeper sharks *Somniosus* spp. range from about 8–10 pups/litter (Ebert et al. 1987; Yano et al. 2007; Kyne and Simpfendorfer 2010) to more than 300 pups/litter (Ebert and Winton 2010). However, the evidence for litter sizes larger than 10 is based on the presence of a high number (>300) of large, vascularized ovarian eggs (Ebert et al. 1987; Yano et al. 2007; Ebert and Winton 2010; Kyne and Simpfendorfer 2010). It is unclear how many of these ovarian eggs are shed into the oviduct at a time (Ebert et al. 1987; Kyne and Simpfendorfer 2010). By comparison, ovary mass and oocyte diameter may vary widely throughout the year in other deep-water sharks (e.g., Baremore 2010). Reproductive output in deep-water hexanchoid and squalid sharks is generally limited but can be up to 108 pups/litter in the Bluntnose Sixgill Shark *Hexanchus griseus* (Kyne and Simpfendorfer 2010), a large-bodied (~480 cm TL), mostly deep-water shark that occurs in the northeast Pacific Ocean (Compagno 1984). In contrast, the average fecundity of Pacific Spiny Dogfish in the GOA is about 8.0 ± 4 pups/litter (mean ± SD; Tribuzio and Kruse 2012).

Empirical data (Cortés 2000) indicate that litter size in sharks tends to be constrained by size of the female body cavity and the energetic requirements of producing large, live young and that larger species tend to have more and larger pups. However, the same study (Cortés 2000) also indicated that a tradeoff exists between litter size and offspring size after the effects of body size are factored out; this tradeoff can be grouped into at least two broad categories. The first category is mainly characterized by species with large litter sizes (median = 41 pups; range = 31–135 pups), variable but generally high longevity (median = 17 years; range = 9–53 years), intermediate to large body size (median = 244 cm TL; range = 155–450 cm TL), small offspring size (median = 39 cm TL; range = 20–78 cm TL), and fairly slow growth (median $\kappa = 0.117$; range = 0.07–0.25; Cortés 2000). Species in this first group can be exemplified by the Blue Shark *Prionace glauca*, a pelagic species that invests in a large number of small young, for which the size at birth represents a low percentage of their maximum size (Cortés 2000). The second category encompasses large species (median = 371 cm TL; range 234–640 cm TL) with large

offspring (median = 85 cm TL; range = 62.5–174 cm TL), a reduced litter size (median = 10 pups; range = 2–14 pups), slow growth (median $\kappa = 0.08$; range = 0.04–0.12), and generally high longevity (median = 22 years; range = 14–39 years; Cortés 2000). Species in the second group include large, slow-growing species such as the Dusky Shark *Carcharhinus obscurus*, which produces a limited number of large pups (Cortés 2000). It is unclear whether the Pacific Sleeper Shark belongs to either of these categories, or to any of the other species groupings identified along the continuum of traits evaluated in Cortés (2000). Consequently, further research should be encouraged on the reproductive correlates identified above (longevity, body size, offspring size, or growth rate) in order to help inform the plausible range of Pacific Sleeper Shark litter size (e.g., species with an intermediate to large body size and a large litter size; or species with a large body size and a reduced litter size).

The reproductive periodicity of Pacific Sleeper Sharks is unknown. However, the high energetic demands associated with the presence of large, vascularized ovarian eggs suggest the possibility of a lengthy reproductive cycle (e.g., Kyne and Simpfendorfer 2010). Biennial or triennial reproductive cycles are plausible for many deep-water shark species (Kyne and Simpfendorfer 2010). For example, deep-water sharks often exhibit a resting period between parturition and the next ovulation, thus extending the reproductive cycle (Kyne and Simpfendorfer 2010). A biennial reproductive cycle has been observed in Pacific Spiny Dogfish within the GOA (Tribuzio and Kruse 2012). The seasonality of the Pacific Sleeper Shark's reproductive cycle is also unknown. Many deep-water species exhibit non-seasonal reproductive cycles that are asynchronous among the population (Kyne and Simpfendorfer 2010). In comparison, Pacific Spiny Dogfish in the GOA potentially give birth from August to November (Tribuzio and Kruse 2012).

Due to the lack of information on the reproductive biology of Pacific Sleeper Sharks in the northeast Pacific Ocean, we assumed that S_t (Equation 2.14) was proportional to annual pup production. The sensitivity of this assumption could be evaluated within the framework of the current operating model. For example, a biennial reproduction cycle could be modeled as $0.5 \times S_t$ (Equation 2.14), which assumes that half of the females reproduce annually. A triennial reproduction cycle could be modeled as $(1/3) \times S_t$ (Equation 2.14). Similarly, because the seasonality of pup production in Pacific Sleeper Sharks is unknown, pupping was assumed to occur over a short period near the middle of each calendar year (~June 1; Equation 2.14).

The expected outcome from changing the scale of S_t (Equation 2.14) would be minimal because of the corresponding change in the scale of S_0 (obtained as $S_0 = R_0\varphi_0$; Equation 2.22) and in the scale of S_{MSY} (obtained as in Appendix 2.A). Consequently, S_{MSY}/S_0 would not be expected to change substantially, although we did not explicitly test this. Such a result is expected because stock productivity in the operating model was determined primarily from the assumed shape of the Beverton–Holt stock–

recruitment relationship obtained under alternative assumptions about h (Equations 2.12, 2.13; Table 2.4). Consequently, it may be more important to evaluate the sensitivity of these simulation results to the assumed shape of the Beverton–Holt stock–recruitment relationship (Equation 2.11), such as in comparison with a survival-based stock–recruitment relationship (Taylor et al. 2013).

The present simulation approach used a grid search to determine the overfishing reference point (U_{MSY}) that maximized the yield per recruit based on the combined effects of length-based selectivity and excess recruitment under equilibrium conditions (Appendix 2.A). The overfished reference point was then set equal to $0.5 \times (S_{MSY}/S_0)$. This approach was intended to be similar to the NPFMC's Tier 3 overfished reference point, which is defined as the instantaneous fishing mortality rate (F) that will reduce the ratio of equilibrium spawning biomass per recruit (i.e., %SPR) to 35% of its unfished equilibrium level ($F_{35\%}$; NMFS 2013; e.g., Clark 1991, 2002; Brodziak 2002). Under NPFMC Tier 3, a stock is defined as undergoing overfishing if the current F exceeds $F_{35\%}$ (NMFS 2013). A stock is deemed to be overfished if (1) the current S is below one-half the spawning stock biomass obtained at $F_{35\%}$ ($S_{35\%}$) or (2) the current S is below $S_{35\%}$ and is also projected to be below $S_{35\%}$ in 10 years (at the target F; NMFS 2013). Within this context, $F_{35\%}$ has been used as an approximation of the fishing mortality rate at MSY (F_{MSY}) for some groundfish species in U.S. waters off Alaska (Clark 1991, 2002; Brodziak 2002).

A difference here is that the overfishing reference point under NPFMC Tier 3 (i.e., F35%) is based on the biological reference point (BRP) of an equilibrium %SPR, whereas the overfishing reference point used in our simulations (U_{MSY}) was determined directly under assumed equilibrium conditions (Appendix 2.A). In general, %SPR reference points are preferred because they may be more robust to uncertainty than other BRPs; however, %SPR reference points can still be influenced by uncertainty about life history parameters and fishing practices (Tsai et al. 2011). For example, %SPR limit reference points as high as $F_{60\%SPR,unfished}$ have been recommended for comparison with F_{MSY} for relatively data-poor, understudied elasmobranch populations in cases where the stock–recruitment relationship is highly uncertain (Clarke and Hoyle 2014). In addition, maximum sustainable values of U are closely linked to stock productivity for teleosts (e.g., Mangel et al. 2010, 2013) and sharks (Brooks and Powers 2007; Forrest et al. 2008; Forrest and Walters 2009; Brooks et al. 2010; Taylor et al. 2013). Consequently, an age-structured operating model approach was employed here along with an explicitly defined stock–recruitment relationship (Equations 2.1–2.14). The U_{MSY} was then approximated indirectly from the assumed stock–recruitment h-value separately for each alternative model configuration under equilibrium conditions by using a grid search (Appendix 2.A; Table 2.5). Within this context, the grid search employed here for U_{MSY} (Appendix 2.A) appeared to provide a reasonable overfishing U reference point for the operating model within the evaluated range of key model parameters because it accounted for the

combined effects of exploitation under length-based selectivity and stock–recruitment steepness on stock productivity in the calculation of MSY.

Another difference here is that the overfished reference point used in the present simulations did not consider the case in which S is below S_{MSY} in the current year and additionally is projected to be below S_{MSY} in 10 years (at the target F), analogous to the second half of the NPFMC Tier 3 approach described above (NMFS 2013). However, this could also be accomplished within the framework of the current operating model (Equations 2.1–2.14)—for example, by re-defining simulation year t = 190 as the "current" year and simulation year t = 200 as the 10-year projection interval from the current year. Within this context, the overfished reference point in the simulations conducted here could be re-defined as either $(\tilde{S}_{t=190}/\tilde{S}_{t=100}) < 0.5 \times (S_{MSY}/S_0)$ or $(\tilde{S}_{t=190}/\tilde{S}_{t=100}) < (S_{MSY}/S_0)$ and $(\tilde{S}_{t=200}/\tilde{S}_{t=100}) < (S_{MSY}/S_0)$.

A simpler definition ($[\tilde{S}_{t=200}/\tilde{S}_{t=100}] < [S_{MSY}/S_0]$) was evaluated in our preliminary model runs (not shown) and resulted in a relatively wide range of uncertainty in the aggregate number (and proportion) of simulations that ended in an overfished condition. For example, the proportion of simulation runs ending in an overfished condition (when defined as $[\tilde{S}_{t=200}/\tilde{S}_{t=100}] < [S_{MSY}/S_0]$) under alternative assumptions about $\bar{U}$ increased from 0.0% under the low-$\bar{U}$ scenario to 81% under the high-$\bar{U}$ scenario, which is similar to the range observed here in aggregate overfishing results under the low-$\bar{U}$ and high-$\bar{U}$ scenarios (8.3–83%; Table 2.6).

In conclusion, the risk analysis results obtained here (the proportion of simulation runs ending in an overfished condition) were most sensitive to the range of uncertainty identified for Pacific Sleeper Shark incidental exploitation rates in the GOA ($\bar{U}$ = 0.006 or 0.145; Equation 2.15; Tables 2.2, 2.5, 2.6). Depending upon which incidental catch data set was chosen for use in the calculation of plausible $\bar{U}$-values (Table 2.2), the aggregate risk of ending in an overfished condition increased from 0.0% under the low-$\bar{U}$ scenario to 59% under the high-$\bar{U}$ scenario (Table 2.6). Given that the high-$\bar{U}$ scenario is at least plausible, the risk of ending in an overfished condition under status quo management may be fairly high (59% after 100 years of exploitation). These results indicate that a priority for management is to reduce the uncertainty in Pacific Sleeper Shark $\bar{U}$ in the GOA. An observer program is now in place to monitor the historically unobserved Pacific Halibut fishery in the GOA, which incidentally catches Pacific Sleeper Sharks; hence, this major uncertainty will be reduced. Risk analysis results were also sensitive to the assumed shape of the length-based selectivity curve (asymptotic or dome shaped) but were less sensitive to the range of assumptions about other key model parameters, including A_{max} and stock productivity.

The simulation model results obtained with this approach should be interpreted cautiously, such as when considering current annual catch limits for Pacific Sleeper Sharks in the GOA. In particular, our

simulation results were based on a minimum estimate of exploitable biomass in the Gulf of Alaska, and were not based on model fits to data (e.g., Hilborn and Mangel 1997) but instead on a range of plausible parameter values that were developed from limited data or were obtained directly from the scientific literature. Consequently, other choices for modeling plausible exploitation rates, length-based selectivity, M from A_{max}, or stock productivity might have resulted in different outcomes than those obtained here.

The additional complexity required to model length-based processes within an age-structured model (Equations 2.1–2.21) was justified here based on the sensitivity of the risk analysis results to the plausible range assumed for length-based selectivity (asymptotic and dome shaped) and, to a lesser extent, based on the plausible range of uncertainty assumed for A_{max} and stock productivity. Simpler models that ignore the plausible range of uncertainty in length-based selectivity, life history, and stock productivity evaluated here (Table 2.4) could lead to different conclusions about stock status. In particular, the availability of length-based data is a common feature among many elasmobranch stock assessments (e.g., Pribac et al. 2005; Punt et al. 2005; Cope and Punt 2009; Cope 2013). Modeling of length-based processes within an age-structured stock assessment model has also become a common practice within many integrated modeling approaches (e.g., Stock Synthesis software), even in some data-limited situations (Wetzel and Punt 2011a, 2011b; Maunder and Punt 2013; Methot and Wetzel 2013; Punt and Maunder 2013).

2.6. Acknowledgements

This research was conceptualized during a National Oceanic and Atmospheric Administration (NOAA) Advanced Studies Program (D. L. C.) in collaboration with the NMFS-AFSC (M. F. S.) and the School of Fisheries and Ocean Sciences, University of Alaska Fairbanks (M. D. A.). Funding (D. L. C.) was provided by the NMFS Auke Bay Laboratory, the NMFS Pacific Islands Fisheries Science Center, and the NMFS Southeast Fisheries Science Center's Panama City Laboratory. The implementation of steepness in the Beverton–Holt stock–recruitment relationship benefited from conversations with Liz Brooks, Jon Brodziak, and Enric Cortés (NOAA Fisheries). The implementation of catch at age and length benefited from conversations with Felipe Hurtado-Ferro (School of Aquatic and Fishery Sciences, University of Washington, Seattle) and from feedback obtained based on preliminary presentations of this work during a Center for the Advancement of Population Assessment Methodology Selectivity Workshop (La Jolla, California; March 2013). Beth Mathews (University of Alaska Southeast, Juneau) contributed to data obtained from Southeast Alaska. The manuscript benefited from comments made by two anonymous reviewers.

2.7. Literature Cited

Aydin, K., and F. Mueter. 2007. The Bering Sea—A dynamic food web perspective. Deep-Sea Research Part II 54:2501–2525.

Baremore, I. E. 2010. Reproductive aspects of the Atlantic angel shark *Squatina dumeril*. Journal of Fish Biology 76:1682–1695.

Baum, J. K., and B. Worm. 2009. Cascading top-down effects of changing oceanic predator abundances. Journal of Animal Ecology 78:699–714.

Benz, G. W., R. Hocking, A. Kowunna Sr., S. A. Bullard, and J. C. George. 2004. A second species of Arctic shark: Pacific sleeper shark *Somniosus pacificus* from Point Hope, Alaska. Polar Biology 27:250–252.

Berkson, J., and J. T. Thorson. 2015. The determination of data-poor catch limits in the United States: is there a better way? ICES Journal of Marine Science 72:237–242.

Borets, L. A. 1986. Ichthyofauna of the Northwestern and Hawaiian submarine ranges. Journal of Ichthyology 26:1–13.

Braccini, M., J. Van Rijn, and L. Frick. 2012. High post-capture survival for sharks, rays and chimaeras discarded in the main shark fishery of Australia? PLoS (Public Library of Science) ONE [online serial] 7:e32547.

Brodziak, J. 2002. In search of optimal harvest rates for west coast groundfish. North American Journal of Fisheries Management 22:258–271.

Brooks, E. N., and J. E. Powers. 2007. Generalized compensation in stock-recruit functions: properties and implications for management. ICES Journal of Marine Science 64:413–424.

Brooks, E. N., J. E. Powers, and E. Cortés. 2010. Analytical reference points for age-structured models: application to data-poor fisheries. ICES Journal of Marine Science 67:165–175.

Carruthers, T. R., A. E. Punt, C. J. Walters, A. MacCall, M. K. McAllister, E. J. Dick, and J. Cope. 2014. Evaluating methods for setting catch limits in data-limited fisheries. Fisheries Research 153:48–68.

Charnov, E. L., D., Berrigan, and R. Shine. 1993. The M/K ratio is the same for fish and reptiles. American Naturalist 142:707–711.

Chen, S., and S. Watanabe. 1989. Age dependence of natural mortality coefficient in fish population dynamics. Nippon Suisan Gakkaishi 55:205–208.

Clark, W. G. 1991. Groundfish exploitation rates based on life-history parameters. Canadian Journal of Fisheries and Aquatic Sciences 48:734–750.

Clark, W. G. 2002. $F_{35\%}$ revisited ten years later. North American Journal of Fisheries Management 22:251–257.

Clark, W. G., and S. R. Hare. 2006. Assessment and management of Pacific halibut: data, methods, and policy. International Pacific Halibut Commission Scientific Report No. 83.

Clarke, S., and S. Hoyle. 2014. Development of limit reference points for elasmobranchs. Western and Central Pacific Fisheries Commission, WCPFC-SC10-2014/ MI-WP-07.

Compagno, L. J. V. 1984. FAO species catalogue. Vol. 4. Sharks of the world. An annotated and illustrated catalogue of shark species known to date, part 1. Hexanchiformes to lamniformes. FAO Fisheries Synopsis 125.

Cope, J. M. 2013. Implementing a statistical catch-at-age model (Stock Synthesis) as a tool for deriving overfishing limits in data-limited situations. Fisheries Research 142:3–14.

Cope, J. M., and A. E. Punt. 2009. Length-based reference points for data-limited situations: applications and restrictions. Marine and Coastal Fisheries: Dynamics, Management, and Ecosystem Science [online serial] 1:169–186.

Cortés, E. 2000. Life history patterns and correlations in sharks. Reviews in Fisheries Science 8:299–344.

Courtney, D., C. Tribuzio, and K. J. Goldman. 2006a. Section 18, BSAI sharks. Pages 1083–1132 *in* Stock assessment and fishery evaluation report for the groundfish resources of the Bering Sea and Aleutian Islands for 2007. North Pacific Fishery Management Council, Anchorage, Alaska.

Courtney, D., C. Tribuzio, K. J. Goldman, and J. Rice. 2006b. Appendix E, GOA sharks. Pages 481–562 *in* Stock assessment and fishery evaluation report for the groundfish resources of the Gulf of Alaska for 2007. North Pacific Fishery Management Council, Anchorage, Alaska.

Courtney, D. L., and R. Foy. 2012. Pacific sleeper shark *Somniosus pacificus* trophic ecology in the eastern North Pacific Ocean inferred from nitrogen and carbon stable-isotope ratios and diet. Journal of Fish Biology 80:1508–1545.

Courtney, D. L. and L. Hulbert. 2007. Shark research in the Gulf of Alaska with satellite, sonic, and archival tags (extended abstract). NOAA Technical Memorandum NMFS-F/SPO-82:26-27.

Courtney, D. L., and M. F. Sigler. 2007. Trends in area-weighted CPUE of Pacific sleeper sharks (*Somniosus pacificus*) in the northeast Pacific Ocean determined from sablefish longline surveys. Alaska Fishery Research Bulletin 12:291–315.

Davis, B., D. L. VanderZwaag, A. Cosandey-Godin, N. E. Hussey, S. T. Kessel, and B. Worm. 2013. The conservation of the Greenland shark (*Somniosus microcephalus*): Setting scientific, law, and policy coordinates for avoiding a species at risk. Journal of International Wildlife Law and Policy 16:300–330.

Ebert, D. A., L. J. V. Compagno, and L. J. Natanson. 1987. Biological notes on the Pacific sleeper shark, *Somniosus pacificus* (chondrichthyes: squalidae). California Fish and Game 73:117–123.

Ebert, D. A., and M. V. Winton. 2010. Chondrichthyans of high latitude seas. Pages 115–158 *in* J. C. Carrier, J. A. Musick, and M. R. Heithaus, editors. Sharks and their relatives II; biodiversity, adaptive physiology, and conservation. CRC Press, Boca Raton, Florida.

Fisk, A. T., S. A. Tittlemier, J. L. Pranschke, and R. J. Norstrom. 2002. Using anthropogenic contaminants and stable isotopes to assess the feeding ecology of Greenland sharks. Ecology 83:2162–2172.

Fordham, S. V. 2005. Piked or spiny dogfish, *Squalus acanthias* Linnaeus, 1758. Pages 226–230 *in* S. L. Fowler, R. D. Cavanagh, M. Camhi, G. H. Burgess, G. M. Cailliet, S. V. Fordham, C. A. Simpfendorfer, and J. A. Musick, editors. Sharks, rays and chimaeras: the status of the chondrichthyan fishes (status survey). International Union for Conservation of Nature, Shark Specialist Group, Gland, Switzerland.

Forrest, R. E., S. J. D. Martell, M. C. Melnychuk, and C. J. Walters. 2008. An age-structured model with leading management parameters, incorporating age-specific selectivity and maturity. Canadian Journal of Fisheries and Aquatic Sciences 65:286–296.

Forrest, R. E., and C. J. Walters. 2009. Estimating thresholds to optimal harvest rate for long-lived, low-fecundity sharks accounting for selectivity and density dependence in recruitment. Canadian Journal of Fisheries and Aquatic Sciences 66:2062–2080.

Francis, R. C., S. R. Hare, A. B. Hollowed, and W. S. Wooster. 1998. Effects of interdecadal climate variability on the oceanic ecosystems of the northeast Pacific. Fisheries Oceanography 7:1–21.

Frid, A., G. G. Baker, and L. M. Dill. 2006. Do resource declines increase predation rates on North Pacific harbor seals? A behavior-based plausibility model. Marine Ecology Progress Series 312:265–275.

Frid, A., G. G. Baker, and L. M. Dill. 2008. Do shark declines create fear released systems? Oikos 117:191–201.

Frid, A., J. Burns, G. G. Baker, and R. E. Thorne. 2009. Predicting synergistic effects of resources and predators on foraging decisions by juvenile Steller sea lions. Oecologia 158:775–786.

Frid, A., L. M. Dill, R. E. Thorne, and G. M. Blundell. 2007a. Inferring prey perception of relative danger in large-scale marine systems. Evolutionary Ecology Research 9:635–649.

Frid, A., M. R. Heithaus, and L. M. Dill. 2007b. Dangerous dive cycles and the proverbial ostrich. Oikos 116:893–902.

Froese, R., and C. Binohlan. 2000. Empirical relationships to estimate asymptotic length, length at first maturity and length at maximum yield per recruit in fishes, with a simple method to evaluate length frequency data. Journal of Fish Biology 56:758–773.

Gabriel, W. L., M. P. Sissenwine, and W. J. Overholtz. 1989. Analysis of spawning stock biomass per recruit: an example for Georges Bank Haddock. North American Journal of Fisheries Management 9:383–391.

Gaichas, S. 2002. Section 15, summary of changes in the Bering Sea–Aleutian Islands squid and other species assessment. Pages 669–700 *in* Stock assessment and fishery evaluation report for the groundfish resources of the Bering Sea and Aleutian Islands for 2003. North Pacific Fishery Management Council, Anchorage, Alaska.

Gaichas, S., L. Fritz, and J. N. Ianelli. 1999. Appendix D, other species considerations for the Gulf of Alaska. *in* Stock assessment and fishery evaluation report for the groundfish resources of the Gulf of Alaska for 2000. North Pacific Fishery Management Council, Anchorage, Alaska.

Goldman, K. J. 2002. Aspects of age, growth, demographics and thermal biology of two lamniform shark species. Doctoral dissertation. Virginia Institute of Marine Science, School of Marine Science, College of William and Mary, Gloucester Point.

Goldman, K. J., and B. Human. 2005. Salmon Shark, *Lamna ditropis* Hubbs & Follett 1947. Pages 260–262 *in* S. L. Fowler, R. D. Cavanagh, M. Camhi, G. H. Burgess, G. M. Cailliet, S. V. Fordham, C. A. Simpfendorfer, and J. A. Musick, editors. Sharks, rays and chimaeras: the status of the chondrichthyan fishes (status survey). International Union for Conservation of Nature, Shark Specialist Group, Gland, Switzerland.

Goldman, K. J., and J. A. Musick. 2006. Growth and maturity of Salmon Sharks (*Lamna ditropis*) in the eastern and western North Pacific, and comments on back-calculation methods. U.S. National Marine Fisheries Service Fishery Bulletin 104:278–292.

Goldman, K. J., and J. A. Musick. 2008. The biology and ecology of the Salmon Shark, *Lamna ditropis*. Pages 95–104 *in* M. D. Camhi, E. K. Pikitch, and E. A. Babcock, editors. Sharks of the open ocean: biology, fisheries and conservation. Blackwell Scientific Publications, Oxford, UK.

Grubbs, R. D. 2010. Ontogenetic shifts in movements and habitat use. Pages 319–350 *in* J. C. Carrier, J. A. Musick, and M. R. Heithaus, editors. Sharks and their relatives II: biodiversity, adaptive physiology, and conservation. CRC Press, Boca Raton, Florida.

Gunderson, D. R., and P. H. Dygert. 1988. Reproductive effort as a predictor of natural mortality rate. ICES Journal of Marine Science 44:200–209.

Haddon, M. 2011. Modelling and quantitative methods in fisheries, 2nd edition. Chapman and Hall/CRC Press, Boca Raton, Florida.

Hansen, P. M. 1963. Tagging experiments with the Greenland Shark (*Somniosus microcephalus* (Bloch and Schneider)) in subarea 1. International Commission for the Northwest Atlantic Fisheries Special Publication 4:172–175.

Hare, S. R., and N. J. Mantua. 2000. Empirical evidence for North Pacific regime shifts in 1977 and 1989. Progress in Oceanography 47:103–145.

He, X., M. Mangel, and A. MacCall. 2006. A prior for steepness in stock–recruitment relationships, based on an evolutionary persistence principle. U.S. National Marine Fisheries Service Fishery Bulletin 104:428–433.

Heithaus, M. R., A. Frid, J. J. Vaudo, B. Worm, and A. J. Wirsing. 2010. Unraveling the ecological importance of elasmobranchs. Pages 611–637 *in* J. C. Carrier, J. A. Musick, and M. R. Heithaus, editors. Sharks and their relatives II: biodiversity, adaptive physiology, and conservation. CRC Press, Boca Raton, Florida.

Heithaus, M. R., A. Frid, A. J. Wirsing, and B. Worm. 2008. Predicting ecological consequences of marine top predator declines. Trends in Ecology and Evolution 23:202–210.

Hewitt, D. A., and J. M. Hoenig. 2005. Comparison of two approaches for estimating natural mortality based on longevity. U.S. National Marine Fisheries Service Fishery Bulletin 103:433–437.

Hilborn, R., and M. Mangel. 1997. The ecological detective: confronting models with data. Princeton University Press, Princeton, New Jersey.

Hilborn, R., and C. J. Walters. 1992. Quantitative fisheries stock assessment: choice, dynamics, and uncertainty. Chapman and Hall, New York.

Hoenig, J. M. 1983. Empirical use of longevity data to estimate mortality rates. U.S. National Marine Fisheries Service Fishery Bulletin 82:898–903.

Hollowed, A. B., and W. S. Wooster. 1992. Variability of winter ocean conditions and strong year-classes of Northeast Pacific groundfish. ICES Marine Science Symposia 195:433–444.

Horning, M., and J.-A. E. Mellish. 2012. Predation on an upper trophic marine predator, the Steller sea lion: evaluating high juvenile mortality in a density dependent conceptual framework. PLoS (Public Library of Science) ONE [online serial] 7(1):e30173.

Horning, M., and J.-A. E. Mellish. 2014. In cold blood: evidence of Pacific Sleeper Shark (*Somniosus pacificus*) predation on Steller sea lions (*Eumetopias jubatus*) in the Gulf of Alaska. U.S. National Marine Fisheries Service Fishery Bulletin 112:297–310.

Hulbert, L. B., M. F. Sigler, and C. R. Lunsford. 2006. Depth and movement behaviour of the Pacific Sleeper Shark in the northeast Pacific Ocean. Journal of Fish Biology 69:406–425.

Hurtado-Ferro, F., A. E. Punt, and K. T. Hill. 2014. Use of multiple selectivity patterns as a proxy for spatial structure. Fisheries Research 158:102–115.

Jensen, A. L. 1996. Beverton and Holt life history invariants result from optimal trade-off of reproduction and survival. Canadian Journal of Fisheries and Aquatic Sciences 53:820–822.

Kitchell, J. F., T. E. Essington, C. H. Boggs, D. E. Schindler, and C. J. Walters. 2002. The role of sharks and longline fisheries in a pelagic ecosystem of the central Pacific. Ecosystems 5:202–216.

Kuker, K., and L. Barrett-Lennard. 2010. A re-evaluation of the role of killer whales *Orcinus orca* in a population decline of sea otters *Enhydra lutris* in the Aleutian Islands and a review of alternative hypotheses. Mammal Review 40:103–124.

Kyne, P. M., and C. A. Simpfendorfer. 2010. Deepwater chondrichthyans. Pages 37–113 *in* J. C. Carrier, J. A. Musick, and M. R. Heithaus, editors. Sharks and their relatives II: biodiversity, adaptive physiology, and conservation. CRC Press, Boca Raton, Florida.

Lorenzen, K. 1996. The relationship between body weight and natural mortality in juvenile and adult fish: a comparison of natural ecosystems and aquaculture. Journal of Fish Biology 49:627–647.

Mace, P. M., and I. J. Doonan. 1988. A generalized bioeconomic simulation model for fish population dynamics. New Zealand Ministry of Agriculture and Fisheries, Research Document 88/4, Wellington.

Mangel, M., J. Brodziak, and G. DiNardo. 2010. Reproductive ecology and scientific inference of steepness: a fundamental metric of population dynamics and strategic fisheries management. Fish and Fisheries 11:89–104.

Mangel, M., A. D. MacCall, J. Brodziak, E. J. Dick, R. E. Forrest, R. Pourzand, and S. Ralston. 2013. A perspective on steepness, reference points, and stock assessment. Canadian Journal of Fisheries and Aquatic Sciences 70:930–940.

Maunder, M. N., and A. E. Punt. 2013. A review of integrated analysis in fisheries stock assessment. Fisheries Research 142:61–74.

McAuley, R. B., C. A. Simpfendorfer, and N. G. Hall. 2007. A method for evaluating the impacts of fishing mortality and stochastic influences on the demography of two long-lived shark stocks. ICES Journal of Marine Science 64:1710–1722.

Mecklenburg, C. W., T. A. Mecklenburg, and L. K. Thorsteinson. 2002. Fishes of Alaska. American Fisheries Society, Bethesda, Maryland.

Menon, M. M. 2004. Spatiotemporal modeling of Pacific Sleeper Shark (*Somniosus pacificus*) and Spiny Dogfish (*Squalus acanthias*) bycatch in the northeast Pacific Ocean. Master's thesis. University of Washington, Seattle.

Menon, M. M., V. F. Gallucci, and L. L. Conquest. 2005. Sampling designs for the estimation of longline bycatch. Pages 851–870 *in* G. H. Kruse, V. F. Gallucci, D. E. Hay, R. I. Perry, R. M. Peterman, T. C. Shirley, P. D. Spencer, B. Wilson, and D. Woodby, editors. Fisheries assessment and management in data-limited situations. Alaska Sea Grant College Program, AK-SG-05-02, University of Alaska, Fairbanks.

Methot, R. D. Jr., and C. R. Wetzel. 2013. Stock Synthesis: a biological and statistical framework for fish stock assessment. Fisheries Research 142:86–99.

Morgan, A., and G. H. Burgess. 2007. At-vessel fishing mortality for six species of sharks caught in the northwest Atlantic and Gulf of Mexico. Gulf and Caribbean Research 19:123–129.

MSRA (Magnuson–Stevens Fishery Conservation and Management Reauthorization Act of 2006). 2006. U.S. Public Law 109-479, 120 Statute 3575.

Mueter, F. J., J. L. Boldt, B. A. Megrey, and R. A. Peterman. 2007. Recruitment and survival of northeast Pacific Ocean fish stocks: temporal trends, covariation, and regime shifts. Canadian Journal of Fisheries and Aquatic Sciences 64:911–927.

Mueter, F. J., and B. L. Norcross. 2002. Spatial and temporal patterns in the demersal fish community on the shelf and upper slope regions of the Gulf of Alaska. U.S. National Marine Fisheries Service Fishery Bulletin 100:559–581.

Murray, B. W., J. Y. Wang, S.-C. Yang, J. D. Stevens, A. Fisk, and J. Svavarsson. 2008. Mitochondrial cytochrome *b* variation in sleeper sharks (Squaliformes: Somniosidae). Marine Biology 153:1015–1022.

Myers, R. A., J. K. Baum, T. D. Shepherd, S. P. Powers, and C. H. Peterson. 2007. Cascading effects of the loss of apex predatory sharks from a coastal ocean. Science 315:1846–1850.

Myers, R. A., K. G. Bowen, and N. J. Barrowman. 1999. Maximum reproductive rate of fish at low population sizes. Canadian Journal of Fisheries and Aquatic Sciences 56:2404–2419.

Myhre, R. J., G. J. Peltonen, G. St-Pierre, B. E. Skud, and R. E. Walden. 1977. The Pacific Halibut fishery: catch, effort and CPUE, 1929–1975. International Pacific Halibut Commission, Technical Report 14.

Newman, D., J. Berkson, and L. Suatoni. 2015. Current methods for setting catch limits for data-limited fish stocks in the United States. Fisheries Research 164:86–93.

NMFS (National Marine Fisheries Service). 2013. Introduction. Pages 1–52 *in* Appendix B, stock assessment and fishery evaluation report for the groundfish resources of the Gulf of Alaska. North Pacific Fishery Management Council, Anchorage, Alaska.

O'Brien, S. M., V. F. Gallucci, and L. Hauser. 2013. Effects of species biology on the historical demography of sharks and their implications for likely consequences of contemporary climate change. Conservation Genetics 14:125–144.

Orlov, A. M. 1999. Capture of especially large Sleeper Shark *Somniosus pacificus* (Squalidae) with some notes on its ecology in northwestern Pacific. Journal of Ichthyology 39:548–553.

Orlov, A. M., and A. A. Baitalyuk. 2014. Spatial distribution and features of biology of Pacific Sleeper Shark *Somniosus pacificus* in the North Pacific. Journal of Ichthyology 54:526–546.

Orlov, A. M., and S. I. Moiseev. 1999a. New data on the biology of the Pacific Sleeper Shark, *Somniosus pacificus* (Squalidae) in the northwestern Pacific Ocean. Pages 177–186 *in* D. MacKinlay, K. Howard, and J. Cech Jr., editors. Fish performance studies. Department of Fisheries and Oceans, Vancouver.

Orlov, A. M., and S. I. Moiseev. 1999b. Some biological features of Pacific Sleeper Shark, *Somniosus pacificus* (Bigelow et Schroeder 1944) (Squalidae) in the northwestern Pacific Ocean. Oceanological Studies 28:3–16.

Pauly, D. 1980. On the interrelationships between natural mortality, growth parameters, and mean environmental temperature in 175 fish stocks. ICES Journal of Marine Science 39:175–192.

Pauly, D., R. Hilborn, and T. A. Branch. 2013. Fisheries: does catch reflect abundance? Nature 494:303–306.

Peterson, I., and J. S. Wroblewski. 1984. Mortality rates of fishes in the pelagic ecosystem. Canadian Journal of Fisheries and Aquatic Sciences 41:1117–1120.

Pribac, F., A. E. Punt, B. L. Taylor, and T. I. Walker. 2005. Using length, age and tagging data in a stock assessment of a length selective fishery for Gummy Shark (*Mustelus antarcticus*). Journal of Northwest Atlantic Fishery Science 35:267–290.

Punt, A. E., and M. N. Maunder. 2013. Stock Synthesis: advancing stock assessment application and research through the use of a general stock assessment computer program. Fisheries Research 142:1–2.

Punt, A. E., F. Pribac, B. L. Taylor, and T. I. Walker. 2005. Harvest strategy evaluation for School and Gummy shark. Journal of Northwest Atlantic Fishery Science 35:387–406.

Punt, A. E., and T. I. Walker. 1998. Stock assessment and risk analysis for the School Shark (*Galeorhinus galeus*) off southern Australia. Marine and Freshwater Research 49:719–731.

Quinn, T. J. II, and R. B. Deriso. 1999. Quantitative fish dynamics. Oxford University Press, New York.

Rodgveller, C. J., C. R. Lunsford, and J. T. Fujioka. 2008. Evidence of hook competition in longline surveys. U.S. National Marine Fisheries Service Fishery Bulletin 106:364–374.

Schaufler, L., R. Heintz, M. Sigler, and L. Hulbert. 2005. Fatty acid composition of Sleeper Shark (*Somniosus pacificus*) liver and muscle reveals nutritional dependence on planktivores. International Council for the Exploration of the Sea, C.M. 2005/N:05, Copenhagen.

Sigler, M. F. 1999. Estimation of Sablefish, *Anoplopoma fimbria*, abundance off Alaska with an age-structured population model. U.S. National Marine Fisheries Service Fishery Bulletin 97:591–603.

Sigler, M. F., L. B. Hulbert, C. R. Lunsford, N. H. Thompson, K. Burek, G. O'Corry-Crowe, and A. C. Hirons. 2006. Diet of Pacific Sleeper Shark, a potential Steller sea lion predator, in the northeast Pacific Ocean. Journal of Fish Biology 69:392–405.

Simpfendorfer, C. A., K. Donohue, and N. G. Hall. 2000. Stock assessment and risk analysis for the Whiskery Shark (*Furgaleus macki* (Whitley)) in southwestern Australia. Fisheries Research 47:1–17.

Smith, C. R. 2006. Bigger is better: the role of whales as detritus in marine ecosystems. Pages 286–300 *in* J. A. Estes, D. P. DeMaster, D. F. Doak, T. M. Williams, and R. L. Brownell Jr., editors. Whales, whaling, and ocean ecosystems. University of California Press, Berkeley.

Smith, C. R., and A. R. Baco. 2003. Ecology of whale falls at the deep-sea floor. Oceanography and Marine Biology: an Annual Review 41:311–354.

Smith, S. E., D. W. Au, and C. Show. 1998. Intrinsic rebound potentials of 26 species of Pacific sharks. Marine and Freshwater Research 49:663–678.

Taylor, I. G., V. Gertseva, R. D. Methot Jr., and M. N. Maunder. 2013. A stock–recruitment relationship based on pre-recruit survival, illustrated with application to Spiny Dogfish shark. Fisheries Research 142:15–21.

Then, A. Y., J. M. Hoenig, N. G. Hall, and D. A. Hewitt. 2015. Evaluating the predictive performance of empirical estimators of natural mortality rate using information on over 200 fish species. ICES Journal of Marine Science 72:82–92.

Thompson, G. G. 1994. Confounding of gear selectivity and the natural mortality rate in cases where the former is a non-monotone function of age. Canadian Journal of Fisheries and Aquatic Sciences 51:2654–2664.

Thompson, W. F., and N. L. Freeman, 1930. History of the Pacific Halibut fishery. International Fisheries Commission, Report 5, Seattle.

Tribuzio, C. A., K. Echave, C. Rodgveller, and P.-J. Hulson. 2012. Section 20: assessment of the shark stock complex in the Bering Sea and Aleutian Islands. Pages 1771–1848 *in* Stock assessment and fishery evaluation report for the groundfish resources of the Bering Sea and Aleutian Islands for 2013. North Pacific Fishery Management Council, Anchorage, Alaska.

Tribuzio, C. A., K. Echave, C. Rodgveller, P.-J. Hulson, and K. J. Goldman. 2011. Chapter 20: assessment of the shark stock complex in the Gulf of Alaska. Pages 1393–1446 *in* Stock assessment and fishery evaluation report for the groundfish resources of the Gulf of Alaska for 2012. North Pacific Fishery Management Council, Anchorage, Alaska.

Tribuzio, C. A., J. R. Gasper, and S. K. Gaichas. 2014. Estimation of bycatch in the unobserved Pacific Halibut fishery off Alaska. NOAA Technical Memorandum NMFS-AFSC-265.

Tribuzio, C. A., and G. H. Kruse. 2011. Demographic and risk analyses of Spiny Dogfish (*Squalus suckleyi*) in the Gulf of Alaska using age- and stage-based population models. Marine and Freshwater Research 62:1395–1406.

Tribuzio, C. A., and G. H. Kruse 2012. Life history characteristics of a lightly exploited stock of Squalus suckleyi. Journal of Fish Biology 80:1159–1180.

Tribuzio, C. A., G. H. Kruse, and J. T. Fujioka. 2010. Age and growth of Spiny Dogfish (*Squalus acanthias*) in the Gulf of Alaska: analysis of alternative growth models. U.S. National Marine Fisheries Service Fishery Bulletin 108:119–135.

Tsai, W.-P., C.-L. Sun, S.-P. Wang, and K.-M. Liu. 2011. Evaluating the impacts of uncertainty on the estimation of biological reference points for the Shortfin Mako Shark, *Isurus oxyrinchus*, in the northwestern Pacific Ocean. Marine and Freshwater Research 62:1383–1394.

U.S. Office of the Federal Register. 2009. Magnuson–Stevens Act provisions; annual catch limits; national standard guidelines. Federal Register 74:11 (16 January 2009):3178–3213.

U.S. Office of the Federal Register. 2012. Groundfish fisheries of the exclusive economic zone off Alaska and Pacific Halibut fisheries; observer program; final rules. Federal Register 77:225(21 November 2012):70062–70173.

Wang, J. Y., and S.-C. Yang. 2004. First records of Pacific Sleeper Sharks (*Somniosus pacificus* Bigelow and Schroeder, 1944) in the subtropical waters of eastern Taiwan. Bulletin of Marine Science 74:229–235.

Wetzel, C. R., and A. E. Punt. 2011a. Model performance for the determination of appropriate harvest levels in the case of data-poor stocks. Fisheries Research 110:342–355.

Wetzel, C. R., and A. E. Punt. 2011b. Performance of a fisheries catch-at-age model (Stock Synthesis) in data-limited situations. Marine and Freshwater Research 62:927–936.

Wiedenmann, J., M. J. Wilberg, and T. J. Miller. 2013. An evaluation of harvest control rules for data-poor fisheries. North American Journal of Fisheries Management 33:845–860.

Wirsing, A. J., M. R. Heithaus, A. Frid, and L. M. Dill. 2008. Seascapes of fear: evaluating sublethal predator effects experienced and generated by marine mammals. Marine Mammal Science 24:1–15.

Wooster, W. S., and C. I. Zhang. 2004. Regime shifts in the North Pacific: early indications of the 1976–1977 event. Progress in Oceanography 60:183–200.

Worm, B., B. Davis, L. Kettemer, C. A. Ward-Paige, D. Chapman, M. R. Heithaus, S. T. Kessel, and S. H. Gruber. 2013. Global catches, exploitation rates, and rebuilding options for sharks. Marine Policy 40:194–204.

Yang, M.-S., and B. N. Page. 1999. Diet of Pacific Sleeper Shark, *Somniosus pacificus*, in the Gulf of Alaska. U.S. National Marine Fisheries Service Fishery Bulletin 97:406–409.

Yano, K., J. D. Stevens, and L. J. V. Compagno. 2004. A review of the systematics of the sleeper shark genus *Somniosus* with redescriptions of *Somniosus (Somniosus) antarcticus* and *Somniosus (Rhinoscymnus) longus* (Squaliformes: Somniosidae). Ichthyological Research 51:360–373.

Yano, K., J. D. Stevens, and L. J. V. Compagno. 2007. Distribution, reproduction and feeding of the Greenland Shark *Somniosus (Somniosus) microcephalus*, with notes on two other sleeper sharks, *Somniosus (Somniosus) pacificus* and *Somniosus (Somniosus) antarcticus*. Journal of Fish Biology 70:374–390.

Yeh, J., and J. C. Drazen. 2009. Depth zonation and bathymetric trends of deep-sea megafaunal scavengers of the Hawaiian Islands. Deep-Sea Research Part I Oceanographic Research Papers 56:251–266.

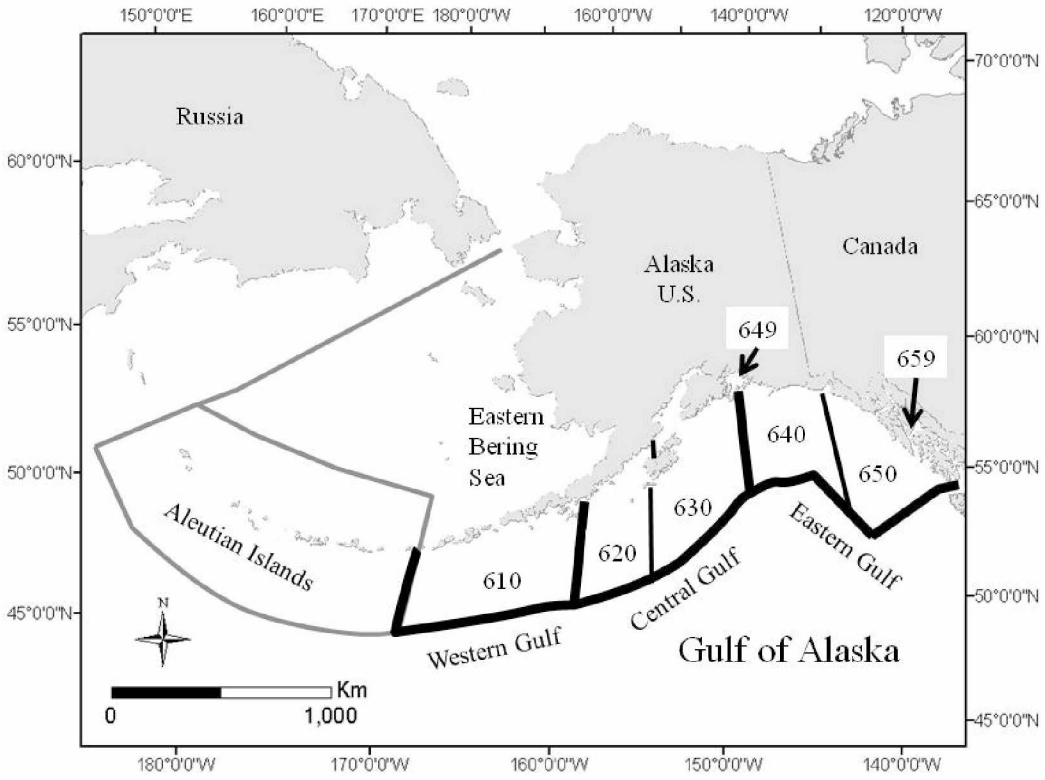

Figure 2.1: Map depicting study area.
Map depicting the U.S. federally managed waters (>5.56 km [3 nautical miles] from shore to 370.4 km [200 nautical miles]) in the Gulf of Alaska (black outline), the Aleutian Islands region (gray outline), and the eastern Bering Sea (gray outline). National Marine Fisheries Service reporting areas within the Gulf of Alaska (610, 620, 630, 640, and 650) are identified, along with area 649 (predominantly Alaska state waters within Prince William Sound) and area 659 (predominantly Alaska state waters within Southeast Alaska).

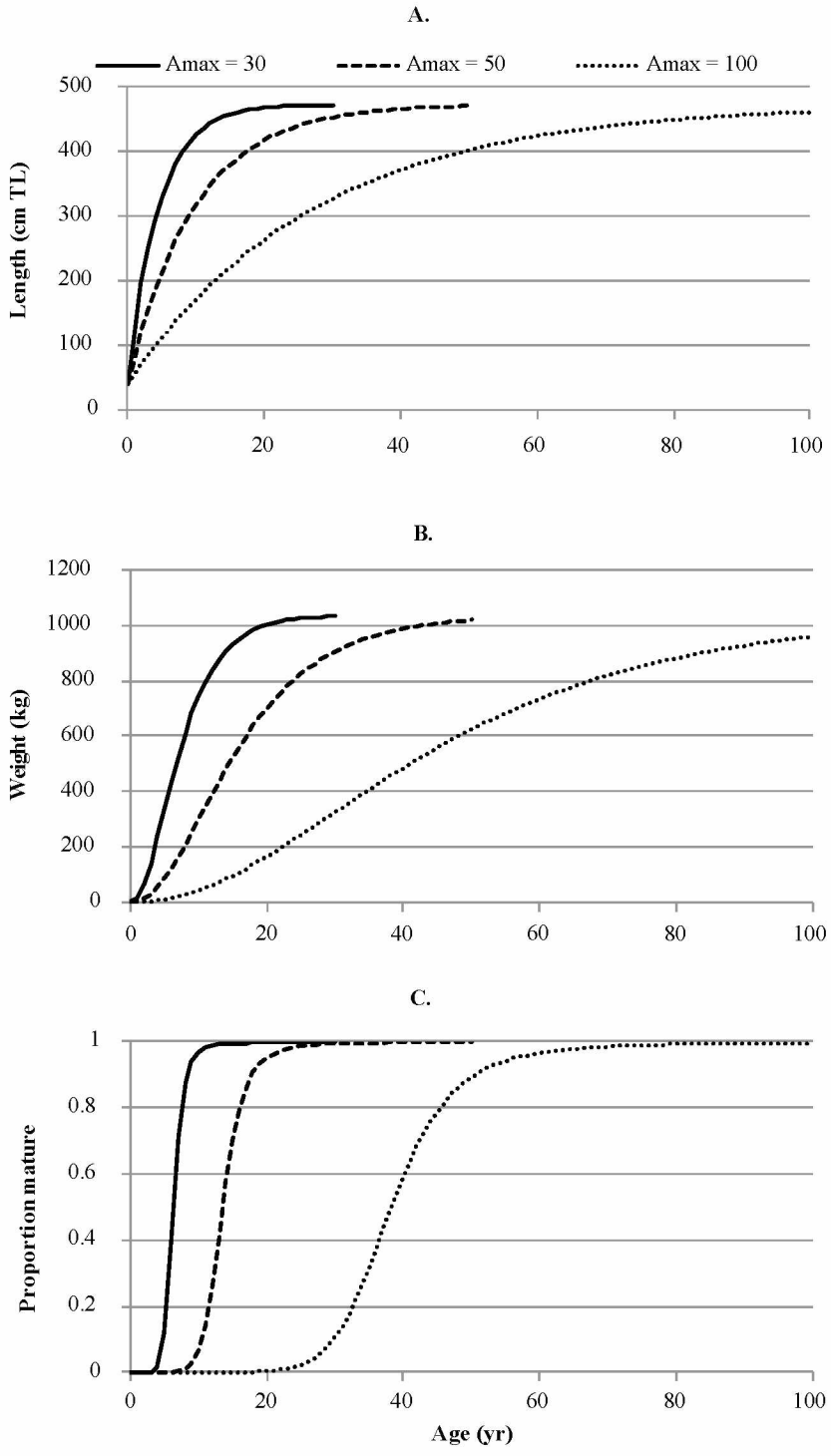

Figure 2.2: Alternative life history scenarios.
(A) Length at age was simulated by using a von Bertalanffy growth model (VBGM; Equation 2.7) for three alternative life history scenarios associated with maximum age (A_{max} = 30, 50, or 100 years; Table 2.4); the resulting (B) weight at age and (C) proportion mature at age back-calculated from the assumed VBGM for each life history scenario (Table 2.4) are shown.

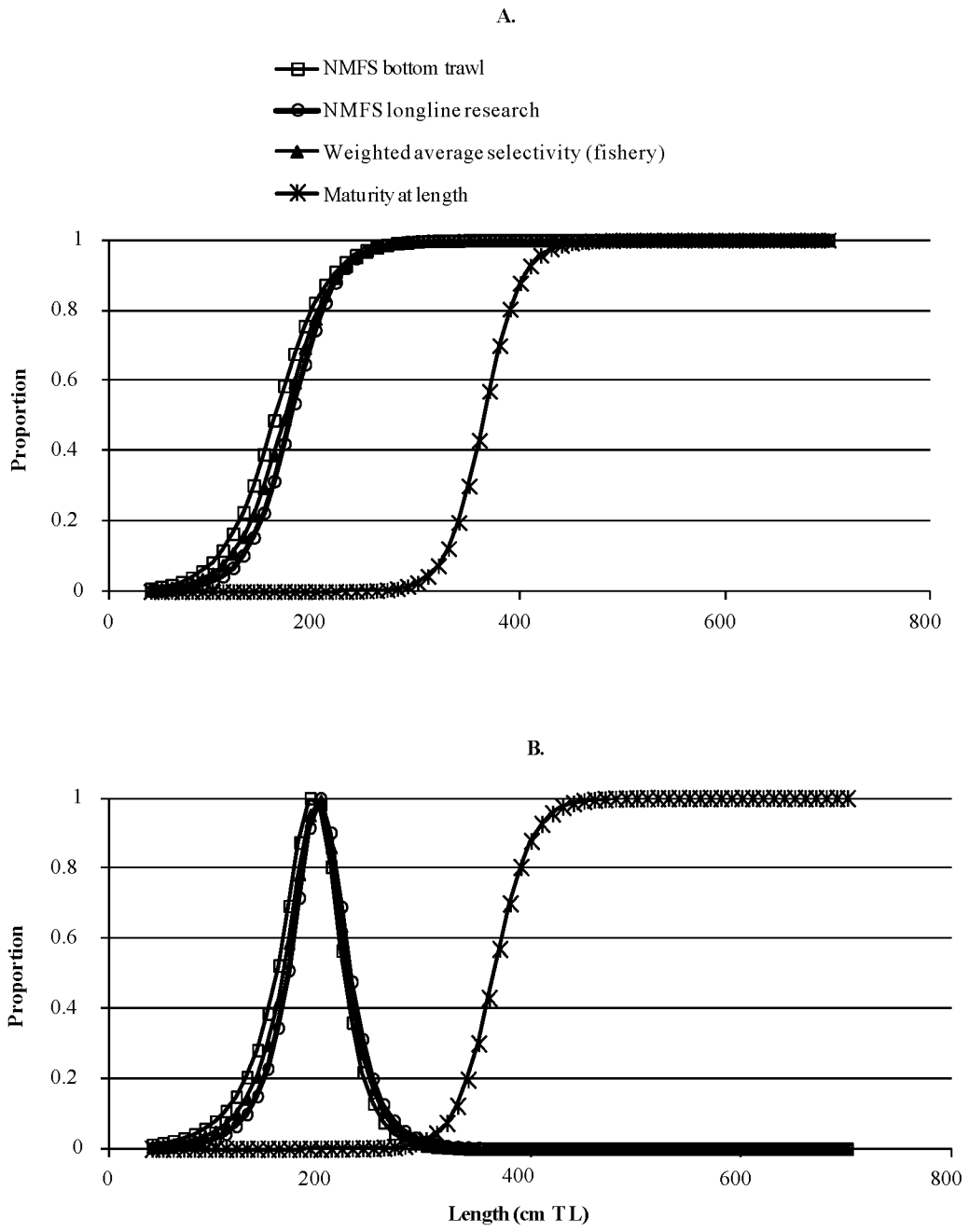

Figure 2.3: Alternative length-based selectivity scenarios.
Length-based selectivity (proportion selected at length) for the National Marine Fisheries Service (NMFS) bottom trawl survey, NMFS longline research, and the weighted average of the two data sets (with weights based on relative catch by gear type in the commercial fishery). Selectivity is plotted under the (A) asymptotic and (B) dome-shaped selectivity scenarios (Table 2.4) along with the assumed proportion mature at length (Table 2.4; see Methods). Proportions are plotted for length bins up to 700+ cm TL for all scenarios.

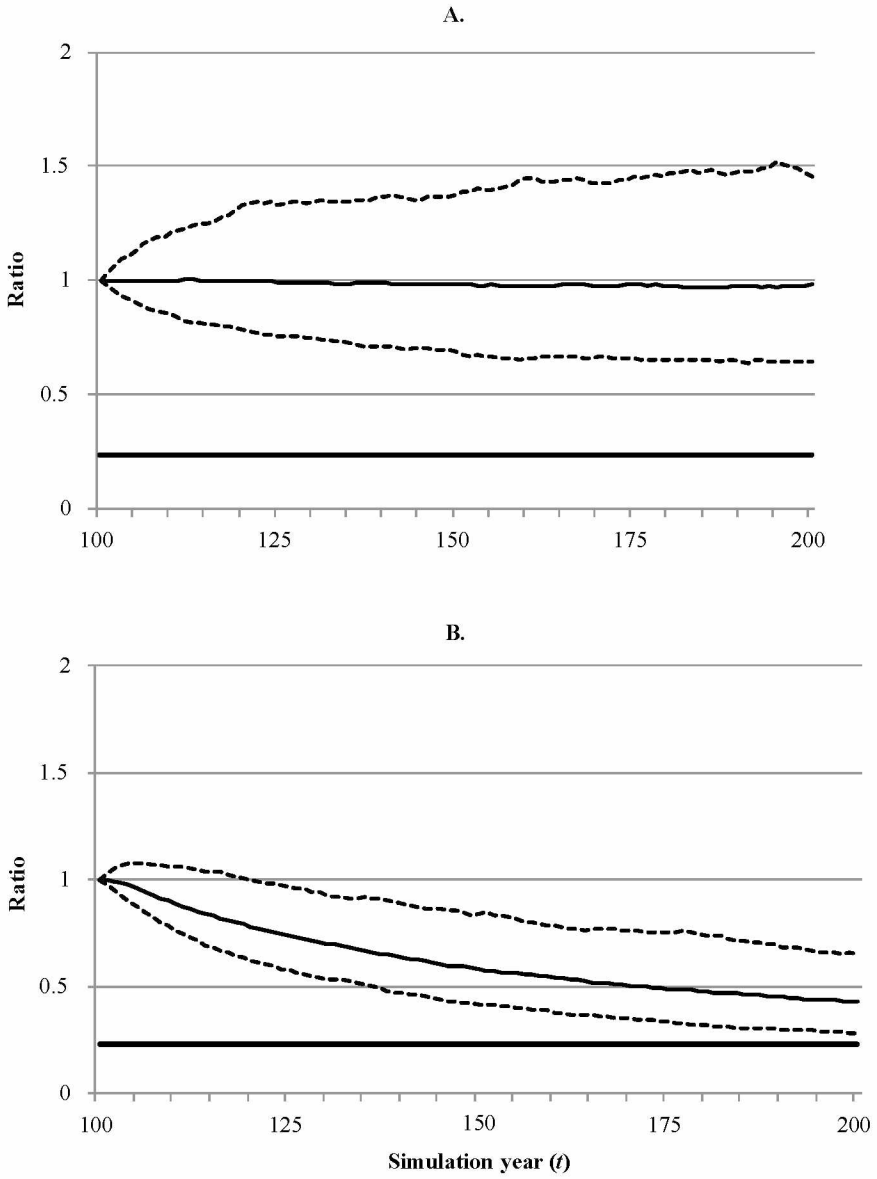

Figure 2.4: Simulation results for model configurations 1 and 2.
Percentiles (thin solid line is 50th; dashed lines are lower 2.5th and upper 97.5th; n = 1,000 simulations) of the ratio $\tilde{S}_t/\tilde{S}_{t=100}$ (where $\tilde{S}_t$ is female spawning stock biomass [S] in intermediate simulation year t; $\tilde{S}_{t=100}$ is female nonequilibrium S at the end of the initialization period but prior to the start of exploitation) obtained during simulation years t = 101–200 for (A) alternative model configuration 1 (relatively short life span, relatively low steepness, dome-shaped selectivity, and low exploitation rate) and (B) alternative model configuration 2 (relatively short life span, relatively low steepness, dome-shaped selectivity, and high exploitation rate), as described in Table 2.5. The bold horizontal line in each panel represents the overfished reference, 0.5 × (S_{MSY}/S_0) (where S_{MSY} is female S at maximum sustainable yield; and S_0 is unexploited equilibrium S of females), which was obtained separately under equilibrium conditions (Appendix 2.A) for each alternative model configuration (Table 2.5).

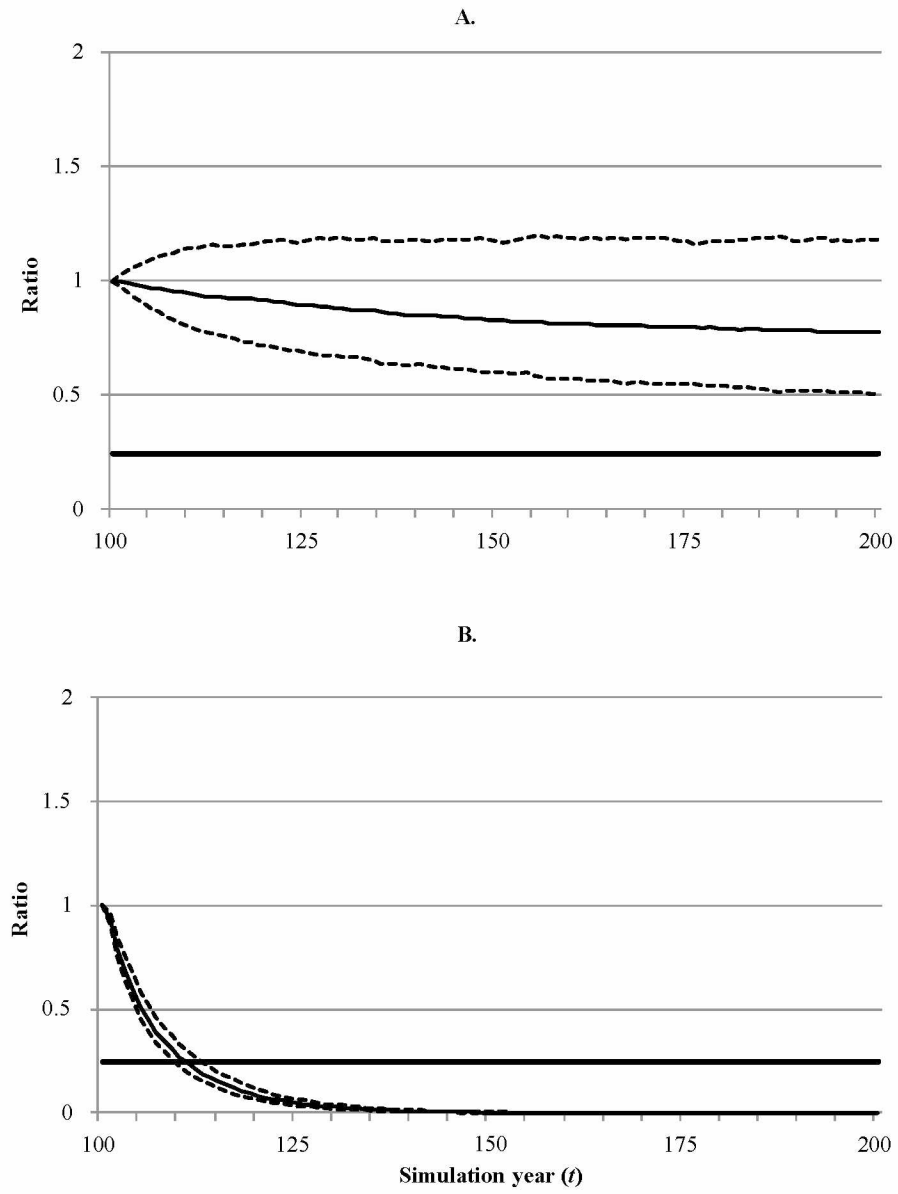

Figure 2.5: Simulation results for model configurations 3 and 4.
Percentiles (thin solid line is 50th; dashed lines are lower 2.5th and upper 97.5th; n = 1,000 simulations) of the ratio $\tilde{S}_t / \tilde{S}_{t=100}$ (where $\tilde{S}_t$ is female spawning stock biomass [S] in intermediate simulation year t; $\tilde{S}_{t=100}$ is female nonequilibrium S at the end of the initialization period but prior to the start of exploitation) obtained during simulation years t = 101–200 for (A) alternative model configuration 3 (relatively short life span, relatively low steepness, asymptotic selectivity, and low exploitation rate) and (B) alternative model configuration 4 (relatively short life span, relatively low steepness, asymptotic selectivity, and high exploitation rate), as defined in Table 2.5. The bold horizontal line in each panel represents the overfished reference, 0.5 × (S_{MSY}/S_0) (where S_{MSY} is female S at maximum sustainable yield; and S_0 is unexploited equilibrium S of females), which was obtained separately under equilibrium conditions (Appendix 2.A) for each alternative model configuration (Table 2.5).

Table 2.1: Time series of Pacific Sleeper Shark incidental catch and biomass.
Time series of Pacific Sleeper Shark incidental catch estimates and biomass estimates (bottom trawl survey) in the Gulf of Alaska, as reported by the National Marine Fisheries Service (NMFS) Alaska Fisheries Science Center (AFSC; Tribuzio et al. 2011; CAS = Catch Accounting System, official estimates of incidental catch in groundfish fisheries; HFICE = Halibut Fishery Incidental Catch Estimation, preliminary estimates of incidental catch in Pacific Halibut fisheries; N_{haul} = total number of bottom trawl survey hauls; $N_{Sleeper}$ = number of survey hauls in which Pacific Sleeper Sharks were captured; biomass = Pacific Sleeper Shark biomass in the survey; CV = coefficient of variation in biomass).

	NMFS-AFSC incidental catch		NMFS-AFSC survey biomass			
Year	CAS	HFICE			Biomass	
(not in sequence)	(metric tons)	(metric tons)	N_{haul}	$N_{Sleeper}$	(metric tons)	CV
1984			929	1	163	1.0
1987			783	8	1,319	0.4
1990			708	3	1,651	0.7
1993			775	13	8,657	0.5
1996			807	11	21,101	0.4
1997	136					
1998	74					
1999	558		764	13	19,362	0.4
2000	608					
2001	249	8,406	489	15	37,695	0.4
2002	226	4,709				
2003	270	5,422	809	28	52,116	0.2
2004	282	6,108				
2005	482	9,618	839	26	57,022	0.3
2006	252	5,168				
2007	295	7,375	820	15	39,635	0.4
2008	65	588				
2009	50	493	884	8	39,688	0.4
2010	161	165				
2011	25		670	5	29,496	0.5

Table 2.2: Plausible range of Pacific Sleeper Shark exploitation rates.

The plausible range of average annual exploitation rates (low $\bar{U} = 0.006$; high $\bar{U} = 0.145$; Equation 2.15) for Pacific Sleeper Sharks in the Gulf of Alaska during 2001–2009 was developed from the time series of incidental catch estimates and bottom trawl survey biomass (Biomass) estimates (see Methods; acronyms are defined in Table 2.1). The low-$\bar{U}$ scenario was calculated as [(CAS)/(Biomass)]. The high-$\bar{U}$ scenario was calculated as [(CAS + HFICE)/(Biomass)].

Year	CAS (metric tons)	HFICE (metric tons)	CAS + HFICE (metric tons)	Biomass (metric tons)	Low-$\bar{U}$ scenario	High-$\bar{U}$ scenario
2001	249	8,406	8,655	37,695	0.0066	0.230
2003	270	5,422	5,692	52,116	0.0052	0.109
2005	482	9,618	10,100	57,022	0.0085	0.177
2007	295	7,375	7,670	39,635	0.0074	0.194
2009	50	493	543	39,688	0.0013	0.014
Plausible range of average annual $\bar{U}$					0.006	0.145

Table 2.3: Independently estimated relationships among life history parameters.
Independently estimated relationships among life history parameters were used to parameterize a range of alternative life history scenarios for Pacific Sleeper Sharks in the Gulf of Alaska.

	Equation	Description	Source
1	$M = e^{(1.44 - 0.982 \times \log_e(A_{max}))}$	Natural mortality (M; yr^{-1}) from maximum age (A_{max})	Hoenig 1983
2	$L_{max} = (4/3) L_{mat}$	Maximum TL (L_{max}; cm) from TL at first maturity (L_{mat})	Cortés 2000
3	$L_\infty = e^{(0.044 + 0.9841 \times \log_e(L_{max}))}$	von Bertalanffy asymptotic growth in length (L_∞; cm TL) from L_{max}	Froese and Binohlan 2000
4	$\kappa = \exp\left(\frac{\log_e(M) + 0.0152 + 0.279 \times \log_e(L_\infty) - 0.04634 \times \log_e(T)}{0.6543}\right)$	von Bertalanffy growth rate coefficient (κ ; cm TL/year) from M, L_∞, and water temperature (T; °C)	Pauly 1980; Quinn and Deriso 1999
5	$w_L = \left(4.257 \times 10^{-6}\right) \times L^{3.135}$	Allometric weight (w_L; kg) from TL (L; cm)	Yano et al. 2007, their Table I
6	TL = 7.8 + 1.15×PCL	Pacific Sleeper Shark TL (cm) from pre-caudal length (PCL; cm)	Sigler et al. 2006; L. B. Hulbert, Alaska Department of Fish and Game, personal communication

Table 2.4: Range of parameter values developed for Pacific Sleeper Sharks.
Range of parameter values developed for Pacific Sleeper Sharks in the Gulf of Alaska (GOA), including life history (three scenarios), stock–recruitment steepness (h; two scenarios), length-based selectivity of incidental catch (two scenarios; asymptotic and dome shaped), along with distributional assumptions for the SD in lognormal recruitment variability (σ_R) and the coefficient of variation (CV) in normally distributed length at age (CV_{L_a}).

Parameter	Description	Alternative scenarios		
	Life history			
Life history scenario		1 Relatively short lived	2 Moderately long lived	3 Relatively long lived
a_{max}	Operating model maximum age bin (years)	150	150	150
A_{max}	Maximum age (years) assumed in each scenario	30	50	100
M	Instantaneous natural mortality rate	0.150	0.091	0.046
T	Ambient water temperature (°C)	5.9	5.9	5.9
l_{max}	Operating model maximum length bin (cm TL)	700	700	700
L_{max}	Maximum observed TL (cm) in the GOA	500	500	500
L_∞	von Bertalanffy asymptotic length (cm TL)	473	473	473
κ	von Bertalanffy growth rate coefficient (cm TL/year)	0.220	0.100	0.036
t_0	von Bertalanffy theoretical age (years) at a length of zero	-0.40	-0.86	-2.40
L_{50}	TL (cm) at 50% maturity	365	365	365
k	Logistic maturity curvature	0.056	0.056	0.056
	Stock recruitment steepness			
Steepness scenario		1 Relatively low steepness	2 Relatively high steepness	
h	Stock recruitment steepness parameter	0.25	0.39	
	Length based selectivity			
Selectivity scenario		1 Dome-shaped	2 Asymptotic	
γ	Exponential-logistic (Equation 2.9)	(0.627, 0.521)	(0.00001, 0.00001)	
β	Exponential-logistic (Equation 2.9)	(200.1, 200.6)	(161.3, 176.9)	
α	Exponential-logistic (Equation 2.9)	(0.086, 0.089)	(0.039, 0.046)	
	Distributions (fixed at the same values for all scenarios)			
σ_R	SD in lognormal recruitment variability (Equation 2.11)		0.4	
CV_{L_a}	CV in normally distributed length at age (Equation 2.7)		0.2	

Table 2.5: Monte Carlo simulation overfishing and overfished results.
Alternative model configurations determined to be in an overfishing condition (average annual exploitation rate [$\bar{U}$] > exploitation rate at maximum sustainable yield [U_{MSY}]) under equilibrium conditions (Appendix 2.A); and the percentage of simulations (n =1,000) conducted with the operating model (Equations 2.1–2.14) that ended in an overfished condition ([$\tilde{S}_{t=200}/\tilde{S}_{t=100}$] < 0.5 × [$S_{MSY}/S_0$], where $\tilde{S}_{t=200}$ is female spawning stock biomass [S] at the end of the exploitation period; $\tilde{S}_{t=100}$ is female nonequilibrium S at the end of the initialization period but prior to the start of exploitation; S_{MSY} is female S at maximum sustainable yield; and S_0 is unexploited S of females) under each alternative model configuration evaluated for the indicated combination of maximum age (A_{max} = 30, 50 or 100 years), stock recruitment steepness (h = 0.25 or 0.39), length-based selectivity (dome-shaped or asymptotic [asym]), and exploitation rate ($\bar{U}$ = 0.006 or 0.140; Equation 2.15; Tables 2.2 and 2.4).

Alternative model configuration	A_{max}	h	Selectivity	$\bar{U}$	Equilibrium results		Simulation results (n=1,000)	
					U_{MSY}	Overfishing	S_{MSY}/S_0	Overfished (%)
1	30	0.25	Dome	0.006	0.100	No	0.464	0.0
2	30	0.25	Dome	0.140	0.100	Yes	0.464	0.1
3	30	0.25	Asym	0.006	0.012	No	0.487	0.0
4	30	0.25	Asym	0.140	0.012	Yes	0.487	100.0
5	30	0.39	Dome	0.006	0.312	No	0.388	0.0
6	30	0.39	Dome	0.140	0.312	No	0.388	0.0
7	30	0.39	Asym.	0.006	0.041	No	0.407	0.0
8	30	0.39	Asym	0.140	0.041	Yes	0.407	100.0
9	50	0.25	Dome	0.006	0.047	No	0.465	0.0
10	50	0.25	Dome	0.140	0.047	Yes	0.465	6.3
11	50	0.25	Asym	0.006	0.007	No	0.464	0.0
12	50	0.25	Asym	0.140	0.007	Yes	0.464	100.0
13	50	0.39	Dome	0.006	0.150	No	0.388	0.0
14	50	0.39	Dome	0.140	0.150	No	0.388	0.0
15	50	0.39	Asym	0.006	0.023	No	0.403	0.0
16	50	0.39	Asym	0.140	0.023	Yes	0.403	100.0
17	100	0.25	Dome	0.006	0.017	No	0.466	0.0
18	100	0.25	Dome	0.140	0.017	Yes	0.466	99.8
19	100	0.25	Asym	0.006	0.003	Yes	0.486	0.0
20	100	0.25	Asym	0.140	0.003	Yes	0.486	100.0
21	100	0.39	Dome	0.006	0.055	No	0.388	0.0
22	100	0.39	Dome	0.140	0.055	Yes	0.388	0.0
23	100	0.39	Asym	0.006	0.010	No	0.416	0.0
24	100	0.39	Asym	0.140	0.010	Yes	0.416	100.0

Table 2.6: Aggregate Monte Carlo simulation overfishing and overfished results.
Aggregate number (percentage in parentheses) of model configurations determined to be in an overfishing condition ($\bar{U} > U_{MSY}$; symbols defined in Table 2.5) under equilibrium conditions (Appendix 2.A); and the aggregate number (percentage) of simulations conducted with the operating model (Equations 2.1–2.14) that ended in an overfished condition ($\tilde{S}_{t=200}/\tilde{S}_{t=100} < 0.5 \times [S_{MSY}/S_0]$; symbols defined in Table 2.5) under alternative assumptions about $\bar{U}$ (0.006 or 0.14; Equation 2.15; Table 2.2), life history (maximum age [A_{max}] = 30, 50, or 100 years), stock-recruitment steepness (h = 0.25 or 0.39), and length-based selectivity (asymptotic or dome-shaped; Table 2.4).

	Equilibrium results		Simulation results	
Alternative assumptions	Configurations evaluated	Configurations in an overfishing condition	Simulations evaluated	Simulations ending in an overfished condition
Exploitation rate				
$\bar{U}$ = 0.006	12	1 (8.3)	12,000	0 (0.0)
$\bar{U}$ = 0.140	12	10 (83.3)	12,000	7,072 (58.9)
Life history				
A_{max} = 30	8	3 (37.5)	8,000	2,001 (25.0)
A_{max} = 50	8	3 (37.5)	8,000	2,072 (25.9)
A_{max} = 100	8	5 (62.5)	8,000	2,999 (37.5)
Stock-recruitment steepness				
h = 0.25	12	7 (58.3)	12,000	4,072 (33.9)
h = 0.39	12	4 (33.3)	12,000	3,000 (25.0)
Length-based selectivity				
Asymptotic	12	7 (58.3)	12,000	6,000 (50.0)
Dome-shaped	12	4 (33.3)	12,000	1,072 (8.9)

2.8. Appendix 2.A. Exploitation Rate at Maximum Sustainable Yield

The operating model was used to implement a grid search to find approximate values for the exploitation rate (U) at equilibrium maximum sustainable yield (U_{MSY}) and the corresponding spawning stock biomass (S) obtained at U_{MSY} (S_{MSY}), as described below.

2.8.1. Grid Search

The grid search was implemented to find the fixed U-value (U_{trial}) that maximized the equilibrium sustainable yield. The grid search utilized the same operating model as the risk analysis (Equations 2.1–2.14) except that the annual U (Equation 2.3) was fixed at a constant value of U_{trial} and annual recruitment (Equation 2.11) was fixed at a constant value of 1.0, as described below. Given these specifications, the operating model was used to project the population forward for 200 years at equilibrium recruitment, with U_{trial} evaluated at values from 0 to 1 in increments of 0.001.

The grid search was implemented once for each of the 24 alternative model configurations evaluated in the simulations (Table 2.5). Equilibrium yield per recruit $\left(Y/R\right)_{U_{\mathrm{trial}}}$ and equilibrium spawning stock biomass per recruit $\left(S/R\right)_{U_{\mathrm{trial}}}$ were calculated from the operating model, given the specifications above, as $Y_{t=200}$ (Equation 2.6) and $S_{t=200}$ (Equation 2.14), respectively, at each value of U_{trial} evaluated for the grid search.

The absolute size of the population was unknown. As a result, the value for the equilibrium recruitment parameter (R_0) was assumed to be unknown and was set equal to 1.0 for all model configurations (with units defined as thousands of recruits). The equilibrium S at U_{trial} under the assumed steepness h (Equations 2.11–2.14, 2.20, 2.22; Brooks et al. 2010: their Appendix 2) was then calculated as

$$S_{U_{\mathrm{trial}}} = \frac{4hR_0\left(S/R\right)_{U_{\mathrm{trial}}} - R_0\varphi_0\left(1-h\right)}{5h-1} = \frac{\hat{\alpha}R_0\left(S/R\right)_{U_{\mathrm{trial}}} - R_0\varphi_0}{\hat{\alpha}-1}, \tag{2.A.1}$$

The value of U_{MSY} was found with the grid search as the U_{trial} that maximized the equilibrium sustainable yield (Brooks et al. 2010: their Appendix 2),

$$Y_{U_{\mathrm{trial}}} = \left(Y/R\right)_{U_{\mathrm{trial}}} \frac{S_{U_{\mathrm{trial}}}}{\left(S/R\right)_{U_{\mathrm{trial}}}}. \tag{2.A.2}$$

2.8.2. Approximation of Equilibrium Conditions

The values obtained for U_{MSY} and S_{MSY} were approximations because (1) they depended on a grid search; and (2) within the current formulation of the operating model (Equations 2.1–2.14), it was not possible to include a "plus" group for the maximum age bin (a_{max}) for some of the equations that were used in the grid search to calculate $Y_{t=200}$ and $S_{t=200}$ (Equations 2.6 and 2.14, respectively). However, an attempt was made to improve the approximations by evaluating U_{trial} over a relatively small grid interval (0.001) and by fixing a_{max} in the operating model to a relatively large value (150 years) within all simulation runs (Table 2.4). Given these specifications, the resulting values calculated for $Y_{t=200}$ and $S_{t=200}$ were similar to those calculated for $Y_{t=199}$ and $S_{t=199}$, respectively (<0.1% absolute difference for all model runs), indicating that approximate equilibrium conditions had been achieved within the grid search algorithm after 200 years of fixed exploitation.

2.8.3. Literature Cited

Brooks, E. N., J. E. Powers, and E. Cortés. 2010. Analytical reference points for age-structured models: application to data-poor fisheries. ICES Journal of Marine Science 67:165–175.

2.9. Supplement 2.A: Length Composition Data[3]

Length composition data used in this study were from Pacific Sleeper Sharks that were captured in the Gulf of Alaska (GOA; Figure 2.S.A.1), as described below.

Size composition data for the incidental catch of GOA Pacific Sleeper Sharks were unavailable because most of the sharks that were captured incidentally in U.S. federally managed commercial groundfish fisheries within the GOA were not measured for length (e.g., Courtney et al. 2006; Tribuzio et al. 2011). Consequently, the length composition (length frequency) of the Pacific Sleeper Shark incidental catch in the GOA was approximated here from three fishery independent data sources. The first source was the National Marine Fisheries Service (NMFS) Alaska Fisheries Science Center (AFSC) bottom trawl survey (n = 86 incidentally captured Pacific Sleeper Sharks) conducted every 2–3 years during 1987–2007 in the western, central, and eastern GOA, primarily within NMFS statistical areas 610, 620, and 630 (Table 2.S.A.1; Figure 2.S.A.1; Dean L. Courtney, unpublished data). The second source was NMFS-AFSC bottom longline research targeting Pacific Sleeper Sharks (n = 198) for diet studies during 2001 and 2002 in the central GOA, primarily NMFS statistical area 630 (Table 2.S.A.2; Figure 2.S.A.1; Sigler et al. 2006; Michael F. Sigler, unpublished data). The third source was the NMFS-AFSC Auke Bay Laboratory's bottom longline research, which targeted Pacific Sleeper Sharks (n = 151) for tagging studies during 2003–2006 in marine waters of Southeast Alaska within NMFS statistical area 659 (Table 2.S.A.3; Figure 2.S.A.1; Courtney and Hulbert 2007; Courtney, unpublished data).

Length measurements from Pacific Sleeper Sharks were recorded variously as FL (tip of snout to fork in tail; Table 2.S.A.1), pre-caudal length (PCL; tip of snout to the dorsal insertion of the caudal peduncle; Table 2.S.A.2), and TL (tip of snout to tip of tail in a natural position; Table 2.S.A.3). For the purposes of this study, all length measurements were converted to TL (cm). Total length was obtained from PCL by use of a previously developed relationship ($TL = 7.8 + 1.15 \times PCL$; Figure 2.S.A.2; Sigler et al. 2006; L. B. Hulbert, Alaska Department of Fish and Game, unpublished data). Total length was obtained from FL by using a ratio ($TL = FL \times 1.07$) obtained here based on a photograph of a 220-cm TL immature male Pacific Sleeper Shark that was captured during tagging studies in Southeast Alaska (Figure 2.S.A.3; Courtney and Hulbert 2007; Courtney, unpublished data).

[3] sm5083 (North American Journal of Fisheries Management 36:523-548, 2016; DOI: 10.1080/02755947.2015.1131779)

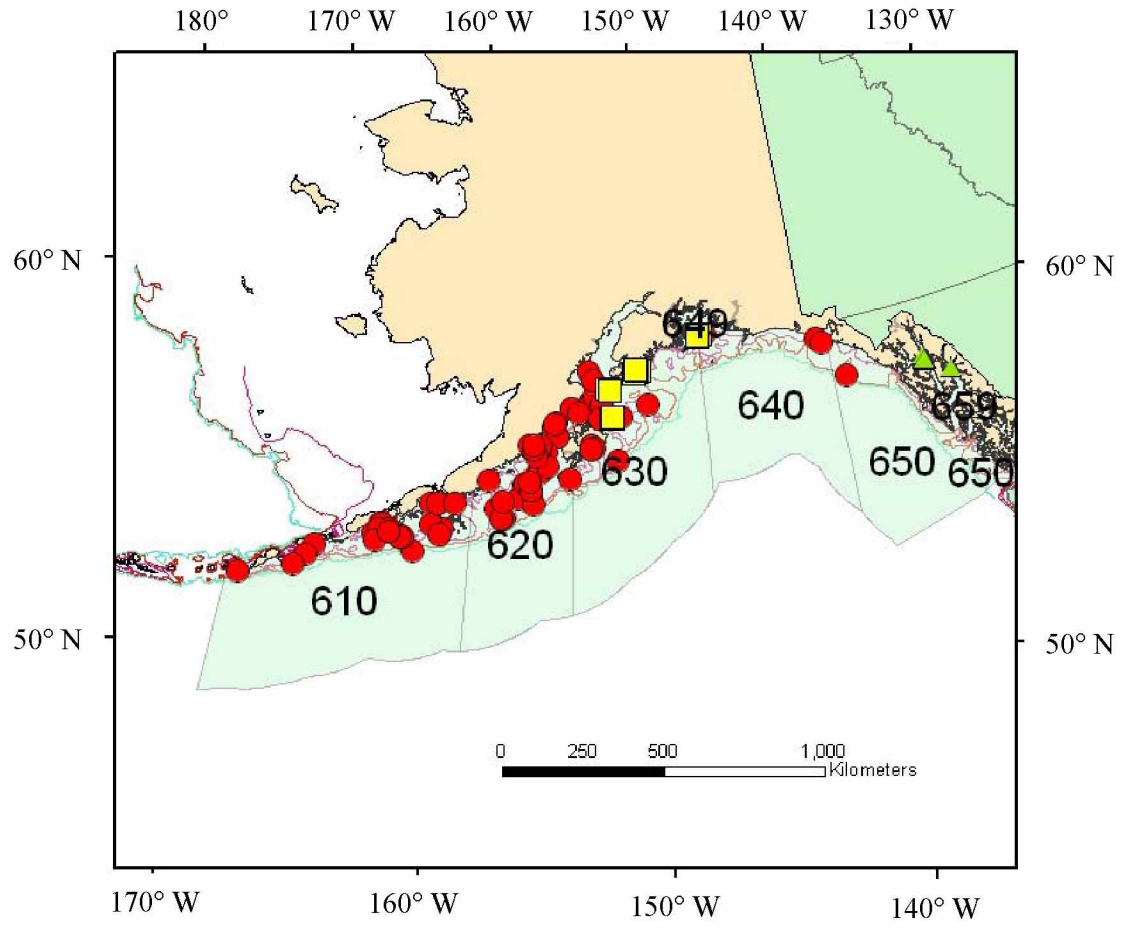

Figure 2.S.A.1: Map depicting length sample locations.
Gulf of Alaska (GOA) locations where Pacific Sleeper Sharks were captured and measured for length: the National Marine Fisheries Service (NMFS) Alaska Fisheries Science Center (AFSC) bottom trawl survey conducted in the GOA every 2–3 years during 1987–2007 (circles within NMFS statistical areas 610, 620, 630, 640, and 650; Table 2.S.A.1; Courtney, unpublished data); diet studies conducted by the NMFS-AFSC with bottom longline gear in the GOA during 2001–2002 (squares within NMFS statistical areas 630 and 649; Table 2.S.A.2; Sigler et al. 2006; Sigler, unpublished data); and tagging studies conducted by the NMFS-AFSC Auke Bay Laboratory with bottom longline gear in marine waters of Southeast Alaska during 2003–2006 (triangles within NMFS statistical area 659; Table 2.S.A.3; Courtney and Hulbert 2007; Courtney, unpublished data). Sampling locations are plotted relative to depth contours (100, 200, and 1,000 m).

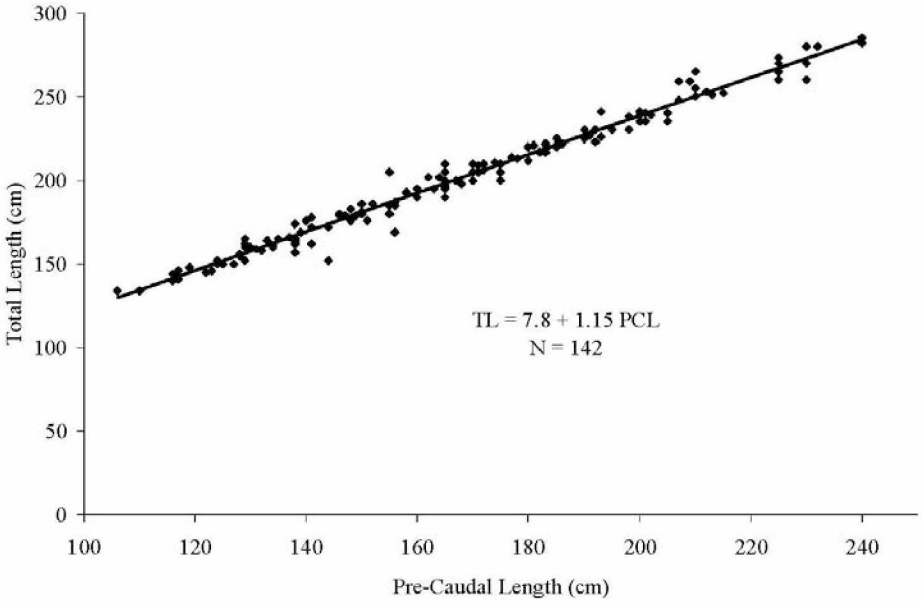

Figure 2.S.A.2: Plot of Pacific Sleeper Shark length conversion relationship.
Observed and predicted relationships between the TL (cm) and pre-caudal length (PCL; cm) of Pacific Sleeper Sharks obtained during National Marine Fisheries Service Alaska Fisheries Science Center research targeting this species for diet studies with bottom longline gear in the Gulf of Alaska during 2001–2002 (Sigler et al. 2006; L. B. Hulbert, unpublished data).

Figure 2.S.A.3: Photograph of Pacific Sleeper Shark for length conversion relationship.
Beth Mathews (University of Alaska Southeast) and D. L. C. on the charted FV *Sea View* with a 220-cm TL (~7-ft) immature male Pacific Sleeper Shark that was captured during tagging studies conducted by the National Marine Fisheries Service Alaska Fisheries Science Center's Auke Bay Laboratory with bottom longline gear in marine waters of Southeast Alaska during 2003–2006. The photograph was printed at a resolution of 8.5 × 11.0 in (21.59 × 27.94 cm); was measured for shark TL (9.25 in [23.49 cm]) and FL (8.625 in [21.91 cm]); and was used to derive the TL–FL relationship (TL = FL×1.07).

Table 2.S.A.1: Pacific Sleeper Shark lengths obtained from bottom trawl surveys.
Size composition (length frequency) of Pacific Sleeper Sharks that were captured incidentally during the National Marine Fisheries Service, Alaska Fisheries Science Center bottom trawl survey conducted in the Gulf of Alaska every 2–3 years over the period 1987–2007 (Courtney, unpublished data). Length measurements were recorded in FL (cm), were converted to TL (cm) with the relationship TL = FL×1.07 (Figure 2.S.A.3), and then were grouped into 10-cm length bins.

Length bin (cm TL)	1987	1990	1996	1999	2001	2003	2005	2007	Total
≤50[a]	0	0	0	0	0	0	1	0	1
60	0	0	0	0	0	0	0	0	0
70	0	0	0	0	0	0	0	0	0
80	0	0	0	0	0	0	0	0	0
90	0	0	0	0	0	0	0	0	0
100	0	0	0	0	0	0	0	0	0
110	0	0	0	0	0	0	0	0	0
120	0	0	0	0	0	0	2	0	2
130	0	0	0	0	0	1	0	0	1
140	0	0	0	0	0	2	2	1	5
150	0	0	0	1	1	2	3	1	8
160	0	0	0	0	1	1	2	1	5
170	0	0	0	0	0	3	1	2	6
180	1	0	0	0	0	1	1	0	3
190	0	0	2	0	3	1	2	1	9
200	0	1	0	2	0	4	3	1	11
210	0	0	0	0	0	2	2	2	6
220	0	0	1	0	2	3	0	0	6
230	0	0	0	0	1	0	1	0	2
240	0	0	0	0	0	3	0	1	4
250	0	0	0	0	0	1	0	1	2
260	0	0	0	0	0	3	0	1	4
270	0	0	1	1	0	0	1	0	3
280	0	0	0	1	0	0	0	1	2
290	0	0	0	0	1	0	0	0	1
300	0	0	0	0	1	0	1	1	3
310	0	0	0	0	0	0	0	1	1
320	0	0	0	0	0	0	0	0	0
330	0	0	0	0	0	0	0	0	0
340	0	0	0	0	0	0	0	1	1
350+	0	0	0	0	0	0	0	0	0
Average TL (cm)	175	200	217	219	213	200	175	223	201
Number measured for length	1	1	4	5	10	27	22	16	86
Number of hauls	1	1	4	4	8	23	20	15	76
Percentage female	NA	NA	100	100	60	64	89	60	72
Number identified for sex	0	0	4	3	10	25	19	15	76

[a] One individual, 32 cm TL (2005 bottom trawl survey, vessel 134, haul 90).

Table 2.S.A.2: Pacific Sleeper Shark lengths obtained from diet studies.
Size composition (length frequency) of Pacific Sleeper Sharks that were captured for diet studies by the National Marine Fisheries Service, Alaska Fisheries Science Center with bottom longline gear in the Gulf of Alaska during 2001–2002 (Sigler et al. 2006; Sigler, unpublished data). Length measurements were recorded in pre-caudal length (PCL; cm), were converted to TL (cm) with the relationship TL = 7.8 + 1.15×PCL (Figure 2.S.A.2; Sigler et al. 2006; L. B. Hulbert, unpublished data), and then were grouped into 10-cm length bins.

Length bin (cm TL)	2001	2002	Total
≤50	0	0	0
60	0	0	0
70	0	0	0
80	0	0	0
90	0	0	0
100	0	0	0
110	0	0	0
120	0	0	0
130	2	0	2
140	5	2	7
150	5	5	10
160	9	9	18
170	14	6	20
180	11	5	16
190	7	6	13
200	9	10	19
210	9	11	20
220	5	11	16
230	7	7	14
240	5	10	15
250	6	6	12
260	3	1	4
270	2	8	10
280	0	2	2
290	0	0	0
300	0	0	0
310	0	0	0
320	0	0	0
330	0	0	0
340	0	0	0
350+	0	0	0
Average TL (cm)	194	209	202
Number measured for length	99	99	198
Number of hauls	14	10	24
Percentage female	60	61	60
Number identified for sex	99	99	198

Table 2.S.A.3: Pacific Sleeper Shark lengths obtained from tagging studies.
Size composition (length frequency) of Pacific Sleeper Sharks that were captured for tagging studies by the National Marine Fisheries Service, Alaska Fisheries Science Center's Auke Bay Laboratory with bottom longline gear in marine waters of Southeast Alaska during 2003–2006 (Courtney and Hulbert 2007; Courtney, unpublished data). Total length measurements were recorded in feet, were converted to centimeters, and then were grouped into 10-cm length bins.

Length (cm TL)[a]	2003	2004	2005	2006	Total
=50	0	0	0	0	0
60	0	0	0	0	0
70	0	0	0	0	0
80	0	0	0	0	0
90	0	0	0	0	0
100	0	0	0	0	0
110	0	0	0	0	0
120	1	0	0	0	1
130	0	0	0	0	0
140	0	0	0	0	0
150	5	2	3	0	10
160	0	0	0	0	0
170	4	0	3	0	7
180	10	10	4	2	26
190	2	0	0	3	5
200	8	6	4	3	21
210	12	3	16	7	38
220	0	0	0	2	2
230	1	4	5	3	13
240	3	3	6	3	15
250	0	0	0	2	2
260	0	0	0	3	3
270	2	1	2	1	6
280	0	0	0	1	1
290	0	0	0	0	0
300	0	0	1	0	1
310	0	0	0	0	0
320	0	0	0	0	0
330	0	0	0	0	0
340	0	0	0	0	0
350+	0	0	0	0	0
Average TL (cm)	196	203	213	224	208
Number measured for length	48	29	44	30	151
Number of hauls	6	4	5	8	23
Percentage female	56	63	52	66	58
Number identified for sex	32	24	42	29	127

[a] During 2003–2006, some of the TL measurements were recorded to the nearest foot (Courtney, unpublished data).

2.9.1. Literature Cited

Courtney, D. L., and L. Hulbert. 2007. Shark research in the Gulf of Alaska with satellite, sonic, and archival tags (extended abstract). NOAA Technical Memorandum NMFS-F/SPO- 82:26–27.

Courtney, D., C. Tribuzio, K. J. Goldman, and J. Rice. 2006. Appendix E, Gulf of Alaska sharks. Pages 481–562 *in* Stock assessment and fishery evaluation report for the groundfish resources of the Gulf of Alaska for 2007. North Pacific Fishery Management Council, Anchorage, Alaska.

Sigler, M. F., L. B. Hulbert, C. R. Lunsford, N. H. Thompson, K. Burek, G. O'Corry-Crowe, and A. C. Hirons. 2006. Diet of Pacific Sleeper Shark, a potential Steller sea lion predator, in the northeast Pacific Ocean. Journal of Fish Biology 69:392–405.

Tribuzio, C. A., K. Echave, C. Rodgveller, P.-J. Hulson, and K. J. Goldman. 2011. Chapter 20: assessment of the shark stock complex in the Gulf of Alaska. Pages 1393–1446 *in* Stock assessment and fishery evaluation report for the groundfish resources of the Gulf of Alaska for 2012. North Pacific Fishery Management Council, Anchorage, Alaska.

2.10. Supplement 2.B: Selectivity and Intermediate-Year Overfished Results[4]

2.10.1. Length-Based Selectivity

For the purposes of these simulations, the observed length composition data for Pacific Sleeper Sharks that were captured in the National Marine Fisheries Service (NMFS) Alaska Fisheries Science Center (AFSC) bottom trawl survey conducted in the Gulf of Alaska (GOA) during 1987–2007 (Table 2.S.A.1 in Supplement 2.A) were pooled into a single length frequency distribution (Figure 2.S.B.1A), which was assumed to approximate the historical length composition of Pacific Sleeper Shark incidental catch taken by commercial bottom trawl gear in the GOA. Similarly, the observed length composition data for Pacific Sleeper Sharks captured in NMFS-AFSC bottom longline research conducted in the GOA during 2001–2002 (Table 2.S.A.2) and 2003–2006 (Table 2.S.A.3) were pooled into a second length frequency distribution (Figure 2.S.B.1B), which was assumed to approximate the historical length composition of Pacific Sleeper Shark incidental catch taken by commercial bottom longline gear in the GOA.

Two length-based selectivity scenarios were developed from the limited available length composition data: (1) asymptotic (Figure 2.S.B.1) and (2) dome shaped (Figures 2.S.B.2, 2.S.B.3), as described in the Methods.

2.10.2. Intermediate-Year Overfished Results

Plots of intermediate-year overfished results (t = 101–200) obtained under each alternative model configuration (Table 2.5) are provided in Figures 2.S.B.4–2.S.B.6. Percentiles of $\tilde{S}_t/\tilde{S}_{t=100}$ (symbols defined in Methods) obtained during simulation years t = 101–200 (n = 1,000 simulations; 50th, lower 2.5th, and upper 97.5th) were compared to the overfished reference line, $0.5 \times (S_{MSY}/S_0)$, which was obtained separately for each alternative model configuration under equilibrium conditions (Table 2.5; Appendix 2.A). A simulation was designated as having resulted in an overfished condition during intermediate simulation year t if $\tilde{S}_t/\tilde{S}_{t=100} < 0.5 \times (S_{MSY}/S_0)$.

[4] sm5077 (North American Journal of Fisheries Management 36:523-548, 2016; DOI: 10.1080/02755947.2015.1131779)

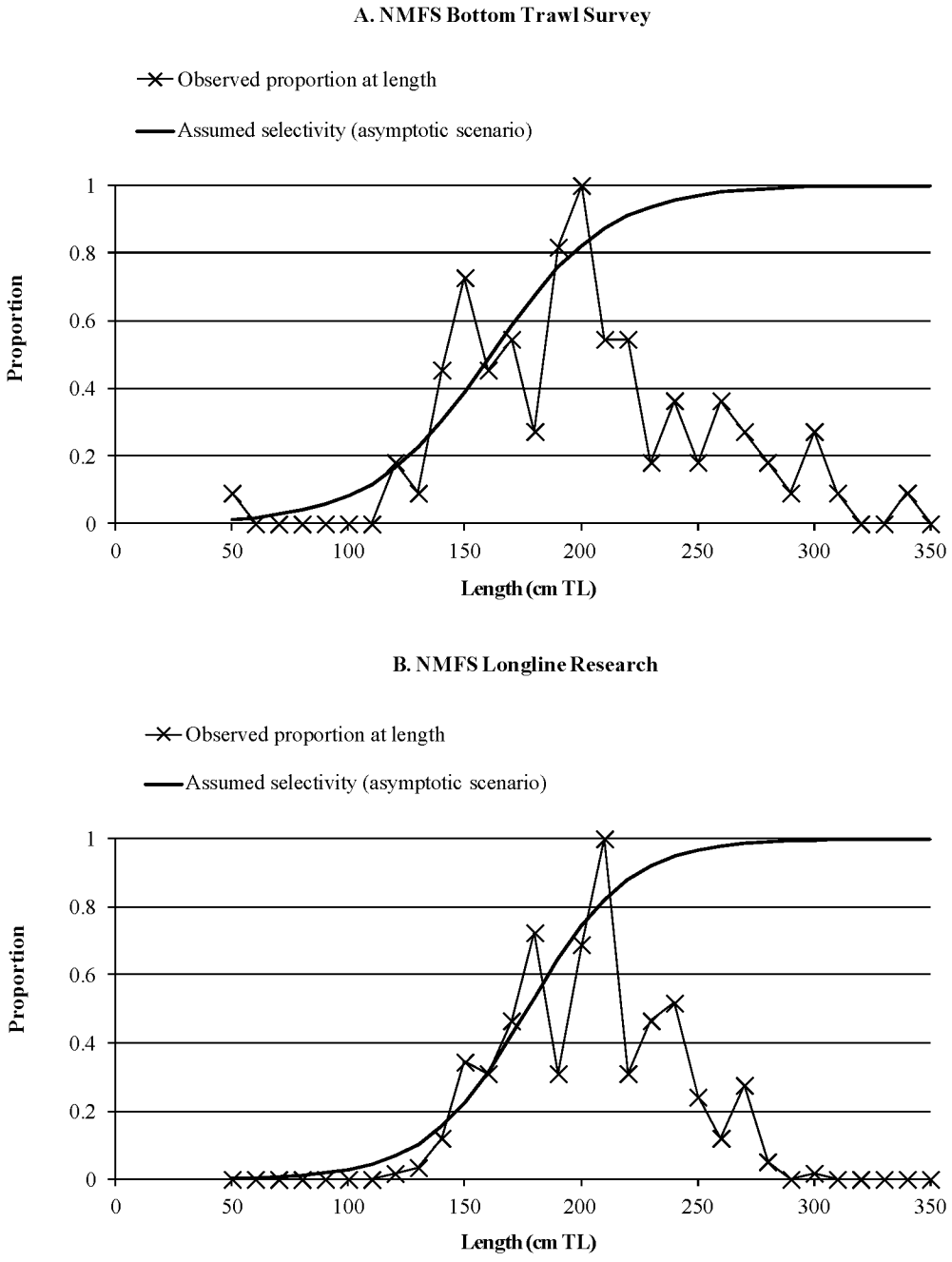

Figure 2.S.B.1: Asymptotic selectivity developed from bottom trawl and longline research. Observed proportions at length obtained from the pooled size composition data developed for Pacific Sleeper Sharks captured in (A) the National Marine Fisheries Service (NMFS) Alaska Fisheries Science Center (AFSC) bottom trawl survey conducted in the Gulf of Alaska (GOA) during 1987–2007 (Table S.A.1); and (B) NMFS-AFSC bottom longline research conducted in the GOA during 2001–2002 (Table S.A.2) and 2003–2006 (Table 2.S.A.3). The assumed selectivity curves under the asymptotic selectivity scenario (described in Methods) are also plotted.

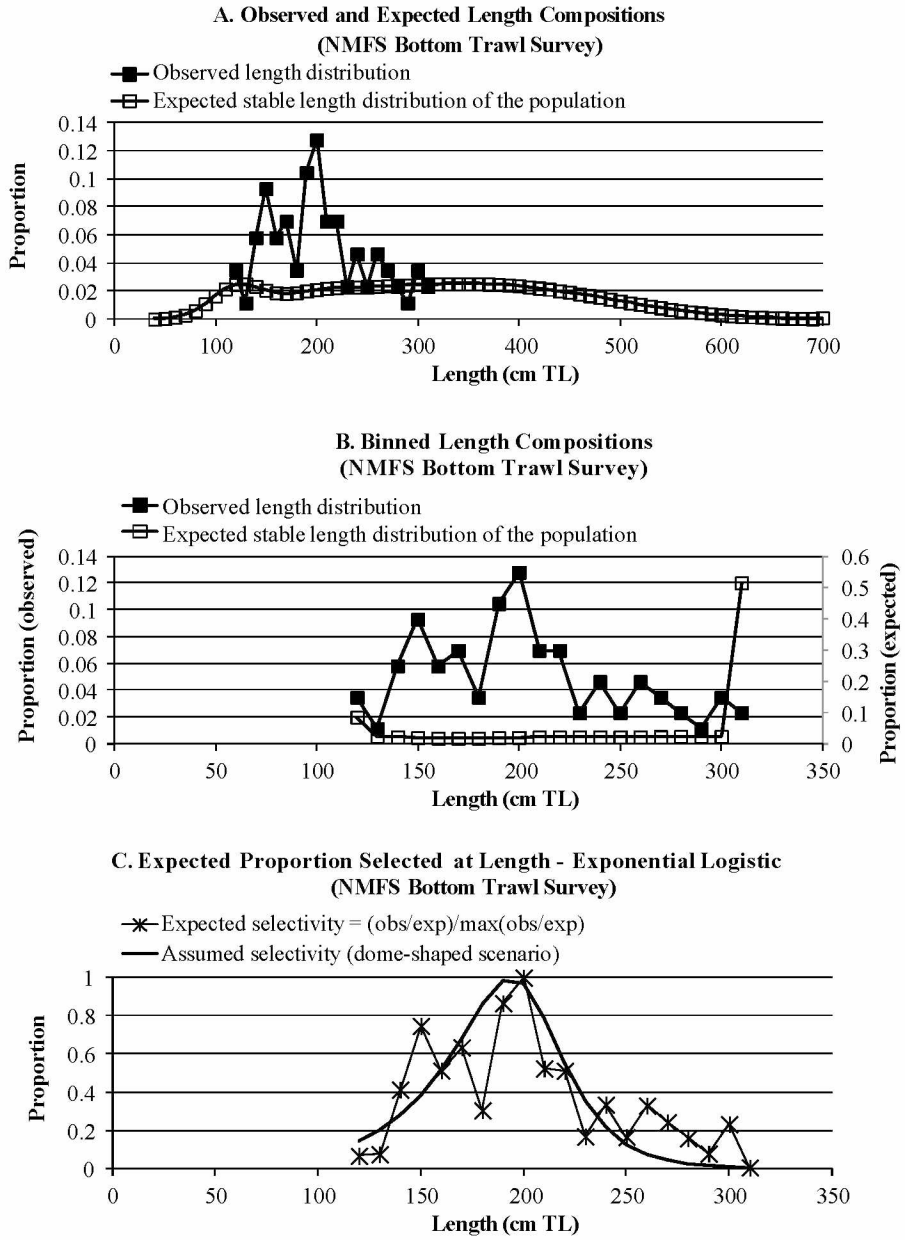

Figure 2.S.B.2: Dome-shaped selectivity developed from bottom trawl research.
(A) Observed proportions at length obtained from the pooled size composition data for Pacific Sleeper Sharks captured in the National Marine Fisheries Service (NMFS) Alaska Fisheries Science Center bottom trawl survey conducted in the Gulf of Alaska during 1987–2007 (Table 2.S.A.1), plotted along with the expected stable length distribution of the population per recruit; (B) the same data binned at the minimum and maximum observed lengths; and (C) the same data converted to expected proportions selected at length, plotted along with the assumed selectivity under the dome-shaped selectivity scenario (described in Methods).

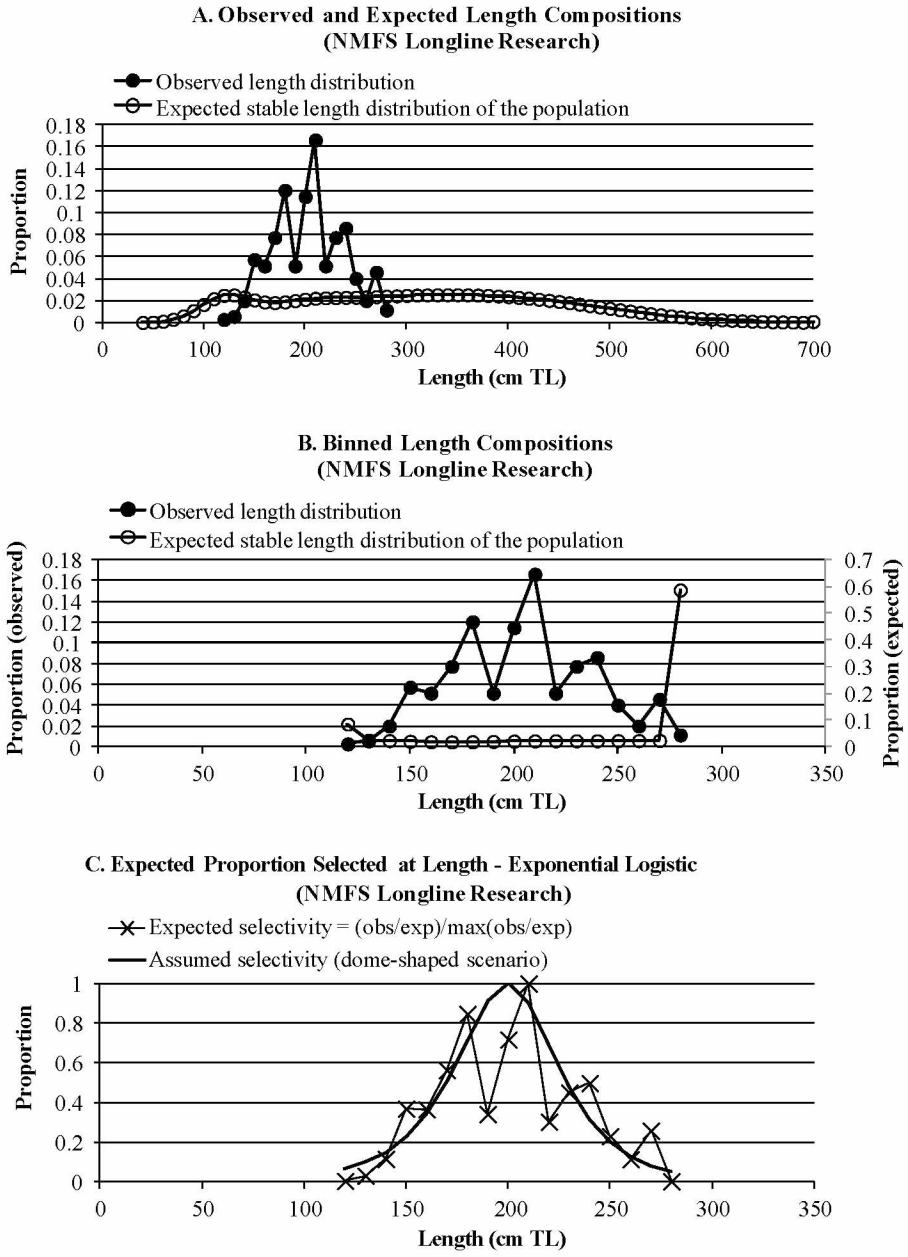

Figure 2.S.B.3: Dome-shaped selectivity developed from bottom longline research.
(A) Observed proportions at length obtained from the pooled size composition data for Pacific Sleeper Sharks captured in National Marine Fisheries Service (NMFS) Alaska Fisheries Science Center bottom longline research conducted in the Gulf of Alaska during 2001–2002 (Table 2.S.A.2) and 2003–2006 (Table 2.S.A.3), plotted along with the expected stable length distribution of the population per recruit; (B) the same data binned at the minimum and maximum observed lengths; and (C) the same data converted to expected proportions selected at length, plotted along with the assumed selectivity under the dome-shaped selectivity scenario (described in Methods).

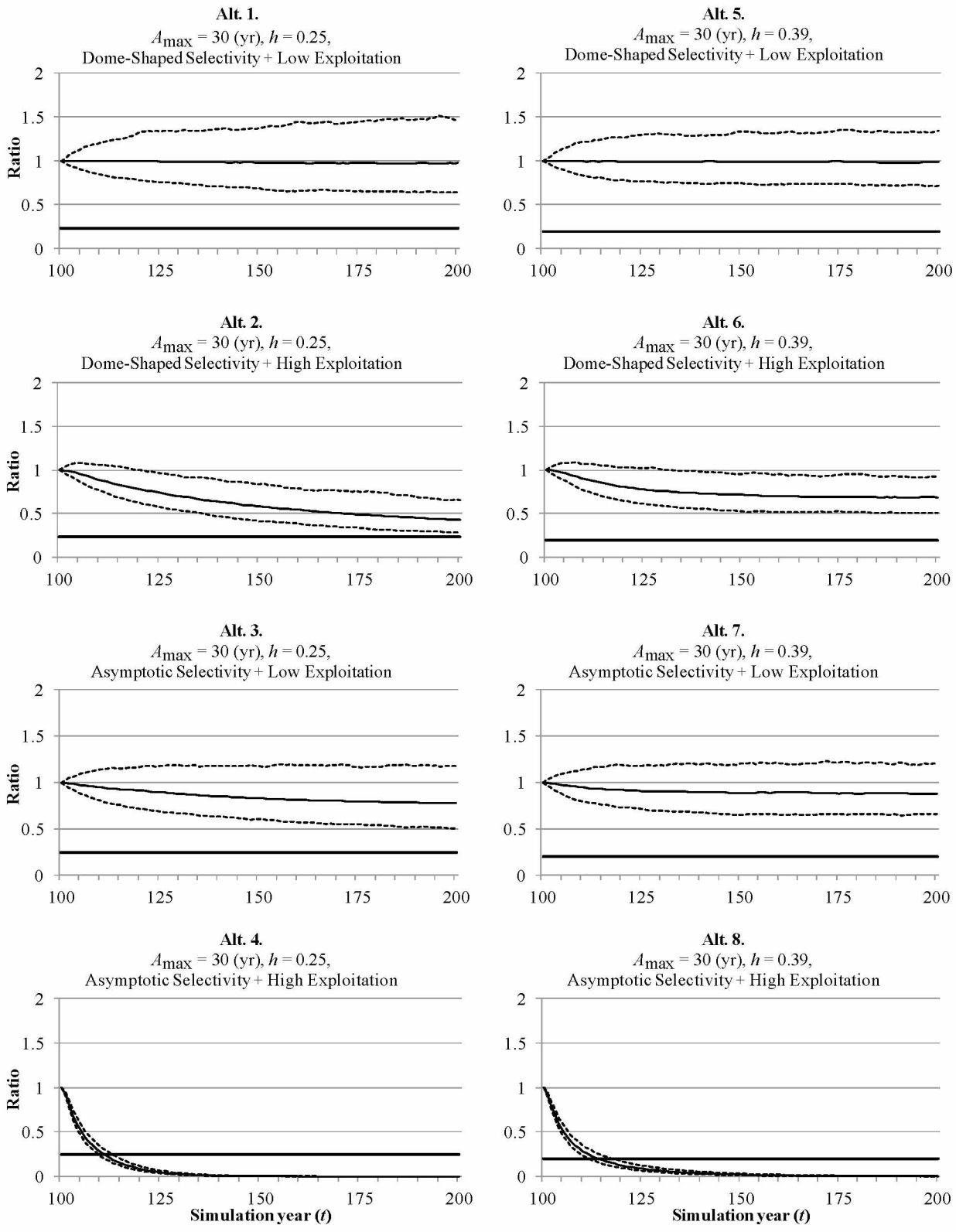

Figure 2.S.B.4: Simulation results for model configurations 1–8.

Figure 2.S.B.4. Continued. Percentiles (thin solid line is 50th; dashed lines are lower 2.5th and upper 97.5th; n = 1,000 simulations) of the ratio $\tilde{S}_t/\tilde{S}_{t=100}$ (where $\tilde{S}_t$ is female spawning stock biomass [S] in intermediate simulation year t; $\tilde{S}_{t=100}$ is female nonequilibrium S at the end of the initialization period but prior to the start of exploitation) obtained during simulation years t = 101–200 for the relatively short life span scenario (A_{max} = 30 years) under relatively low and relatively high productivity (steepness h = 0.25 and 0.39, respectively), dome-shaped and asymptotic selectivity, and low and high exploitation (Table 2.5). The bold horizontal line in each panel represents the overfished reference, 0.5 × (S_{MSY}/S_0) (where S_{MSY} is female S at maximum sustainable yield; and S_0 is unexploited equilibrium S of females), which was obtained separately under equilibrium conditions (Appendix 2.A) for each alternative model configuration (Table 2.5).

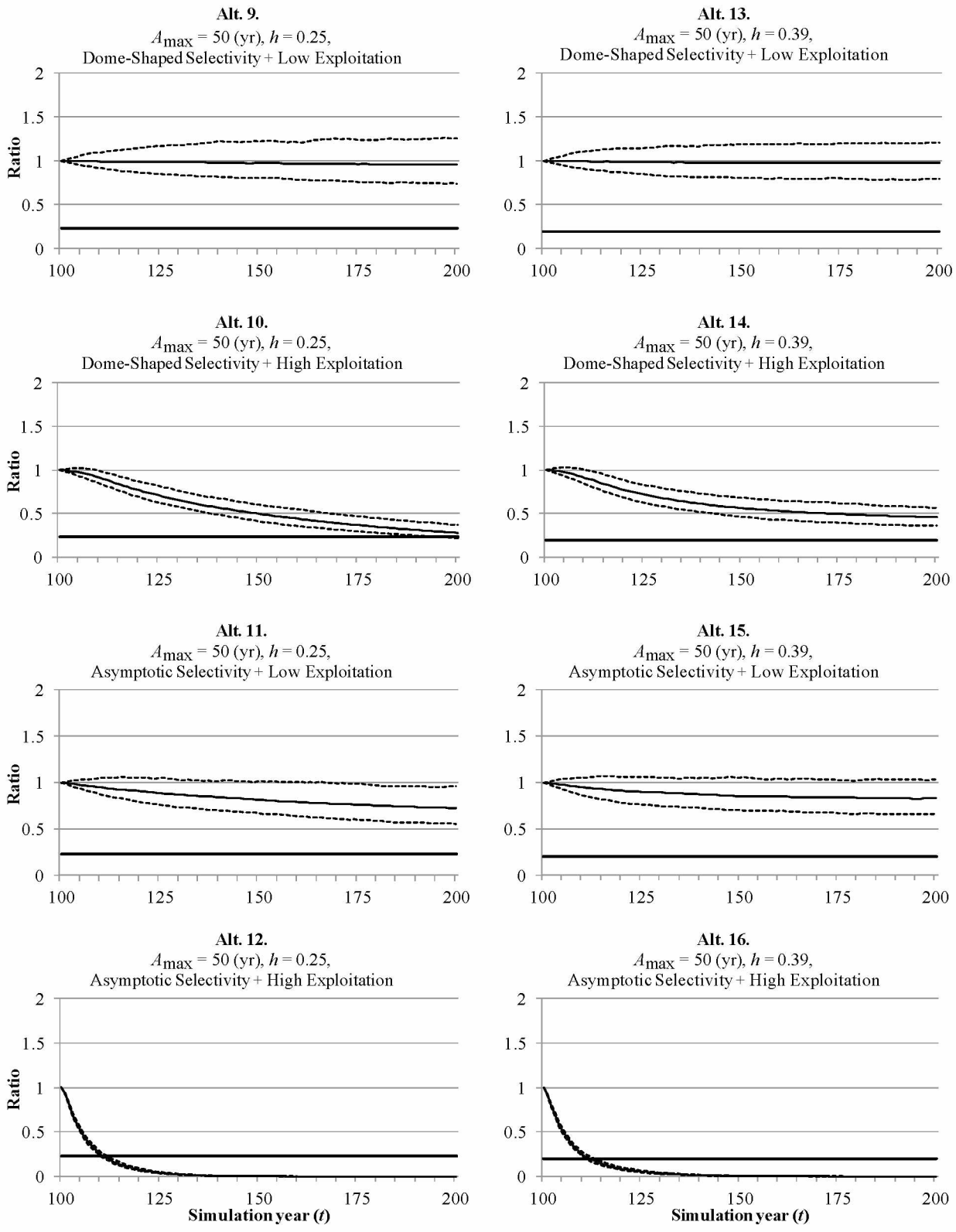

Figure 2.S.B.5: Simulation results for model configurations 9–16.

Figure 2.S.B.5. Continued. Percentiles (thin solid line is 50th; dashed lines are lower 2.5th and upper 97.5th; n = 1,000 simulations) of the ratio $\tilde{S}_t/\tilde{S}_{t=100}$ (where $\tilde{S}_t$ is female spawning stock biomass [S] in intermediate simulation year t; $\tilde{S}_{t=100}$ is female nonequilibrium S at the end of the initialization period but prior to the start of exploitation) obtained during simulation years t = 101–200 for the moderately long life span scenario (A_{max} = 50 years) under relatively low and relatively high productivity (steepness h = 0.25 and 0.39, respectively), dome-shaped and asymptotic selectivity, and low and high exploitation (Table 2.5). The bold horizontal line in each panel represents the overfished reference, 0.5 × (S_{MSY}/S_0) (where S_{MSY} is female S at maximum sustainable yield; and S_0 is unexploited equilibrium S of females), which was obtained separately under equilibrium conditions (Appendix 2.A) for each alternative model configuration (Table 2.5).

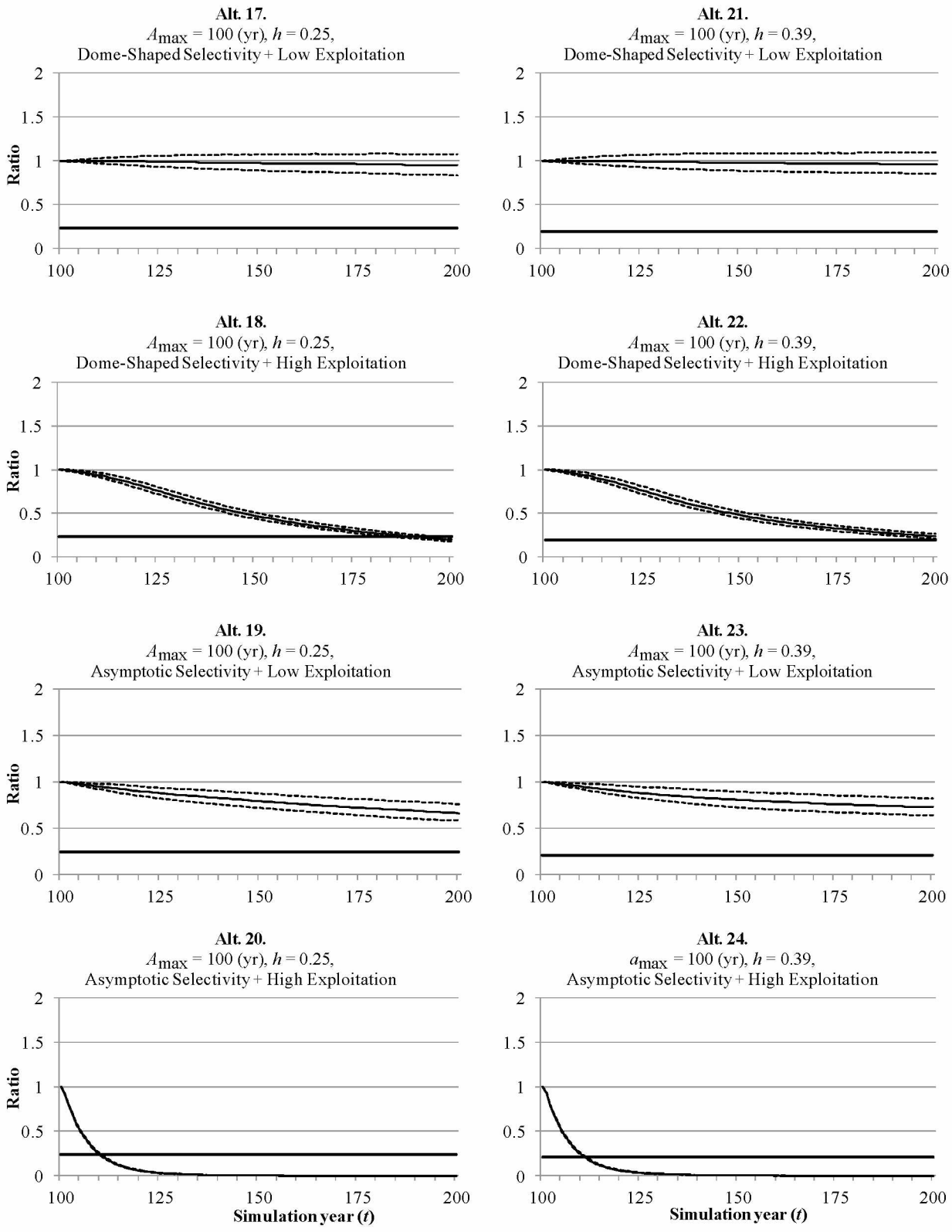

Figure 2.S.B.6: Simulation results for model configurations 17–24.

Figure 2.S.B.6. Continued. Percentiles (thin solid line is 50th; dashed lines are lower 2.5th and upper 97.5th; n = 1,000 simulations) of the ratio $\tilde{S}_t/\tilde{S}_{t=100}$ (where $\tilde{S}_t$ is female spawning stock biomass [S] in intermediate simulation year t; $\tilde{S}_{t=100}$ is female nonequilibrium S at the end of the initialization period but prior to the start of exploitation) obtained during simulation years t = 101–200 for the relatively long life span scenario (A_{max} = 100 years) under relatively low and relatively high productivity (steepness h = 0.25 and 0.39, respectively), dome-shaped and asymptotic selectivity, and low and high exploitation (Table 2.5). The bold horizontal line in each panel represents the overfished reference, 0.5 × (S_{MSY}/S_0) (where S_{MSY} is female S at maximum sustainable yield; and S_0 is unexploited equilibrium S of females), which was obtained separately under equilibrium conditions (Appendix 2.A) for each alternative model configuration (Table 2.5).

3. Chapter 3 Pacific Sleeper Shark Trophic Ecology[5]

3.1. Abstract

Stable-isotope ratios of nitrogen ($\delta^{15}N$) and lipid-normalized carbon ($\delta^{13}C'$) were used to examine geographic and ontogenetic variability in the trophic ecology of a high latitude benthopelagic elasmobranch, the Pacific sleeper shark *Somniosus pacificus*. Mean muscle tissue $\delta^{13}C'$ values of *S. pacificus* differed significantly among geographic regions of the eastern North Pacific Ocean. Linear models identified significant ontogenetic and geographic variability in muscle tissue $\delta^{15}N$ values of *S. pacificus*. The trophic position of *S. pacificus* in the eastern North Pacific Ocean estimated here from previously published stomach-content data (4.3) was within the range of *S. pacificus* trophic position predicted from a linear model of *S. pacificus* muscle tissue $\delta^{15}N$ (3.3–5.7) for fish of the same mean total length (L_T; 201.5 cm), but uncertainty in predicted trophic position was very high (95% prediction intervals ranged from 2.9 to 6.4). The relative trophic position of *S. pacificus* determined here from a literature review of $\delta^{15}N$ by taxa in the eastern North Pacific Ocean was also lower than would be expected based on stomach-content data alone when compared to fishes, squid and filter feeding whales. Stable-isotope analysis revealed wider variability in the feeding ecology of *S. pacificus* in the eastern North Pacific Ocean than shown by diet data alone, and expanded previous conclusions drawn from analyses of stomach-content data to regional and temporal scales meaningful for fisheries management.

[5]Courtney, D. L., and R. Foy. 2012. Pacific sleeper shark *Somniosus pacificus* trophic ecology in the eastern North Pacific Ocean inferred from nitrogen and carbon stable isotope ratios and diet. Journal of Fish Biology 80:1508–1545.

3.2. Introduction

The Pacific sleeper shark *Somniosus pacificus* Bigelow & Schroeder 1944 is a benthopelagic elasmobranch common to the continental shelves and the upper continental slopes of the high latitude North Pacific Ocean (Compagno, 1984; Ebert et al., 1987; Orlov, 1999; Orlov & Moiseev, 1999a, b; Mecklenburg et al., 2002; Yano et al., 2004, 2007; Murray et al., 2008; Ebert & Winton, 2010), but also occurs in both the Arctic (Benz et al., 2004) and the lower latitude North Pacific Oceans (Borets, 1986; Wang & Yang, 2004; Yeh & Drazen, 2009). In the eastern North Pacific Ocean, *S. pacificus* occur primarily at depths between 250 and 450 m (61% of observations), but make regular ascents to depths <100 m (58% of days observed) (Hulbert et al., 2006). *Somniosus pacificus* may attain large size [c. 7 m total length (L_T)], but specimens >430 cm L_T have only been reported from estimated lengths (Compagno, 1984; Ebert et al., 1987; Orlov, 1999; Wang & Yang, 2004; Yano et al., 2004, 2007). The diet of *S. pacificus* varies ontogenetically as well as by season, geographic region and capture depth, probably in response to prey availability (Bright, 1959; Gotshall & Jow, 1965; Ebert et al., 1987; Orlov, 1999; Orlov & Moiseev, 1999a, b; Yang & Page, 1999; Smith & Baco, 2003; Wang & Yang, 2004; Taggart et al., 2005; Sigler et al., 2006; Yano et al., 2007). As a result, the trophic ecology of *S. pacificus* in the eastern North Pacific Ocean is uncertain (Hulbert et al., 2006; Sigler et al., 2006; McMeans et al., 2007).

Understanding the trophic ecology of *S. pacificus* is important because of the potential ecological consequences of changes in *S. pacificus* abundance in the eastern North Pacific Ocean. In particular, catch rates of *S. pacificus* have increased noticeably in fisheries independent surveys for groundfishes in some regions of the eastern North Pacific Ocean (Mueter & Norcross, 2002; Courtney & Sigler, 2007). *Somniosus pacificus* are also captured as by-catch in Alaskan commercial groundfish fisheries, but discard mortality rates for *S. pacificus* are uncertain because shark by-catch is currently managed as part of a non-target data-poor species complex (Reuter et al., 2010). Large-bodied *Somniosus* spp. are assumed to be slow growing (Hansen, 1963) and long lived (Fisk et al., 2002); as a result, *S. pacificus* may be relatively more vulnerable to overfishing than the teleost target species they are captured with (Smith et al., 1998; Forrest & Walters, 2009; Kyne & Simpfendorfer, 2010). Ecosystem-based fishery management requires the collection of data on species interactions in order to minimize the risk of irreversible changes to natural assemblages of species and ecosystem processes from the effects of fishing (Pikitch et al., 2004). While the potential ecological effects of changes in *S. pacificus* abundance in the eastern North Pacific Ocean are uncertain (Frid et al., 2006, 2007a, b, 2008, 2009; Wirsing et al., 2008; Heithaus et al., 2008; Kuker & Barrett-Lennard, 2010; Heithaus et al., 2010; Horning & Mellish, 2012), changes in elasmobranch abundance in other ecosystems have been indicative of or in response to ecosystem level restructuring following the effects of fishing (Kitchell et al., 2002; Myers et al., 2007; Baum & Worm,

2009). Furthermore, sharks may be at or near the apex of trophic structures that support them and, as a result, may function as keystone predators and be essential to the maintenance and stability of food webs (Myers et al., 2007).

Reliance on stomach contents alone to quantify the diet of elasmobranchs has limits (Wetherbee & Cortés, 2004). Consequently, the use of stable isotopes to examine trophic position and feeding in different food webs can improve the understanding of *S. pacificus* trophic ecology in the eastern North Pacific Ocean. Stable-isotope analysis of nitrogen ($\delta^{15}N$) and carbon ($\delta^{13}C$) (DeNiro & Epstein, 1978, 1981; Minagawa & Wada, 1984) is a useful predictor of trophic relationships in aquatic ecosystems (Vander Zanden et al., 1997; Post, 2002; Martínez del Rio et al., 2009) and has been used to investigate the trophic ecology of elasmobranchs (Estrada et al., 2003, 2006; Domi et al., 2005; MacNeil et al., 2005; Kerr et al., 2006; Andrews & Foy, 2009; Andrews, 2010; Matich et al., 2010a; Papastamatiou et al., 2010; Sampson et al., 2010; Borrell et al., 2011; Dale et al., 2011; Kim et al., 2011; Vaudo & Heithaus, 2011; Woodland et al., 2011), including *S. pacificus* and *Somniosus microcephalus* (Bloch & Schneider 1801) (Fisk et al., 2002; McMeans et al., 2010). The nitrogen stable-isotope technique is based on the empirical evidence that during the ingestion of food and the excretion of wastes, there is an enrichment of the heavier nitrogen isotope, ^{15}N, in animal tissues relative to the lighter nitrogen isotope, ^{14}N, in a process known as fractionation (DeNiro & Epstein, 1981; Minagawa & Wada, 1984). The $\delta^{15}N$ of an animal's tissues generally reflects that of its diet with a mean isotopic enrichment within an ecosystem of *c.* 3.4‰ (DeNiro & Epstein, 1981; Minagawa & Wada, 1984; Vander Zanden & Rasmussen, 2001; Post, 2002). As a result, $\delta^{15}N$ can be used to calculate trophic position by quantifying how many times the biomass consumed by an organism has been metabolically processed within the food chain (Vander Zanden et al., 1997; Post, 2002). In contrast, $\delta^{13}C$ is on average enriched less than $\delta^{15}N$ (*c.* <1‰ relative to its diet) (DeNiro & Epstein, 1978; Vander Zanden & Rasmussen, 2001; Post, 2002). As a result, $\delta^{13}C$ is useful for examining feeding in different food webs because it can be used to distinguish between different sources of primary productivity, *e.g.* benthic or nearshore *v.* pelagic (McConnaughey & McRoy, 1979a, b; Hobson & Welch, 1992; Schell et al., 1998; Hobson et al., 2002; Post, 2002; Kline, 2009).

This study examined the trophic ecology of *S. pacificus* in the eastern North Pacific Ocean by using mathematically lipid-normalized carbon stable-isotope ratios ($\delta^{13}C'$) to determine *S. pacificus* food-web utilization, and by using $\delta^{15}N$ to determine *S. pacificus* trophic position. A non-parametric Wilcoxon rank-sum test was used to evaluate geographic variability in the $\delta^{13}C'$ values of *S. pacificus* muscle tissue. A linear model was used to evaluate geographic and ontogenetic variability in the $\delta^{15}N$ values of *S. pacificus* muscle tissue and to predict the trophic position of *S. pacificus* from muscle tissue $\delta^{15}N$ values by region for fish of the same mean L_T. In order to validate the use of *S. pacificus* muscle tissue $\delta^{15}N$ as a

relative measure of trophic position, the trophic position of *S. pacificus* predicted from the linear model was compared to that predicted from previously published diet data in the same region for *S. pacificus* of the same mean L_T. In order to place the relative trophic position of *S. pacificus* determined from muscle tissue $\delta^{15}N$ into an ecosystem context, mean $\delta^{15}N$ of other aquatic organisms from the eastern North Pacific Ocean were reviewed from the primary literature and graphically compared to that of *S. pacificus* by taxa.

3.3. Materials and Methods

Somniosus pacificus were sampled from the eastern Bering Sea (EBS), western and central Gulf of Alaska (GOA) and northern Southeast Alaska (NSE) (Figure 3.1). Within the EBS, fish (n = 169) were sampled during the period 19 January 2007 to 29 October 2007 by the National Marine Fisheries Service (NMFS), Alaska Fisheries Science Center (AFSC) North Pacific Groundfish Observer Program (Stevenson & Lewis, 2010). Fisheries observers sampled incidentally captured *S. pacificus* on board commercial fishing vessels operating pelagic trawls (n = 147), bottom trawls (n = 3) and longlines (n = 2), as well as from port deliveries (n = 17). Up to five incidentally captured *S. pacificus* were sampled per observer trip or port delivery. *Somniosus pacificus* for this study were encountered and sampled along the outer continental shelf and upper continental slope of the EBS (Figure 3.1). Within the GOA, *S. pacificus* (n = 15) were sampled during the period 9 June 2007 to 11 July 2007 on board chartered commercial fishing vessels conducting the NMFS GOA bottom-trawl survey (von Szalay et al., 2008), which is conducted biannually by the NMFS AFSC Resource Assessment and Conservation Engineering (RACE) Division to assess groundfish abundance along the continental shelf and upper continental slope of the U.S. exclusive economic zone from 170° to 132° 40' W (Figure 3.1). *Somniosus pacificus* are regularly encountered in NMFS bottom trawl surveys in the GOA, but sample sizes are low (Mueter & Norcross, 2002). *Somniosus pacificus* for this study were encountered and sampled in the western and central GOA (Figure 3.1). Within the NSE, tissue samples were collected opportunistically from *S. pacificus* captured in Chatham Strait (n = 7) during the period 7 July 2006 to 9 July 2006 by commercial longline vessels chartered by the NMFS AFSC Auke Bay Laboratories (ABL) (Courtney & Hulbert, 2007), from one *S. pacificus* captured in Stephens Passage on 10 July 2006 (B. Mathews, pers. comm.), and from one *S. pacificus* sampled in port by ABL staff on 27 August 2007 from a commercial longline vessel delivery in Juneau, Alaska.

Tissue samples were obtained by excising a single piece (*c.* 2.5 cm^3) of white muscle from the dorsal region of each *S. pacificus*. Muscle tissue was stored on ice or frozen, and shipped on ice or frozen to ABL. Stable-isotope ratios were processed as described below. Other data recorded for each *S. pacificus* and used in this study included L_T from the tip of the snout to the tip of tail in a natural position,

capture latitude, capture longitude and bottom depth. Capture locations were not available for the *S. pacificus* sampled at port. In addition, three of the nine *S. pacificus* captured in the NSE were returned whole to ABL and stored frozen. These three *S. pacificus* were used to evaluate variability in $\delta^{15}N$ and $\delta^{13}C$ of *S. pacificus* muscle tissue, which provided information on the allocation of regional sampling effort in the EBS and GOA for this study.

Once at ABL, each of these three *S. pacificus* was partially thawed at room temperature and three small pieces (*c.* 2.5 cm^3) of white muscle were excised (dorsal, ventral and lateral). Stable-isotope ratios were processed as described below. For the purposes of this study, the mean value of the four white muscle samples (three taken in the laboratory and one taken in the field) was used in the analyses of muscle tissue stable-isotope ratios of $\delta^{15}N$ and $\delta^{13}C$ as described below, except that a muscle sample taken in the field was lost for one of the *S. pacificus*. Low variability in muscle tissue $\delta^{15}N$ and $\delta^{13}C$ sampled at different intervals along the length of individual sharks in other studies (Hussey et al., 2010a) suggests that stable-isotope values of shark muscle tissue are consistent among different locations of the body.

Once at ABL, each muscle tissue sample was partially thawed at room temperature, and a small piece of clean white muscle was excised, placed in a glass vial, freeze-dried for at least 24 h and homogenized with a glass rod. Freeze-dried samples were sent to the University of Alaska Fairbanks (UAF), Alaska Stable Isotope Facility, where stable-isotope analysis was conducted. A sub-sample (*c.* 0.2–0.4 mg) of each freeze-dried muscle homogenate was weighed, placed in a tin capsule and processed with a Costech ECS4010 elemental analyzer (EA) (www.costechanalytical.com) interfaced through a CONFLO III to a Finnigan Delta^{plus}XP isotope ratio mass spectrometer (continuous flow EA-IRMS; www.thermoscientific.com). EA-IRMS results were reported in delta (δ) notation $\delta^{15}N = 1000\left[\left(R_{sample}R_{standard}^{-1}\right)-1\right]$, where R_{sample} was the ratio of heavy to light isotopes in the sample, $R_{standard}$ was the isotopic ratio (*e.g.* ^{15}N:^{14}N or ^{13}C:^{12}C) of a standard reference gas and units were parts 1000^{-1} (‰). The reference gas for nitrogen was atmospheric air, N_2(atm) and the reference gas for carbon was Vienna-PeeDee Belemnite (V-PDB). Measurement of each sample with EA-IRMS was either followed or preceded by the measurement of the standard reference gas. Replicate measurements of $\delta^{15}N$ and $\delta^{13}C$ were also obtained from a known compound (peptone), which was processed simultaneously with the freeze-dried muscle homogenate. On the basis of the replicate peptone measurements (n = 28), variability (± S.D.) of EA-IRMS was ± 0.38 and ± 0.27‰ for $\delta^{15}N$ and $\delta^{13}C$, respectively. Measurement bias of EA-IRMS (the average of the expected standard subtracted from the peptone replicates) was 0.12 and −0.02‰ for $\delta^{15}N$ and $\delta^{13}C$, respectively.

3.3.1. Data Analysis

For statistical analysis, the data were post-stratified within the EBS south-east (SE-EBS) and north-west (NW-EBS) of longitude 170° W (Figure 3.1). Preliminary analyses indicated that post stratification of the data east and west of 170° W was necessary to isolate the possible confounding effects of geographic region (NW-EBS and SE-EBS) from season (summer and winter) within the EBS. Sample sizes for statistical analysis were reduced within the EBS from 169 to 145, within the GOA from 15 to 11 and within the NSE from nine to four because of missing data for either *S. pacificus* L_T, $\delta^{15}N$, $\delta^{13}C$ or capture location, and because of the removal of one outlier in L_T from the EBS (453.0 cm L_T, bottom depth = 70 m, $\delta^{15}N$ =14.1‰, $\delta^{13}C$ = −22.9‰, C:N = 7·7, $\delta^{13}C'$ = −20.8‰). Data from the GOA and the NSE were pooled because of low sample size in the NSE. These changes resulted in four strata for statistical analysis: NW-EBS-Summer (n = 54), SE-EBS-Summer (n = 41), SE-EBS-Winter (n = 50) and GOA–NSE-Summer (n = 15) (Table 3.1). Statistical analysis was conducted with R statistical software version 2.12.1 (R Development Core Team; www.r-project.org).

3.3.2. Lipid Normalization of $\delta^{13}C$

Calculation of lipid normalized $\delta^{13}C$ followed equations in McConnaughey & McRoy (1979a), Kline (1997, 1999, 2009), Andrews (2010) and Sweeting et al. (2006):

$$\delta^{13}C' = \delta^{13}C + D\left\{(-0.207 + 3.900)\left[(1 + 287)L^{-1}\right]^{-1}\right\}, \tag{3.1}$$

where $L = 93\,[1 + (0.246x - 0.775)^{-1}]^{-1}$. The parameter x(C:N) was the ratio of carbon to nitrogen in mass measured in each *S. pacificus* muscle tissue sample. The parameter L was the calculated lipid proxy based on the ratio of C:N in mass. The parameter D was the isotopic difference between protein and lipid (6‰) derived by McConnaughey & McRoy (1979a) from the literature. The resulting $\delta^{13}C'$ value was the lipid-normalized $\delta^{13}C$ value. The $\delta^{13}C'$ value was normalized to be less negative than the $\delta^{13}C$ value for fatty (C:N ratios >4·0) animals (McConnaughey & McRoy, 1979a; Sweeting et al., 2006).

3.3.3. Analysis of $\delta^{13}C'$ and $\delta^{15}N$

Variability in the $\delta^{13}C'$ values of *S. pacificus* muscle tissue among strata (Table 3.1) was analyzed with non-parametric Kruskal–Wallis and Wilcoxon rank-sum tests (Sokal & Rohlf, 1995). Preliminary analysis of the pooled $\delta^{13}C'$ data with a normal probability plot indicated that the $\delta^{13}C'$ values of *S. pacificus* muscle tissue were not normally distributed (one-sample Shapiro–Wilk normality test, n = 160, $P < 0.001$; Table 3.1; Crawley, 2007). The $\delta^{13}C'$ values of *S. pacificus* muscle tissue also had significantly

unequal variance among strata (Fligner–Killeen non-parametric test of homogeneity of variances, d.f. = 4, $P < 0.05$; Table 3.1; Crawley, 2007). The $\delta^{13}C'$ values, however, did not differ significantly between GOA-Summer and NSE-Summer (non-parametric Wilcoxon rank-sum test, $P > 0.05$; Table 3.1; Crawley, 2007). The $\delta^{13}C'$ values also did not differ significantly among NW-EBS-Summer, SE-EBS-Summer and SE-EBS-Winter (non-parametric Kruskal–Wallis rank-sum test, d.f. = 2, $P > 0.05$; Table 3.1; Crawley 2007). As a result, the $\delta^{13}C'$ values of *S. pacificus* muscle tissue were pooled within the GOA–NSE-Summer (mean ± S.E.: −19.9 ± 0.2‰, $n = 15$) and within the EBS (mean ± S.E.: −21.1 ± 0.01‰, $n = 145$). The pooled $\delta^{13}C'$ values were compared between the GOA–NSE-Summer and the EBS using a non-parametric Wilcoxon rank-sum test. The $1 - \alpha$ significance level ($\alpha = 0.05$) was corrected for multiple hypotheses tests using the Bonferroni method $\alpha' = \alpha \times \kappa^{-1}$. The value for κ was set equal to 3 ($\alpha' = 0{\cdot}02$) in order to account for the two implicit hypothesis tests associated with pooling data as well as the explicit hypothesis test comparing the pooled $\delta^{13}C'$ values between the GOA–NSE-Summer and the EBS.

Sample size in the NSE-Summer was very small ($n = 4$; Table 3.1), and neither the $\delta^{15}N$ values of *S. pacificus* muscle tissue (ln transformed) nor *S. pacificus* L_T (ln transformed) differed significantly between GOA-Summer and NSE-Summer (Welch two-sample t -tests, $P > 0.05$; Crawley, 2007). As a result, *S. pacificus* muscle tissue $\delta^{15}N$ values (mean ± S.E.: 15.2 ± 0.3‰, $n = 15$) and L_T data (mean ± S.E.: 204.2 ± 10.5‰, $n = 15$) were pooled within the GOA–NSE-Summer for the following analyses. The effect of L_T on the muscle tissue $\delta^{15}N$ values of *S. pacificus* was then analyzed among the remaining four strata (Z) (NW-EBS-Summer, SE-EBS-Summer, SE-EBS-Winter and GOA–NSE-Summer) with a linear regression model:

$$\delta^{15}\mathrm{N} = \beta_0 + \beta_1 L_T + \beta_{2,i} Z + \beta_{3,i} \left(L_T \times Z\right) + \varepsilon, \tag{3.2}$$

Dummy variables were used to represent each stratum within Z ($i = 4$) (Kleinbaum et al., 1988; Criddle, 2005). The main effects and interaction terms were systematically removed from the model, and the reduced models were evaluated based on differences in the Akaike information criterion with a correction for small sample sizes (AICc; U) calculated as $\Delta U = U - U_{\text{minimum}}$ (Burnham & Anderson, 2002). The best model for $\delta^{15}N$ had the minimum AICc score and was used to test for significant differences in $\delta^{15}N$ among strata (Z) of the main effect (stratum) by systematically setting each factor level as the contrast (Criddle, 2005). Coefficients of the remaining strata were then evaluated relative to the contrast. The test statistic followed a t-distribution with $n - k - 1$ d.f. at the $1 - \alpha$ significance level ($\alpha = 0.05$) (Criddle, 2005; Crawley, 2007).

3.3.4. $\delta^{15}N$ Predicted from *S. pacificus* Total Length

For prediction, the best linear model for $\delta^{15}N$ (minimum AICc score) was simplified with a stepwise a posteriori procedure (Crawley, 2007) in which strata (Z) of the main effect (stratum) with the most similar coefficients were systematically aggregated. Partial F-statistics (F_p) were evaluated after each aggregation in order to test for the significance of the full *v.* aggregated model (Crawley, 2007). The AICc score of each simplified model was also evaluated. The simplified linear model was used to predict muscle tissue $\delta^{15}N$ of *S. pacificus* ($\delta^{15}\hat{N}$) from *S. pacificus* L_T. For prediction, the simplified linear model was run with an additional dummy variable assigned a value of −1 for the forecast observation and a value of 0 for all other observations (Criddle, 2005). The estimated coefficient on the dummy variable was the point forecast ($\delta^{15}\hat{N}$), and the S.E. of the estimated coefficient on the dummy variable was the estimated standard error ($s_{\delta^{15}\hat{N}}$). The 95% prediction interval (P.I.) for $\delta^{15}\hat{N}$ was estimated following Criddle (2005):

$$(1-\alpha)\% = \delta^{15}\hat{N} \pm \left(t_{\alpha,n-k-1}\right)\left(s_{\delta^{15}\hat{N}}\right), \tag{3.3}$$

where n is the sample size, k is the number of estimated coefficients from the simplified model for $\delta^{15}N$ and $\alpha = 0.05$ is the significance level.

The forecast observation for *S. pacificus* L_T was the mean L_T of *S. pacificus* (201.5 cm) from three independent diet studies in the eastern North Pacific Ocean weighted by the number of *S. pacificus* examined for diet in each study (Yang & Page, 1999; Sigler et al., 2006; Yano et al., 2007). Average *S. pacificus* L_T from Yang & Page (1999) was mean ± S.E.: 264.5 ± 6.9 cm L_T (n = 13). Average L_T from Sigler et al. (2006) was mean ± S.E.: 201.6 ± 2.6 cm L_T (n = 198) (M. Sigler, pers. comm.). Average *S. pacificus* L_T from Yano et al. (2007) was approximated here as 149.5 cm for n = 16 *S. pacificus* examined for diet in the EBS, GOA and Aleutian Islands (AI) (Yano et al., 2007). *Somniosus pacificus* L_T was reported by Yano et al. (2007) as the mode in female L_T (150–199 cm) and the mode in male L_T (100–149 cm) from n = 34 *S. pacificus* examined for diet in the North Pacific Ocean. For the purposes of this study, average *S. pacificus* L_T from Yano et al. (2007) was approximated here as the average of the median of the mode in female L_T and the median of the mode in male L_T.

3.3.5. Trophic Position Determined from $\delta^{15}N$ (T_{PN})

Somniosus pacificus trophic position from $\delta^{15}N$ (T_{PN}):

$$T_{PN} = T_{Pbaseline} + \left(\delta^{15}N_{consumer} - \delta^{15}N_{baseline}\right)\left(\Delta_n\right)^{-1}, \quad (3.4)$$

followed equations in Vander Zanden et al. (1997) and Post (2002), as reviewed by Martínez del Rio et al. (2009). Within each stratum, the mean $\delta^{15}N$ value from copepods (Schell et al., 1998; Kline, 2009) was assumed to approximate the $\delta^{15}N$ value of primary consumers at the base of the food web ($\delta^{15}N_{baseline}$). The baseline trophic position ($T_{Pbaseline}$) of primary consumers (copepods) was assumed to be 2.3 (Kline, 2009) in all strata, as discussed below. Within each stratum, consumer $\delta^{15}N$ ($\delta^{15}N_{consumer}$) was the estimated point forecast of muscle tissue $\delta^{15}N$ for *S. pacificus* ($\hat{\delta^{15}N}$) from the simplified linear model. The trophic discrimination factor (Δ_n) was the assumed mean consumer to diet discrimination factor, ($\Delta^{15}N$) = ($\delta^{15}N_{consumer} - \delta^{15}N_{diet}$), for an unknown number (n) of trophic links between *S. pacificus* and copepods in the eastern North Pacific Ocean. Uncertainty in Δ_n was incorporated in this study by including four different point estimates of $\Delta^{15}N$ obtained from the literature as estimates of Δ_n in Equation (3.4). Two point estimates of $\Delta^{15}N$ were obtained from ecosystem level meta-analyses of consumer to diet discrimination factors: 3.4‰ (Minagawa & Wada, 1984; Vander Zanden & Rasmussen, 2001; Post, 2002) and 2.7‰ (Vanderklift & Ponsard, 2003; Dale et al., 2011). Two point estimates of $\Delta^{15}N$ were obtained from muscle tissue to diet discrimination factors specifically estimated for large carnivorous sharks: 2.3‰ (Hussey et al., 2010a) and 4.0‰ (McMeans et al., 2010).

For the purposes of this study, the mean $\delta^{15}N$ value of copepods in the GOA was obtained from previously published results for individually sampled *Neocalanus cristatus* (mean ± S.E.: 7.3 ± 0.1‰, n = 1588) (Kline, 2009). *Neocalanus cristatus* samples were collected primarily at 13 stations along the Seward Line (Figure 3.1) extending from nearshore station GAK 1; (59° 50.7' N; 149° 28.0' W) to offshore station GAK 13 (*c.* 2000 m depth contour; 59° 5.9' N; 147° 47.6' W) during the years 1998–2004 (Kline, 2009) (Figure 3.1). In the GOA, *N. cristatus* is principally herbivorous during the spring bloom, with a 30% contribution by microzooplankton (assumed trophic position = 2), resulting in a trophic position of *c.* 2.3 (Liu et al., 2005; Kline, 2009).

For the purposes of this study, the mean $\delta^{15}N$ value of copepods in the EBS was calculated here from previously published results for composite calanoid copepods collected during the years 1985–1990 and 1993–1995 from the western Bering Sea (WB; Schell et al. 1998; Figure 3.1; mean ± S.E.: 8.7 ± 0.2‰), the central Bering Sea (CB; Schell et al. 1998; Figure 3.1; mean ± S.E.: 9.6 ± 0.2‰) and the eastern Bering Sea (EB; Schell et al. 1998; Figure 3.1; mean ± S.E.: 9.8 ± 0.2‰). Copepods from the WB were collected from 64 stations in continental shelf waters from roughly west of 170° W. Copepods from

the CB were collected from 132 stations in continental-shelf waters roughly straddling the 170° W longitude line. Copepods from the EB were collected from 64 stations in continental-shelf waters roughly east of 170° W. Comparisons of zooplankton isotope ratios among years and cruises within the same region revealed no significant differences (Schell et al., 1998). The approximate locations for WB and CB from Schell et al. (1998) corresponded roughly with the NW-EBS in this study (Figure 3.1). The approximate locations of CB and EB from Schell et al. (1998) corresponded roughly with the SE-EBS in this study (Figure 3.1). Consequently, for the purposes of this study, reference $\delta^{15}N$ for the NW-EBS (Figure 3.1) during the year 2007 (9.2‰) was estimated here as the average of composite calanoid copepod $\delta^{15}N$ values from the WB (8.7‰) and CB (9.6‰) (Schell et al., 1998). Similarly, reference $\delta^{15}N$ for the SE-EBS (Figure 3.1) during the year 2007 (9.7‰) was estimated here as the average of composite calanoid copepod $\delta^{15}N$ values from the CB (9.6‰) and EB (9.8‰) (Schell et al., 1998).

3.3.6. Trophic Position Determined from Diet

The trophic position (T_P) of *S. pacificus* in the eastern North Pacific Ocean was determined from diet (T_{PD}) based on results from three previously published diet studies (Yang & Page, 1999; Sigler et al., 2006; Yano et al., 2007). Most *S. pacificus* examined for diet (n = 211) in the previously published studies were captured during summer months in the NMFS central GOA regulatory area (Yang & Page, 1999; Sigler et al., 2006) (Figure 3.1). The exact capture locations and capture dates were not available for some *S. pacificus* (n = 16) examined for diet in the EBS, GOA and AI (Yano et al., 2007).
An index of standardized diet composition (P_j) was calculated from 11 prey categories (j) following Cortés (1999):

$$P_j = \sum_{i=1}^{3} P_{ij} \times N_i \times \left(\sum_{j=1}^{11} \left(\sum_{i=1}^{3} P_{ij} * N_i \right) \right)^{-1}, \tag{3.5}$$

The parameter P_{ij} was the proportion of prey in category j and study i. The variable N_i was the number of stomachs with food used to calculate P_{ij} in study i. For each study, P_{ij} was calculated using the quantitative method from the original study. Indices were included from the original study based on hierarchical criteria following methods in Cortés (1999) and Ebert & Bizzarro (2007). Compound indices were used if available. If a compound index was not available but more than one single index was available, then an index of importance was calculated on a percentage basis by averaging all available indices. The percent frequency of occurrence was not included in the hierarchical criteria for this study because it may not be a robust estimate of diet when species are combined at higher taxonomic levels than those reported in the original study (Cortés, 1997). Based on these criteria, the compound index of

relative importance (%*R*) was included from Sigler et al. (2006), the index of percent mass (%*W*) was included from Yang & Page (1999) and the index of per cent number (%*N*) was included from Yano et al. (2007).

The T_{PD} was then calculated following Cortés (1999):

$$T_{PD} = 1 + \left(\sum_{j=1}^{11} P_j * T_{Pj} \right), \tag{3.6}$$

The parameter T_{Pj} was the trophic position of each prey category *j* taken directly from Cortés (1999).

3.3.7. Review of $\delta^{15}N$ by Taxa in the Eastern North Pacific Ocean

In order to place the relative trophic position of *S. pacificus* into an ecosystem context, the $\delta^{15}N$ values of other aquatic organisms in the eastern North Pacific Ocean were reviewed here from previously published literature (Appendices 3.A and 3.B). Taxonomic groupings and subdivisions of aquatic organisms were based on the original publications (Appendices 3.A and 3.B). For comparison with *S. pacificus* in this study, the $\delta^{15}N$ values of other aquatic organisms in the eastern North Pacific Ocean were then further grouped into the following taxa: killer whales *Orcinus orca*, pinnipeds, spiny dogfish *Squalus acanthias* L. 1758, humpback whales *Megaptera novaeangliae*, fishes and squid, other invertebrates and zooplankton.

The $\delta^{15}N$ values of other aquatic organisms from the EBS and AI (Hobson et al., 1997; Schell et al., 1998; Hirons et al., 2001; Kurle & Worthy, 2001; Herman et al., 2005; Krahn et al., 2007; Witteveen et al., 2009; Andrews, 2010) were compared to the mean $\delta^{15}N$ values of *S. pacificus* muscle tissue sampled in this study from the NW-EBS-Summer, SE-EBS-Summer and SE-EBS-Winter (Table 3.1). The $\delta^{15}N$ values of other aquatic organisms from the GOA and Southeast Alaska (Hobson et al., 1997; Hirons et al., 2001; Herman et al., 2005; Krahn et al., 2007; Kline, 2009; Witteveen et al., 2009; Andrews, 2010; Marsh, 2010) were compared to the mean muscle tissue $\delta^{15}N$ values of *S. pacificus* sampled in this study from the GOA-Summer and NSE-Summer (Table 3.1). The $\delta^{15}N$ values of aquatic organisms from Prince William Sound (PWS) (Figure 3.1) were specifically excluded, except for *S. acanthias*, because of significant differences in baseline $\delta^{15}N$ between the GOA and PWS (Kline, 2009).

3.4. Results

3.4.1. Analysis of $\delta^{13}C'$ and $\delta^{15}N$

The $\delta^{13}C'$ values of *S. pacificus* muscle tissue within the pooled summer strata (GOA-Summer + NSE-Summer; mean ± S.E.: −19·9 ± 0.2‰ , n = 15; Table 3.1) were significantly enriched (less negative) relative to those within the pooled EBS strata (NW-EBS-Summer + SE-EBS-Summer + SE-EBS-Winter; mean ± S.E.: −21.1 ± 0.03‰, n = 145; Table 3.1) at the Bonferroni corrected $\alpha' = 0.02$ (nonparametric Wilcoxon rank-sum test with continuity correction, $P < 0.001$).

The best linear model for *S. pacificus* muscle tissue $\delta^{15}N$ (Equation 3.2) was the full model (L_T + stratum + L_T × stratum; minimum AICc score = 414.6; Table 3.2). There was weak evidence ($2 < \Delta AICc < 4$) to rule out the next best model for $\delta^{15}N$ ($\Delta AICc = 3.2$) and very strong evidence ($10 < \Delta AICc$) to rule out the remaining models (Table 3.2). The full model (Equation 3.2) explained 54% of the observed variability in $\delta^{15}N$ ($r^2 = 0.54$, F-test, k d.f. = 7, $n - k - 1$ d.f. = 152, $P < 0.001$; Table 3.2). The evaluation of contrast coefficients among strata (Z) (NWEBS-Summer, SE-EBS-Summer, SE-EBS-Winter and GOA–NSE-Summer) fitted in the full model (L_T + stratum + L_T × stratum; Table 3.2) indicated that *S. pacificus* length (L_T) had a significant effect on *S. pacificus* muscle tissue $\delta^{15}N$ within each of the four strata (t-tests, $n - k - 1$ d.f. = 152, $P < 0.001$; Figure 3.2 and Table 3.3). The effect of L_T on *S. pacificus* muscle tissue $\delta^{15}N$ also differed significantly among some strata (L_T × stratum, t-tests, $n - k - 1$ d.f. = 152, $P < 0.05$; Figure 3.2 and Table 3.3). The residuals from the full model (Table 3.2) were normally distributed (one-sample Shapiro–Wilk normality test, n = 160, $P > 0.05$). The variances of muscle tissue $\delta^{15}N$ values (Fligner–Killeen test of homogeneity of variances, d.f. = 3, $P > 0.05$) and *S. pacificus* L_T (Fligner–Killeen test of homogeneity of variances, d.f. = 3, $P > 0.05$) did not differ significantly among the four strata (NW-EBS-Summer, SE-EBS-Summer, SE-EBS-Winter and GOA–NSE-Summer).

3.4.2. Trophic Position Determined from $\delta^{15}N$ and from Diet

The full model (Table 3.2) was simplified with a posteriori stepwise model simplification for prediction of muscle tissue $\delta^{15}N$ from shark L_T (Table 3.4). Among the four strata included in the full model (Table 3.2), SE-EBS-Summer and GOA–NSE-Summer had the most similar contrast coefficient estimates, and NW-EBS-Summer and SE-EBS-Winter had the next most similar coefficient estimates (Table 3.3). As a result, the first stepwise simplification aggregated SE-EBS-Summer with GOA–NSE-Summer within the full model, and the second stepwise simplification aggregated NW-EBS-Summer with SE-EBS-Winter within the first simplified model. The first simplification was justified ($P > \alpha' = 0.025$; Table 3.4), but the second was not ($P < \alpha' = 0.025$; Table 3.4). The remaining coefficients were all larger

than those already examined for model simplification. As a result, further model simplification was not justified. The ΔAICc of the first simplified model relative to full model was −4.4 (Table 3.4). Consequently, there was definite evidence ($4 < \Delta AICc \leq 7$) to rule out the full model (Table 3.2) in favor of the first simplified model (Table 3.4).

Point forecasts ± S.E. of *S. pacificus* (mean L_T 201.5 cm) muscle tissue $\hat{\delta}^{15}N$ obtained from the first simplified model ranged from 13.7 ± 0.9‰ to 15.1 ± 0.9‰ (Table 3.5). The corresponding 95% P.I. (Equation 3.3) ranged from 11.9 to 16.8‰ (Table 3.5). *Somniosus pacificus* (mean L_T = 201.5 cm) trophic position determined from $\delta^{15}N$ (T_{PN}) (Equation 3.4) ranged from 3.3 to 5.7 (Table 3.6). The corresponding 95% P.I. ranged from 2.9 to 6.4 (Table 3.6). The wide range in 95% P.I. calculated for *S. pacificus* T_{PN} (*c.* 3.5 trophic levels; Table 3.6) resulted from the wide range of uncertainty in $\hat{\delta}^{15}N$ predicted for *S. pacificus* muscle tissue (*c.* 3.4‰ between 95% P.I. within each stratum from the first simplified model; Table 3.5), the wide range in geographic variability of the assumed $\delta^{15}N_{baseline}$ values (*c.* 2.4‰ among strata; Table 3.6) and the wide range in point estimates of $\Delta^{15}N$ assumed for Δn (*c.* 1.7‰ among $\Delta^{15}N$ estimates; Table 3.6). The trophic position of *S. pacificus* (mean L_T = 201.5 cm) in the eastern North Pacific Ocean determined here from previously published diet data (T_{PD} = 4.3; Equation 3.6; Table 3.7) was within the range of the point estimates of *S. pacificus* T_{PN} by stratum (3.5–5.7) for *S. pacificus* of the same mean L_T (Table 3.6).

3.4.3. Review of $\delta^{15}N$ by Taxa in the Eastern North Pacific Ocean

Based on the literature review of mean $\delta^{15}N$ values of aquatic organisms in the eastern North Pacific Ocean by taxa (Appendices 3.A and 3.B), the $\delta^{15}N$ values of *S. pacificus* muscle tissue from this study (Table 3.1) were within the range of those of fishes (Teleostei) and squid (teuthoidea), enriched relative to those of filter feeding whales (*M. novaeangliae*) and *S. acanthias*, and depleted relative to those of pinnipeds and *O. orca* (Figure 3.3).

3.5. Discussion

3.5.1. Analysis of $\delta^{13}C'$

In this study on the ecological role of *S. pacificus* in the eastern North Pacific Ocean, there was significant (*c.* 1‰) enrichment in the mean $\delta^{13}C'$ value of *S. pacificus* muscle tissue from the pooled GOA–NSE-Summer strata (GOA-Summer + NSE-Summer) relative to the mean value from the pooled EBS strata (NW-EBS-Summer + SE-EBS-Summer + SE-EBS-Winter) (Table 3.1). This significant difference in the feeding ecology of *S. pacificus* between regions is consistent with previous results from

electronic tagging studies which suggest that there is relatively little annual interchange of individual *S. pacificus* between the EBS and the GOA. In particular, 76% of electronically tagged *S. pacificus* in the GOA were recovered within 100 km of their release location up to *c.* 1 year after release (Hulbert et al., 2006). In contrast, numerically tagged *S. microcephalus* at liberty for >1 year exhibited longer distance movements (Hansen, 1963). Isotopic differences would be expected to be minimal if there were more mixing between the regions because of the slow isotopic turnover of $\delta^{13}C$ in elasmobranch muscle tissue (95% turnover in elasmobranch white muscle $\delta^{13}C$ occurs between *c.* 555 and 786 days; Logan & Lutcavage, 2010a).

A probable explanation of this enrichment in $\delta^{13}C$ is that *S. pacificus* may have been feeding on different prey in the two regions. In particular, benthic or nearshore prey may have been relatively more important in the diet of *S. pacificus* in the GOA and NSE than in the EBS. Specific evidence of spatial variability in $\delta^{13}C$ in the eastern North Pacific Ocean was observed in *N. cristatus* where more nearshore Prince William Sound $\delta^{13}C$ levels (mean ± S.E.: −20.4 ± 1.4‰) were enriched by *c.* 2.6‰ relative to more offshore GOA $\delta^{13}C$ levels (mean ± S.E.: −23.0 ± 2.0‰) (Kline, 2009). A second possible explanation of this enrichment is that the $\delta^{13}C$ values of the same prey may have differed among regions. For example, the observed magnitude of differences in the $\delta^{13}C$ values of primary consumers (copepods) between the GOA and the EBS (*c.* 1‰) (Schell et al., 1998; Kline, 2009) is large enough to account for the enrichment found in this study. There is also significant geographic variability in the $\delta^{13}C$ values of copepods in both the EBS and the GOA, and the fine scale patterns of enrichment and depletion are quite complex (Schell et al., 1998; Kline, 2009). The typical direction of these differences, however, shows enrichment in the $\delta^{13}C$ values of EBS copepods relative to those from the GOA (Schell et al., 1998; Kline, 2009) unlike in this study.

Lipid content can have an effect on elasmobranch muscle tissue $\delta^{13}C$ values (Sweeting et al., 2006; Post et al., 2007; Hussey et al., 2010a; Reum, 2011). In general, it is important to account for lipid content in the muscle tissue of aquatic organisms when the ratio of C:N is >3.5 for all samples or when comparing samples with variable lipid content (Post et al., 2007). The relationship between C:N and $\Delta\delta^{13}C$ ($\delta^{13}C_{uncorrected} - \delta^{13}C'$) for aquatic organisms may also be non-linear at C:N ratios > *c.* 6·9 (McConnaughey & McRoy, 1979a; Post et al., 2007; Reum, 2011). In this study, mean C:N ratios (by mass) of *S. pacificus* muscle tissue were high (>3.5), but similar among strata (mean ± S.E.: 7.1 ± 1.1 to 8.0 ± 0.8; Table 3.1). The range of individual variation, however, in C:N ratios (by mass) of *S. pacificus* muscle tissue was quite wide (3.2–15.6; Table 3.1). The C:N ratios (by mass) of *S. pacificus* muscle tissue observed in this study (Table 3.1) were within the range of other lipid-rich animals examined in the Bering Sea (McConnaughey & McRoy, 1979a). Consequently, for the purpose of comparing *S. pacificus*

muscle tissue $\delta^{13}C$ among geographic regions in this study, the $\delta^{13}C'$ values of *S. pacificus* muscle tissue were mathematically normalized to a constant lipid content following the non-linear relationship developed by McConnaughey & McRoy (1979a) for taxa within the Bering Sea (Equation 3.1). In this study, $\delta^{13}C'$ (Equation 3.1) and $\delta^{13}C_{uncorrected}$ were consistent in both the magnitude (*c.* 1‰) and the direction of stable-isotope carbon ratio enrichment in the GOA and NSE relative to the EBS (Table 3.1). Lipid normalization also had the anticipated effect of reducing variability in $\delta^{13}C'$ (smaller S.E.) relative to $\delta^{13}C_{uncorrected}$ in most regions (Table 3.1). The reduced variability of $\delta^{13}C'$ was necessary to detect the significant regional difference in carbon stable isotope ratios between the pooled EBS strata and the pooled GOA–NSE-Summer strata.

Lipid normalization of $\delta^{13}C$ following the non-linear relationship of McConnaughey & McRoy (1979a) (Equation 3.1) has not been validated for *S. pacificus*. As a result, the lipid-normalized $\delta^{13}C'$ values for *S. pacificus* in this study may be biased relative to $\delta^{13}C$ values anticipated from lipid extracted tissue (Post et al., 2007; Reum, 2011). For example, all other things being equal, a sample with high lipid concentration (C:N of 3.5–6.9) that has not been lipid extracted or mathematically normalized is expected to be c. 3–4‰ more negative than an extracted or normalized sample (Post et al., 2007). In this study, the mean $\Delta\delta^{13}C$ of *S. pacificus* muscle tissue within each stratum was c. 2‰ (Table 3.1), which suggests that lipid normalization may have underestimated the change in $\delta^{13}C$ anticipated from lipid extraction by *c.* 1–2‰. The lower than expected $\Delta\delta^{13}C$ relative to that anticipated from lipid extraction may have resulted from applying a mathematical lipid-normalization relationship to elasmobranchs that was parameterized from multispecies studies of teleosts (Reum, 2011). In particular, Reum (2011) hypothesized that high nitrogenous waste in elasmobranch tissues could lead to higher lipid content for the same C:N ratio relative to that of teleosts, which could negatively bias mathematical lipid correction models developed for teleosts when applied to elasmobranchs. Consequently, species-specific and tissue-specific lipid correction models for elasmobranchs are preferable to those parameterized using multispecies data (Reum, 2011).

Mathematical lipid correction models parameterized specifically for elasmobranch muscle tissue (Reum, 2011) were not applied in this study because the C:N ratios (by mass) of *S. pacificus* muscle tissue observed in this study (Table 3.1) were higher than those used to parameterize lipid correction equations for elasmobranch muscle tissue (Reum, 2011). In particular, the maximum C:N ratios (by mass) of *S. pacificus* muscle tissue observed among strata in this study (10.1–15.6; Table 3.1) were within the range of elasmobranch liver tissue (Reum, 2011). Lipid extracted C:N ratios differ significantly between elasmobranch muscle and liver tissue (Reum, 2011). Consequently, it may not be appropriate to apply lipid correction models parameterized from elasmobranch liver tissue to elasmobranch muscle tissue

(Reum, 2011). In this study, the potential bias associated with the use of a lipid-normalization relationship was assumed to have had a minimal effect on the relative differences in $\delta^{13}C'$ of *S. pacificus* muscle tissue among strata because the same lipid-normalization relationship (Equation 3.1) was applied to each tissue sample, and because mean C:N ratios (by mass) of *S. pacificus* muscle tissue were similar among strata (Table 3.1). Because of the potential for a negative bias in lipid-normalized $\delta^{13}C'$ values relative to $\delta^{13}C$ values anticipated from lipid extracted tissue, however, the $\delta^{13}C'$ values of *S. pacificus* muscle tissue calculated in this study were not compared directly to $\delta^{13}C$ values of other taxa from the eastern North Pacific Ocean.

3.5.2. Analysis of $\delta^{15}N$

The significant increase in the $\delta^{15}N$ values of *S. pacificus* muscle tissue with *S. pacificus* length found in this study (Table 3.2 and Figure 3.2) is consistent with previous studies of *S. pacificus* stomach contents which found evidence of an ontogenetic shift in diet in both the eastern and the western North Pacific Ocean (Orlov, 1999; Orlov & Moiseev, 1999a, b; Sigler et al., 2006; Yano et al., 2007). In comparison, similar ontogenetic shifts in prey have also been reported for the Antarctic sleeper shark *Somniosus antarcticus* Whitley 1939 and for the *S. microcephalus* (Cherel & Duhamel, 2004; Yano et al., 2007).

The significant difference in the effect of L_T on muscle tissue $\delta^{15}N$ of *S. pacificus* by stratum (L_T × stratum; Table 3.3) between NW-EBS-Summer and SE-EBS-Summer and between NW-EBS-Summer and GOA–NSE-Summer (Figure 3.2) may reflect patterns similar to those hypothesized above for $\delta^{13}C'$. Differences in L_T among EBS strata may, however, also have been influenced by commercial fishing operations. Most importantly, because of time and vessel constraints, large *S. pacificus* may have been pre-sorted by length on commercial vessels and removed from the catch before NMFS observers had an opportunity to sample the catch. In addition, fishing locations differed between the winter and the summer in the SE-EBS (Figure 3.1), and *S. pacificus* were also captured over deeper bottom depths and were relatively smaller in the SE-EBS-Winter than in the SE-EBS-Summer (Table 3.1). In addition, it is also possible that muscle tissue $\delta^{15}N$ values of smaller *S. pacificus* near the size at birth (*c.* 42 cm L_T) (Yano et al., 2007) (Figure 3.2) may have been influenced by a maternal signature in muscle tissue $\delta^{15}N$ (McMeans et al., 2009; Matich et al., 2010b; Vaudo et al., 2010; Olin et al., 2011), which was not considered in this study.

3.5.3. Trophic Position Determined from $\delta^{15}N$ and from Diet

T_{PN} (Table 3.6) and T_{PD} (Table 3.7) estimated for *S. pacificus* in the GOA were both based on data collected predominantly from the same geographic region, the NMFS central GOA regulatory area (Figure 3.1; Yang & Page, 1999; Sigler et al., 2006; Yano et al., 2007; Kline, 2009), which corresponds with the center of the surveyed distribution of *S. pacificus* in the GOA (Mueter & Norcross, 2002; Menon, 2004; Menon et al., 2005; Courtney & Sigler, 2007). The T_{PD} value estimated for *S. pacificus* in this study (4.3; Table 3.7) was the same as that previously estimated for *S. pacificus* (4.3; Cortés, 1999; Table 3.7) and was within the range of *S. pacificus* T_{PN} estimated here by stratum (3.5–5.7; Table 3.6) for fish of the same mean L_T (201.5 cm). The uncertainty in *S. pacificus* T_{PN} among strata, however, was quite large; the 95% P.I. among strata ranged from 2.9 to 6.4 (Table 3.6). In this study, the estimated T_{PN} of *S. pacificus* was also higher in the GOA–NSE-Summer (4.3–5.7; Table 3.6) than in the NW-EBS-Summer, SE-EBS-Summer and SE-EBS-Winter (3.3–4.7; Table 3.6) primarily as a result of differences in the $\delta^{15}N_{baseline}$ (Equation 3.4) estimated for the EBS (9.2–9.7‰; Table 3.6) relative to the GOA (7.3‰; Table 3.6). This result suggests that there may be important regional differences in the trophic position of *S. pacificus* between the EBS and the GOA similar to patterns hypothesized above for $\delta^{13}C'$.

Calculating the trophic position of large upper trophic level elasmobranchs from $\delta^{15}N$, however, is complex (Hussey et al., 2011, 2012). As a result, individual estimates of *S. pacificus* T_{PN} predicted in this study (Equation 3.4; Table 3.6) should be interpreted with caution. First, consumer tissue to diet discrimination factors ($\Delta^{15}N = \delta^{15}N_{consumer} - \delta^{15}N_{diet}$) for large elasmobranchs are uncertain. In particular, an estimate of $\Delta^{15}N$ available for large carnivorous sharks obtained under semi-controlled experimental conditions (mean ± S.E.: 2.3 ± 0.2‰; Hussey et al., 2010a) differs from that estimated in the field for *S. microcephalus* (4.0‰; McMeans et al., 2010), an Atlantic congener of *S. pacificus*. Both estimates differ from that estimated for elasmobranch muscle tissue under controlled conditions (mean ± S.D.: 3.7 ± 0.4%; Kim et al., 2011) and from that estimated in the field for large pelagic filter feeding rays (*c.* 3.2‰; Sampson et al., 2010). Second, $\Delta^{15}N$ may vary with each step of the food web (Hussey et al., 2012), which could result in a propagation of errors when estimating the T_{PN} of upper trophic level elasmobranchs from lower level baseline organisms with Equation (3.4). In particular, while a $\Delta^{15}N$ value of 3.4‰ may be valid when averaged over the multiple trophic pathways within an ecosystem (Post, 2002), individual estimates of $\Delta^{15}N$ vary among taxonomic groups of organisms, among taxonomically related species, between tissue types, with diet quality and with environment and feeding rate (Vander Zanden & Rasmussen, 2001; Post, 2002; Vanderklift & Ponsard, 2003; Caut et al., 2009; Martínez del Rio et al., 2009; Wolf et al., 2009; Hussey et al., 2010a, b). In particular, the $\Delta^{15}N$ estimated for carnivores (2.7‰; Vanderklift & Ponsard, 2003; Dale et al., 2011), which is similar to that obtained from

muscle tissue of fishes, birds and terrestrial animals (Caut et al., 2009), is lower than that typically assumed for ecosystem level studies (*c.* 3.4‰; Minagawa & Wada, 1984; Vander Zanden & Rasmussen, 2001; Post, 2002). Third, there may be a negative relationship between the $\Delta^{15}N$ of predators with the $\delta^{15}N$ of their prey (Hussey et al., 2012), i.e. $\Delta^{15}N$ decreases as $\delta^{15}N$ (and presumably trophic level) of prey increases. Consequently, using a single $\Delta^{15}N$ in Equation (3.4) could bias the trophic position estimated for upper trophic level predators if lower trophic level organisms, e.g. copepods (Table 3.6), are used as the reference baseline organisms.

This study incorporated uncertainty in $\Delta^{15}N$ by including four point estimates of $\Delta^{15}N$ obtained from the literature as estimates of Δ_n in Equation (3.4): 3.4‰ (Minagawa & Wada, 1984; Vander Zanden & Rasmussen, 2001; Post, 2002), 2.7‰ (Vanderklift & Ponsard, 2003; Dale et al., 2011), 2.3‰ (Hussey et al., 2010a) and 4.0‰ (McMeans et al., 2010) (Table 3.6). As more estimates of $\Delta^{15}N$ become available for elasmobranchs, meta-analysis may provide a more accurate estimate of the uncertainty in $\Delta^{15}N$ (Vander Zanden & Rasmussen, 2001; Vanderklift & Ponsard, 2003). An advantage of meta-analysis is that it would incorporate both the variability among $\Delta^{15}N$ estimates from each study as well as the variability within each study (Borenstein et al., 2009). Another approach that may also provide more accurate estimates of the uncertainty in $\Delta^{15}N$ for elasmobranchs is compound-specific stable-isotope analysis (Dale et al., 2011). An advantage of compound-specific stable-isotope analysis is that both baseline $\delta^{15}N$ values and the trophic enrichment in $\delta^{15}N$ ($\Delta^{15}N$) can be determined from individual amino acids of consumer tissues (Chikaraishi et al., 2009; Martínez del Rio et al., 2009; Wolf et al., 2009; Dale et al., 2011). Another advantage is that compound-specific stable-isotope analysis integrates the effects of variable consumer to diet discrimination factors at lower trophic levels of a consumer's diet.

The retention of urea in elasmobranch tissues may also bias the estimation of elasmobranch trophic position from $\delta^{15}N$ (Fisk et al., 2002; Hussey et al., 2010a; Dale et al., 2011; Kim & Koch, 2012). For example, although Logan & Lutcavage (2010b) found that nitrogen stable isotope values of elasmobranch white muscle were not affected by tissue urea content, Hussey et al. (2010a) found a large decrease in total N following lipid extraction of muscle tissue from three large sand tiger sharks *Carcharias taurus* Rafinesque 1810 and one large lemon shark *Negaprion brevirostris* (Poey 1868), providing evidence for the removal of nitrogenous waste products following lipid extraction. Similarly, Kim & Koch (2012) found that $\delta^{15}N$ values of elasmobranch muscle tissue increased (*c.* 2‰) following treatment with deionized water, as well as lipid extraction, presumably due to the removal of urea. In this study, allowing for a negative bias in the untreated $\delta^{15}N$ values of elasmobranch muscle tissue due to the retention of urea (*c.* 2‰; Kim & Koch, 2012) would result in higher $\delta^{15}N$ values for *S. pacificus* (*c.* 2‰; Table 3.1) and higher T_{PN} values for *S. pacificus* [*c.* $2(\Delta_n)^{-1}$‰; Equation 3.4; Table 3.6]. In this case, the

range of *S. pacificus* T_{PN} estimates within the NW-EBS-Summer, SE-EBS-Winter and SE-EBS-Summer (Table 3.6) would be more consistent with, or higher than, the *S. pacificus* T_{PD} estimate (4.3; Table 3.7), and the range of *S. pacificus* T_{PN} estimates in the GOA–NSE-Summer (Table 3.6) would be consistently higher than the *S. pacificus* T_{PD} estimate (4.3; Table 3.7).

Finally, the results of this study highlight an additional source of uncertainty in the estimation of trophic position from $\delta^{15}N$ with Equation (3.4) for large opportunistic upper trophic level predators, namely the wide range in muscle tissue $\delta^{15}\hat{N}$ predicted for *S. pacificus* of the same mean L_T (Table 3.5). In this study, $\delta^{15}N_{consumer}$ (Equation 3.4) was the point forecast of *S. pacificus* muscle tissue $\delta^{15}\hat{N}$ within each stratum (Table 3.5) estimated from the simplified linear model (Table 3.4). Even after accounting for ontogenetic and geographic variability in *S. pacificus* muscle tissue $\delta^{15}N$ values with the linear model (Table 3.5), however, the range of uncertainty in the 95% P.I. for $\delta^{15}\hat{N}$ within each stratum was still relatively large (*c.* 3.4‰ between 95% P.I. within each stratum from the first simplified model; Table 3.5). This uncertainty was propagated into the 95% P.I. calculated for T_{PN} ($\delta^{15}N_{consumer}$; Table 3.6) and was relatively larger than other sources of uncertainty included in Equation (3.4) for both $\delta^{15}N_{baseline}$ (*c.* 2.4‰ among strata; Table 3.6) and Δ_n (*c.* 1.7‰ among $\Delta^{15}N$ estimates; Table 3.6). This contrasts with results from a simulation study of aquatic carnivores (Vander Zanden & Rasmussen, 2001), which found that variability in $\delta^{15}N_{consumer}$ is relatively less influential than variability in both $\delta^{15}N_{baseline}$ and $\Delta^{15}N$ on the resulting uncertainty in estimated trophic position of aquatic carnivores. An explanation for this difference is that the S.E. for $\delta^{15}N_{consumer}$ (Equation 3.4) estimated in this study (*c.* 0.9‰; Table 3.5) was larger than that assumed for aquatic carnivores in the simulation study (Vander Zanden & Rasmussen, 2001). A relatively larger S.E. for $\delta^{15}N_{consumer}$ of *S. pacificus* seems reasonable because *S. pacificus* is a large opportunistic upper trophic level predator with a diet that varies not only ontogenetically and by geographic region, but also by season and capture depth, probably in response to prey availability (Bright, 1959; Gotshall & Jow, 1965; Ebert et al., 1987; Orlov, 1999; Orlov & Moiseev, 1999a, b; Yang & Page, 1999; Smith & Baco, 2003; Wang & Yang, 2004; Sigler et al., 2006; Yano et al., 2007).

3.5.4. Review of $\delta^{15}N$ by Taxa in the Eastern North Pacific Ocean

The enrichment of *S. pacificus* muscle tissue $\delta^{15}N$ values relative to those of fish and squid in the eastern North Pacific Ocean (Figure 3.3; Appendices 3.A and 3.B) was lower than would be expected based on stomach-content data alone. The available stomach-content data suggest that fishes and squid are important prey of *S. pacificus* in the eastern North Pacific Ocean. In particular, in the high latitude eastern North Pacific Ocean, teleosts are the most important prey group of *S. pacificus* in August (%*R c.* 64; Sigler et al., 2006). Important teleost prey include walleye pollock *Theragra chalcogramma* (Pallas

1814), pink salmon *Oncorhynchus gorbuscha* (Walbaum 1792) and chum salmon *Oncorhynchus keta* (Walbaum 1792). Cephalopods are the most important prey group (%*R c.* 61) in May, made up of both squid (teuthoidea) (%*N c.* 56) and giant Pacific Ocean octopus *Octopus dofleini* (per cent mass; %*M c.* 25; Sigler et al., 2006). In comparison, important prey items for *S. pacificus* in the high latitude western North Pacific include red squid *Berryteuthis magister* (%*N c.* 93), giant grenadier *Albatrossia pectoralis* (Gilbert 1892) (%*M c.* 18), fish offal (%*M c.*16), Kamchatka flounder *Atheresthes evermanni* Jordan & Starks 1904 (%*M c.* 15) and *O. keta* (%*M c.* 14) (Orlov, 1999; Orlov & Moiseev, 1999a, b). In the western North Pacific Ocean, the importance of prey taxa in *S. pacificus* stomach contents changes with capture depth mostly in relation to the vertical distribution of prey (Orlov & Moiseev, 1999b). In lower latitudes, *S. pacificus* stomach contents also include fast-swimming epipelagic teleosts such as albacore tuna *Thunnus alalunga* (Bonnaterre 1788), mahi-mahi *Coryphaena hippurus* L. 1758, wahoo *Acanthocybium solandri* (Cuvier 1832) and striped bonito *Sarda orientalis* (Temminck & Schlegel 1844) (Ebert et al., 1987; Wang & Yang, 2004).

The enrichment of *S. pacificus* muscle tissue $\delta^{15}N$ values relative to those of humpback whales (*M. novaeangliae*) in the eastern North Pacific (Figure 3.3; Appendices 3.A and 3.B) was also lower than would be expected based on stomach-content data and other information sources. The available stomach-content data suggest that filter feeding whale carrion may be an energetically important component of *S. pacificus* diet in the eastern North Pacific Ocean. In particular, cetaceans comprise about one-third of *S. pacificus* stomach contents by mass in the high latitude eastern North Pacific Ocean (at least 70% probably scavenged) and, as a result, appear to be energetically important (Sigler et al., 2006). Preliminary analysis of the fatty acid composition of *S. pacificus* liver and muscle from the Gulf of Alaska also revealed nutritional dependence on planktivores (Schaufler et al., 2005), which is consistent with scavenging on filter feeding whales (Schaufler et al., 2005). In the lower latitude Pacific Ocean, *S. pacificus* are dominant scavengers of whale carcasses at the deep sea floor (Smith & Baco, 2003). Cetaceans also occur occasionally in the stomach contents of *S. pacificus* in Southeast Alaska (Taggart et al., 2005) and in the low latitude Pacific Ocean (Wang & Yang, 2004). In comparison, unidentified cetacean also occurred in 33% of *S. antarcticus* stomachs examined from the Tasman Sea, Macquarie Island, South Africa and Namibia (Yano et al., 2007), and cetacean tissues also occur in the stomach contents of *S. microcephalus* from Icelandic waters (McMeans et al., 2010).

Somniosus pacificus muscle tissue $\delta^{15}N$ ($\delta^{15}N_{consumer}$) was enriched less than 3.4‰ relative to the $\delta^{15}N$ values of their putative prey ($\delta^{15}N_{diet}$) including fish, squid, and whale carrion (Figure 3.3; Appendices 3.A and 3.B). One possible explanation for the lower than expected enrichment is that *S. pacificus* muscle tissue diet discrimination factors ($\Delta^{15}N = \delta^{15}N_{consumer} - \delta^{15}N_{diet}$) may be lower than that typically assumed in ecosystem level studies (*i.e. c.* 3·4‰; Minagawa & Wada, 1984; Vander Zanden &

Rasmussen, 2001; Post, 2002). As discussed above, $\Delta^{15}N$ for large upper trophic level elasmobranchs ranges from 2.3‰ (Hussey et al., 2010a) to 4.0‰ (McMeans et al., 2010). Results of the comparison of *S. pacificus* muscle tissue $\delta^{15}N$ with that of its putative prey including fishes, squid and whale carrion (Figure 3.3; Appendices 3.A and 3.B) suggest *S. pacificus* muscle tissue $\Delta^{15}N$ may be at the lower end of the estimated range in $\Delta^{15}N$ (*e.g. c.* 2.3‰, Hussey et al., 2010a). This would be consistent with the estimated $\Delta^{15}N$ for carnivores (2.7‰; Vanderklift & Ponsard, 2003; Dale et al., 2011), which is similar to that obtained from muscle tissue of fishes, birds and terrestrial animals (Caut et al., 2009), and would also be consistent with a negative relationship between the $\Delta^{15}N$ of predators and the $\delta^{15}N$ of their prey (Caut et al, 2009; Hussey et al., 2012). Another possible explanation for the lower than expected enrichment in *S. pacificus* muscle tissue $\delta^{15}N$ values is that, as discussed above, the retention of urea may negatively bias $\delta^{15}N$ of elasmobranch muscle tissue (Kim & Koch, 2012). Allowing for both a negative bias in $\delta^{15}N$ resulting from the retention of urea in elasmobranch muscle tissue (*c.* 2‰; Kim & Koch, 2012; Table 3.1) and assuming that *S. pacificus* muscle tissue $\Delta^{15}N$ is at the lower end of the estimated range in $\Delta^{15}N$, *c.* 2.3‰ (Hussey et al., 2010a) or 2.7‰ (Vanderklift & Ponsard, 2003; Caut et al., 2009; Dale et al., 2011), would result in a relatively higher predicted trophic position for *S. pacificus* relative to fishes, squid and filter feeding whales (Figure 3.3; Appendices 3.A and 3.B) and would be more consistent with the available stomach-content data discussed above.

In this study, *S. pacificus* muscle tissue $\delta^{15}N$ values were depleted relative to those of *O. orca* and pinnipeds in the eastern North Pacific Ocean (Figure 3.3; Appendices 3.A and 3.B). These results are consistent with observations of offshore *O. orca* predation on *S. pacificus* in Southeast Alaska (Ford et al., 2011) and with the limited occurrence of pinnipeds in the stomach contents of *S. pacificus* in the Gulf of Alaska (Sigler et al., 2006). In particular, a directed study of *S. pacificus* diet (n = 198 stomachs examined) near *E. jubatus* rookeries in the Gulf of Alaska found no evidence of *S. pacificus* predation on *E. jubatus*. In the same study, harbor seal *Phoca vitulina* comprised only about 3% of *S. pacificus* stomach contents by mass (Sigler et al., 2006). In comparison, harbor seal comprise about 2% of *S. pacificus* stomach contents by mass in the high latitude western North Pacific Ocean (Orlov, 1999; Orlov & Moiseev, 1999a, b). Direct comparisons of *S. pacificus* muscle tissue $\delta^{15}N$ values with those of marine mammals (Figure 3.3) should, however, be interpreted cautiously because a variety of marine mammal tissue types were sampled, which may have had an effect on the resulting marine mammal $\delta^{15}N$ values (Appendices 3.A and 3.B). In addition, the relatively low occurrence of pinnipeds in the stomach contents of *S. pacificus* in the eastern North Pacific Ocean could result from sampling bias (Taggart et al., 2005). It is also possible that predation by individual 'specialist' (Matich et al., 2010a) sharks could have an effect on pinniped populations (Brodie & Beck, 1983; Lucas & Stobo, 2000; Taggart et al., 2005). The slow

isotopic turnover rates of elasmobranch muscle tissue $\delta^{15}N$ may also mask temporal variation in $\delta^{15}N$ associated with diet switching, especially in scavenging or omnivorous elasmobranchs (MacNeil et al., 2005, 2006; Matich et al., 2010a). As a result, estimates of trophic position from muscle tissue $\delta^{15}N$ of scavenging or omnivorous elasmobranchs may have considerable uncertainty (MacNeil et al., 2006).

In conclusion, stable-isotope analysis revealed wider variability in the feeding ecology of *S. pacificus* in the eastern North Pacific Ocean than shown by diet data alone. The use of lipid-normalized carbon stable isotopes ($\delta^{13}C'$) to determine food web utilization and the use of $\delta^{15}N$ to determine trophic position revealed significant regional differences in the feeding ecology of *S. pacificus* in the eastern North Pacific Ocean. For example, the stable-isotope results from this study revealed that *S. pacificus* in the eastern North Pacific Ocean switch prey and, potentially, feeding areas with increasing size. Stable-isotope analysis and stomach-content analysis were consistent in suggesting that changes in *S. pacificus* abundance could have direct effects on the eastern North Pacific Ocean ecosystem, most probably on relatively lower trophic level populations of fishes and squid. Stable-isotope analysis, however, expanded previous conclusions drawn from geographically and temporally limited snapshots of stomach-content data to the broader geographic regions within the EBS, GOA and NSE sampled in this study and to an annual time scale inferred from seasonal sampling in this study combined with the slow isotopic turnover rates of $\delta^{13}C$ and $\delta^{15}N$ in elasmobranch muscle tissue.

3.6. Acknowledgements

We thank the NMFS AFSC Observer Program, the NMFS AFSC RACE Division and the NMFS AFSC ABL for specimen collections in the EBS, GOA and NSE (respectively). The manuscript benefited from reviews by K. Criddle (UAF School of Fisheries and Ocean Sciences), W. Walsh and J. O'Malley (NMFS Pacific Islands Fisheries Science Center) and two anonymous reviewers. This project was funded by the NMFS AFSC ABL (D. L. C.) and by a grant from the Pollock Conservation Cooperative Research Center (PCCRC) (R. F.) for investigation of by-catch and the ecology of sharks in the Bering Sea.

3.7. Literature Cited

Andrews, A. G. III (2010). *Variation in the Trophic Position of Spiny Dogfish (Squalus acanthias) in the Northeastern Pacific Ocean: An Approach Using Carbon and Nitrogen Stable Isotopes*. MS Thesis, University of Alaska Fairbanks, AK.

Andrews, A. G. & Foy, R. J. (2009). Geographical variation in the carbon and nitrogen stable isotope ratios of spiny dogfish, *Squalus acanthias*, in the northeastern Pacific Ocean. In *Biology and Management of Dogfish Sharks* (Gallucci, V. F., McFarlane, G. A. & Bargmann, G. G., eds), pp. 269–276. Bethesda, MD: American Fisheries Society.

Baum, J. K. & Worm, B. (2009). Cascading top-down effects of changing oceanic predator abundances. *Journal of Animal Ecology* **78,** 699–714.

Benz, G. W., Hocking, R., Kowunna, A. Sr., Bullard, S. A. & George, J. C. (2004). A second species of Arctic shark: Pacific sleeper shark *Somniosus pacificus* from Point Hope, Alaska. *Polar Biology* **27,** 250–252.

Borenstein, M., Hedges, L. V., Higgins, J. P. T. & Rothstein, H. R. (2009). *Introduction to Meta-Analysis*, New York, NY: John Wiley and Sons, Ltd.

Borets, L. A. (1986). Ichthyofauna of the Northwestern and Hawaiian submarine ranges. *Journal of Ichthyology* **26,** 1–13.

Borrell, A., Cardona, L., Kumarran, R. P. & Aguilar, A. (2011). Trophic ecology of elasmobranchs caught off Gujarat, India, as inferred from stable isotopes. *ICES Journal of Marine Science* **68,** 547–554.

Bright, D. B. (1959). The occurrence and food of the sleeper shark, *Somniosus pacificus*, in a central Alaska bay. *Copeia* **1959,** 76–77.

Brodie, P. & Beck, B. (1983). Predation by sharks on the grey seal (*Halichoerus grypus*) in eastern Canada. *Canadian Journal of Fisheries and Aquatic Sciences* **40,** 267–271.

Burnham, K. P. & Anderson, D. R. (2002). *Model Selection and Multimodel Inference: A Practical Information-Theoretic Approach*, 2nd edn. New York, NY: Springer-Verlag.

Caut, S., Angulo, E. & Courchamp, F. (2009). Variation in discrimination factors (Δ^{15}N and Δ^{13}C): the effect of diet isotopic values and applications for diet reconstruction. *Journal of Applied Ecology* **46,** 443–453.

Cherel, Y. & Duhamel, G. (2004). Antarctic jaws: cephalopod prey of sharks in Kerguelen waters. *Deep Sea Research I* **51,** 17–31.

Chikaraishi, Y., Ogawa, N. O., Kashiyama, Y., Takano, Y., Suga, H., Tomitani, A., Miyashita, H., Kitazato, H. & Ohkouchi, N. (2009). Determination of aquatic food-web structure based on compound-specific nitrogen isotopic composition of amino acids. *Limnology and Oceanography-Methods* **7,** 740–750.

Compagno, L. J. V. (1984). FAO species catalogue. Vol. 4. Sharks of the world. An annotated and illustrated catalogue of shark species known to date, Part 1. Hexanchiformes to Lamniformes. *FAO Fisheries Synopsis* **125,** 1–249.

Cortés, E. (1997). A critical review of methods of studying fish feeding based on analysis of stomach contents: application to elasmobranch fishes. *Canadian Journal of Fisheries and Aquatic Sciences* **54,** 726–738.

Cortés, E. (1999). Standardized diet compositions and trophic levels of sharks. *ICES Journal of Marine Science* **56,** 707–717.

Courtney, D. L. & Sigler, M. F. (2007). Trends in area-weighted CPUE of Pacific sleeper sharks (*Somniosus pacificus*) in the northeast Pacific Ocean determined from sablefish longline surveys. *Alaska Fishery Research Bulletin* **12,** 291–315.

Crawley, M. J. (2007). *The R Book*. John Wiley & Sons, Ltd.

Criddle, K. R. (2005). *Intermediate Statistics and Applied Regression Analysis*. Auke Bay, AK: East-West Bridge Publishing House.

Dale, J. J., Wallsgrove, N. J., Popp, B. N. & Holland, K. N. (2011). Nursery habitat use and foraging ecology of the brown stingray *Dasyatis lata* determined from stomach contents, bulk and amino acid stable isotopes. *Marine Ecology Progress Series* **433,** 221–236.

DeNiro, M. J. & Epstein, S. (1978). Influence of diet on distribution of carbon isotopes in animals. *Geochimica et Cosmochimica Acta* **42,** 495–506.

DeNiro, M. J. & Epstein, S. (1981). Influence of diet on the distribution of nitrogen isotopes in animals. *Geochimica et Cosmochimica Acta* **45,** 341–351.

Domi, N., Bouquegneau, J. M. & Das, K. (2005). Feeding ecology of five commercial shark species of the Celtic Sea through stable isotope and trace metal analysis. *Marine Environmental Research* **60,** 551–569.

Ebert, D. A. & Bizzarro, J. J. (2007). Standardized diet compositions and trophic levels of skates (Chondrichthyes: Rajiformes: Rajoidei). *Environmental Biology of Fishes* **80,** 221–237.

Ebert, D. A. & Winton, M. V. (2010). Chondrichthyans of high latitude seas. In *Sharks and their Relatives II; Biodiversity, Adaptive Physiology, and Conservation* (Carrier, J. C., Musick, J. A. & Heithaus, M. R., eds), pp. 115–158. Boca Raton, FL: CRC Press.

Ebert, D. A., Compagno, L. J. V. & Natanson, L. J. (1987). Biological notes on the Pacific sleeper shark, *Somniosus pacificus* (Chondrichthyes: Squalidae). *California Fish and Game* **73,** 117–123.

Estrada, J. A., Rice, A. N., Lutcavage, M. E. & Skomal, G. B. (2003). Predicting trophic position in sharks of the north-west Atlantic Ocean using stable isotope analysis. *Journal of the Marine Biological Association of the United Kingdom* **83,** 1347–1350.

Estrada, J. A., Rice, A. N., Natanson, L. J. & Skomal, G. B. (2006). Use of isotopic analysis of vertebrae in reconstructing ontogenetic feeding ecology in white sharks. *Ecology* **87,** 829–834.

Fisk, A. T., Tittlemier, S. A., Pranschke, J. L. & Norstrom, R. J. (2002). Using anthropogenic contaminants and stable isotopes to assess the feeding ecology of Greenland sharks. *Ecology* **83,** 2162–2172.

Ford, J. K. B., Ellis, G. M., Makin, C. O., Wetklo, M. H., Barrett-Lennard, L. G. & Withler, R. E. (2011). Shark predation and tooth wear in a population of northeastern Pacific killer whales. *Aquatic Biology* **11,** 213–224.

Forrest, R. E. & Walters, C. J. (2009). Estimating thresholds to optimal harvest rate for longlived, low-fecundity sharks accounting for selectivity and density dependence in recruitment. *Canadian Journal of Fisheries and Aquatic Sciences* **66,** 2062–2080.

Frid, A., Baker, G. G. & Dill, L. M. (2006). Do resource declines increase predation rates on North Pacific harbor seals? A behavior-based plausibility model. *Marine Ecology Progress Series* **312,** 265–275.

Frid, A., Dill, L. M., Thorne, R. E. & Blundell, G. M. (2007a). Inferring prey perception of relative danger in large-scale marine systems. *Evolutionary Ecology Research* **9,** 635–649.

Frid, A., Heithaus, M. R. & Dill, L. M. (2007b). Dangerous dive cycles and the proverbial ostrich. *Oikos* **116,** 893–902. doi: 10.1111/j.2007.0030-1299.15766.x

Frid, A., Baker, G. G. & Dill, L. M. (2008). Do shark declines create fear-released systems? *Oikos* **117,** 191–201. doi: 10.1111/j.2007.0030-1299.16134.x

Frid, A., Burns, J., Baker, G. G. & Thorne, R. E. (2009). Predicting synergistic effects of resources and predators on foraging decisions by juvenile Steller sea lions. *Oecologia* **158,** 775–786.

Gotshall, D. W. & Jow, T. (1965). Sleeper sharks (*Somniosus pacificus*) off Trinidad, California, with life history notes. *California Fish and Game* **51,** 294–298.

Hansen, P. M. (1963). Tagging experiments with the Greenland shark (*Somniosus microcephalus* (Bloch and Schneider)) in Subarea 1. *International Commission Northwest Atlantic Fisheries Special Publication* **4,** 172–175.

Heithaus, M. R., Frid, A., Wirsing, A. J. & Worm, B. (2008). Predicting ecological consequences of marine top predator declines. *Trends in Ecology and Evolution* **23,** 202–210.

Heithaus, M. R., Frid, A., Vaudo, J. J., Worm, B. & Wirsing, A. J. (2010). *Unraveling the ecological importance of elasmobranchs. In Sharks and Their Relatives II; Biodiversity, Adaptive Physiology, and Conservation* (Carrier, J. C., Musick, J. A. & Heithaus, M. R., eds), pp. 611–637. Boca Raton, FL: CRC Press.

Herman, D. P., Burrows, D. G., Wade, P. R., Durban, J. W., Matkin, C. O., LeDuc, R. G., Barrett-Lennard, L. G. & Krahn, M. M. (2005). Feeding ecology of eastern North Pacific killer whales *Orcinus orca* from fatty acid, stable isotope, and organochlorine analyses of blubber biopsies. *Marine Ecology Progress Series* **302,** 275–291.

Hirons, A. C., Schell, D. M. & Finney, B. P. (2001). Temporal records of $\delta^{13}C$ and $\delta^{15}N$ in North Pacific pinnipeds: inferences regarding environmental change and diet. *Oecologia* 129, 591–601.

Hobson, K. A. & Welch, H. E. (1992). Determination of trophic relationships within a high arctic marine food web using $\delta^{13}C$ and $\delta^{15}N$ analysis. *Marine Ecology Progress Series* **84,** 9–18.

Hobson, K. A., Sease, J. L., Merrick, R. L. & Piatt, J. F. (1997). Investigating trophic relationships of pinnipeds in Alaska and Washington using stable isotope ratios of nitrogen and carbon. *Marine Mammal Science* **13,** 114–132.

Hobson, K. A., Fisk, A., Karnovsky, N., Holst, M., Gagnon, J.-M. & Fortier, M. (2002). A stable isotope ($\delta^{13}C$, $\delta^{15}N$) model for the North Water food web: implications for evaluating trophodynamics and the flow of energy and contaminants. *Deep Sea Research II* **49,** 5131–5150.

Horning, M. & Mellish, J.-A. E. (2012). Predation on an upper trophic marine predator, the Stellar Sea Lion: evaluating high juvenile mortality in a density dependent conceptual frame work. *PLoS One* **7,** e30173. doi: 10.1371/journal.pone0030173

Hulbert, L. B., Sigler, M. F. & Lunsford, C. R. (2006). Depth and movement behaviour of the Pacific sleeper shark in the eastern North Pacific Ocean. *Journal of Fish Biology* **69,** 406–425.

Hussey, N. E., Brush, J., McCarthy, I. D. & Fisk, A. T. (2010*a*). $\delta^{15}N$ and $\delta^{13}C$ diet-tissue discrimination factors for large sharks under semi-controlled conditions. *Comparative Biochemistry and Physiology A* **155,** 445–453.

Hussey, N. E., MacNeil, M. A. & Fisk, A. T. (2010*b*). The requirement for accurate diet tissue discrimination factors for interpreting stable isotopes in sharks. *Hydrobiologia* **654,** 1–5.

Hussey, N. E., Dudley, S. F. J., McCarthy, I. D., Cliff, G. & Fisk, A. T. (2011). Stable isotope profiles of large marine predators: viable indicators of trophic position, diet, and movement in sharks? *Canadian Journal of Fisheries and Aquatic Sciences* **68,** 2029–2045. doi: 10.1139/2011-115

Hussey, N. E., MacNeil, M. A., Olin, J. A., McMeans, B. C., Kinney, M. J., Chapman, D. D. & Fisk, A. T. (2012). Stable isotopes and elasmobranchs: tissue types, methods, applications and assumptions. *Journal of Fish Biology* **80,** 1449–1484. doi:10.1111/j.1095-8649.2012.03251.x

Kerr, L. A., Andrews, A. H., Cailliet, G. M., Brown, T. A. & Coale, K. H. (2006). Investigations of $\Delta^{14}C$, $\delta^{13}C$, and $\delta^{15}N$ in vertebrae of white shark (*Carcharodon carcharias*) from the eastern North Pacific Ocean. *Environmental Biology of Fishes* **77,** 337–353.

Kim, S. L. & Koch, P. L. (2012). Methods to collect, preserve, and prepare elasmobranch tissues for stable isotope analysis. *Environmental Biology of Fishes* **95,** 53–63.

Kim, S., Caspar, D., Galván-Magaña, F., Ochoa-Díaz, R., Hernández-Aguilar, S. & Koch, P. (2011). Carbon and nitrogen discrimination factors for elasmobranch soft tissues based on a long-term controlled feeding study. *Environmental Biology of Fishes* **95,** 37–52.

Kitchell, J. F., Essington, T. E., Boggs, C. H., Schindler, D. E. & Walters, C. J. (2002). The role of sharks and longline fisheries in a pelagic ecosystem of the Central Pacific. *Ecosystems* **5,** 202–216.

Kleinbaum, D. G., Kupper, L. L. & Muller, K. E. (1988). *Applied Regression Analysis and Other Multivariate Methods*, 2nd edn. Belmont, CA: Duxbury Press.

Kline, T. C., Jr. (1997). Confirming forage fish food web dependencies in Prince William Sound using natural stable isotope tracers. In *Forage Fishes in Marine Ecosystems. Proceedings of the International Symposium on the Role of Forage Fishes in Marine Ecosystems*, pp. 257–269. *Alaska Sea Grant College Program Report No.* 97-01. Fairbanks, AK: University of Alaska Fairbanks.

Kline, T. C. Jr. (1999). Temporal and spatial variability of $^{13}C/^{12}C$ and $^{15}N/^{14}N$ in pelagic biota of Prince William Sound, Alaska. *Canadian Journal of Fisheries and Aquatic Sciences* **56,** 94–117.

Kline, T. C. Jr. (2009). Characterization of carbon and nitrogen stable isotope gradients in the northern Gulf of Alaska using terminal feed stage copepodite-V *Neocalanus cristatus*. *Deep Sea Research Part II-Topical Studies in Oceanography* **56,** 2537–2552.

Krahn, M. M., Herman, D. P., Matkin, C. O., Durban, J. W., Barrett-Lennard, L., Burrows, D. G., Dahlheim, M. E., Black, N., LeDuc, R. G. & Wade, P. R. (2007). Use of chemical tracers in assessing the diet and foraging regions of eastern North Pacific killer whales. *Marine Environmental Research* **63,** 91–114.

Kuker, K. & Barrett-Lennard, L. (2010). A re-evaluation of the role of killer whales *Orcinus orca* in a population decline of sea otters *Enhydra lutris* in the Aleutian Islands and a review of alternative hypotheses. *Mammal Review* **40,** 103–124.

Kurle, C. M. & Worthy, G. A. J. (2001). Stable isotope assessment of temporal and geographic differences in feeding ecology of northern fur seals (*Callorhinus ursinus*) and their prey. *Oecologia* **126,** 254–265.

Kyne, P. M. & Simpfendorfer, C. A. (2010). Deepwater chondrichthyans. *In Sharks and their Relatives II; Biodiversity, Adaptive Physiology, and Conservation* (Carrier, J. C., Musick, J. A. & Heithaus, M. R., eds), pp. 37–113. Boca Raton, FL: CRC Press.

Liu, H., Dagg, M. J. & Strom, S. (2005). Grazing by the calanoid copepod *Neocalanus cristatus* on the microbial food web in the coastal Gulf of Alaska. *Journal of Plankton Research* **27,** 647–662.

Logan, J. M. & Lutcavage, M. E. (2010*a*). Stable isotope dynamics in elasmobranch fishes. *Hydrobiologia* **644,** 231–244.

Logan, J. M. & Lutcavage, M. E. (2010*b*). Reply to Hussey et al.: The requirement for accurate diet-tissue discrimination factors for interpreting stable isotopes in sharks. *Hydrobiologia* **654,** 7–12.

Lucas, Z. & Stobo, W. T. (2000). Shark-inflicted mortality on a population of harbour seals (*Phoca vitulina*) at Sable Island, Nova Scotia. *Journal of Zoology* **252,** 405–414.

MacNeil, M. A., Skomal, G. B. & Fisk, A. T. (2005). Stable isotopes from multiple tissues reveal diet switching in sharks. *Marine Ecology Progress Series* **302,** 199–206.

MacNeil, M. A., Drouillard, K. G. & Fisk, A. T. (2006). Variable uptake and elimination of stable nitrogen isotopes between tissues in fish. *Canadian Journal of Fisheries and Aquatic Sciences* **63,** 345–353.

Marsh, J. M. (2010). *Ontogenetic Considerations in the Trophic Level of Commercial Groundfish Species in the Gulf of Alaska*. MS Thesis, University of Alaska Fairbanks, AK.

Martínez del Rio, C., Wolf, N., Carleton, S. A. & Gannes, L. Z. (2009). Isotopic ecology ten years after a call for more laboratory experiments. *Biological Reviews* **84,** 91–111.

Matich, P., Heithaus, M. R. & Layman, C. A. (2010*a*). Contrasting patterns of individual specialization and trophic coupling in two marine apex predators. *Journal of Animal Ecology* **80,** 294–305.

Matich, P., Heithaus, M. R. & Layman, C. A. (2010*b*). Size-based variation in intertissue comparisons of stable carbon and nitrogen isotopic signatures of bull sharks (*Carcharhinus leucas*) and tiger sharks (*Galeocerdo cuvier*). *Canadian Journal of Fisheries and Aquatic Sciences* **67,** 877–885.

McConnaughey, T. & McRoy, C. P. (1979*a*). Food-web structure and the fractionation of carbon isotopes in the Bering Sea. *Marine Biology* **53,** 257–262.

McConnaughey, T. & McRoy, C. P. (1979*b*). ^{13}C label identifies eelgrass (*Zostera marina*) carbon in an Alaskan estuarine food web. *Marine Biology* **53,** 263–269.

McMeans, B. C., Borga, K., Bechtol, W. R., Higginbotham, D. & Fisk, A. T. (2007). Essential and non-essential element concentrations in two sleeper shark species collected in Arctic waters. *Environmental Pollution* **148,** 281–290.

McMeans, B. C., Olin, J. A. & Benz, G. W. (2009). Stable-isotope comparisons between embryos and mothers of a placentatrophic shark species. *Journal of Fish Biology* **75,** 2464–2474.

McMeans, B. C., Svavarsson, J., Dennard, S. & Fisk, A. T. (2010). Diet and resource use among Greenland sharks (*Somniosus microcephalus*) and teleosts sampled in Icelandic waters, using $\delta^{13}C$, $\delta^{15}N$, and mercury. *Canadian Journal of Fisheries and Aquatic Sciences* **67,** 1428–1438.

Mecklenburg, C. W., Mecklenburg, T. A. & Thorsteinson, L. K. (2002). *Fishes of Alaska*. Bethesda, MD: American Fisheries Society.

Menon, M. M. (2004). *Spatio-Temporal Modeling of Pacific Sleeper Shark (*Somniosus pacificus*) and Spiny Dogfish (*Squalus acanthias*) Bycatch in the Northeast Pacific Ocean*. Seattle, WA: University of Washington.

Menon, M. M., Gallucci, V. F. & Conquest, L. L. (2005). Sampling designs for the estimation of longline bycatch. In *Fisheries Assessment and Management in Data-limited Situations* (Kruse, G. H., Gallucci, V. F., Hay, D. E., Perry, R. I., Peterman, R. M., Shirley, T. C., Spencer, P. D., Wilson, B. & Woodby, D., eds), pp. 851–870. *Alaska Sea Grant College Program Report No.* 05-02. Fairbanks, AK: University of Alaska Fairbanks.

Minagawa, M. & Wada, E. (1984). Stepwise enrichment of ^{15}N along food chains: further evidence and the relation between ^{15}N and animal age. *Geochimica et Cosmochimica Acta* **48,** 1135–1140.

Mueter, F. J. & Norcross, B. L. (2002). Spatial and temporal patterns in the demersal fish community on the shelf and upper slope regions of the Gulf of Alaska. *Fishery Bulletin* **100,** 559–581.

Murray, B. W., Wang, J. Y., Yang, S.-C., Stevens, J. D., Fisk, A. & Svavarsson, J. (2008). Mitochondrial cytochrome *b* variation in sleeper sharks (Squaliformes: Somniosidae). *Marine Biology* **153,** 1015–1022.

Myers, R. A., Baum, J. K., Shepherd, T. D., Powers, S. P. & Peterson, C. H. (2007). Cascading effects of the loss of apex predatory sharks from a coastal ocean. *Science* **315,** 1846–1850.

Olin, J. A., Hussey, N. E., Fritts, M., Heupel, M. R., Simpfendorfer, C. A., Poulakis, G. R. & Fisk, A. T. (2011). Maternal meddling in neonatal sharks: implication for interpreting stable isotopes in young animals. *Rapid Communications in Mass Spectrometry* **25,** 1008–1016. doi: 10.1002/rcm.4946

Orlov, A. M. (1999). Capture of especially large sleeper shark *Somniosus pacificus* (Squalidae) with some notes on its ecology in northwestern Pacific. *Journal of Ichthyology* **39,** 548–553.

Orlov, A. M. & Moiseev, S. I. (1999*a*). New data on the biology of the Pacific sleeper shark, *Somniosus pacificus* (Squalidae) in the northwestern Pacific Ocean. In *Fish Performance Studies* (MacKinlay, D., Howard, K. & Cech, J. Jr., eds), pp. 177–186. Vancouver, BC: Department of Fisheries and Oceans.

Orlov, A. M. & Moiseev, S. I. (1999*b*). Some biological features of Pacific sleeper shark, *Somniosus pacificus* (Bigelow and Schroeder 1944) (Squalidae) in the northwestern Pacific Ocean. *Oceanological Studies* **28,** 3–16.

Papastamatiou, Y. P., Friedlander, A. M., Caselle, J. E. & Lowe, C. G. (2010). Long-term movement patterns and trophic ecology of blacktip reef sharks (*Carcharhinus melanopterus*) at Palmyra Atoll. *Journal of Experimental Marine Biology and Ecology* **386,** 94–102.

Pikitch, E. K., Santora, C., Babcock, E. A., Bakun, A., Bonfil, R., Conover, D. O., Dayton, P., Doukakis, P., Fluharty, D., Heneman, B., Houde, E. D., Link, J., Livingston, P. A., Mangel, M., McAllister, M. K., Pope, J. G., & Sainsbury, K. J. (2004). Ecosystem based fishery management. *Science* **305,** 346–347.

Post, D. M. (2002). Using stable isotopes to estimate trophic position: models, methods, and assumptions. *Ecology* **83,** 703–718.

Post, D. M., Layman, C. A., Arrington, D. A., Takimoto, G., Quattrochi, J. & Montaña, C. G. (2007). Getting to the fat of the matter: models, methods and assumptions for dealing with lipids in stable isotope analyses. *Oecologia* **152,** 179–189.

Reum, J. C. P. (2011). Lipid correction model of carbon stable isotopes for a cosmopolitan predator, spiny dogfish *Squalus acanthias*. *Journal of Fish Biology* **79,** 2060–2066. doi: 10.1111/j.1095-8649.2011.03120.x

Reuter, R. F., Conners, M. E., Dicosimo, J., Gaichas, S., Ormseth, O. & Tenbrink, T. T. (2010). Managing non-target, data-poor species using catch limits: lessons from the Alaskan groundfish fishery. *Fisheries Management and Ecology* **17,** 323–335. doi:10.1111/j.1365-2400.2009.00726.x

Sampson, L., Galván-Magaña, F., De Silva-Dávila, R., Aguíñiga-García, S. & O'Sullivan, J. B. (2010). Diet and trophic position of the devil rays *Mobula thurstoni* and *Mobula japanica* as inferred from stable isotope analysis. *Journal of the Marine Biological Association of the United Kingdom* **90,** 969–976.

Schell, D. M., Barnett, B. A. & Vinette, K. A. (1998). Carbon and nitrogen isotope ratios in zooplankton of the Bering, Chukchi and Beaufort Seas. *Marine Ecology Progress Series* **162,** 11–23.

Sigler, M. F., Hulbert, L. B., Lunsford, C. R., Thompson, N. H., Burek, K., O'Corry-Crowe, G. & Hirons, A. C. (2006). Diet of Pacific sleeper shark, a potential Steller sea lion predator, in the eastern North Pacific Ocean. *Journal of Fish Biology* **69,** 392–405.

Smith, C. R. & Baco, A. R. (2003). Ecology of whale falls at the deep-sea floor. In *Oceanography and Marine Biology: An Annual Review* **41,** 311–354.

Smith, S. E., Au, D. W. & Show, C. (1998). Intrinsic rebound potentials of 26 species of Pacific sharks. *Marine and Freshwater Research* **49,** 663–678.

Sokal, R. R. & Rohlf, F. J. (1995). *Biometry*, 3rd edn. New York, NY: W. H. Freeman and Company.

Stevenson, D. E. & Lewis, K. A. (2010). Observer-reported skate bycatch in the commercial groundfish fisheries of Alaska. *Fishery Bulletin* **108,** 208–217.

Sweeting, C. J., Polunin, N. V. C. & Jennings, S. (2006). Effects of chemical lipid extraction and arithmetic lipid correction on stable isotope ratios of fish tissues. *Rapid Communications in Mass Spectrometry* **20,** 595–601.

Taggart, S. J., Andrews, A. G., Mondragon, J. & Mathews, E. A. (2005). Co-occurrence of Pacific sleeper sharks *Somniosus pacificus* and harbor seals *Phoca vitulina* in Glacier Bay. *Alaska Fishery Research Bulletin* **11,** 113–117.

Vander Zanden, M. J. & Rasmussen, J. B. (2001). Variation in $\delta^{15}N$ and $\delta^{13}C$ trophic fractionation: implications for aquatic food web studies. *Limnology and Oceanography* **46**, 2061–2066.

Vander Zanden, M. J., Cabana, G. & Rasmussen, J. B. (1997). Comparing trophic position of freshwater fish calculated using stable nitrogen isotope ratios ($\delta^{15}N$) and literature dietary data. *Canadian Journal of Fisheries and Aquatic Sciences* **54,** 1142–1158.

Vanderklift, M. A. & Ponsard, S. (2003). Sources of variation in consumer-diet $\delta^{15}N$ enrichment: a meta-analysis. *Oecologia* **136,** 169–182.

Vaudo, J. J. & Heithaus, M. R. (2011). Dietary niche overlap in a nearshore elasmobranch mesopredator community. *Marine Ecology Progress Series* **425,** 247–260.

Vaudo, J. J., Matich, P. & Heithaus, M. R. (2010). Mother-offspring isotope fractionation in two species of placentatrophic sharks. *Journal of Fish Biology* **77,** 1724–1727.

Wang, J. Y. & Yang, S.-C. (2004). First records of Pacific sleeper sharks (*Somniosus pacificus* Bigelow and Schroeder, 1944) in the subtropical waters of eastern Taiwan. *Bulletin of Marine Science* **74,** 229–235.

Wetherbee, B. M. & Cortés, E. (2004). Food consumption and feeding habits. In *Biology of Sharks and their Relatives* (Carrier, J. C., Musick, J. A. & Heithaus, M. R., eds), pp. 225–246. Boca Raton, FL: CRC Press.

Wirsing, A. J., Heithaus, M. R., Frid, A. & Dill, L. M. (2008). Seascapes of fear: evaluating sublethal predator effects experienced and generated by marine mammals. *Marine Mammal Science* **24,** 1–15.

Witteveen, B. H., Worthy, G. A. J., Wynne, K. M. & Roth, J. D. (2009). Population structure of North Pacific humpback whales on their feeding grounds revealed by stable carbon and nitrogen isotope ratios. *Marine Ecology Progress Series* **379,** 299–310.

Wolf, N., Carleton, S. A. & Martínez del Rio, C. M. (2009). Ten years of experimental animal isotopic ecology. *Functional Ecology* **23,** 17–26.

Woodland, R. J., Secor, D. H. & Wedge, M. E. (2011). Trophic resource overlap between small elasmobranchs and sympatric teleosts in Mid-Atlantic Bight nearshore habitats. *Estuaries and Coasts* **34,** 391–404.

Yang, M.-S. & Page, B. N. (1999). Diet of Pacific sleeper shark, *Somniosus pacificus*, in the Gulf of Alaska. *Fishery Bulletin* **97,** 406–409.

Yano, K., Stevens, J. D. & Compagno, L. J. V. (2004). A review of the systematics of the sleeper shark genus *Somniosus* with redescriptions of *Somniosus (Somniosus) antarcticus* and *Somniosus (Rhinoscymnus) longus* (Squaliformes: Somniosidae). *Ichthyological Research* **51,** 360–373.

Yano, K., Stevens, J. D. & Compagno, L. J. V. (2007). Distribution, reproduction and feeding of the Greenland shark *Somniosus (Somniosus) microcephalus*, with notes on two other sleeper sharks, *Somniosus (Somniosus) pacificus* and *Somniosus (Somniosus) antarcticus*. *Journal of Fish Biology* **70,** 374–390.

Yeh, J. & Drazen, J. C. (2009). Depth zonation and bathymetric trends of deep-sea megafaunal scavengers of the Hawaiian Islands. *Deep Sea Research* ***I*** **56,** 251–266.

3.8. Electronic References

Courtney, D. L. & Hulbert, L. B. (2007). Shark research in the Gulf of Alaska with satellite, sonic, and archival tags. In *Report of the National Marine Fisheries Service Workshop on Advancing Electronic Tag Technologies and their Use in Stock Assessments, August 23–25, 2005* (Sheridan, P., Ferguson, J. W. & Downing, S. L., eds), pp. 26–27 (extended abstract). *U.S. Department of Commerce, NOAA Technical Memorandum NMFS-F/SPO-82*. Available at http://spo.nwr.noaa.gov/tm/tm82.pdf/ (accessed 1 June 2011).

Schaufler, L., Heintz, R., Sigler, M. & Hulbert, L. B. (2005). Fatty acid composition of sleeper shark (*Somniosus pacificus*) liver and muscle reveals nutritional dependence on planktivores. *ICES CM 2005/N:05*. Available at http://www.ices.dk/products/CMdocs/2005/N/N0505.pdf/ (accessed 1 June 2011).

von Szalay, P. G., Wilkins, M. E. & Martin, M. M. (2008). Data Report: 2007 Gulf of Alaska bottom trawl survey. *U.S. Department of Commerce, NOAA Technical Memorandum NMFS-AFSC-189*. Available at http://www.afsc.noaa.gov/publications/AFSC-TM/NOAA-TM-AFSC-189/NOAA-TM-AFSC-189.pdf/ (accessed 1 June 2011).

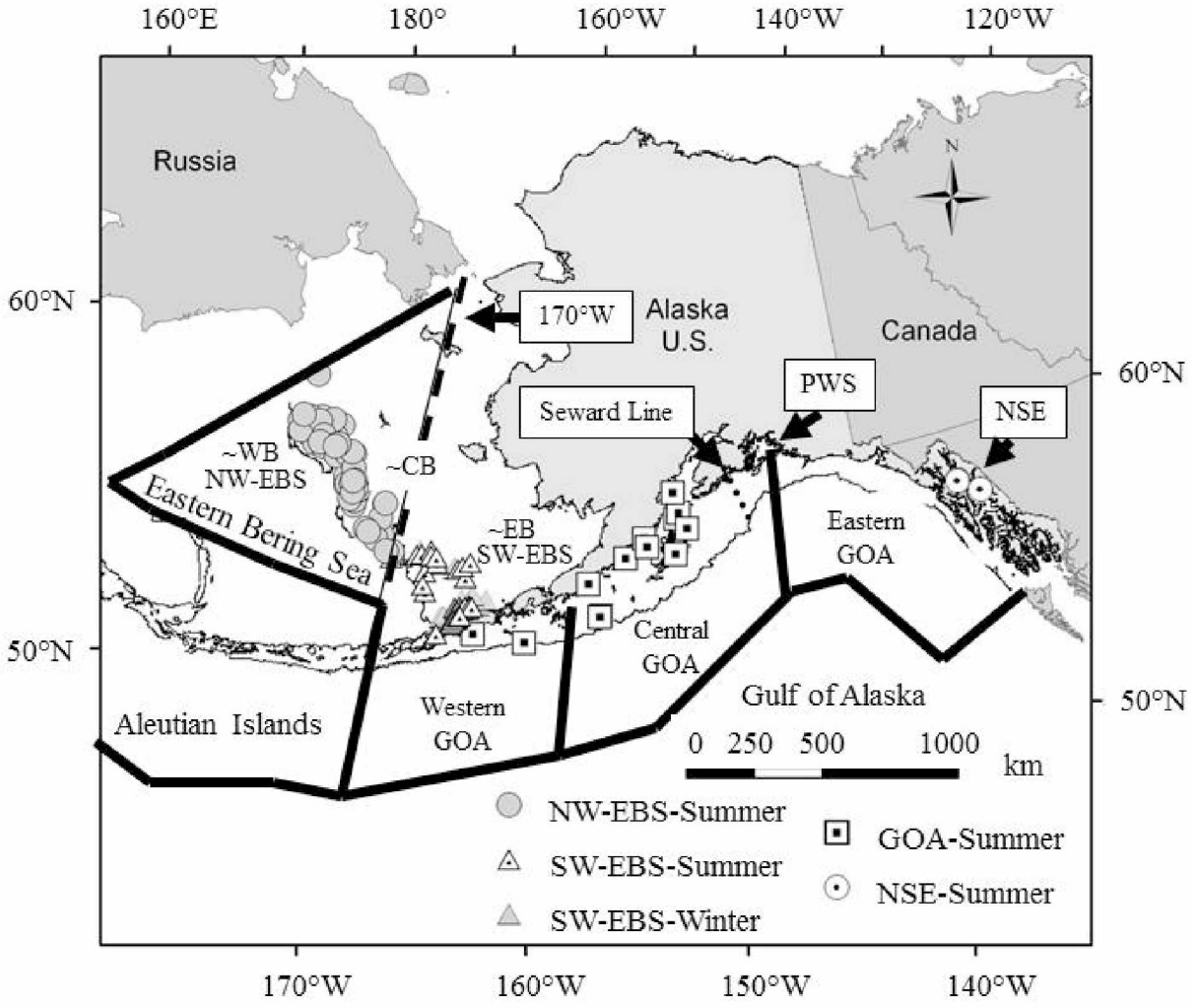

Figure 3.1: Map depicting the study area.
Somniosus pacificus were sampled for $\delta^{15}N$ and $\delta^{13}C$ from the north-western region of the eastern Bering Sea (NW-EBS) west of longitude 170° W (stippled line), from the south-eastern region of the EBS (SE-EBS) east of longitude 170° W, from the western and central Gulf of Alaska (GOA) and from northern region of Southeast Alaska (NSE) within U.S. National Marine Fisheries Service (NMFS) regulatory areas of the EBS, Aleutian Islands (AI) and western, central and eastern GOA; Trophic position from diet was estimated from previously published stomach-content data collected from *S. pacificus* captured in the EBS, AI and central GOA (Yang & Page, 1999; Sigler et al., 2006; Yano et al., 2007). The $\delta^{15}N_{baseline}$ (Equation 3.4) values of copepods were estimated here from previously published mean $\delta^{15}N$ values of copepods obtained from the western Bering Sea (c. WB; Schell et al. 1998), central Bering Sea (c. CB; Schell et al. 1998) and eastern Bering Sea (c. EB; Schell et al. 1998), and from the GOA continental shelf waters along the Seward Line (dotted line; Kline, 2009).

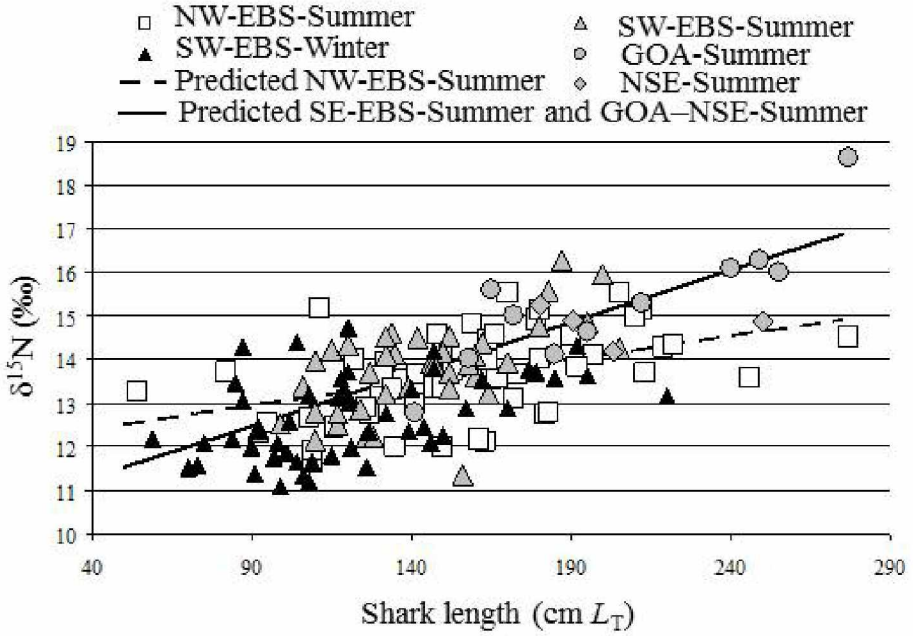

Figure 3.2: Observed and predicted nitrogen stable isotope ratios.

Observed $\delta^{15}N$ and predicted $\delta^{15}\hat{N}$ of *Somniosus pacificus* muscle tissue obtained from a simplified linear model (Equation 3.2 with three strata: NW-EBS-Summer, n = 54; SE-EBS-Winter, n = 50 and pooled SE-EBS-Summer + GOA-Summer + NSE-Summer, n = 56; Table 3.4) as a function of *S. pacificus* total length (L_T).

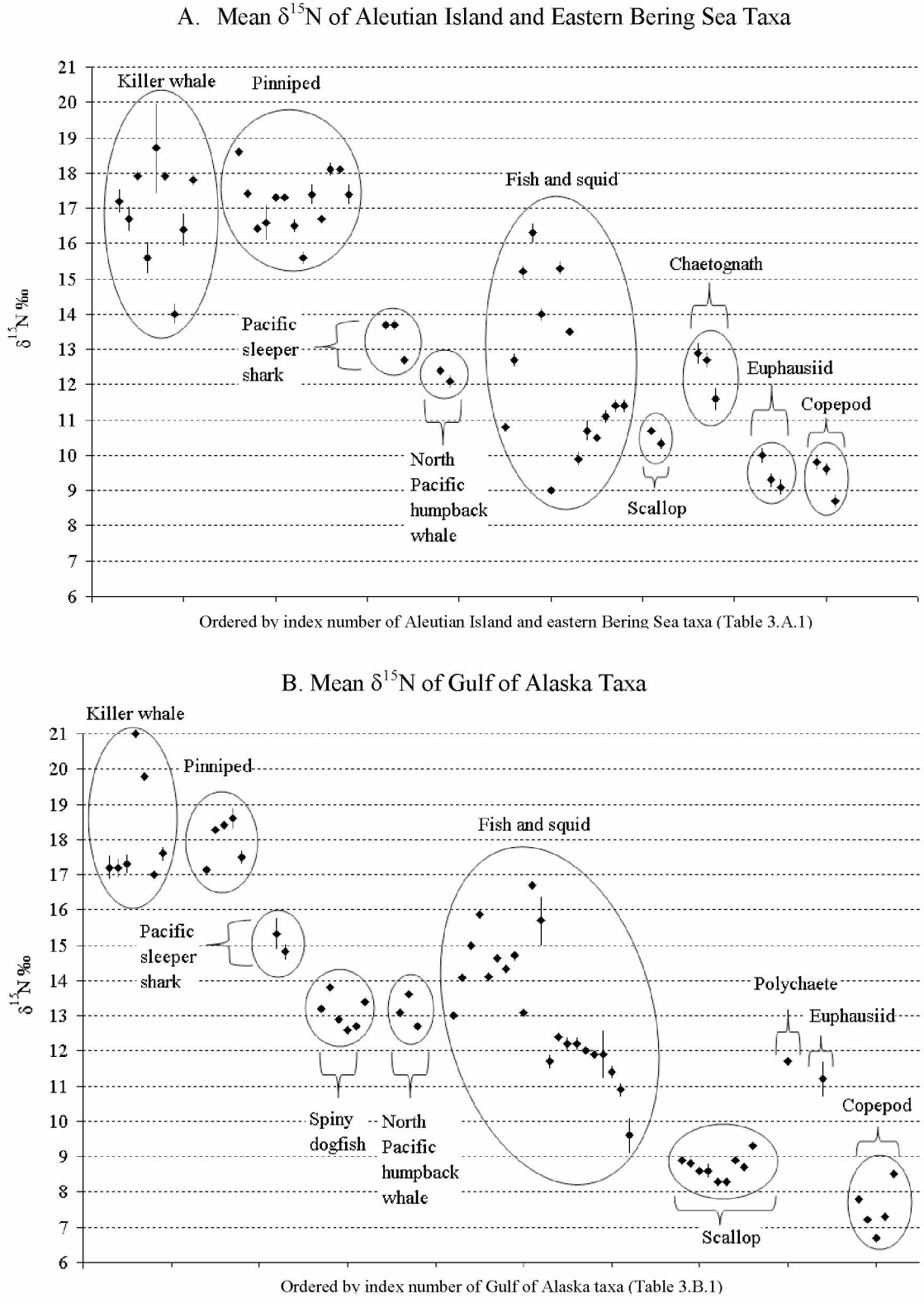

Figure 3.3: Mean $\delta^{15}N$ by taxa (Aleutian Islands, eastern Bering Sea, and Gulf of Alaska).

Figure 3.3 Continued. Mean $\delta^{15}N$ of *Somniosus pacificus* muscle tissue from the eastern Bering Sea by strata (Table 3.1; Figure 3.1) compared to the mean $\delta^{15}N$ values of other aquatic organisms from the Aleutian Islands and eastern Bering Sea (Panel A) and from the Gulf of Alaska (Panel B) obtained from a literature review (Appendices 3.A and 3.B); taxonomic groupings and subdivisions of other aquatic organisms were based on the original publications.

Table 3.1: Stable isotope values by region and season.
Values of $\delta^{15}N$, $\delta^{13}C$, $\delta^{13}C'$ and C:N of *Somniosus pacificus* muscle tissue from the eastern Bering Sea (EBS), Gulf of Alaska (GOA) and the northern region of Southeast Alaska (NSE), mean total length (L_T) and mean bottom depth at capture, post-stratified by region and sampling dates (*a*–*e*).

	Mean ± S.E.	Minimum	Maximum
(a) North-western eastern Bering Sea Summer (NW-EBS-Summer); 22 June 2007 – 29 October 2007 (n = 54)			
$\delta^{15}N$ (‰)	13.7 ± 0.1	11.6	15.5
$\delta^{13}C$ (‰)	−23.2 ± 0.1	−24.3	−20.9
$\delta^{13}C'$ (‰)	−21.1 ± 0.0	−21.9	−20.3
C:N (mass)	7.7 ± 0.2	3.9	10.9
Shark length (cm L_T)	158.2 ± 5.6	54.0	277.0
Bottom depth (m)	73.1 ± 3.1	48.0	165.0
(b) South-eastern eastern Bering Sea Summer (SE-EBS-Summer); 22 June 2007 – 29 October 2007 (n = 41)			
$\delta^{15}N$ (‰)	13.7 ± 0.2	11.3	16.3
$\delta^{13}C$ (‰)	−23.1 ± 0.1	−24.4	−20.8
$\delta^{13}C'$ (‰)	−21.1 ± 0.0	−21.8	−20.5
C:N (mass)	7.6 ± 0.3	3.6	12.4
Shark length (cm L_T)	141.9 ± 4.5	92.0	205.0
Bottom depth (m)	84.7 ± 5.5	44.0	160.0
(c) South-eastern eastern Bering Sea Winter (SE-EBS-Winter); 19 January 2007 – 17 March 2007 (n = 50)			
$\delta^{15}N$ (‰)	12.7 ± 0.1	11.1	14.7
$\delta^{13}C$ (‰)	−23.2 ± 0.1	−24.5	−20.2
$\delta^{13}C'$ (‰)	−21.1 ± 0.1	−22.4	−19.0
C:N (mass)	8.0 ± 0.3	3.2	15.6
Shark length (cm L_T)	122.7 ± 5.1	59.0	220.0
Bottom depth (m)	181.2 ± 13.7	49.0	300.0
(d) Gulf of Alaska Summer (GOA-Summer); 9 June 2007 – 11 July 2007 (n = 11)			
$\delta^{15}N$ (‰)	15.3 ± 0.5	12.8	18.6
$\delta^{13}C$ (‰)	−22.1 ± 0.4	−23.5	−20.2
$\delta^{13}C'$ (‰)	−20.0 ± 0.2	−20.7	−18.5
C:N (mass)	8.0 ± 0.8	5.6	14.1
Shark length (cm L_T)	204.5 ± 13.6	141.0	277.0
Bottom depth (m)	166.9 ± 19.9	91.0	309.0
(e) Northern Southeast Alaska Summer (NSE-Summer); 7 July 2006 – 10 July 2006 (n = 4)			
$\delta^{15}N$ (‰)	14.8 ± 0.2	14.2	15.3
$\delta^{13}C$ (‰)	−21.4 ± 0.2	−21.8	−21.1
$\delta^{13}C'$ (‰)	−19.5 ± 0.3	−20.1	−19.0
C:N (mass)	7.1 ± 1.1	5.1	10.1
Shark length (cm L_T)	206.0 ± 15.4	180.5	250.0
Bottom depth (m)	498.3 ± 90.5	226.8	588.9

Table 3.2: Linear model of $\delta^{15}N$ by shark length and stratum.
Linear regression model results (Equation 3.2) for *Somniosus pacificus* muscle tissue $\delta^{15}N$ as a function of total length (L_T) and stratum (NW-EBS-Summer, SE-EBS-Summer, SE-EBS-Winter and GOA–NSE-Summer; see Figure 3.1).

Main effects	k_F	$n - k_F - 1$	F	r^2	AIC	AIC_c	ΔAIC_c
Shark length (L_T)	1	158	121.8 ***	0.43	434.3	434.5	19.8
Stratum	3	156	24.4 ***	0.32	468.2	468.6	53.9
L_T + Stratum	4	155	40.5 ***	0.51	417.3	417.8	3.2
L_T + Stratum + L_T × Stratum	7	152	25.5 ***	0.54	413.5	414.6	0.0

*** $P < 0.001$.

Table 3.3: Contrast coefficients of linear model for $\delta^{15}N$.
Contrast coefficients among strata (Z) (NW-EBS-Summer, SE-EBS-Summer, SE-EBS-Winter and GOA–NSE-Summer; see Figure 3.1) fitted in the full model (L_T + stratum + L_T × stratum; as defined in Table 3.2).

	Contrast			
Coefficient	NW-EBS-Summer	SE-EBS-Summer	SE-EBS-Winter	GOA–NSE-Summer
Intercept	11.974 ***	10.363 ***	11.189 ***	10.022 ***
Shark length (L_T)	0.011 ***	0.024 ***	0.012 ***	0.025 ***
NW-EBS-Summer	NA	1.611	0.785	1.952
SE-EBS-Summer	–1.611	NA	–0.826	0.341
SE-EBS-Winter	–0.785	0.826	NA	1.167
GOA–NSE-Summer	–1.952	–0.341	–1.167	NA
L_T × NW-EBS-Summer	NA	–0.013 *	–0.002	–0.015 *
L_T × SE-EBS-Summer	0.013 *	NA	0.011	–0.002
L_T × SE-EBS-Winter	0.002	–0.011	NA	–0.013
L_T × GOA–NSE-Summer	0.015 *	0.002	0.013	NA

The test statistic for each contrast coefficient followed a t-distribution with $n - k_F - 1$ d.f. (152) from the full model (Table 3.2) and was evaluated at the $1 - \alpha$ significance level ($\alpha = 0.05$). * $P < 0{\cdot}05$; *** $P < 0{\cdot}001$.

Table 3.4: Model simplification for predicted $\delta^{15}N$.
Stepwise *a posteriori* model simplification of the full model (Table 3.2). The first stepwise model simplification aggregated SE-EBS-Summer with GOA–NSE-Summer within the full model (Table 3.2). The second stepwise model simplification aggregated NW-EBS-Summer with SE-EBS-Winter within the first simplified model (see Figure 3.1).

Model	F_p	k_p	$n - k_P - 1$	F(regression)	r^2	AIC	AIC_c	ΔAIC_c
1st stepwise model simplification	0.04	5	154	36.1 ***	0.54	409.6	410.3	–4.4
2nd stepwise model simplification	4.44*	3	156	54.9 ***	0.52	414.5	414.9	0.2

Table 3.5: Point forecasts of predicted $\delta^{15}N$ from simplified model.

Point forecasts of *Somniosus pacificus* muscle tissue $\delta^{15}N$ ($\delta^{15}\hat{N}$) estimated from the first simplified model (Equation 2; Table 3.4) with three strata (NW-EBS-Summer, $n = 54$; SE-EBS-Winter, $n = 50$ and pooled SE-EBS-Summer + GOA–NSE-Summer, $n = 56$) for *S. pacificus* of mean total length (L_T) 201.5 cm along with 95% prediction intervals (P.I.; Equation 3.3) (see Figure 3.1 for strata).

	$\delta^{15}\hat{N}$ (‰)			
Strata	Point forecast	S.E.	Lower 95% P.I.	Upper 95% P.I.
NW-EBS-Summer	14.1	0.9	12.4	15.8
SE-EBS-Winter	13.7	0.9	11.9	15.5
SE-EBS-Summer + GOA–NSE-Summer	15.1	0.9	13.4	16.8

Table 3.6: Trophic position determined from $\delta^{15}N$.

Somniosus pacificus trophic position calculated from $\hat{\delta^{15}N}$ (T_{PN}; Equation 3.4) within four strata (NW-EBS-Summer, SE-EBS-Summer, SE-EBS-Winter and GOA–NSE-Summer; see Figure 3.1) for *S. pacificus* of mean total length (L_T) 201.5 cm.

			T_{PN}		
Strata	$\delta^{15}N_{baseline}$ (‰)[1]	$\Delta^{15}N$ (‰)[2]	Point forecast	Lower 95% P.I.	Upper 95% P.I.
NEBS-Summer	9.2	4.0	3.5	3.1	4.0
		3.4	3.8	3.3	4.3
		2.7	4.1	3.5	4.8
		2.3	4.5	3.7	5.2
SEBS-Winter	9.7	4.0	3.3	2.9	3.7
		3.4	3.5	3.0	4.0
		2.7	3.8	3.1	4.4
		2.3	4.0	3.3	4.8
SEBS-Summer	9.7	4.0	3.7	3.2	4.1
		3.4	3.9	3.4	4.4
		2.7	4.3	3.7	4.9
		2.3	4.7	3.9	5.4
GOA-NSE-Summer	7.3	4.0	4.3	3.8	4.7
		3.4	4.6	4.1	5.1
		2.7	5.2	4.6	5.8
		2.3	5.7	5.0	6.4

[1] The $\delta^{15}N_{baseline}$ value within each stratum was the mean $\delta^{15}N$ value of copepods estimated here from results presented in Schell et al. (1998) and Kline (2009) and was assumed to approximate the $\delta^{15}N$ value of primary consumers at the base of the food web in each stratum.

[2] Uncertainty in $\Delta^{15}N$ was incorporated in this study by including four point estimates of $\Delta^{15}N$ obtained from the literature as estimates of Δn in Equation (3.4): 3.4‰ (Minagawa & Wada, 1984; Vander Zanden & Rasmussen, 2001; Post, 2002), 2.7‰ (Vanderklift & Ponsard, 2003; Dale et al., 2011), 2.3‰ (Hussey et al., 2010a) and 4.0‰ (McMeans et al., 2010).

Table 3.7: Trophic position determined from diet.
Standardized diet compositions (P_j ; Equation 3.5) and trophic position determined from diet (T_{PD}; Equation 3.6) for *S. pacificus* in the eastern North Pacific Ocean (4.26) (mean total length 201.5 cm) compared to T_{PD} of *S. pacificus* obtained from previous diet studies (4.25).

		T_{PD}						
		This study, eastern North Pacific Ocean					Previous studies, Pacific Ocean	
Species group [5]	Trophic level [5]	%M [1]	%R [2]	%N [3]	P_j(%)	T_{PD}	P_j (%)[4]	T_{PD}[4]
Teleosts	3.24	93.91	33.6	3.55	34.3	4.26	33.3	4.25
Cephalopods (squids, octopuses)	3.2	5.42	59.9	96.22	59.4		38.9	
Mollusks (excluding cephalopods)	2.1	0.68	0	0	0.0		5.6	
Decapod crustaceans (shrimps, crabs, prawns, lobsters)	2.52	0.02	0.3	0	0.3		5.6	
Other invertebrates (except mollusks, crustaceans, and zooplankton)	2.5	0	0	0	0.0		0	
Zooplankton (mainly euphausiids krill)	2.2	0	0	0	0.0		0	
Seabirds	3.87	0	0	0	0.0		0	
Marine reptiles (sea turtles and sea snakes)	2.4	0	0	0	0.0		0	
Marine mammals (cetaceans, pinnipeds, mustelids)	4.02	0	6.7	0	5.7		16.7	
Chondrichthyes (sharks, skates, rays, and chimaeras)	3.65	0	0.3	0	0.3		0	
Plants (marine plants and algae)	1	0	0	0	0.0		0	
Total		100.0	100.8	99.8	100.0		100.1	
N_i = number of stomachs with food		11	165	16	(245)		(13)	

[1] Diet items of *S. pacificus* expressed as per cent mass (%M) (Yang & Page, 1999).
[2] Diet items of *S. pacificus* expressed as a per cent index of relative importance (%R) (Sigler et al., 2006).
[3] Diet items of *S. pacificus* expressed as per cent number (%N) (Yano et al., 2007).
[4] P_j and T_{PD} of *S. pacificus* from previous studies (n = 6) in the Pacific Ocean were reproduced here from Cortés (1999); their Table 2; also see Cortés (1999) online supplemental material available at:www.flmnh.ufl.edu/fish/Sharks/references/diet.htm; accessed 1 June 2011.
[5] Prey categories and trophic levels used to calculate standardized diet compositions of sharks were reproduced here from Cortés (1999); their Table 1.

3.9. Appendix 3.A. Mean $\delta^{15}N$ of Aleutian Islands and eastern Bering Sea Taxa.

Mean $\delta^{15}N$ of taxa from the Aleutian Islands and eastern Bering Sea obtained from a scientific literature review.

Table 3.A.1: $\delta^{15}N$ by taxa from the Aleutian Islands and eastern Bering Sea.
Literature review of $\delta^{15}N$ values of taxa from the Aleutian Islands (AI) and eastern Bering Sea (EBS): mean ± S.E., minimum, maximum and sample size (*n*); summarized from the primary literature and compared to the mean $\delta^{15}N$ values of *Somniosus pacificus* from the north-west (NW-)EBS-Summer, south-east (SE-)EBS-Summer and SE-EBS-Winter in this study (see Figure 3.1). Taxonomic groups were subdivided based on differences in $\delta^{15}N$ values identified in the original publications. A brief description of each taxonomic subdivision is provided based on criteria from the original publication.

(Index) AI and EBS taxa	Description	$\delta^{15}N$ (‰)	S.E.	Min., Max.	*n*
Killer whale *Orcinus orca*					
(1) *O. orca* [1]	Eastern AI and GOA, offshore, adult	17.2	0.3		3
(2) *O. orca* [1]	Eastern AI, resident, adult	16.7	0.4		11
(3) *O. orca* [1]	Eastern AI, transient, adult	17.9	0.2		9
(4) *O. orca* [1]	Central AI, resident, adult	15.6	0.5		11
(5) *O. orca* [1]	Central AI, transient, adult	18.7	1.3		2
(6) *O. orca* [1]	AI, resident, juvenile	17.9			1
(7) *O. orca* [2]	Central AI, resident, mixed age	14.0	0.3		3
(8) *O. orca* [2]	Eastern AI, resident, mixed age	16.4	0.5		13
(9) *O. orca* [2]	Eastern AI, transient, mixed age	17.8	0.2		23
Pinnipeds					
(10) Steller sea lion *Eumetopias jubatus* [3]	EBS	*c.* 18.6		*c.* 16.4, 21.9	19
(11) Harbor seal *Phoca vitulina* [3]	EBS	*c.* 17.4		*c.* 14.4, 20.5	15
(12) Northern fur seal *Callorhinus ursinus* L. 1758 [3]	EBS	*c.* 16.4		*c.*15.5, 17.2	8
(13) *C. ursinus* [4]	EBS, Pribilof Islands	16.6	0.5		7
(14) *C. ursinus* [5]	EBS, St. Paul Island, July –August, female, adult	17.3	0.1		46
(15) *C. ursinus* [5]	EBS, St. George Island, July –August, female, adult	17.3	0.1		46
(16) *C. ursinus* [5]	EBS, St. Paul Island, July –August, male, juvenile	16.5	0.2		20
(17) *C. ursinus* [5]	EBS, St. Paul Island, July –August, male, juvenile	15.6	0.2		5
(18) *C. ursinus* [5]	EBS, St. Paul Island, July –August, male, juvenile	17.4	0.3		11
(19) *C. ursinus* [5]	EBS, St. George Island, July –August, male, juvenile	16.7	0.1		28
(20) *C. ursinus* [5]	EBS, St. Paul Island, November, female, adult	18.1	0.2		15
(21) *C. ursinus* [5]	EBS, St. George Island, November, female, adult	18.1	0.1		3
(22) *C. ursinus* [5]	EBS, St. Paul Island, July – August, nulliparous female	17.4	0.3		2

Table 3.A.1. Continued.

(Index) AI and EBS taxa	Description	$\delta^{15}N$ (‰)	S.E.	Min., Max.	*n*
Pacific sleeper shark *Somniosus pacificus*					
(23) *S. pacificus* [6]	Northwestern EBS in summer (NW-EBS-Summer)	13.7	0.1	11.6, 15.5	54
(24) *S. pacificus* [6]	South-eastern eastern Bering Sea in summer (SE-EBS-Summer)	13.7	0.2	11.3, 16.3	41
(25) *S. pacificus* [6]	South-eastern eastern Bering Sea in winter (SE-EBS-Winter)	12.7	0.1	11.1, 14.7	50
Humpback whale *Megaptera novaeangliae*					
(26) *M. novaeangliae* [7]	EBS	12.4	0.1	7.4, 15.7	122
(27) *M. novaeangliae* [7]	Eastern AI	12.1	0.2	9.1, 14.9	56
Fish (Teleostei) and squid (Teuthoidea)					
(28) Walleye pollock *Theragra chalcogramma* [5]	EBS, age 0, 3.2 (cm) mean L_s	10.8	0.1		10
(29) *T. chalcogramma* [5]	EBS, age 1-2, 14.6 (cm) mean L_s	12.7	0.2		10
(30) *T. chalcogramma* [5]	EBS, age 2-3, 24.4 (cm) mean L_s	15.2	0.2		5
(31) *T. chalcogramma* [5]	EBS, age 3-4, 29.9 (cm) mean L_s	16.3	0.3		4
(32) Eulachon *Thaleichthys pacificus* (Richardson 1836) [5]	EBS, medium, 19.2 (cm) mean L_s	14.0	0.2		10
(33) Pacific sand lance *Ammodytes hexapterus* Pallas 1814 [5]	EBS, large, 24.2 (cm) mean L_s	9.0	0.0		10
(34) Pacific herring *Clupea pallasii* Valenciennes 1847 [5]	EBS, small, 23.2 (cm) mean L_s	15.3	0.2		5
(35) *C. pallasii* [5]	EBS, large, 28.9 (cm) mean L_s	13.5	0.1		8
(36) Atka mackerel *Pleurogrammus monopterygius* (Pallas 1810) [5]	EBS, small, 23.8 (cm) mean L_s	9.9	0.2		5
(37) *P. monopterygius* [5]	EBS, large, 39.8 (cm) mean L_s	10.7	0.3		5
(38) Chum salmon *Oncorhynchus keta* (Walbaum 1792) [5]	EBS, medium, 46.0 (cm) mean L_s	10.5			1
(39) Squid *Gonatopsis borealis* Sasaki 1923 [5]	EBS, small, 7.7 (cm) mean L_{DM}	11.1	0.2		3
(40) Squid *Berryteuthis magister* [5]	EBS, small, 5.4 (cm) mean L_{DM}	11.4	0.2		3
(41) *B. magister* [5]	EBS, medium, 10.0 (cm) mean L_{DM}	11.4	0.2		9

Table 3.A.1. Continued.

(Index) AI and EBS taxa	Description	$\delta^{15}N$ (‰)	S.E.	Min., Max.	*n*
Weathervane scallop *Patinopecten caurinus*					
(42) *P. caurinus*[8]	EBS, 2005	10.7	0.1		10
(43) *P. caurinus*[8]	EBS, 2006	10.3	0.2		10
Zooplankton					
(44) Chaetognath (Composite)[9]	Eastern Bering (*c.* EB[10])	12.9	0.3		35
(45) Chaetognath (Composite)[9]	Central Bering (*c.* CB[10])	12.7	0.2		64
(46) Chaetognath (Composite)[9]	Western Bering (*c.* WB[10])	11.6	0.3		27
(47) Euphausiid (Composite)[9]	Eastern Bering (*c.* EB[10])	10.0	0.2		33
(48) Euphausiid (Composite)[9]	Central Bering (*c.* CB[10])	9.3	0.2		47
(49) Euphausiid (Composite)[9]	Western Bering (*c.* WB[10])	9.1	0.2		32
(50) Copepod (Composite)[9]	Eastern Bering (*c.* EB[10])	9.8	0.2		64
(51) Copepod (Composite)[9]	Central Bering (*c.* CB[10])	9.6	0.2		132
(52) Copepod (Composite)[9]	Western Bering (*c.* WB[10])	8.7	0.2		64

L_S, standard length; L_{DM}, dorsal mantle length.
[1] Lipid extracted blubber (Herman et al., 2005);
[2] lipid extracted epidermis (Krahn et al., 2007);
[3] lipid extracted and demineralized bone collagen (Weighted average of data by region from Hirons et al., 2001);
[4] lipid extracted skeletal muscle—including deceased animals (Hobson et al., 1997);
[5] skin (pinniped) and homogenized whole (fish and squid) (Kurle & Worthy, 2001);
[6] white muscle (this study, Table 3.1);
[7] lipid extracted skin (Witteveen et al., 2009);
[8] adductor muscle (scallop) (Andrews, 2010);
[9] demineralized composite (Schell et al., 1998);
[10] approximate locations for the eastern Bering (~EB), central Bering (~CB), and western Bering (~WB) regions from Schell et al. (1998) are identified in Figure 3.1.

3.10. Appendix 3.B. Mean $\delta^{15}N$ of Gulf of Alaska and Southeast Alaska Taxa.

Mean $\delta^{15}N$ of taxa from the Gulf of Alaska and Southeast Alaska obtained from a scientific literature review.

Table 3.B.1: $\delta^{15}N$ by taxa from the Gulf of Alaska and Southeast Alaska.
Literature review of $\delta^{15}N$ values of taxa from the Gulf of Alaska (GOA) and Southeast Alaska: mean ± S.E., minimum, maximum and sample size (*n*); summarized from the primary literature and compared to the mean $\delta^{15}N$ values of *Somniosus pacificus* from the GOA-Summer and NSE-Summer in this study (see Figure 3.1). Taxonomic groups were subdivided based on differences in $\delta^{15}N$ values identified in the original publications. A brief description of each taxonomic subdivision is provided based on criteria from the original publication.

(Index) GOA and Southeast Alaska taxa	Description	$\delta^{15}N$ (‰)	S.E.	Min., Max.	*n*
Killer whale *Orcinus orca*					
(1) *O. orca* [1]	Eastern AI and GOA, offshore, adult	17.2	0.3		3
(2) *O. orca* [1]	GOA, resident, adult	17.2	0.3		8
(3) *O. orca* [1]	GOA, transient, adult	17.3	0.3		2
(4) *O. orca* [1]	GOA, resident, sub adult	21.0			1
(5) *O. orca* [1]	GOA, transient, yearling	19.8			1
(6) *O. orca* [2]	Kenai Fjords and Southeast Alaska, offshore, mixed ages	17.0	0.0		5
(7) *O. orca* [2]	GOA, resident, mixed ages	17.6	0.2		6
Pinnipeds					
(8) Harbor seal *Phoca vitulina* [3]	GOA	*c.* 17.1		*c.* 14.7, 20.2	48
(9) Steller sea lion *Eumetopias jubatus* [3]	GOA	*c.* 18.3		*c.* 17.0, 20.4	12
(10) Northern fur seal *Callorhinus ursinus* L. 1758 [3]	GOA	*c.* 18.4		*c.* 16.7, 20.1	5
(11) *P. vitulina* [4]	GOA, Copper River Delta	18.6	0.3		9
(12) *E. jubatus* [4]	GOA, Copper River Delta	17.5	0.2		13
Pacific sleeper shark *Somniosus pacificus*					
(13) *S. pacificus* [5]	GOA in summer (GOA-summer)	15.3	0.5	12.8, 18.6	11
(14) *S. pacificus* [5]	Northern Southeast Alaska in summer (NSE-summer)	14.8	0.2	14.2, 15.3	4
Spiny dogfish *Squalus acanthias*					
(15) *S. acanthias* [6]	GOA, Kodiak	13.2	0.1	11.7, 15.6	86
(16) *S. acanthias* [6]	GOA, Cook Inlet	13.8	0.1	11.8, 15.0	32
(17) *S. acanthias* [6]	GOA, Prince William Sound	12.9	0.1	10.8, 14.0	45
(18) *S. acanthias* [6]	GOA, north-eastern	12.6	0.1	10.8, 14.1	45
(19) *S. acanthias* [6]	GOA, Yakutat	12.7	0.1	10.8, 14.2	126
(20) *S. acanthias* [6]	GOA, Southeast	13.4	0.1	11.0, 14.7	76
Humpback whale *Megaptera novaeangliae*					
(21) *M. novaeangliae* [7]	Western GOA	13.1	0.1	11.3, 15.3	104
(22) *M. novaeangliae* [7]	Northern GOA	13.6	0.1	8.8, 16.2	199
(23) *M. novaeangliae* [7]	Southeast Alaska	12.7	0.1	7.8, 15.1	227

Table 3.B.1. Continued.

(Index) GOA and Southeast Alaska taxa	Description	$\delta^{15}N$ (‰)	S.E.	Min., Max.	*n*
Fish (Teleostei) and Squid (Teuthoidea)					
(24) Walleye pollock *Theragra chalcogramma* [8]	CGOA[10] < L_T at 50% maturity	13.0	0.1	11.2, 16.1	148
(25) *T. chalcogramma* [8]	CGOA[10] > L_T at 50% maturity	14.1	0.1	11.5, 18.2	81
(26) Pacific cod *Gadus macrocephalus* Tilesius 1810 [8]	CGOA[10] < L_T at 50% maturity	15.0	0.1	12.9, 16.6	68
(27) *G. macrocephalus* [8]	CGOA[10] > L_T at 50% maturity	15.9	0.1	14.3, 17.3	78
(28) Arrowtooth flounder *Atheresthes stomias* (Jordan & Gilbert 1880) [8]	CGOA[10] < L_T at 50% maturity	14.1	0.1	12.4, 15.9	47
(29) *A. stomias* [8]	CGOA[10] > L_T at 50% maturity	14.6	0.1	13.1, 16.4	54
(30) Pacific halibut *Hippoglossus stenolepis* Schmidt 1904 [8]	CGOA[10] < 50 cm L_T	14.3	0.1	13.6, 15.2	25
(31) *H. stenolepis* [8]	CGOA[10] > 50 cm L_T	14.7	0.1	12.8, 17.1	44
(32) Eulachon *Thaleichthys pacificus* [8]	CGOA[10] (mean ± S.D.) 17.6 ± 1.9 L_T	13.1	0.1	11.6, 14.8	41
(33) Squid unidentified (Cephalopoda) [4]	GOA, large	16.7			1
(34) *T. chalcogramma* [4]	GOA, large	15.7	0.7		2
(35) Atka mackerel *Pleurogrammus monopterygius* [4]	GOA, large	11.7	0.2		6
(36) Capelin *Mallotus villosus* (Müller 1776) [4]	GOA, small	12.4	0.1		13
(37) *P. monopterygius* [4]	GOA, small	12.2	0.2		3
(38) Prowfish *Zaprora silenus* Jordan 1896 [4]	GOA, small	12.2	0.2		12
(39) Rockfish (Scorpaenidae) [4]	GOA, small	12.0	0.0		2
(40) Pacific Sand Lance *Ammodytes hexapterus* [4]	GOA, small	11.9	0.1		8
(41) Mackerel (Unidentified) [4]	GOA, small	11.9	0.7		5
(42) *G. macrocephalus* [4]	GOA, small	11.4	0.2		19
(43) *T. chalcogramma* [4]	GOA, small	10.9	0.2		24
(44) Squid unidentified (Cephalopoda) [4]	GOA, small	9.6	0.5		4

Table 3.B.1. Continued.

(Index) GOA and Southeast Alaska taxa	Description	$\delta^{15}N$ (‰)	S.E.	Min., Max.	*n*
Weathervane scallop *Patinopecten caurinus*					
(45) *P. caurinus* [6]	WGOA[10] Shumagin Island, 2006	8.9	0.1		10
(46) *P. caurinus* [6]	WGOA[10] north of Shumagin Island, 2006	8.8	0.1		10
(47) *P. caurinus* [6]	CGOA[10] South of Cape Douglas, 2006	8.6	0.1		10
(48) *P. caurinus* [6]	CGOA[10] Northeast Kodiak, 2006	8.6	0.2		10
(49) *P. caurinus* [6]	EGOA[10] Southwest of Kayak Island, 2006	8.3	0.1		10
(50) *P. caurinus* [6]	EGOA[10] Northwest of Icy Bay, 2006	8.3	0.1		10
(51) *P. caurinus* [6]	EGOA[10] South of Icy Bay, 2005	8.9	0.0		10
(52) *P. caurinus* [6]	EGOA[10] South of Yakutat Bay, 2006	8.7	0.1		10
(53) *P. caurinus* [6]	EGOA[10] North of Lituya Bay, 2006	9.3	0.1		10
Other invertebrates					
(54) Polychaete (Annelida) [4]	GOA	11.7			1
Zooplankton					
(55) Euphausiid (Composite) [4]	GOA	11.2	0.5		9
(56) Copepod *Neocalanus cristatus*[9]	GOA Seward Line[11] Inner shelf stations, 1998–2004	7.8	0.1		354
(57) *N. cristatus* [9]	GOA Seward Line[11] outer shelf stations, 1998–2004	7.2	0.1		505
(58) *N. cristatus* [9]	GOA Seward Line[11] slope stations, 1998–2004	6.7	0.1		434
(59) *N. cristatus* [9]	GOA Seward Line[11] all stations combined, 1995–2004	7.3	0.1		1,588
(60) Copepod (Composite) [4]	GOA	8.5			1

L_T, total length.
[1] Lipid extracted blubber (Herman *et al.,* 2005);
[2] lipid extracted epidermis (Krahn *et al.,* 2007);
[3] lipid extracted and demineralized bone collagen (Weighted average of data by region; Hirons *et al*., 2001);
[4] lipid extracted skeletal muscle (pinnipeds—including deceased animals), lipid extracted muscle (fish and squid), and demineralized composite (invertebrates) (Hobson *et al.*, 1997);
[5] white muscle (this study, Table 3.1);
[6] white muscle (Andrews, 2010);
[7] lipid extracted skin (Witteveen *et al.*, 2009);
[8] homogenized whole (Marsh, 2010);
[9] individual terminal-feeding copepodite-V stage *N. cristatus* (Kline, 2009);
[10] U.S. National Marine Fisheries Service (NMFS) regulatory areas for the western Gulf of Alaska (WGOA), central Gulf of Alaska (CGOA) and Gulf of Alaska (EGOA) are identified in Figure 3.1;
[11] the approximate location of the GOA Seward Line is identified in Figure 3.1.

4. Chapter 4 Pacific Sleeper Shark Habitat Use[6]

4.1. Abstract

This study characterized Pacific sleeper shark vertical movement patterns in the Gulf of Alaska, which are important for improving commercial fisheries bycatch estimates and identifying potential ecological interactions with an endangered subpopulation of Steller sea lions. A structural model relating vertical movements to environmental data was combined with an iterative time series error correction procedure. A strong autoregressive process at a lag of one hourly time step was identified in the average hourly depth profile obtained from one shark during June – November, 2002. None of the environmental factors explored were included in the most parsimonious model. However, the iterative approach required a structural explanatory variable (in this case month of the year) to achieve stationary residuals for time series analysis. This indicated that Pacific sleeper shark movement behavior over relatively longer time periods (in this case one month) could be explained largely by a change in average depth over time. Our results demonstrate that statistical inference about habitat utilization can be drawn from an entire time series depth profile stored on electronic archival tags. Specifically, we found a simple autoregressive relationship governing short-term movements throughout the time series, which included substantial variation in longer time period movement patterns.

[6] Courtney, D. L., and K. R. Criddle. In Prep. Characterizing habitat use of Pacific sleeper sharks in the Gulf of Alaska using time-series analysis of archived electronic tag and nearby environmental data.

4.2. Introduction

Understanding Pacific sleeper shark vertical movement patterns in the Gulf of Alaska is important for characterizing their potential interactions with commercial fishery operations (Courtney et al. 2016). It could also be used to discriminate among two alternative hypotheses proposed for their ecological interactions with an endangered Steller sea lion subpopulation in the eastern North Pacific Ocean west of 144° W (Figure 1): 1) direct effects of predation (Horning and Mellish 2014), and 2) indirect effects of antipredator behavior in response to predation risk (Frid et al. 2009).

The Pacific sleeper shark is commonly encountered at bottom depths of 200 to 700 m as well as pelagic depths of 100 to 200 m associated with the continental shelfs and upper continental slopes of the high-latitude North Pacific Ocean and the Bering Sea (Compagno 1984; Ebert et al. 1987; Orlov 1999; Orlov and Moiseev 1999a, b; Mecklenburg et al. 2002; Yano et al. 2004, 2007; Ebert and Winton 2010; Orlov and Baitalyuk 2014). In the Gulf of Alaska, Pacific sleeper sharks are captured incidentally in commercial fisheries for demersal fish species. The incidentally captured sharks are discarded and assumed to die, which is a potential conservation concern (Courtney et al. 2006; Tribuzio et al. 2011). Pacific sleeper sharks are assumed to be long-lived and to have slow growth rates based on their morphological similarity to the Greenland shark, which may live for hundreds of years (Nielsen et al. 2016). Given their assumed life history and the range of uncertainty in their bycatch estimates, Pacific sleeper shark incidental exploitation rates in the Gulf of Alaska are unsustainable under some simulated conditions (Courtney et al. 2016).

Pacific sleeper sharks are large predators capable of consuming fast swimming prey including large teleosts and marine mammals, and their diet varies ontogenetically as well as by season, geographic region, and capture depth, likely in response to prey availability (Bright 1959; Gotshall and Jow 1965; Ebert et al. 1987; Orlov 1999; Orlov and Moiseev 1999a, 1999b; Yang and Page 1999; Smith and Baco 2003; Wang and Yang 2004; Sigler et al. 2006; Yano et al. 2007). Pacific sleeper sharks have also been implicated as predators of an endangered Steller sea lion subpopulation in the eastern North Pacific Ocean west of 144° W (Horning and Mellish 2014). However, a directed diet study of Pacific sleeper sharks sampled near four large rookeries of the endangered Steller sea lion subpopulation concluded that although the species ranges overlapped, predation on Steller sea lions was unlikely, at least near rookeries where pups first enter the water (August) or occur during weaning (May) (Sigler et al. 2006; Hulbert et al. 2006; Figure 4.1). Instead, diet was dominated by cephalopods in May and teleosts in August (Sigler et al. 2006). Marine mammal tissues were identified in 15% of stomachs examined, but no Steller sea lion tissue was detected. Marine mammal tissue was primarily cetacean (probably scavenged), but also included harbor seal (possibly consumed alive) (Sigler et al. 2006). Stable isotope analysis of Pacific

sleeper shark muscle tissue from the Gulf of Alaska and the eastern Bering Sea was also consistent with a variable diet, possibly including pinnipeds, but also including a large proportion of relatively lower trophic level prey such as fishes, squid, elasmobranchs, or filter feeding whales (Courtney and Foy 2012).

However, even when direct predation events are rare, long-lived species including marine mammals are predicted to engage in antipredator behavior in response to predation risk (Heithaus et al. 2008). For example, in Prince William Sound, both harbor seals and Steller sea lions are predicted to change their foraging behavior in response to predation risk from large predators including Pacific sleeper sharks and Killer whales, and to reverse their foraging preferences in response to simulated removals of large predators, leading to increased seal predation on some teleost taxa and relaxed predation on others (Frid et al. 2007, 2008, 2009; Heithaus et al. 2010).

In order to characterize habitat utilization of Pacific sleeper sharks from their vertical movement patterns, we re-analyzed archived electronic tag time series data previously obtained from the Gulf of Alaska (Hulbert et al. 2006). Three types vertical movement behavior have been described for Pacific sleeper sharks in the Gulf of Alaska based on observed patterns in the time-series depth profile recorded from electronic archival tags (Hulbert et al. 2006). These include a diel vertical movement pattern, a systematic vertical oscillation movement pattern, and an irregular vertical movement pattern (Figures 4.S.A.1–4.S.A.3). We hypothesized that the complex patterns previously described in the depth profile data could be modeled efficiently as simple time series processes (Supplement 4.A; Figures 4.S.A.1–4.S.A.3). We hypothesized that a long memory process would be consistent with expected shark vertical movement behavior because patterns in shark depth profiles over time are likely to respond predictably to cues obtained from their environment. For example shark depth profiles may respond predictably to changes in prey availability at hourly, daily, weekly, or seasonal time scales, which would produce patterns in the observed time series of depth data consistent with a long memory time series process. In order to test our hypothesis, we postulated that tide stage (a surrogate for current strength and direction), light (daylight, twilight, moonlight, dark), and season (month of the year) would influence depth occupied at long time scales (days to months) while simple autoregressive processes would characterize movement at finer time scales (hours).

Our approach was to fit and then remove autocorrelation in the depth profile obtained from archived electronic tag data with a time series model, iteratively, within a structural model developed from independent environmental data. The structural model was implemented as a first-pass filter in order to test our hypothesis that a long memory process exists in the time series data and that it can be explained by fits to environmental data collected for a nearby location. An advantage of this approach is that statistical inference about model selection can be drawn from the entire depth profile, and that once fit,

the structural model can be used to predict habitat utilization while accounting for autocorrelation within the depth profile time series.

4.3. Materials and Methods

4.3.1. Data Sources

As a proof of concept, tag depth, temperature, and light intensity observations were obtained, at one minute intervals, from a previously satellite tagged (Wildlife Computers-PSAT) Pacific sleeper shark during June 1, 2002– November 30, 2002 (Hulbert et al. 2006; their tag #21). We chose this tagged shark because its depth profile included all of the complex patterns previously described in Pacific sleeper shark depth profiles (Supplement 4.A; Figures 4.S.A.1, 4.S.A.2, and 4.S.A.3). The tag was released offshore of Cape Hinchinbrook, Hinchinbrook Island, Alaska (Figure 4.1). The tag was physically recovered, but the tag never transmitted and a recovery location was not determined exactly (Hulbert et al. 2006). Most (76%) of the tags released on Pacific sleeper sharks by Hulbert et al. (2006) were recovered within 100 km of their release site up to one year after release. Consequently the habitat occupied by the Pacific sleeper shark analyzed in this study potentially ranged from the deep marine waters of Prince William Sound (> 200 m), to the continental shelf (~200 m), continental shelf gullies (~300 m), and the shelf break (~200 m to abyssal depths) (Figure S4).

Environmental data were obtained for the same period (June 1, 2002– November 30, 2002) at the approximate location where the tagged shark was released (Cape Hinchinbrook, Hinchinbrook Island, Alaska, 60.2383° N, 146.6467° W). Predicted tide depth each minute along with predicted times of high and low tide each day were obtained from the University of South Carolina Biological Sciences tide predictor (Pentcheff 2016; e.g., Coutré et al. 2017). Times of nautical dawn, sunrise, sunset, nautical dusk, moonrise, and moonset each day were obtained from the archives of the Naval Observatory (U.S. Naval Observatory 2016, e.g., Coutré et al. 2017). Phase of the moon and percent of the moon illuminated at midnight local time each day were obtained from the archives of the Naval Observatory (U.S. Naval Observatory 2016).

4.3.2. Data Transformations

All data were converted to Alaska Standard Time (AKST) calculated as Greenwich Mean Time (GMT) – 9 hr. Average tag depth, temperature, and light were computed each hour. Average tag depth, and tag temperature were transformed with the natural log (*Ln-Tag-Depth*, and *Ln-Tag-Temp*) to reduce the effect of an observed increase in variability over time. Our primary goal in these analyses was to investigate patterns in habitat utilization associated with changes in depth. Consequently, *Ln-Tag-Depth*

was included as the dependent variable. Because of concerns over a lack of independence and possible collinearity, *Ln-Tag-Temp* was not investigated as an explanatory variable. Instead, *Ln-Tag-Temp* was included in diagnostic tests as described below to evaluate unexplained autocorrelation in the final model residuals. *Tag-Light* was not included in these analyses because the light readings may have been below detection levels.

4.3.3. Candidate Explanatory Variables

Tag data were assigned to one of four tidal stages (*Tide-Stage*): High-slack (hour in which high tide occurred and the hour after), Low-slack (hour in which low tide occurred and the hour after), Ebb (hours between high-slack and low-slack), or Flood (hours between low-slack and high-slack). Tag data were assigned to one of four light stages (*Light-Stage*): Daylight (sunrise to sunset), Twilight (sunset to nautical dusk or nautical dawn to sunrise), Moonlight (nautical dusk to nautical dawn and moon above the horizon with at least 50% of the moon illuminated), or Dark (nautical dusk to nautical dawn and moon below or above the horizon with less than 50% of the moon illuminated). Tag data were assigned to one of two tide strength stages associated with a lunar cycle (*Tide-Strength*): Spring tides or Neap tides. Spring tides were defined as the maximum semi-diurnal tidal ranges associated with either a New Moon or a Full Moon and approximated here as one-hour periods with less than 25 percent of the moon illuminated or more than 75 percent of the moon illuminated. Neap tides were defined as the minimum semi-diurnal tidal ranges associated with either a First Quarter Moon or a Last Quarter Moon and approximated here as one hour time periods with at least 25 percent but not more than 75 percent of the moon illuminated.

Light-Stage was investigated because previous analyses of this tag data indicated that the shark sometimes occupied shallower water at night compared to daylight (Hulbert et al. 2006; Supplement 4.A). *Tide-Strength* and *Tide-Stage* were investigated as proxies for current speed in the coastal fjords and continental shelf gullies where Pacific sleeper sharks occur (Hulbert et al. 2006; Courtney and Sigler 2007). Large bodied sleeper sharks have very slow swimming speeds for their body size relative to other species (Watanabe et al. 2012). Consequently, current speed may affect both prey distribution and sleeper shark movement rates (Supplement 4.A).

Environmental data with significant linear correlations to *Ln-Tag-Depth* were included as potential explanatory variables in the structural models (SMs). *Light-Stage* was negatively correlated with *Ln-Tag-Depth* ($r = -0.38$, $p < 0.01$; Supplement 4.A) and *Tide-Strength* was positively correlated with *Ln-Tag-Depth* ($r = 0.16$, $p < 0.01$; Supplement 4.A). *Tide-Stage* was not significantly correlated with *Ln-Tag-Depth* ($r = 0.02$, $p > 0.01$; Supplement 4.A) and was excluded as a potential explanatory variable.

However, *Tide-Stage*, along with *Ln-Tag-Temp*, was included in diagnostic tests, as described below, to evaluate unexplained autocorrelation in final model residuals.

4.3.4. Elimination of Non-stationarity

Preliminary residual analyses for models of *Ln-Tag-Depth* indicated statistically significant non-stationarity. To correct for this, tag depth data were assigned to one of six monthly time stages (*Date-Month*): June, July, August, September, October, or November. The explanatory variable *Date-Month* was then included as a categorical variable in all model runs evaluated with *Ln-Tag-Depth* as a response variable.

4.3.5. Model Formulation

A generalization of the Cochrane and Orcutt (1949) iterative error correction procedure was used to address complex serial correlation observed in preliminary analyses of the tag data. Examples of this error correction procedure using Aoki (1990) State Space Time Series methods are available from Criddle and Havenner (1991), Criddle and Herrmann (2008), and Steiner et al. (2011). An example using vector autoregression methods is available from Yasumiishi et al. (2016). As a continuation of our proof of concept, a simple univariate approach was used here to specify lagged and contemporaneous relationships among multiple time series observations simultaneously from a single depth series profile (Appendix A).

In our error correction procedure, residuals of a candidate structural model, SM, were modelled in tandem with a candidate time series model (TSM) within the iterative approach (SM+TSM). In step-1, each candidate SM was fit to the observed tag data and the residuals from the SM were subsequently fit with a candidate TSM. In step-2 the TSM fit to the residuals was subtracted from the observed tag data, the SM was re-fit to the error-corrected data, and the new error corrected residuals (raw response variable data versus the updated SM) were re-fit with the TSM. The process was repeated for 100 iterations and evaluated for convergence based on agreement in the sum of all estimated SM + TSM coefficients to within four significant digits.

4.3.6. Candidate SM Models

Simple linear regression with ordinary least squares was implemented in R statistical software (CRAN.R base stats package function "lm") for the SM. Thirteen SMs, were used, which included *Ln-Tag-Depth* as the response variable and *Date-Month*, *Light-Stage*, and *Tide-Strength* as explanatory variables along with their interactions (Table 4.1).

4.3.7. Candidate TSM Models

An autoregressive (AR) time series model was fit to residuals from the SM by ordinary least squares in R statistical software (CRAN.R base stats package function "ar.ols"). Preliminary analyses revealed a strong AR relationship in the lagged residuals of SMs that included *Ln-Tag-Depth* as the response variable. Values of residuals in the current period were explained by the values of the residuals in previous periods at lagged time steps of 1, 2, and 3, as well as a weaker AR relationship observed in the SM residuals at longer lags of up to ~30 time steps. Consequently, an AR process was implemented for the TSM with lags of 1, 2, and 3, along with a lag length selected to minimize the Akaike information criterion (AIC; Shumway and Stoffer 2015), and each SM was evaluated with four TSMs: AR(1), AR(2), AR(3), and AR(AIC) (Table 4.1).

4.3.8. Model Validation

Time series analysis with AR models requires both trend and level stationarity in the times series data (e.g., Chatfield 2004). Trend stationarity of SM residuals (the TSM dependent variable) was assumed because the residuals resulted from a structural model. Level stationarity of SM residuals was evaluated with a KPSS-test (Kwiatkowski et al. 1992) implemented in the CRAN.R package "urca", function ur.kpss (TS, type="mu", lags='long'; e.g., Pfaff 2006, 2008).

Goodness-of-fit of the converged TSM model was evaluated with a Henriksson–Merton turning point test (Henriksson and Merton 1981) in order to evaluate the ability to accurately predict a change in direction from increasing depth to decreasing depth, or vice versa. Naik and Leuthold's ratio of accurate turning points (NL-TP) was also evaluated for the TSM component at the converged parameter estimates in order to provide an ordinal ranking of overall relative TSM model performance (Naik and Leuthold 1986; Criddle 2007).

Goodness of fit for a converged candidate SM + TSM was determined from the root mean squared error (RMSE), the coefficient of determination (R^2), and an F-statistic (F) obtained from combined model residuals. The coefficient of determination, R^2, for the combined SM + TSM model represents the percentage of the observed variation in *Ln-Tag-Depth* explained by the combined model fit, and for ordinary least squares regression ranges from zero (model fit no more accurate than the mean of the observations) to one (model fit exactly equal the observations) (e.g., Criddle 2007). The statistical significance for the combined SM + TSM model was calculated here with an F-statistic as $F = (R^2/(k + l))/((1 - R^2)/(\text{d.f.}))$, where $k + l$ is the total number of explanatory and lagged variables, respectively, in the combined (SM + TSM) model and d.f. is the degrees of freedom of the combined model, as defined in Appendix 4.A.

Normality of the combined SM + TSM model residuals at the converged parameter estimates was tested with a Lilliefors test. The combined SM + TSM model residuals were evaluated for randomness over time with a Wald-Wolfowitz runs test (CRAN.R package "randtests" Caeiro and Mateus 2014; e.g., Carvalho et al. 2017). Residuals were visually inspected for non-normality (qqnorm plot) and evaluated for trends and unequal variance over time and relative to model fit (e.g., Criddle 2007). The autocorrelation function (ACF) and partial autocorrelation function (PACF) of the combined SM + TSM model residuals were evaluated as a diagnostic for significant unexplained autocorrelation in the residuals (Shumway and Stoffer 2015; e.g., Pfaff 2008). The combined model fit along with *Tide-Stage*, and *Ln-Tag-Temp* were evaluated individually in a cross correlation function (CCF; Shumway and Stoffer 2015) with the combined SM + TSM model residuals as a diagnostic to evaluate unexplained autocorrelation in the residuals.

Substantial uncertainty was identified in some SM coefficient estimates (CV > 0.5) which included *Ln-Tag-Depth* as the response variable. SM coefficient CVs > 0.5 were interpreted here as an indication of possible model misspecification and excluded from further analysis. In contrast, TSM coefficient CVs > 0.5 for AR(AIC) were allowed because the structure of the AR model necessarily includes lower order AR processes if higher order processes are significant.

4.3.9. Model Selection

Converged models, which met the model validation criteria described above, were evaluated for model selection. The combined SM + TSM model fit was evaluated with the AIC with bias correction (AICc) (Burnham and Anderson 2002; Anderson and Burnham 2002). AICc differences (Δ_i) (Burnham and Anderson 2002; Burnham et al. 2011) were used to quantify the relative strength of evidence for each candidate combined model compared to the best approximating model in the model set (smallest AIC for the given data).

The AICc was calculated here as AICc = log[RSS/(n – l)]+[(n – l + P)/(n – l – P – 2)] following Shumway and Stoffer 2015 (their Equation 2.19 p. 54-55), where $P = (k + l + 2)$ is the total number of explanatory and lagged variables, $k + l$, in the combined (SM + TSM) model plus two intercepts. For ordinary least squares regression, the log likelihood, log(L) is equivalent to ($-n$/2)log(RSS/n) where RSS denotes the residual fitted sum of squares from the fitted model; the AIC, which equals –2Log(L) + 2k, is then equal to (n)log(RSS/n) + 2k and the bias corrected AIC, AICc, is then equal to (n)log(RSS/n) + 2k + (2k(k + 1))/(n – k – 1) (Burnham et al. 2011). Additionally, for ordinary least squares, the number of estimable parameters, k, includes the estimated model coefficients, the intercept, and the residual variance (Burnham and Anderson 2002; Anderson and Burnham 2002).

For each model in a set i, the AICc difference, Δ_i, was calculated as $AICc_i - AICc_{min}$. As a rule of thumb, models within the set with Δ_i values between 1 and 2 are considered to be indistinguishable from the best approximating model for the given data; models with Δ_i values between 2 and 7 have some support and inference should be drawn based on all models in the set (for example based on model likelihoods, probabilities, and evidence ratios, as discussed below); and models with Δ_i values greater than about 14 are implausible relative to the best approximating model for the given data (Burnham et al. 2011).

4.3.10. Akaike Weights

The relative maximum likelihood of each model in the model set being the best approximating model in the set given the data was calculated as $L_i = \exp((-1/2)\ \Delta_i)$. The probability of each model being the best approximating model in the set given the data was calculated as the Akaike weight, $w_i = L_i \Big/ \sum_i L_i$ (Burnham et al. 2011).

A table showing the combined model (SM + TSM) number of explanatory and lagged variables, $k + l$, the value of information criterion, AICc, the AICc differences Δ_i, the value of relative maximum likelihood, L_i, and the Akaike weight, w_i, was provided for each model evaluated within the reduced model set (Anderson and Burnham 2002). The weight of evidence for each model in the set was calculated from the ratios of the Akaike weights ($\exp(\Delta i)$, Burnham and Anderson 2002, their p 77).

All analyses were carried out using the R language for statistical computing version 3.2.0. (R Core Team, 2015). Use of additional packages is identified by a cited CRAN.R package library or the publication in which the package function is defined.

4.4. Results

4.4.1. Model Validation

All combined model (SM + TSM) combinations converged within 100 iterations. However, only sixteen of the SM + TSM combinations resulted in SM coefficient estimates with all CVs ≤ 0.5 (Tables 4.2 and 4.3). The results from this subset of sixteen models are summarized below. However, the results obtained from the subset models are representative of all candidate SM + TSM combinations examined.

All sixteen of the candidate SM + TSM combinations resulted in stationary SM residuals (KPSS-test P-value > 0.10; Table 4.3). However, model residuals were neither normally distributed (Lilliefors-test P-value < 0.001) nor randomly distributed over time (Wald-Wolfowitz "runs" test P -value < 0.001)

(Table 4.3). In addition, the ratio of accurate turning point predictions was very low (NL-TP Ratio accurate < 0.23; Table 4.3).

In contrast, the goodness-of-fit obtained from the subset of candidate SM + TSM combinations was generally very high ($R^2 > 0.79$) and statistically significant (F-stat P -value < 0.001) (Table 4. 4). Similarly, each TSM obtained from the subset of candidate SM + TSM combinations was able to predict turning points in the SM residual time series better than those that would be obtained at random (HM-test P -value < 0.001 Table 4.4 and Figure 4.S.A.10).

4.4.2. Model Selection

Values for the AICc Δ_i for all candidate SM + TSM combinations were less than two, indicating that there was no evidence to identify the best approximating model (Table 4.5). There was also very little support for the best model based on the relative weight of evidence for each model. The selected best model SM.1 + TSM.4 had Akaike weight of only 0.054, i.e., a probability of 0.05 of being the best model. The evidence ratio for the best model versus the worst model, 1.07, was also very low and indicated that the best model was only about 1.1 times as likely as the worst model. Consequently, results from the most parsimonious model (SM.1 + TSM.1) were presented below.

4.4.3. Model Fit

Analysis of model residuals from the combined model (SM.1 + TSM.1) fit (Figure 4.2) indicated periods of increasing variability beginning in September, and a trend for positive residuals at shallower depths and negative residuals at deeper depths. Plots of the response variable (*Ln-Tag-Depth*) after implementation of the error correction procedure (Figure 4.3) revealed a structural change in the response variable after about 2,000 hours (September), followed by periods of increasing variability.

Analysis of the structural model, SM.1, residuals before implementation of the error correction procedure (Figure 4.4) indicated a slow decay of the autocorrelation function, ACF, along with a rapid decay of the partial autocorrelation function, PACF, which was diagnostic for a strong (PACF > 0.8) positive autoregressive process at a lag of 1 hour and relatively weaker (PACF < 0.2) positive AR processes at lags 2 and 3 hours. There was also some indication of relatively weaker (PACF << 0.2) positive AR processes at lags of between about 10-24 hours. In contrast, analysis of the combined model, SM.1 + TSM.1, residuals after implementation of the error correction procedure (Figure 4.5) indicated a rapid decay of the autocorrelation function (ACF), which was diagnostic for negligible autocorrelation remaining in the residuals.

Analysis of the structural model, SM.1, residual autocorrelations at lagged periods of 1, 2, 3, and 4 hours (Figure 4.6) identified strong lagged autocorrelation patterns before implementation of the error

correction procedure and the absence of lagged autocorrelation patterns after error correction. Analysis of the CCF of lagged residuals of the combined model, SM.1 + TSM.1, did not indicate strong correlations with lagged *Tide-Stage* at lags of up to 720 hrs (~1 month; CCF within stippled lines; Figure 4.7, upper panel). In contrast, the CCF of lagged residuals of the combined model, SM.1 + TSM.1, identified significant positive correlations with lagged model fit at lags up to about 200 hours (~ 1 week; CCF outside stippled lines; Figure 4.7, middle panel). This result indicated that an important un-modelled process in the residuals was correlated with model fit at lags of up to 1 week. Similarly, the CCF of lagged residuals identified significant negative correlations with lagged *Ln-Tag-Temp* at lags up to about 200 hours (~ 1 week; Figure 4.7, lower panel). This result indicated that the same (or similar) un-modelled process in the residuals was also correlated with the tag temperature. Additionally, the CCF analysis identified that the un-modelled process in the residuals was strongly correlated with both model fit and *Ln-Tag-Temp* at lags of up to 30 hrs (Figure 4.8).

The CCF analysis results suggest that including either *Tide-Stage* or *Ln-Tag-Temp* in the combined SM.1 + TSM.1 fit to *Ln-Tag-Depth* would probably not have improved the combined model fit to the observed long memory process in the residuals. *Tide-Stage* was not significantly correlated with the residuals at any lag, and both *Ln-Tag-Temp* and the model fit showed a similar lagged relationship to the model residuals. However, the CCF analysis results suggest that there were two important unmodeled long memory processes remaining in the residuals of the combined SM.1 + TSM.1 model: the first at lags of up to about 1 day and the second at lags up to about 1 week.

4.5. Discussion

Implementation of the iterative error correction procedure identified a strong AR(1) process in the response variable (*Ln-Tag-Depth*) (Figure 4.4) in the most parsimonious combined SM.1 + TSM.1 model (Table 4.5). This result indicated that the vertical movement patterns of this Pacific sleeper shark over relatively short time periods, defined here as the average depth each hour, could be explained largely by a deterministic time series process based on the sharks' average depth in the previous hour. This result is consistent with the extremely slow swimming speed (relative to body size) documented for large bodied sleeper sharks (Watanabe et al. 2012).

A structural explanatory variable (in this case *Date-Month*) was required as a first pass filter in order to achieve stationary residuals within all of the combined SM + TSM models examined. This result indicates that the vertical movement patterns of this Pacific sleeper over longer periods (in this case one month) could be explained largely by a change in average depth over time (in this case average depth each month). This result suggests that a change in primary vertical habitat utilization occurred in September followed by a period of increasing variability (Figure 4.3), perhaps in response to changes in

prey distributions over time. For example, pelagic prey will typically be shallower in summer and deeper in winter (a response to seasonal production in the photic zone). The time series for this tagged shark intersected this seasonal change, although in the opposite direction, suggesting that pelagic prey may intersect with Pacific sleeper shark vertical habitat during dark nights in the winter. September-November also marked a period of diel vertical migration (Figure 4.S.A.1) and systematic vertical oscillation (Figure 4.S.A.2) patterns previously described for this shark (Hulbert et al. 2006). Diel vertical migration may be a foraging strategy for vertically migrating prey such as squid, while systematic vertical oscillation is characteristic of an efficient foraging strategy for diffuse epipelagic prey (Hulbert et al. 2006). Periods of increasing variability observed in the SM.1 residuals after mid-September (Figures 4. 2 – 4.5) could also be associated with changes in local weather patterns. For example, in the northeastern Gulf of Alaska, low pressure systems typically deepen beginning in September resulting in high winds, unsettled seas, and strong near shore currents.

However, the importance of the structural explanatory variable (*Date-Month*) is difficult to validate within the limited time frame of this study (6 months of observations) which precludes repeated observations of month over multiple years. For example, there was no consistent seasonal pattern in either the depth range or its variability among all tagged sharks described in Hulbert et al. (2006). Consequently, the movement behavior of Pacific sleeper sharks at monthly time scales may change less predictably over time than at hourly time scales, or may change in response to factors outside the scope of the current study.

We addressed the periods of increasing variability observed in the depth profile over time with a log transformation of the response variable. We also investigated splitting the analyses carried out above into two periods (not shown): June–August and September–November. We re-ran the entire analysis separately for each period. However, the results were similar to those obtained for the combined data set. We also investigated a reduced candidate structural model set (not shown) which removed *Date-Month*. However, all candidate structural model sets that removed *Date-Month* resulted in significant non-stationarity in the SM residuals (KPSS P-value < 0.05). Future research, beyond the scope of the current proof of concept study, could explore alternative TSM formulations that can accommodate unequal variance over time such as a generalized autoregressive conditionally heteroskedastic (GARCH; e.g., Chatfield 2004) model or its equivalents.

The goodness of model fit based on computation of RMSE, R^2, and F-stat P-values for these model runs (Table 4.4) should be interpreted cautiously because of significant runs remaining in the residuals (Table 4.3). Runs in the residuals would be expected to result in inflated R^2 values and biased F-stat P-values, which would make it more likely to conclude that a model is significant (Appendix 4.A). Similarly, AICc for these model runs were obtained from least squares regression based on the

assumption that ordinary least squares regression and maximum likelihood results are equivalent. However, this is only true if the assumptions of the ordinary least squares regression, including independent and normally distributed residuals, are met. Residuals from these model runs failed the Lilliefors normality test (Table 4.3). If the combined model (SM + TSM) residuals are over-dispersed, then the AICc would be expected to result in less evidence for selection among models. This interpretation is consistent with our CCF results which identified important lagged processes remaining in the residuals of the most parsimonious combined model, SM.1 + TSM.1, fit to *Ln-Tag-Depth* (Figures 4.8 and 4.9). In contrast, CCF plots of residuals from a higher order autoregressive process in the combined model, SM.1 + TSM.4 (Figures 4.S.A.11–4.S.A.S13), showed that the important lagged processes remaining in the residuals of the combined SM.1 + TSM.1 model fit to *Ln-Tag-Depth* (Figures 4.8 and 4.9) were accounted for with a higher order AR model, in this case an AR(30). However, the higher order AR model was not identified as the best model based on AICc (Table 4.5).

A range of transformed response variables (not shown) was explored in order to address the observed non-normality of residuals. In addition to *Ln-Tag-Depth*, the following transformations were explored as a response variable: *Ln-Tag-Temp*, the ratio of *Ln-Tag-Depth* to *Ln-Tag-Temp*, the average movement rate (meters per minute) each hour, the absolute vertical movement rate (meters per hour), the natural log of the absolute vertical movement (meters per hour), and the logit transform of the proportion of time (minutes) in each hour spent above 150 meters. However, none of the transformations explored were successful at achieving normality in residuals of the combined SM + TSM model at the converged solution for all model combinations.

For example, when the absolute vertical movement rate (meters per hour) was included as the response variable for the combined model SM.1 + TSM.1, the combined model residuals were both trend and level stationary (i.e., passed the runs test, P-value = 0.06) and were not significantly auto correlated (runs test P-value > 0.05). This result indicated that the seasonal factor (*Date-Month*) was not necessary in the model. The combined model at the converged solution also had a relatively lower R^2 (0.37) compared to the same model run with *Ln-Tag-Depth* as the response variable (R^2 = 0.79). This result was consistent with our expectation, as discussed above, that significant runs in the residuals of the combined model with *Ln-Tag-Depth* as the response variable may have resulted in an inflated R^2. Another explanation is that the new model may simply have had worse explanatory power. However, when we re-ran the entire analysis with the absolute vertical movement rate (meters per hour) included as the response variable, the results (not shown) were similar to those summarized above with *Ln-Tag-Depth* as the response variable, except that R^2 was consistently lower in the new model. In addition, with increasing model complexity in the SM, the combined model, SM + TSM, residuals no longer passed the runs test (P -value < 0.05). This result was concerning because it may imply that adding unnecessary factors in the

SM resulted in time series artifacts manifest as runs in the combined the combined model, SM + TSM, residuals.

Nonlinearity was also observed in the smoothed response variable (Supplement 4.A; Figures 4.S.A.6 – 4.S.A.8), which may have contributed to a lack of power for discriminating among candidate linear SMs. Consequently, future research, beyond the scope of this proof of concept study, could explore multivariate vector autoregression methods (Appendix 4.A; e.g., Yasumiishi et al. 2016) or multivariate Aoki (1990) State Space Time Series methods (Criddle and Havenner 1991; Criddle and Herrmann 2008; Steiner et al. 2011). An advantage of multivariate time series methods is that seemingly complex nonlinearity over time can be modeled by lagged relationships among variables within multivariate time series analysis. It is also possible to model non-linearity directly within the SM, for example with a generalized additive model (GAM; Supplement 4.A). However, we did not pursue GAMs in the SM because of a concern that increasing the complexity of the SM might introduce artifacts into the residuals, and compromise the TSM analyses.

In conclusion, the results of this study demonstrate that statistical inference about habitat utilization can be drawn from simultaneous analysis of an entire time series depth profile stored on an electronic archival tag. Pacific sleeper shark vertical movement behavior over relatively short periods (hours) was explained largely by a deterministic time series process based on the shark's average depth in the previous hour, which was consistent with a slow sleeper shark swim speed. Vertical movement behavior over longer periods (months) was explained largely by a change in primary vertical habitat utilization in mid-September, suggestive of movement among habitats perhaps in response to changing prey vertical distributions over time.

4.6. Literature Cited

Anderson, D. R., and K. P. Burnham. 2002. Avoiding pitfalls when using information-theoretic methods. Journal of Wildlife Management 66:912–918.

Aoki, M. 1990. State space modeling of time series, Springer-Verlag, NY.

Bright, D. B. 1959. The occurrence and food of the sleeper shark, *Somniosus pacificus*, in a central Alaska bay. Copeia 1959:76–77.

Burnham, K. P., and D. R. Anderson. 2002. Model selection and multimodel inference, Second edition, Springer.

Burnham, K. P., D. R. Anderson, and K. P. Huyvaert. 2011. AIC model selection and multimodel inference in behavioral ecology: some background, observations, and comparisons. Behavioral Ecology and Sociobiology 65:23–35.

Caeiro, F., and A. Mateus. 2014. randtests: Testing randomness in R. R package version 1.0. http://CRAN.R-project.org/package=randtests

Carvalho, F., A. E. Punt, Y.-J. Chang, M. N. Maunder, and K. R. Piner. 2017. Can diagnostic tests help identify model misspecification in integrated stock assessments? Fisheries Research 192:28–40.

Chatfield, C. 2004. The analysis of time series, an introduction. Chapman and Hall/CRC texts in Statistical Science (sixth ed.).

Cochrane, D., and G. H. Orcutt. 1949. Application of least squares regressions to relationships containing autocorrelated error terms. Journal of the American Statistical Association 44:32–61.

Compagno, L. J. V. 1984. FAO species catalogue. Vol. 4. Sharks of the world. An annotated and illustrated catalogue of shark species known to date, part 1 - hexanchiformes to lamniformes. FAO Fisheries Synopsis 125:1–249.

Courtney, D. L., M. D. Adkison, and M. F. Sigler. 2016. Risk analysis of plausible incidental exploitation rates for the Pacific Sleeper Shark, a data-poor species in the Gulf of Alaska. North American Journal of Fisheries Management 36:523–548.

Courtney, D. L., and R. Foy. 2012. Pacific sleeper shark *Somniosus pacificus* trophic ecology in the eastern North Pacific Ocean inferred from nitrogen and carbon stable-isotope ratios and diet. Journal of Fish Biology 80:1508–1545.

Courtney, D. L., and M. F. Sigler. 2007. Trends in area-weighted CPUE of Pacific sleeper sharks (*Somniosus pacificus*) in the northeast Pacific Ocean determined from sablefish longline surveys. Alaska Fishery Research Bulletin 12:291–315.

Courtney, D., C. Tribuzio, K. J. Goldman, and J. Rice. 2006. Appendix E, GOA sharks. Pages 481–562 *in* Stock assessment and fishery evaluation report for the groundfish resources of the Gulf of Alaska for 2007. North Pacific Fishery Management Council, 605 W 4th Ave, Suite 306, Anchorage, AK 99501. http://www.afsc.noaa.gov/refm/docs/2006/GOAsharks.pdf (last accessed 5 November 2015).

Coutré, K. M., A. H. Beaudreau, D. Courtney, F. Mueter, P. W. Malecha, and T. L. Rutecki. 2017. Vertical movement patterns of juvenile Sablefish in coastal Southeast Alaska. Marine and Coastal Fisheries 9:161–169 (DOI: 10.1080/19425120.2017.1285377).

Criddle K. R. 2007. Intermediate statistics and applied regression analysis, Third Edition. East-West Bridge Publishing, Providence, UT.

Criddle, K. R., and A. Havenner. 1991. An encompassing approach to modeling fishery dynamics: Modeling dynamic nonlinear systems. Natural Resource Modeling 5:55–90.

Criddle, K. R., and Herrmann, M. 2008. A state space bioeconomic model of Pacific halibut. Natural Resource Modeling 21:29–60.

Ebert, D. A., L. J. V. Compagno, and L. J. Natanson. 1987. Biological notes on the Pacific sleeper shark, *Somniosus pacificus* (chondrichthyes: squalidae). California Fish and Game 73:117–123.

Ebert, D. A., and M. V. Winton. 2010. Chondrichthyans of high latitude seas. Pages 115–158 *in* J. C. Carrier, J. A. Musick, and M. R. Heithaus, editors. Sharks and their relatives II; biodiversity, adaptive physiology, and conservation. CRC Press, Boca Raton, FL.

Frid, A., G. G. Baker, and L. M. Dill. 2008. Do shark declines create fear-released systems? Oikos 117:191–201.

Frid, A., J. Burns, G. G. Baker, and R. E. Thorne. 2009. Predicting synergistic effects of resources and predators on foraging decisions by juvenile Steller sea lions. Oecologia 158:775–786.

Frid, A., L. M. Dill, R. E. Thorne, and G. M. Blundell. 2007. Inferring prey perception of relative danger in large-scale marine systems. Evolutionary Ecology Research 9:635–649.

Gotshall, D. W., and T. Jow. 1965. Sleeper sharks (*Somniosus pacificus*) off Trinidad, California, with life history notes. California Fish and Game 51:294–298.

Heithaus, M. R., A. Frid, J. J. Vaudo, B. Worm, and A. J. Wirsing. 2010. Unraveling the ecological importance of elasmobranchs. Pages 611–638 *in* J. C. Carrier, J. A. Musick, and M. R. Heithaus, editors. Sharks and their relatives II; biodiversity, adaptive physiology, and conservation. CRC Press, Boca Raton, FL.

Heithaus, M. R., A. Frid, A. J. Wirsing, and B. Worm. 2008. Predicting ecological consequences of marine top predator declines. Trends in Ecology and Evolution 23:202–210.

Henriksson, R. D., and R. C. Merton. 1981. On market timing and investment performance. II. Statistical procedures for evaluating forecasting skills. Journal of Business 54:513–533.

Horning, M., and J. A. E. Mellish. 2014. In cold blood: evidence of Pacific sleeper shark (*Somniosus pacificus*) predation on Steller sea lions (*Eumetopias jubatus*) in the Gulf of Alaska. Fishery Bulletin 112:297–310.

Hulbert, L. B., M. F. Sigler, and C. R. Lunsford. 2006. Depth and movement behaviour of the Pacific sleeper shark in the northeast Pacific Ocean. Journal of Fish Biology 69:406–425.

Kwiatkowski, D., P. C. Phillips, P. Schmidt, and Y. Shin. 1992. Testing the null hypothesis of stationarity against the alternative of a unit root: How sure are we that economic time series have a unit root? Journal of Econometrics 54:159–178.

Mecklenburg, C. W., T. A., Mecklenburg, and L. K. Thorsteinson. 2002. Fishes of Alaska. American Fisheries Society, Bethesda, MD.

Naik, G., and R. M. Leuthold. 1986. A note on qualitative forecast evaluation. American Journal of Agricultural Economics 68:721–726.

Nielsen, J., R. B. Hedeholm, J. Heinemeier, P. G. Bushnell, J. S. Christiansen, J. Olsen, C. B. Ramsey, R. W. Brill, M. Simon, K. F. Steffensen, and J. F. Steffensen. 2016. Eye lens radiocarbon reveals centuries of longevity in the Greenland shark *Somniosus microcephalus*. Science 6300:702–704.

Orlov, A. M. 1999. Capture of especially large sleeper shark *Somniosus pacificus* (Squalidae) with some notes on its ecology in northwestern Pacific. Journal of Ichthyology 39:548–553.

Orlov, A. M., and A. A. Baitalyuk. 2014. Spatial distribution and features of biology of Pacific sleeper shark *Somniosus pacificus* in the North Pacific. Journal of Ichthyology 54:526–546.

Orlov, A. M., and S. I. Moiseev. 1999a. New data on the biology of the Pacific sleeper shark, *Somniosus pacificus* (Squalidae) in the northwestern Pacific Ocean. Pages 177–186 *in* D. MacKinlay, K. Howard, and J. Cech Jr., editors. Fish performance studies. Department of Fisheries and Oceans, Vancouver, BC.

Orlov, A. M., and S. I. Moiseev. 1999b. Some biological features of Pacific sleeper shark, *Somniosus pacificus* (Bigelow et Schroeder 1944) (Squalidae) in the northwestern Pacific Ocean. Oceanological Studies 28:3–16.

Pentcheff, D. 2016. WWW Tide/Current Predictor for Cape Hinchinbrook, Hinchinbrook Island, Alaska (May 2002-March 2003). Biological Sciences, University of South Carolina, Columbia SC 29208 USA. http://tbone.biol.sc.edu/tide

Pfaff, B. 2006. Analysis of integrated and cointegrated time series with R. Springer.

Pfaff, B. 2008. Analysis of integrated and cointegrated time series with R. Second edition. Springer-Verlag New York.

Shumway, R. H., and D. S. Stoffer. 2015. Time series analysis and it applications, with R examples, third edition. Springer.

Sigler, M. F., L. B. Hulbert. C. R. Lunsford, N. H. Thompson, K. Burek, G. O'Corry-Crowe, and A. C. Hirons. 2006. Diet of Pacific sleeper shark, a potential Steller sea lion predator, in the eastern North Pacific Ocean. Journal of Fish Biology 69:392–405.

Smith, C. R., and A. R. Baco. 2003. Ecology of whale falls at the deep-sea floor. Oceanography and Marine Biology: an Annual Review 41:311–354.

Steiner, E. M., K. R. Criddle, and M. D. Adkison. 2011. Balancing biological sustainability with the economic needs of Alaska's sockeye salmon fisheries. North American Journal of Fisheries Management 31:431–444.

Tribuzio, C. A., K. Echave, C. Rodgveller, P.-J. Hulson, and K. J. Goldman. 2011. Chapter 20: Assessment of the shark stock complex in the Gulf of Alaska. Pages 1393–1446 *in* Stock assessment and fishery evaluation report for the groundfish resources of the Gulf of Alaska for 2012. North Pacific Fishery Management Council, 605 W 4th Ave, Suite 306, Anchorage, AK 99501. http://www.afsc.noaa.gov/REFM/docs/2011/GOAshark.pdf (last accessed 5 November 2015).

U.S. Naval Observatory. 2016. Sunrise, sunset, and nautical twilight tables (May 2002-March 2003) for 60° 14' N, 146° 39' W. http://aa.usno.navy.mil/data/

Wang, J. Y. and S.-C. Yang. 2004. First records of Pacific sleeper sharks (*Somniosus pacificus* Bigelow and Schroeder, 1944) in the subtropical waters of eastern Taiwan. Bulletin of Marine Science 74:229–235.

Watanabe, Y. Y., C. Lydersen, A. T. Fisk, and K. M. Kovacs. 2012. The slowest fish: Swim speed and tail-beat frequency of Greenland sharks. Journal of Experimental Marine Biology and Ecology 426–427:5–11.

Yang, M.-S. and B. N. Page. 1999. Diet of Pacific sleeper shark, *Somniosus pacificus*, in the Gulf of Alaska. Fishery Bulletin 97:406–409.

Yano, K., J. D. Stevens, and L. J. V. Compagno. 2004. A review of the systematics of the sleeper shark genus *Somniosus* with redescriptions of *Somniosus (Somniosus) antarcticus* and *Somniosus (Rhinoscymnus) longus* (Squaliformes: Somniosidae). Ichthyological Research 51:360–373.

Yano, K., J. D. Stevens, and L. J. V. Compagno. 2007. Distribution, reproduction and feeding of the Greenland shark *Somniosus (Somniosus) microcephalus*, with notes on two other sleeper sharks, *Somniosus (Somniosus) pacificus* and *Somniosus (Somniosus) antarcticus*. Journal of Fish Biology 70:374–390.

Yasumiishi, E. C. M., K. R. Criddle, J. H. Helle, N. Hillgruber and F. J. Mueter. 2016. Effect of population abundance and climate on the growth of 2 populations of chum salmon (*Oncorhynchus keta*) in the eastern North Pacific Ocean. Fishery Bulletin 114:203–219.

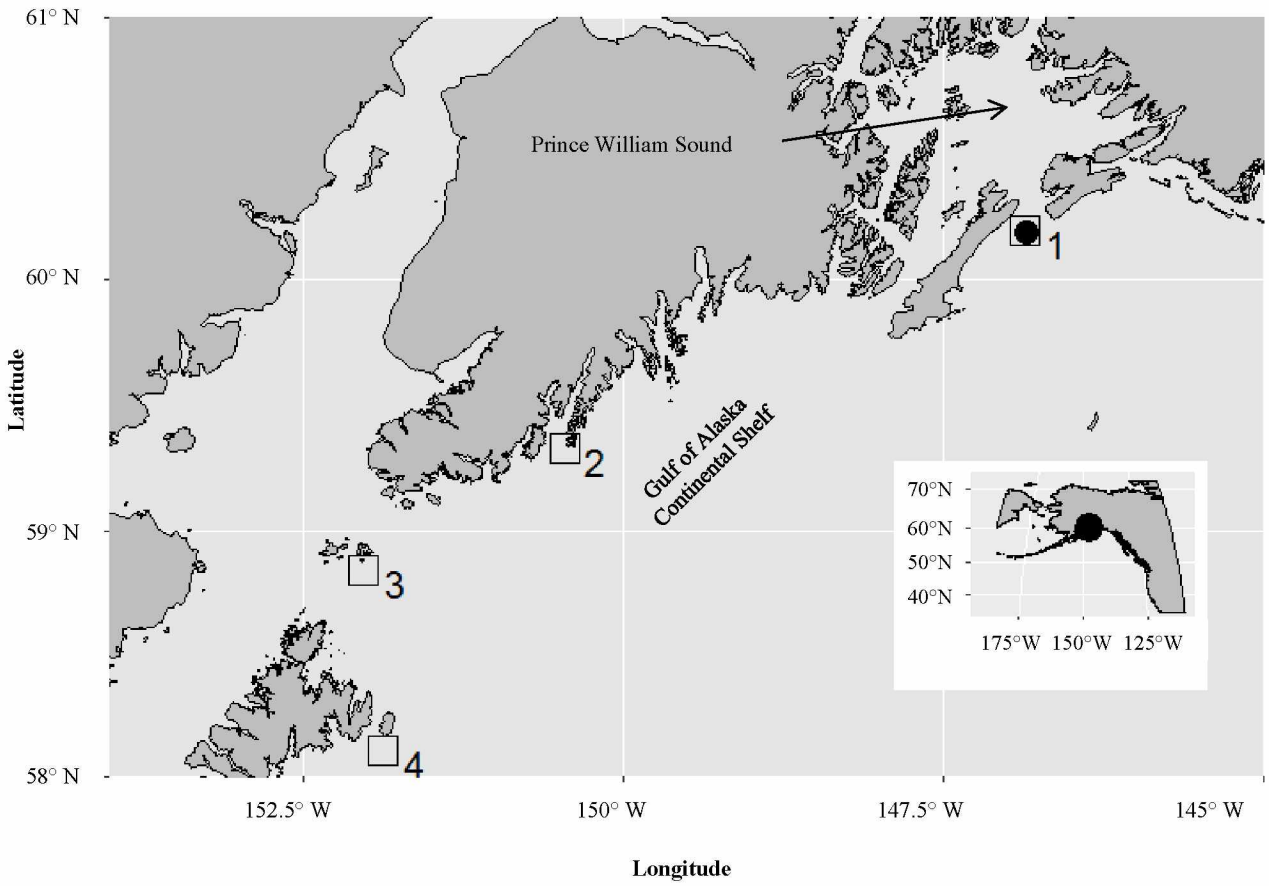

Figure 4.1: Map depicting Pacific sleeper shark tag release location.
Pacific sleeper shark tag release location (solid circle) near Cape Hinchinbrook, Hinchinbrook Island, Alaska (Hulbert et al. 2006, their tag #21; approximate location 60.2383° N, 146.6467° W; solid circle) in the northern Gulf of Alaska relative to the average longline set location of Pacific sleeper shark sampling near four large rookeries of the endangered Steller sea lion subpopulation west of 144° W (squares; adapted from Hulbert et al. 2006, their Figure 1), including Seal Rocks (1), Outer Pye Island (2), Sugarloaf Island (3), and Marmot Island (4). The tag was physically recovered, but the tag never transmitted and a recovery location was not determined exactly.

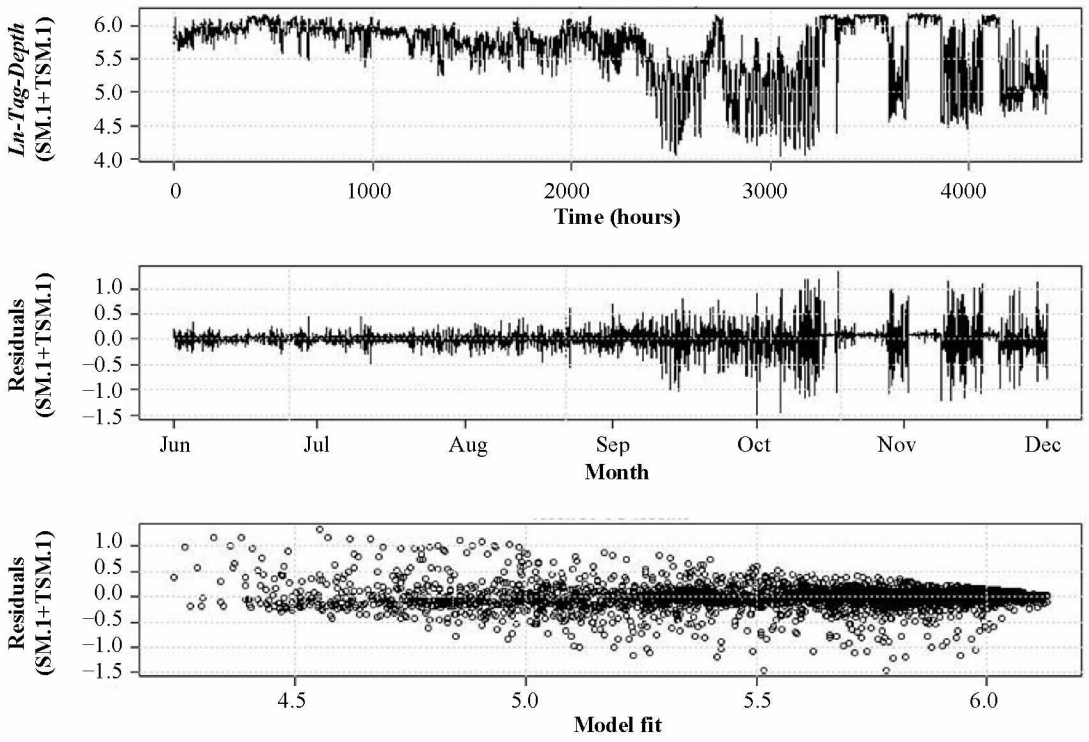

Figure 4.2: Combined model (SM.1+TSM.1) response variable *Ln-Tag-Depth* and residuals. Combined model (SM.1+TSM.1) response variable *Ln-Tag-Depth* (upper panel; deeper depths correspond to larger absolute values) at the converged parameter estimates after 100 iterations; combined model residuals (middle panel) indicated periods of increasing variability beginning in September; combined model residuals versus fit (lower panel) indicated a trend of positive residuals at shallower depths and negative residuals at deeper depths.

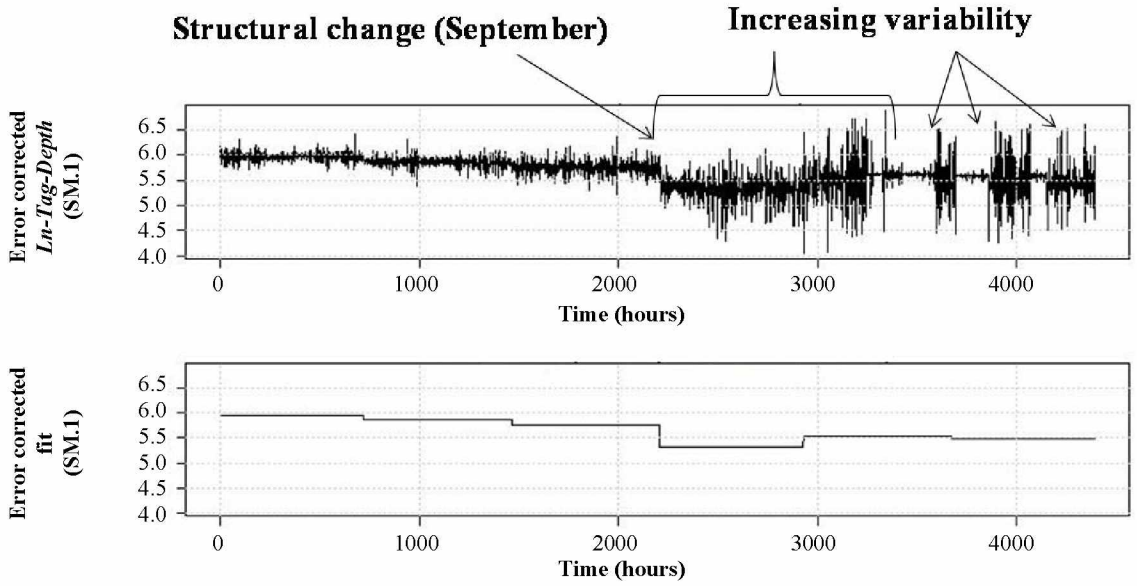

Figure 4.3: Structural model (SM.1) error corrected response variable *Ln-Tag-Depth.*
Analysis of the error corrected structural model (SM.1) response variable (*Ln-Tag-Depth*) after implementation of step-2 of the error correction procedure (upper panel) identified a structural change after about 2,000 hours (September) followed by periods of increasing variability; the error corrected fit of the structural model is shown in the bottom panel.

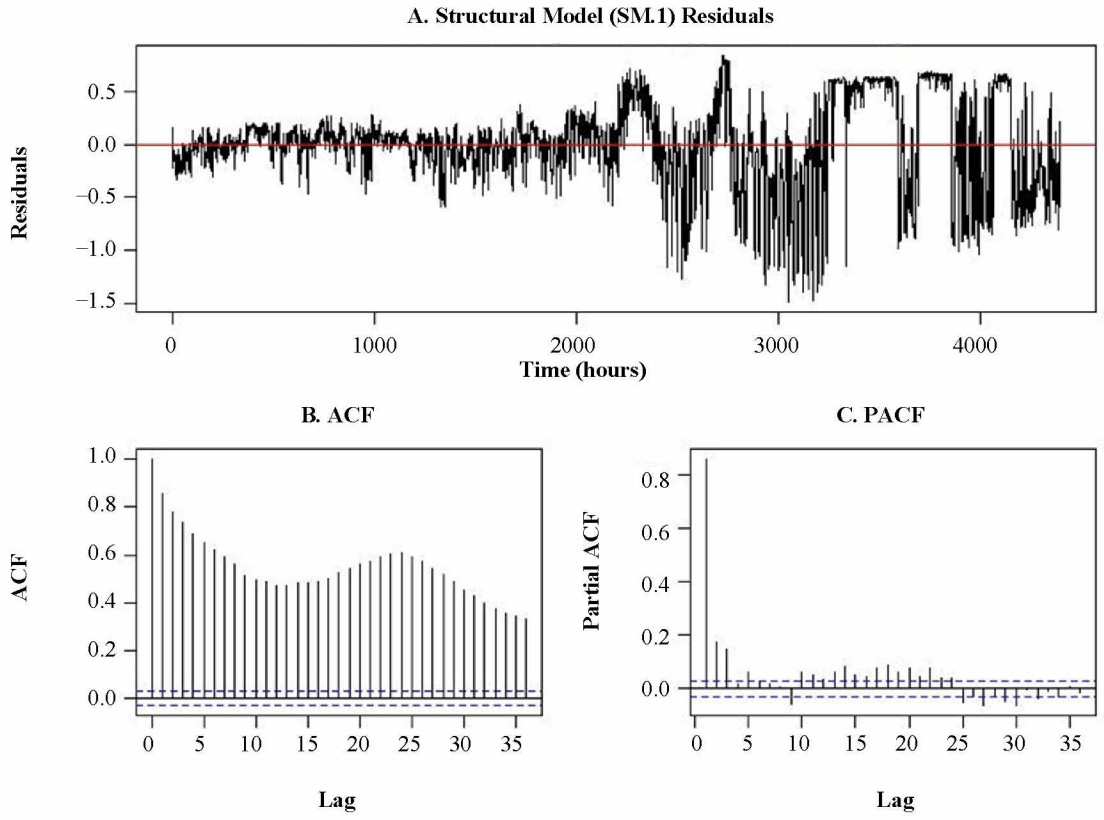

Figure 4.4: Analysis of the structural model (SM.1) residuals.
Analysis of the structural model (SM.1) residuals (Panel A) before implementation of error correction identified a slow decay of the autocorrelation function (ACF; Panel B) at increasing lag length and a rapid decay of the partial autocorrelation function (PACF; Panel C) at increasing lag length, which was diagnostic for a strong positive autoregressive process at a lag of 1 hour (PACF near 0.8), a relatively weaker positive AR processes at lags 2 and 3 hours (PACF near 0.2), and a very weak positive AR processes at lags of between about 10-24 hrs (PACF < 0.2); the stippled lines (lower panels) represent the approximate 95% confidence intervals for lagged AR processes.

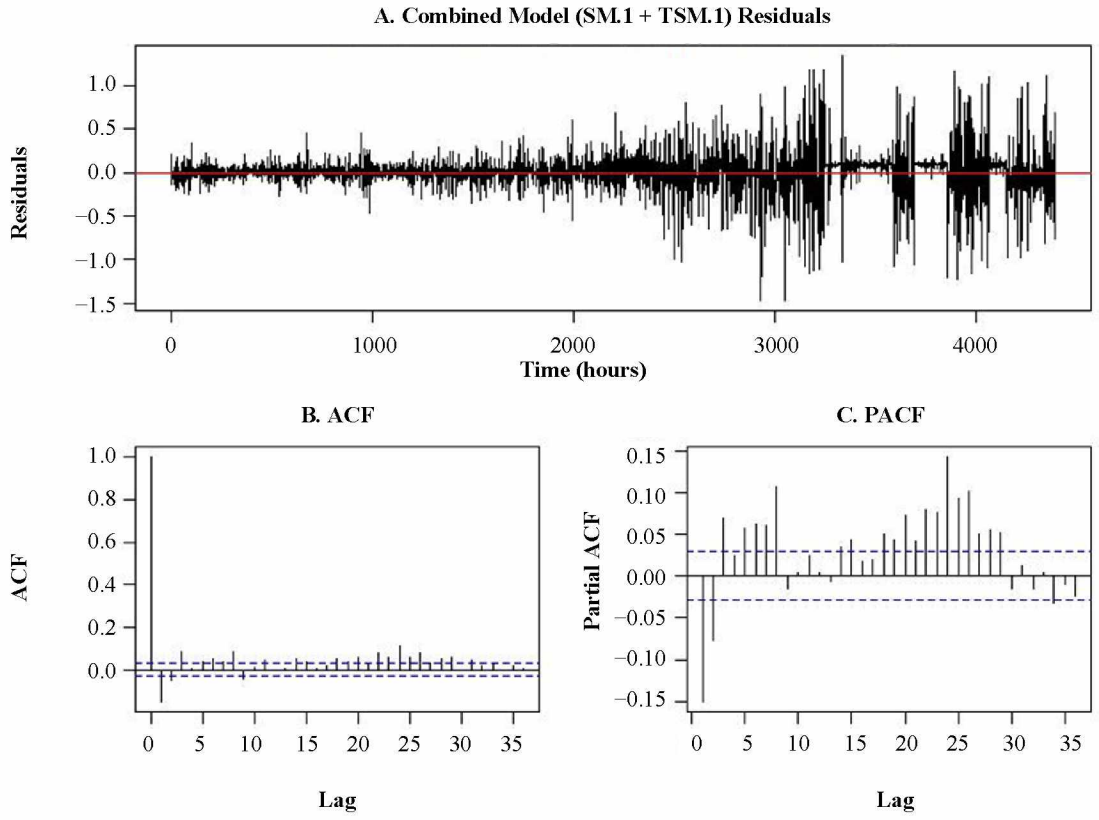

Figure 4.5: Analysis of the combined model (SM.1 + TSM.1) residuals.
Analysis of the combined model (SM.1 + TSM.1) residuals (Panel A) at the converged parameter estimates after 100 iterations; a rapid decay of the autocorrelation function (ACF; Panel B) was diagnostic for negligible autocorrelation remaining within the combined model (SM.1 + TSM.1) residuals at the converged parameter estimates; the stippled lines (lower panels) represent the approximate 95% confidence intervals for lagged AR processes.

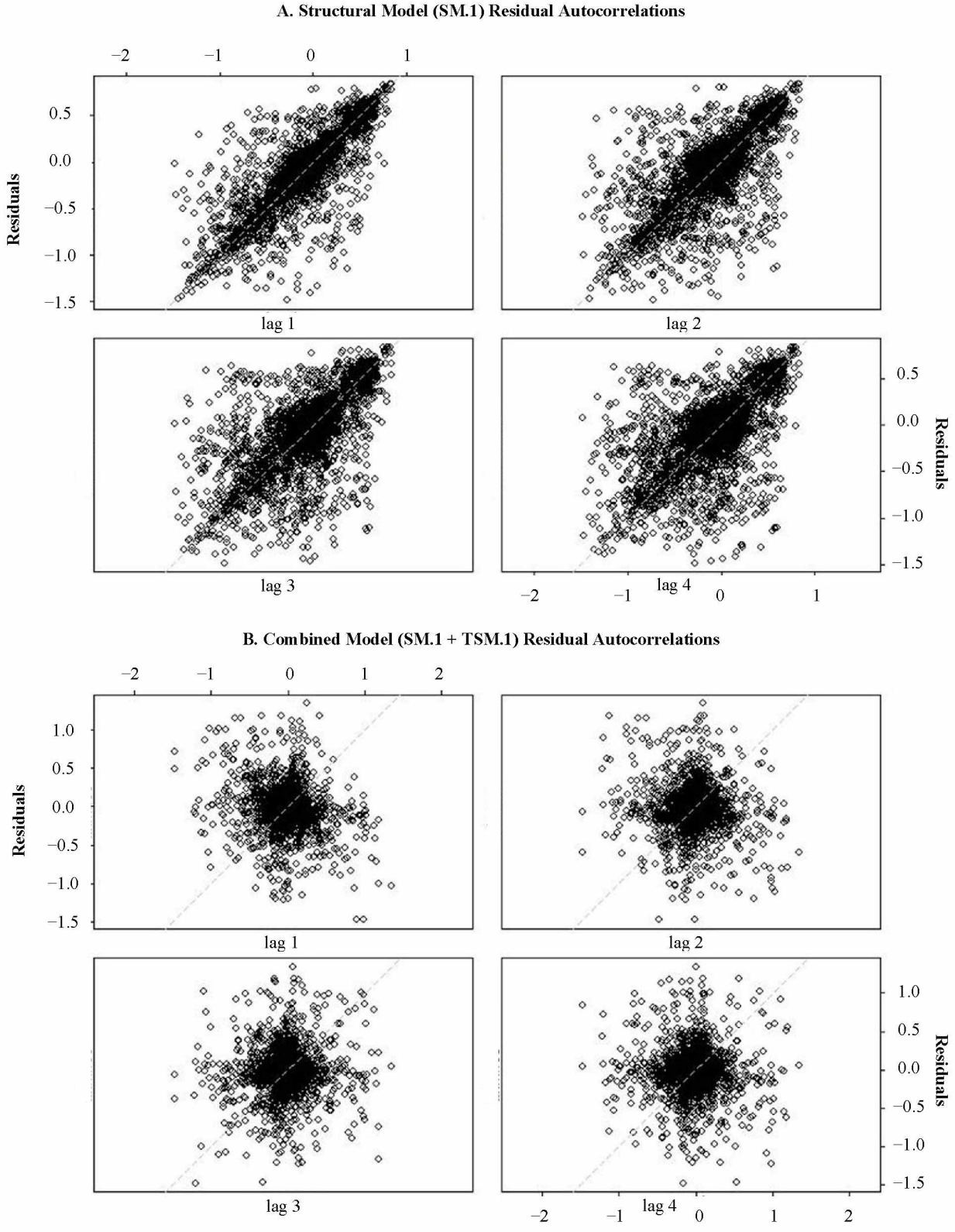

Figure 4.6: Analysis of model residual autocorrelations at lags 1–4.

Figure 4.6. Continued. Analysis of the structural model (SM.1) residual autocorrelations (Panel A) at lagged time periods of 1, 2, 3, and 4 hours identified strong lagged autocorrelation patterns; analysis of the combined model (SM.1 + TSM.1) residual autocorrelations (Panel B) at lagged time periods of 1, 2, 3, and 4 hours identified an absence of lagged autocorrelation patterns, which was diagnostic for negligible lagged autocorrelation remaining within the model residuals at the converged parameter estimates of the combined (SM.1 + TSM.1) model after 100 iterations.

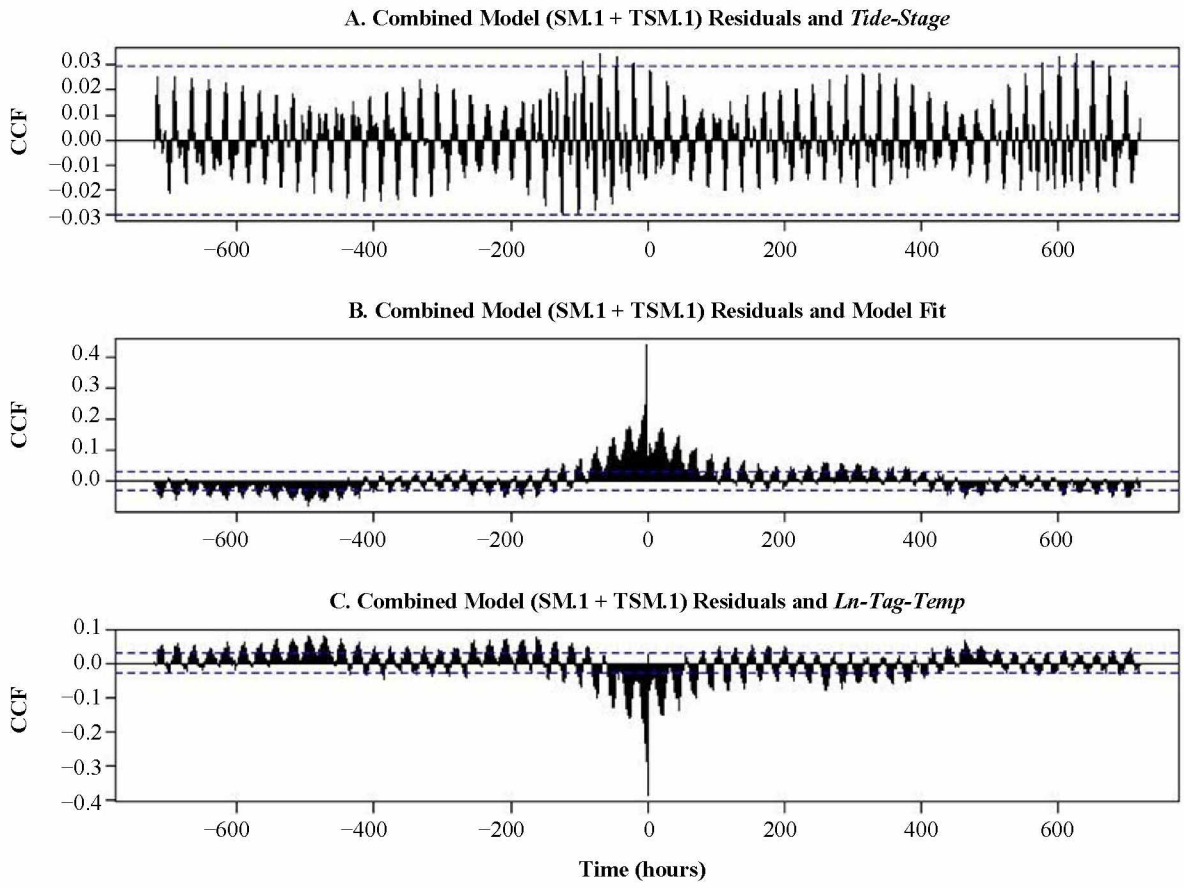

Figure 4.7: Cross correlation function of SM.1 + TSM.1 lagged residuals (c. 1 month).
Cross correlation function (CCF) of lagged residuals (moving to the left from zero) of the combined model (SM.1 + TSM.1) after 100 iterations plotted against lagged (moving to the right from zero) *Tide-Stage* (Panel A), model fit (Panel B), and *Ln-Tag-Temp* (Panel C) for lags of up to 720 hours (c. 1 month); the stippled lines represent the approximate 95% confidence intervals for lagged AR processes.

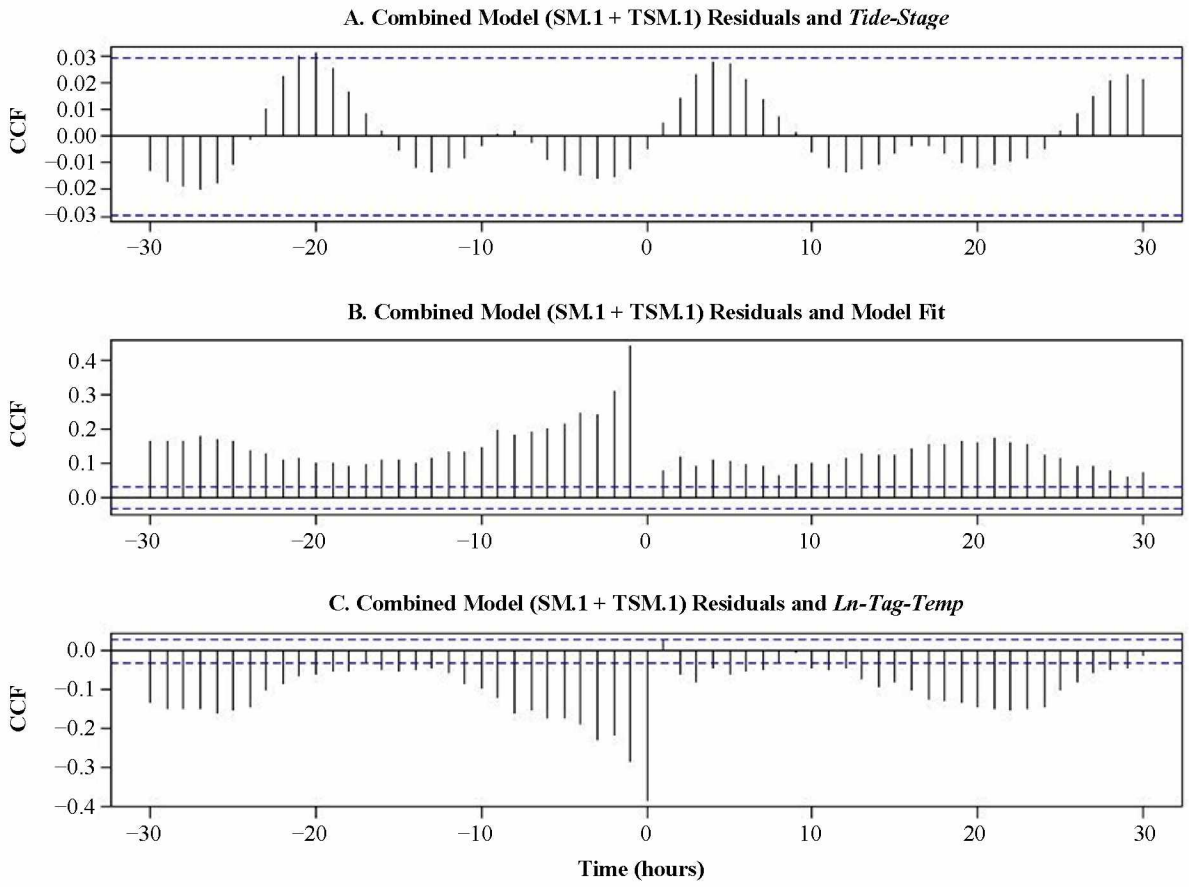

Figure 4.8: Cross correlation function of SM.1 + TSM.1 lagged residuals (c. 1 day).
Cross correlation function (CCF) of lagged residuals (moving to the left from zero) of the combined model (SM.1 + TSM.1) after 100 iterations plotted against lagged (moving to the right from zero) *Tide-Stage* (Panel A), model fit (Panel B), and *Ln-Tag-Temp* (Panel C) for lags of up to 30 hours (c. 1 day); the stippled lines represent the approximate 95% confidence intervals for lagged AR processes.

Table 4.1: Structural model (SM) and time series model (TSM) descriptions.
Thirteen structural models (SMs) were implemented, which included *Ln-Tag-Depth* as the response variable and *Date-Month*, *Light-Stage*, and *Tide-Strength* as explanatory variables along with their interactions; four time series models (TSM) were evaluated for each SM: AR(1), AR(2), AR (3), and AR(AIC).

A. Structural Models (SM)

SM	Description
SM.1	*Date-Month*
SM.2	*Date-Month* + *Light-Stage*
SM.3	SM.2 + *Date-Month* × *Light-Stage*
SM.4	*Date-Month* + *Tide-Strength-Stage*
SM.5	SM.4 + *Date-Month* × *Tide-Strength-Stage*
SM.6	*Date-Month* + *Light-Stage* + *Tide-Strength-Stage*
SM.7	SM.6 + *Date-Month* × *Light-Stage*
SM.8	SM.6 + *Date-Month* × *Tide-Strength-Stage*
SM.9	SM.6 + *Light-Stage* × *Tide-Strength-Stage*
SM.10	SM.6 + *Date-Month* × *Light-Stage* + *Date-Month* × *Tide-Strength-Stage*
SM.11	SM.6 + *Date-Month* × *Light-Stage* + *Light-Stage* × *Tide-Strength-Stage*
SM.12	SM.6 + *Date-Month* × *Tide-Strength-Stage* + *Light-Stage* × *Tide-Strength-Stage*
SM.13	SM.6+ *Date-Month* × *Light-Stage* + *Date-Month* × *Tide-Strength-Stage* + *Light-Stage* × *Tide-Strength-Stage*

B. Time Series Models (TSM) evaluated for each SM

TSM	Description
TSM.1	Autoregressive with lag 1; AR(1)
TSM.2	Autoregressive with lag 2; AR(2)
TSM.3	Autoregressive with lag 3; AR(3)
TSM.4	Autoregressive with lag determined by minimum AIC; AR(AIC)

Table 4.2: Subset of SM + TSM model combinations evaluated for model selection.
A subset of sixteen SM + TSM model combinations for which all SM coefficient estimates CVs were ≤ 0.5, was evaluated for model selection.

Structural model Time series model
SM.1: *Date-Month*
TSM.1: Autoregressive with lag 1; AR(1)
TSM.2: Autoregressive with lag 2; AR(2)
TSM.3: Autoregressive with lag 3; AR(3)
TSM.4: Autoregressive with lag determined by minimum AIC; AR(30)
SM.2: *Date-Month* + *Light-Stage*
TSM.1: Autoregressive with lag 1; AR(1)
TSM.2: Autoregressive with lag 2; AR(2)
TSM.3: Autoregressive with lag 3; AR(3)
TSM.4: Autoregressive with lag determined by minimum AIC; AR(30)
SM.4: *Date-Month* + *Tide-Strength-Stage*
TSM.1: Autoregressive with lag 1; AR(1)
TSM.2: Autoregressive with lag 2; AR(2)
TSM.3: Autoregressive with lag 3; AR(3)
TSM.4: Autoregressive with lag determined by minimum AIC; AR(30)
SM.6: *Date-Month* + *Light-Stage* + *Tide-Strength-Stage*
TSM.1: Autoregressive with lag 1; AR(1)
TSM.2: Autoregressive with lag 2; AR(2)
TSM.3: Autoregressive with lag 3; AR(3)
TSM.4: Autoregressive with lag determined by minimum AIC; AR(30)

Table 4.3: SM + TSM model results (diagnostic tests).
Results of SM residual level stationarity KPSS-test (level stationarity is rejected if P-value ≤ 0.05), SM coefficient of variation (CV) evaluation (accepted if all CVs ≤ 0.5), combined model (SM + TSM) residuals Lilliefors normality test (normality rejected if P-value ≤ 0.05), combined model (SM + TSM) residuals Wald-Wolfowitz runs test (significant runs if P-value ≤ 0.05), and TSM model Naik and Leuthold's ratio of accurate turning points (NL-TP).

Model	KPSS-test P-value	All SM coef. CV's ≤ 0.5	Lilliefors-test P-value	Runs-test P-value	NL-TP Ratio accurate
SM.1 + TSM.1	> 0.10	Yes	< 0.001	< 0.001	0.21
SM.1 + TSM.2	> 0.10	Yes	< 0.001	< 0.001	0.20
SM.1 + TSM.3	> 0.10	Yes	< 0.001	< 0.001	0.20
SM.1 + TSM.4	> 0.10	Yes	< 0.001	< 0.001	0.23
SM.2 + TSM.1	> 0.10	Yes	< 0.001	< 0.001	0.21
SM.2 + TSM.2	> 0.10	Yes	< 0.001	< 0.001	0.21
SM.2 + TSM.3	> 0.10	Yes	< 0.001	< 0.001	0.21
SM.2 + TSM.4	> 0.10	Yes	< 0.001	< 0.001	0.22
SM.4 + TSM.1	> 0.10	Yes	< 0.001	< 0.001	0.21
SM.4 + TSM.2	> 0.10	Yes	< 0.001	< 0.001	0.21
SM.4 + TSM.3	> 0.10	Yes	< 0.001	< 0.001	0.21
SM.4 + TSM.4	> 0.10	Yes	< 0.001	< 0.001	0.23
SM.6 + TSM.1	> 0.10	Yes	< 0.001	< 0.001	0.22
SM.6 + TSM.2	> 0.10	Yes	< 0.001	< 0.001	0.21
SM.6 + TSM.3	> 0.10	Yes	< 0.001	< 0.001	0.21
SM.6 + TSM.4	> 0.10	Yes	< 0.001	< 0.001	0.22

Table 4.4: SM + TSM model results (goodness of fit tests).
Number of observations (n – *l*), along with the combined model (SM + TSM) number of explanatory variables (*k* + *l*), degrees of freedom d.f. = (n – *l*) – (*k* + *l* + 2), root mean squared error of residuals (RMSE), coefficient of determination (R^2), significance of the *F*-stat (*P*-value), and significance of the Henriksson–Merton turning point test (HM-test), as defined above in the methods section.

Model	*n* – *l*	*k* + *l*	d.f.	RMSE	R^2	*F*-stat *P*-value	HM-test *P*-value
SM.1 + TSM.1	4391	6	4383	0.212	0.79	< 0.001	< 0.001
SM.1 + TSM.2	4390	7	4381	0.209	0.80	< 0.001	< 0.001
SM.1 + TSM.3	4389	8	4379	0.206	0.80	< 0.001	< 0.001
SM.1 + TSM.4	4362	35	4325	0.199	0.82	< 0.001	< 0.001
SM.2 + TSM.1	4391	9	4380	0.214	0.79	< 0.001	< 0.001
SM.2 + TSM.2	4390	10	4378	0.210	0.80	< 0.001	< 0.001
SM.2 + TSM.3	4389	11	4376	0.206	0.80	< 0.001	< 0.001
SM.2 + TSM.4	4362	38	4322	0.200	0.82	< 0.001	< 0.001
SM.4 + TSM.1	4391	7	4382	0.212	0.79	< 0.001	< 0.001
SM.4 + TSM.2	4390	8	4380	0.209	0.80	< 0.001	< 0.001
SM.4 + TSM.3	4389	9	4378	0.207	0.80	< 0.001	< 0.001
SM.4 + TSM.4	4362	36	4324	0.199	0.82	< 0.001	< 0.001
SM.6 + TSM.1	4391	10	4379	0.214	0.79	< 0.001	< 0.001
SM.6 + TSM.2	4390	11	4377	0.210	0.80	< 0.001	< 0.001
SM.6 + TSM.3	4389	12	4375	0.206	0.80	< 0.001	< 0.001
SM.6 + TSM.4	4362	39	4321	0.200	0.82	< 0.001	< 0.001

Table 4.5: SM + TSM model results (Akaike information criterion)
Akaike information criterion with bias correction (AICc), along with the combined model (SM + TSM) number of explanatory variables ($k + l$), the AICc differences Δi, the value of relative maximum likelihood, $L(g_i|x)$, the Akaike weight, w_i, and the weight of evidence for each model in the set calculated from the ratios of the Akaike weights, as defined in the methods section.

	Min AICc			Total	Total	
	– 2.22			18.4	1.00	
Model	AICc	$k + l$	Δ_i	L	w_i	Evidence ratio
SM.1 + TSM.1**	–2.10	6	0.12	0.94	0.051	1.06
SM.1 + TSM.2	–2.13	7	0.08	0.96	0.052	1.04
SM.1 + TSM.3	–2.15	8	0.06	0.97	0.053	1.03
SM.1 + TSM.4*	–2.22	35	0.00	1.00	0.054	1.00
SM.2 + TSM.1	–2.08	9	0.14	0.93	0.051	1.07
SM.2 + TSM.2	–2.12	10	0.10	0.95	0.052	1.05
SM.2 + TSM.3	–2.15	11	0.06	0.97	0.053	1.03
SM.2 + TSM.4	–2.21	38	0.01	0.99	0.054	1.01
SM.4 + TSM.1	–2.10	7	0.11	0.94	0.051	1.06
SM.4 + TSM.2	–2.13	8	0.09	0.96	0.052	1.04
SM.4 + TSM.3	–2.15	9	0.06	0.97	0.053	1.03
SM.4 + TSM.4	–2.21	36	0.00	1.00	0.054	1.00
SM.6 + TSM.1	–2.08	10	0.13	0.94	0.051	1.07
SM.6 + TSM.2	–2.12	11	0.10	0.95	0.052	1.05
SM.6 + TSM.3	–2.15	12	0.06	0.97	0.053	1.03
SM.6 + TSM.4	–2.20	39	0.01	0.99	0.054	1.01

* Minimum AICc
**Most parsimonious model of those examined.

4.7. Appendix 4.A. Addressing Complex Serial Correlation

Suppose that the true system is described by:

$$Y_t = f\left(X_{t,1},\ldots,X_{t-l,k},Y_{t-1},\ldots,Y_{t-l}\right)+\varepsilon_t, \tag{4.A.1}$$

and

$$\varepsilon_t = g\left(\varepsilon_{t-1},\ldots,\varepsilon_{t-l}\right)+u_t \quad u_t \sim N\left(0,\sigma^2\right), \tag{4.A.2}$$

where ε_t is a serially correlated random variable and u_t is clean of serial correlation.

If $f(\bullet)$ and $g(\bullet)$ are sequentially estimated in the presence of serial correlation in ε_t, estimates of $f(\bullet)$ will be inefficient (not minimum variance unbiased estimates) and $g(\bullet)$ may be miss-specified because it is based on $\hat{\varepsilon}_t$ instead of ε_t. As a consequence, the standard errors of the coefficients will be underestimated and thus the corresponding *P*-values will be inflated as will the estimated value of R^2, which could lead to erroneous conclusions about the statistical significance of model elements. Maximum likelihood or simultaneous equation approaches avoid this problem by jointly estimating both $f(\bullet)$ and $g(\bullet)$.

However, in practice, it is often necessary to impose restrictive and unrealistic assumptions about the nature of $f(\bullet)$ and $g(\bullet)$. A flexible alternative is to adopt an extension of the Cochrane-Orcutt (Cochrane and Orcutt 1949) algorithm. This approach can be applied to models that exhibit complex patterns of serial correlation in ε_t by using specialized time series models to generate estimates of structural model residuals and using those estimates to adjust the dependent variable of the structural models. The regression and time-series error-correction models can be iterated until the coefficients and covariance matrices of both models converge to an acceptable degree of precision.

The algorithm begins with estimates of $f(\bullet)$ which are used to generate estimates of Y_t :

$$\hat{Y}_t = \hat{f}\left(X_{t,1},\ldots,X_{t-l,k},Y_{t-1},\ldots,Y_{t-l}\right). \tag{4.A.3}$$

Those estimates, $\hat{Y}_t$, are used to generate estimates of ε_t:

$$\hat{\varepsilon}_t = Y_t - \hat{Y}_t, \tag{4.A.4}$$

which are used to obtain estimates of $g(\bullet)$ and $\hat{\hat{\varepsilon}}_t$:

$$\hat{\hat{\varepsilon}}_t = \hat{g}\left(\hat{\varepsilon}_{t-1},...,\hat{\varepsilon}_{t-l}\right). \tag{4.A.5}$$

The next iteration begins by removing estimates of the serially correlated errors from the dependent variable:

$$Y_t^* = Y_t - \hat{\hat{\varepsilon}}_t. \tag{4.A.6}$$

Those values are used to obtain revised estimates of $f(\bullet)$, which are used to generate revised estimates of the dependent variable:

$$\hat{Y}_t^* = \hat{\hat{f}}\left(X_{t,1},\ldots,X_{t-l,k},Y_{t-1},\ldots,Y_{t-l}\right). \tag{4.A.7}$$

Those estimates, $\hat{Y}_t^*$, are used to generate new estimates of ε_t:

$$\hat{\hat{\varepsilon}}_t = Y_t - \hat{Y}_t^*, \tag{4.A.8}$$

which are used to obtain revised estimates of $g(\bullet)$ and $\hat{\hat{\hat{\varepsilon}}}_t$:

$$\hat{\hat{\hat{\varepsilon}}}_t = \hat{\hat{g}}\left(\hat{\hat{\hat{\varepsilon}}}_{t-1},...,\hat{\hat{\hat{\varepsilon}}}_{t-l}\right). \tag{4.A.9}$$

The algorithm loops between Equation (4.A.6) and Equation (4.A.9) until there is convergence in the estimated parameters of $f(\bullet)$, in the parameters and specification of $g(\bullet)$, and in estimates of the

elements of the covariance matrices for ε_t and u_t. The degrees of freedom for the combined model can be calculated as d.f. = $(n - l) - (k + l + 2)$, where n is the number of observations, k is the total number of explanatory variables in $f(\bullet)$, l is the number of lagged variables in $g(\bullet)$, and $(k + l + 2)$ represents the total number of parameters in the combined model including intercepts from both $f(\bullet)$ and $g(\bullet)$.

This approach can be generalized to equation systems where $\mathbf{Y}_t$ is a vector:

$$\begin{pmatrix} Y_{1,t} \\ \vdots \\ Y_{n,t} \end{pmatrix} = f\left(X_{t,1},\ldots,X_{t-l,k}, \begin{pmatrix} Y_{1,t-1} & \cdots & Y_{1,t-l} \\ \vdots & \ddots & \vdots \\ Y_{n,t-1} & \cdots & Y_{n,t-l} \end{pmatrix} \right) + \begin{pmatrix} \varepsilon_{1,t} \\ \vdots \\ \varepsilon_{n,t} \end{pmatrix}, \tag{4.A.10}$$

$$\mathbf{Y}_t = f\left(\mathbf{X}_t,\ldots,\mathbf{X}_{t-l},\mathbf{Y}_t,\ldots,\mathbf{Y}_{t-l}\right) + \boldsymbol{\varepsilon}_t$$

and where the time series process includes co-varying time series observations (TSOs):

$$\boldsymbol{\eta}_t = \begin{pmatrix} \boldsymbol{\varepsilon}_t \\ \vdots \\ \mathbf{Z}_t \end{pmatrix} = g\left(\boldsymbol{\varepsilon}_{t-1},\ldots,\boldsymbol{\varepsilon}_{t-l},\ldots,\mathbf{Z}_{t-1},\ldots,\mathbf{Z}_{t-l}\right) + \mathbf{u}_t . \tag{4.A.11}$$

4.8. Supplement 4.A. Additional Analyses and Diagnostic Plots.

We hypothesized that complex patterns previously described in the depth profile obtained from Pacific sleeper shark archived electronic tag time series data in the Gulf of Alaska (Hulbert et al. 2006; Figures 4.S.A.1–4.S.A.3) could be efficiently modeled as simple time series processes. Three types of vertical movement behavior have been described for Pacific sleeper sharks in the Gulf of Alaska based on observed patterns in the fine scale (1 minute) time-series depth profile recorded from electronic archival tags (Hulbert et al. 2006). These include a diel vertical movement pattern, a systematic vertical oscillation movement pattern, and an irregular vertical movement pattern (4.S.A.1–4.S.A.3). As a proof of concept, we fit the three previously described patterns using a single autoregressive (AR) time series model at lagged time steps of 1, 2, and 3 minutes: AR(3) (Figures 4.S.A.1 – 4.S.A.3). That is, depth in the current time period (minute) was closely predicted by depth in the previous three periods (minutes), regardless of the complex patterns apparent in the data. Similarly, an AR(2) process fit to the first difference of the raw depth data (not shown) produced reasonable fits to the first differenced depth data with highly significant coefficients. Preliminary analyses (not shown) also indicated that the first difference of the raw depth data produced a stationary time series, which was consistent with either a random walk process or a long memory process.

Environmental data collected from near the tag release location (Figure 4.S.A.4) with significant linear correlations to *Ln-Tag-Depth* (Figure 4.S.A.5) were included as potential explanatory variables in the structural models (SMs). Preliminary analysis of smoothed trends in average hourly tag depth were investigated and found to be relatively shallower during hours of Night compared to hours of Twilight and Day and relatively shallower during hours of Night compared to hours of Moonlight (Figures 4.S.A.6–4.S.A.8). The smoothed trends were nonlinear over time, and there were no hours with Night or Moonlight during the months of June or July. Density plots of average tag depth each hour were investigated by month separately for Spring and Neap tides; deeper depths had relatively higher density during Spring tides than Neap tides during the months of September, October, and November; and the densities during Spring tides were strongly bimodal in the months of October and November (Figure 4.S.A.9).

Additional model diagnostics are provided in Figures 4.S.A.10–4.S.A.13, as described in the main text of Chapter 4 above.

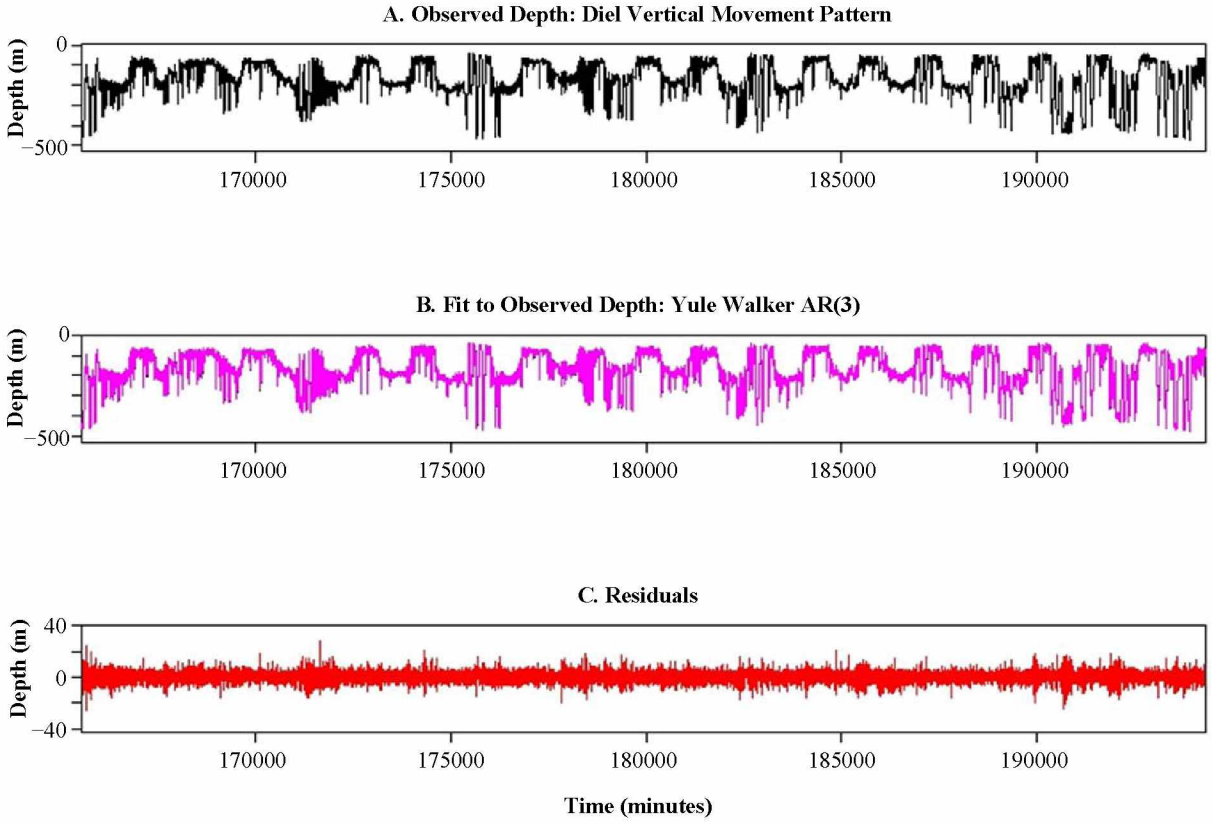

Figure 4.S.A.1: Example of diel vertical movement pattern in tag depth.
Example of a diel vertical movement pattern in tag depth recorded at 1 minute intervals during the period 9/24/2002–10/14/2002 (Panel A); adapted from Hulbert et al. (2006, their Figure 4), fit here in R statistical software using a Yule-Walker autoregressive function with lag 3, AR(3) (Panel B), along with the residuals (Panel C).

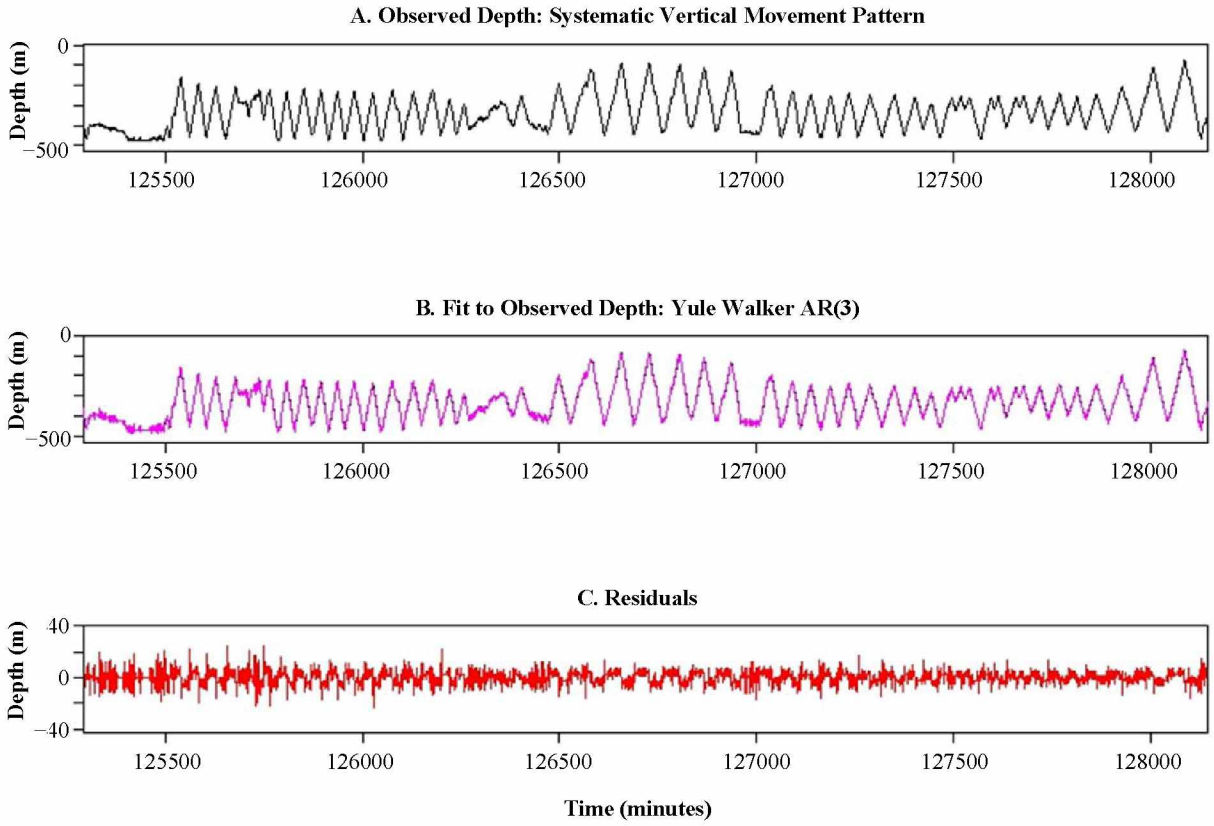

Figure 4.S.A.2: Example of systematic vertical oscillation movement pattern in tag depth.
Example of a systematic vertical oscillation movement pattern in tag depth recorded at 1 minute intervals during the period 8/27/2002–8/28/2002 (Panel A); adapted from Hulbert et al. (2006, their Figure 5a), fit here in R statistical software using a Yule-Walker autoregressive function with lag 3, AR(3) (Panel B), along with the residuals (Panel C).

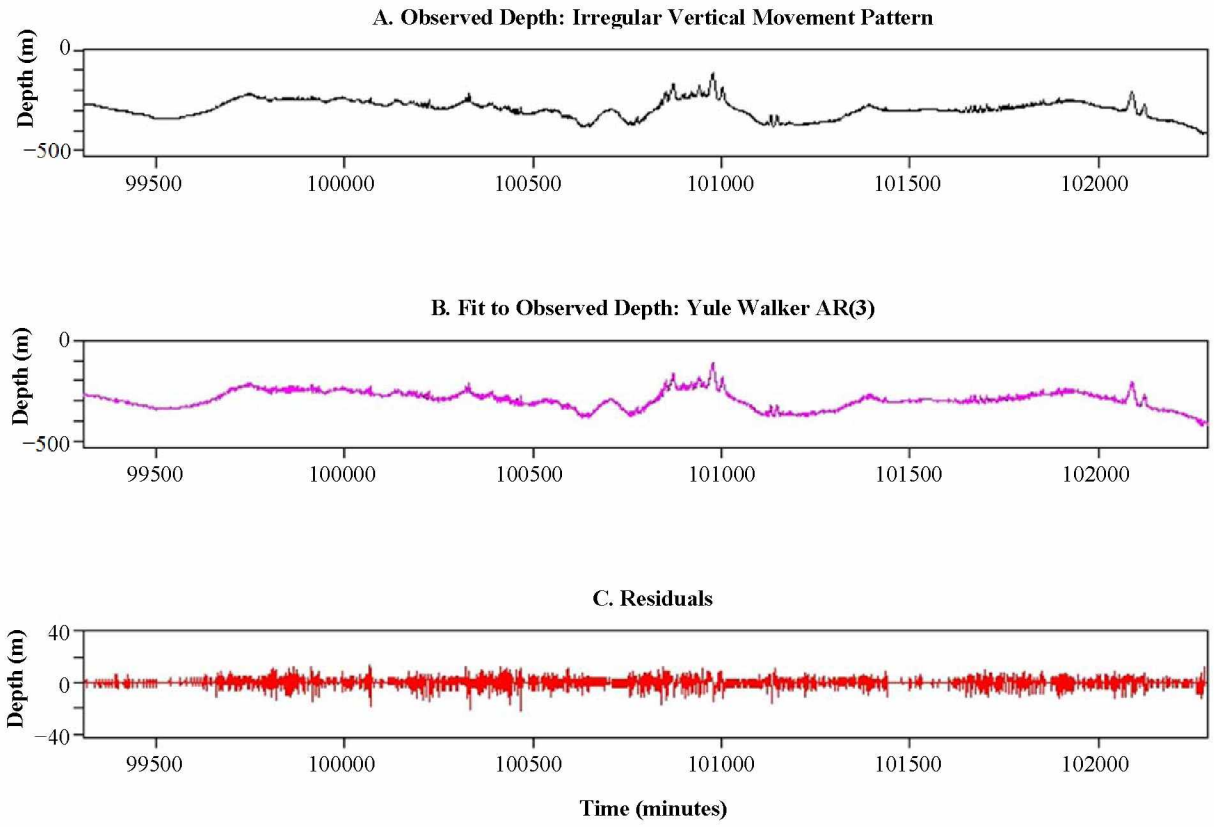

Figure 4.S.A.3: Example of irregular vertical movement pattern in tag depth.
Example of an irregular vertical movement pattern in tag depth recorded at 1 minute intervals during the period 8/9/2002–8/10/2002 (Panel A); adapted from Hulbert et al. (2006, their Figure 5b), fit here in R statistical software using a Yule-Walker autoregressive function with lag 3, AR(3) (Panel B), along with the residuals (Panel C).

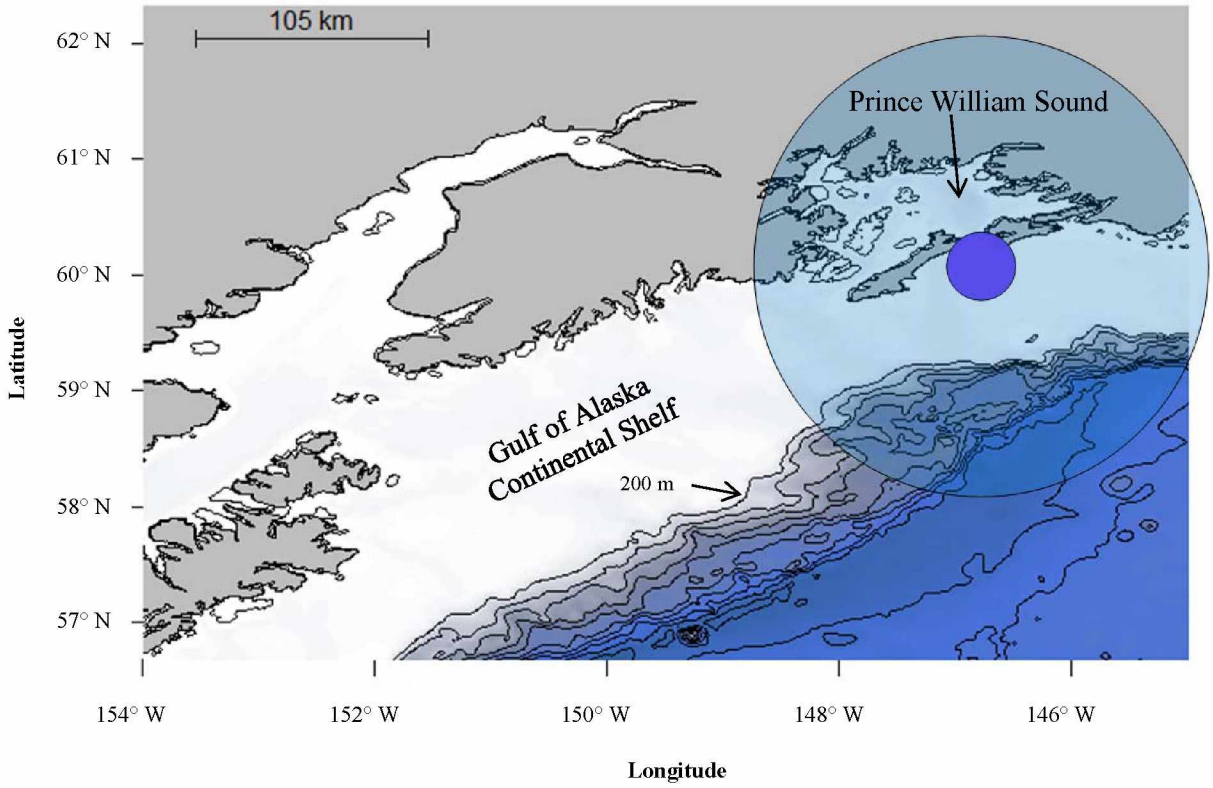

Figure 4.S.A.4: Tagged Pacific sleeper shark release location and possible range.
Tagged Pacific sleeper shark release location (near Cape Hinchinbrook, Hinchinbrook Island, Alaska; approximate location 60.24° N, 146.65° W; small solid circle); the tag data investigated in this study was previously analyzed by Hulbert et al. (2006 their tag #21); most (76%) of the tags released on Pacific sleeper sharks in the Hulbert et al. (2006) study were recovered within 100 km (diameter of larger circle) up to one year after release; consequently, the potential habitat occupied by the tagged Pacific sleeper shark investigated in this study (June–November, 2002) includes the deep waters of Prince William Sound (> 200 m), the Gulf of Alaska (GOA) continental shelf (c. 200 m), GOA continental shelf gullies (c. 300 m) and the GOA shelf break (c. 200 m to abyssal depths).

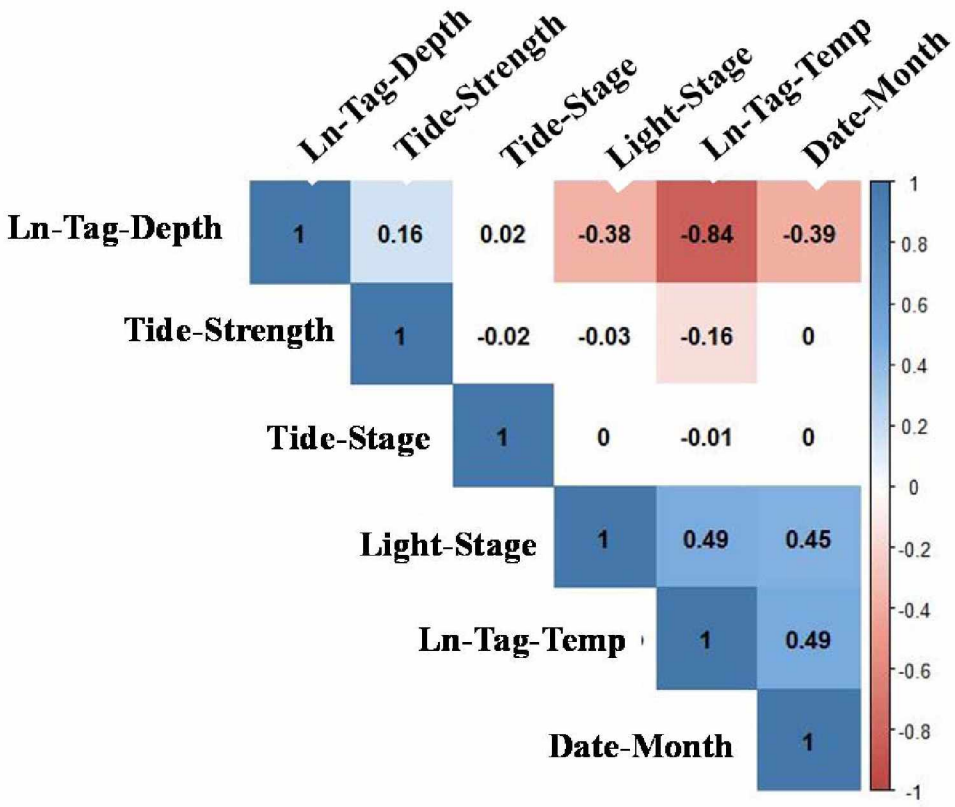

Figure 4.S.A.5: Linear correlation coefficients among environmental and tag data.
Linear correlation coefficients among environmental and tag data (shaded cells have significant correlation, P-values ≤ 0.01) as defined in the methods of the main document.

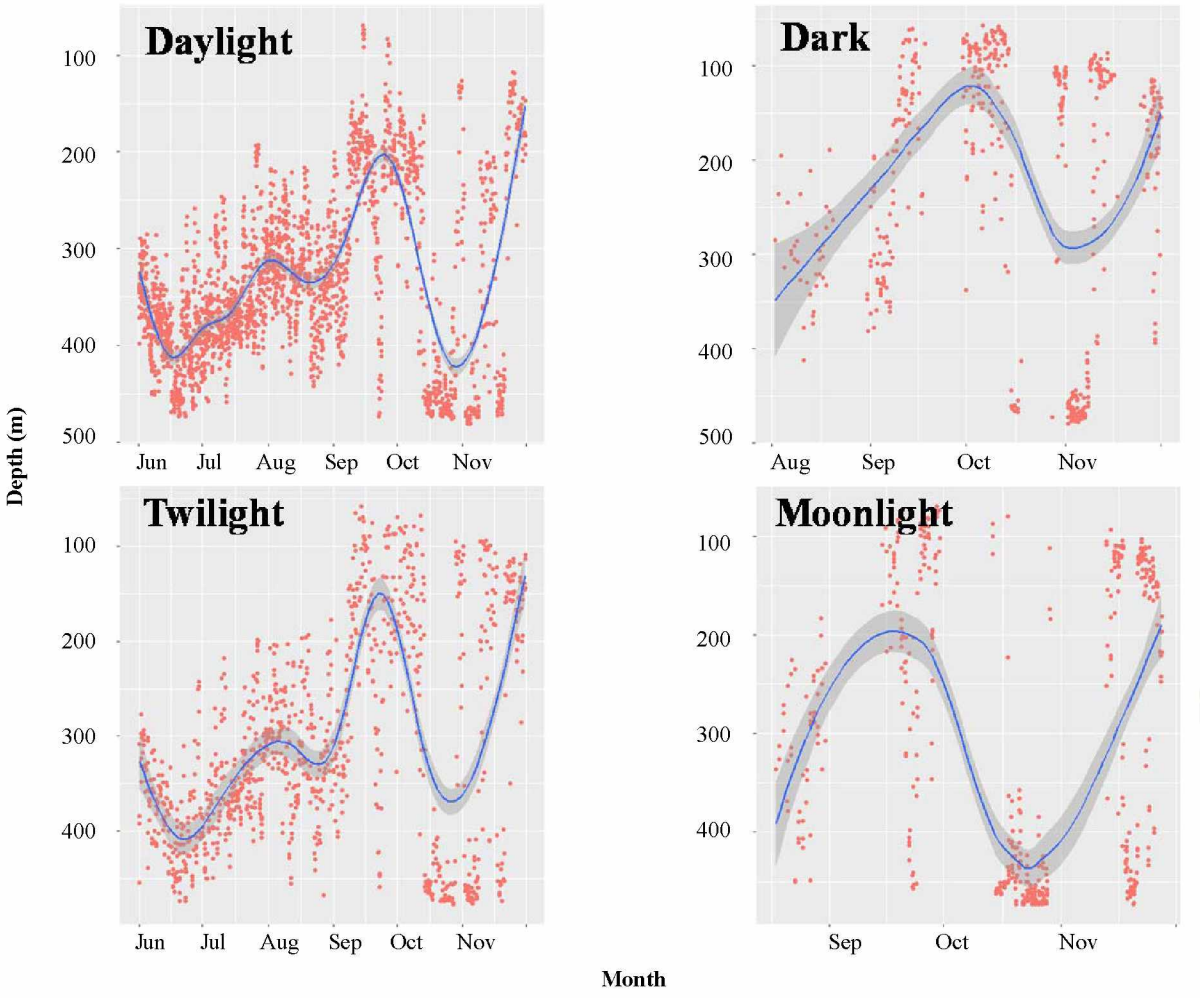

Figure 4.S.A.6: Smoothed trends in tag depth (Daylight, Twilight, Moonlight, and Dark). Smoothed trends in average tag depth each hour fit separately by *Light-Stage* (Daylight, Twilight, Moonlight, and Dark), as defined in the methods of the main document.

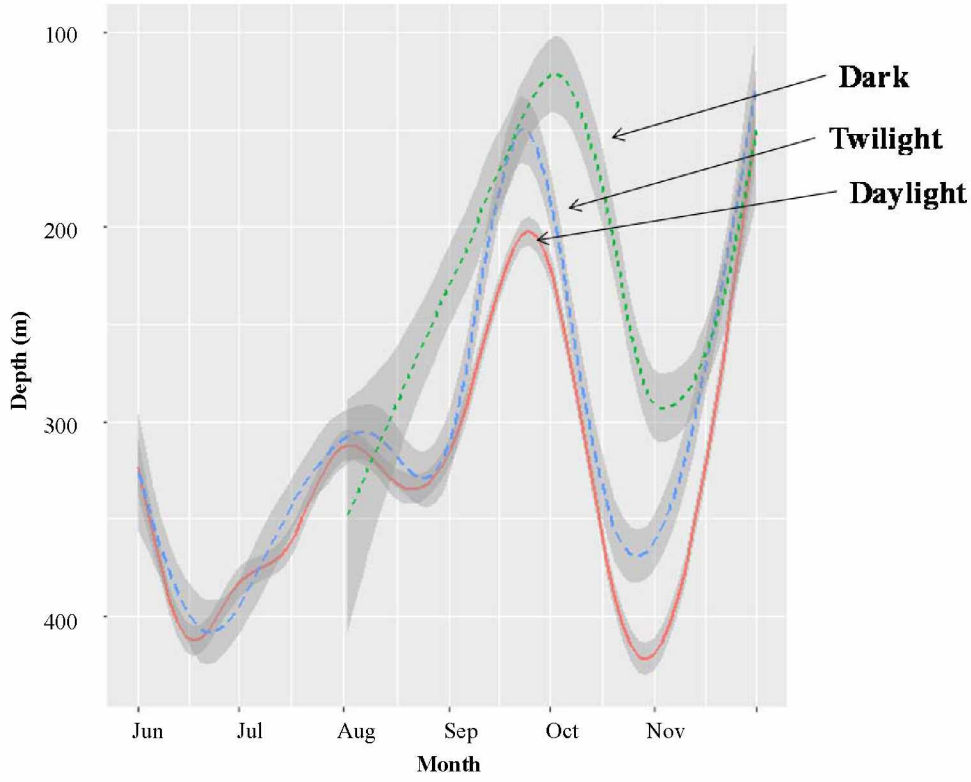

Figure 4.S.A.7: Smoothed trends in tag depth (Dark, Twilight, and Daylight).
Smoothed trends in average tag depth each hr. fit separately by *Light-Stage* (Dark, Twilight, and Daylight), as defined in the methods of the main document, were relatively shallower at Dark and Twilight, respectively, than during Daylight. Smoothed trends were nonlinear over time, and there were no hours of Dark in June or July.

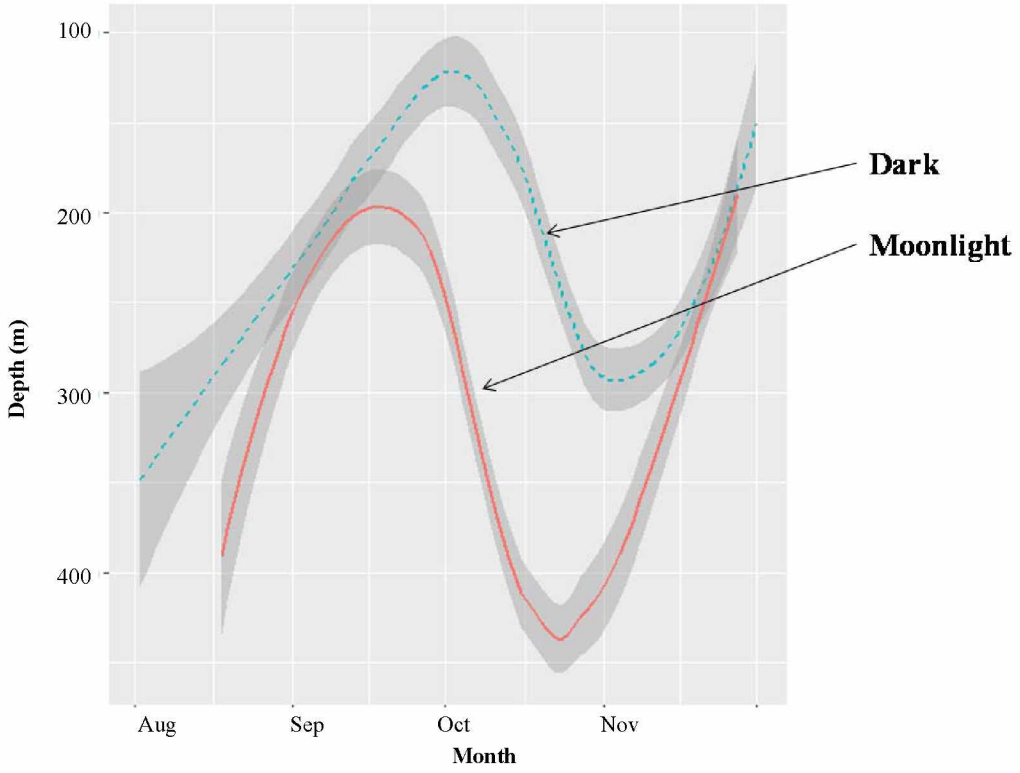

Figure 4.S.A.8: Smoothed trends in tag depth (Dark and Moonlight).
Smoothed trends in average tag depth each hr. fit separately by *Light-Stage* (Dark and Moonlight), as defined in the methods of the main document, were relatively shallower at Dark than Moonlight. Smoothed trends were nonlinear over time, and there here were no hours of Dark or Moonlight in June or July.

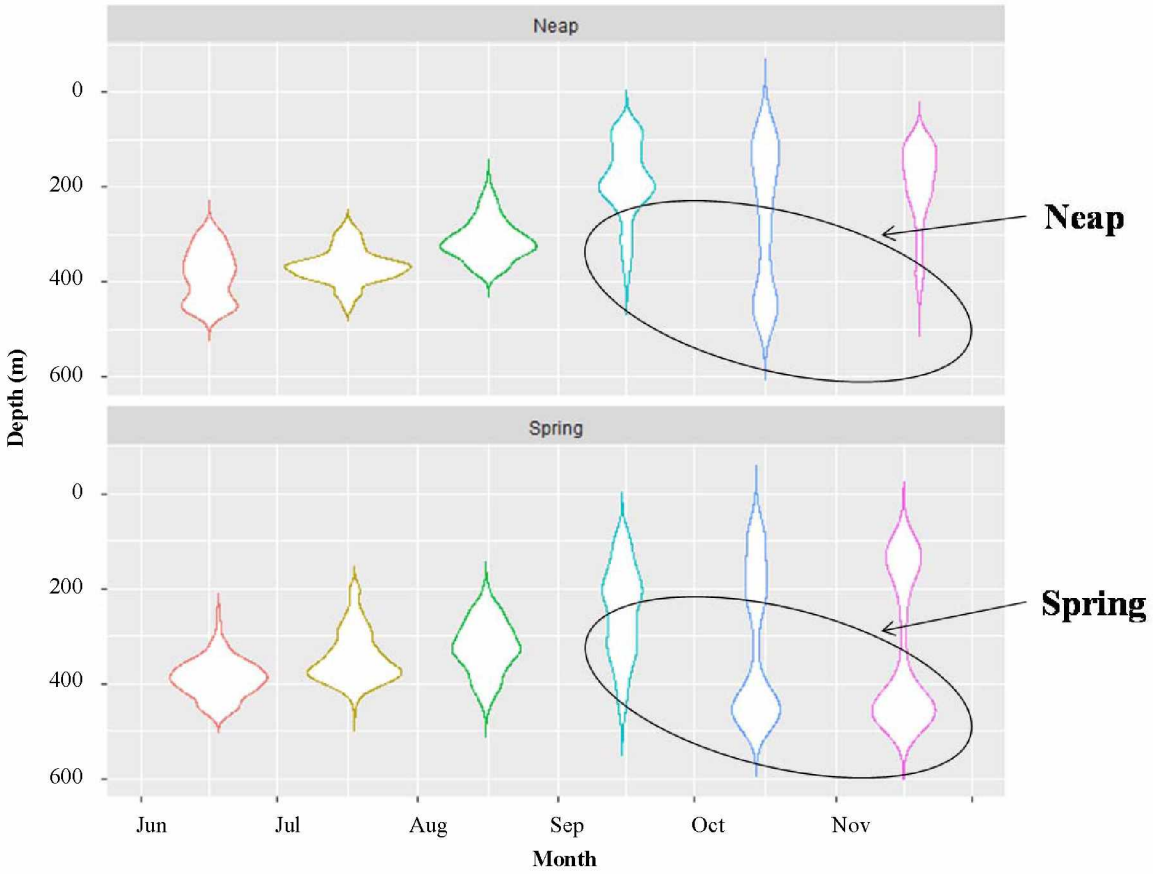

Figure 4.S.A.9: Density plots of tag depth (Spring and Neap).
Density plots of average hourly tag depth by *Date-Month* (June, July, August, September, October, and November) and *Tide-Strength* (Spring and Neap), as defined in the methods of the main document. Deeper depths had relatively higher density during Spring tides compared to Neap tides during the months of September, October, and November. The densities during Spring tides were strongly bimodal in the months of October and November.

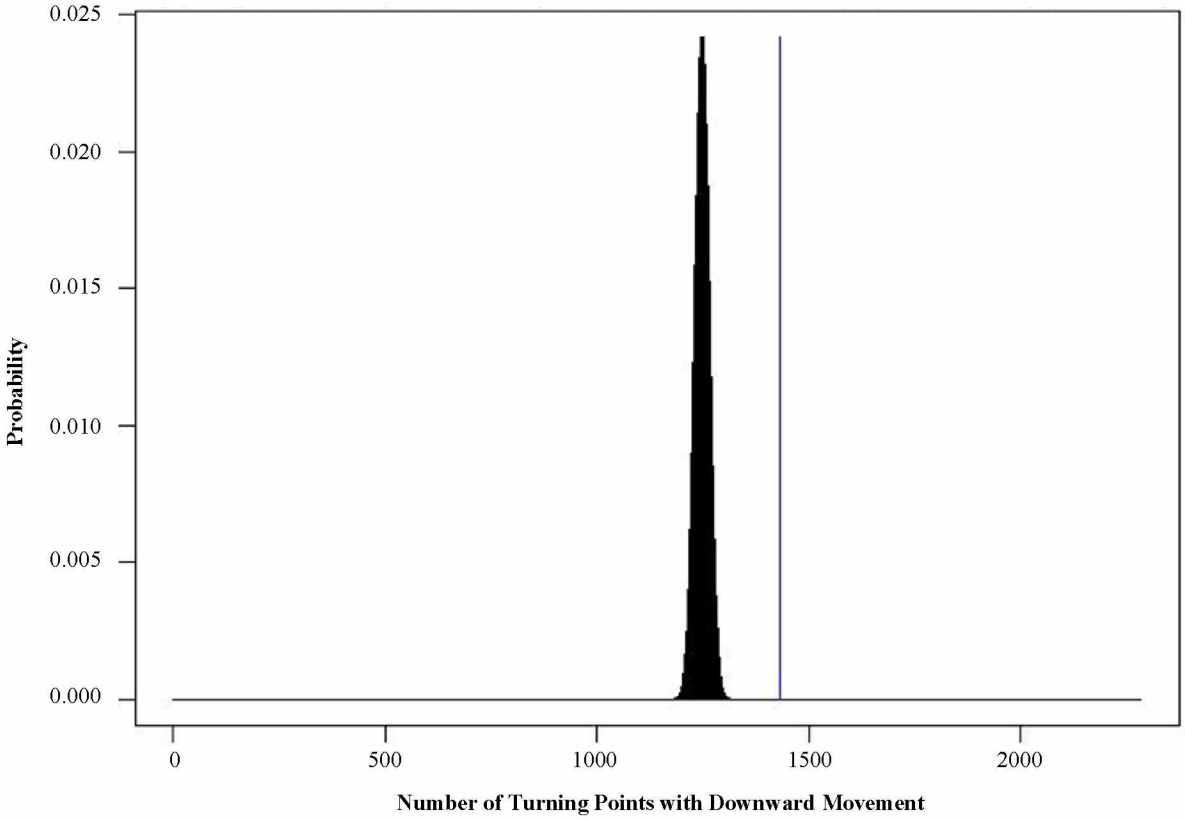

Figure 4.S.A.10: Henriksson–Merton's turning point test predictions.
Correct turning point predictions of downward movement obtained with the Henriksson–Merton's turning point test for TSM.1 (1433; line) were significantly larger than would have been obtained at random (hypergeometric distribution; black histogram P-value <0.001) for the combined (SM.1 + TSM.1) model at the converged parameter estimates after 100 iterations.

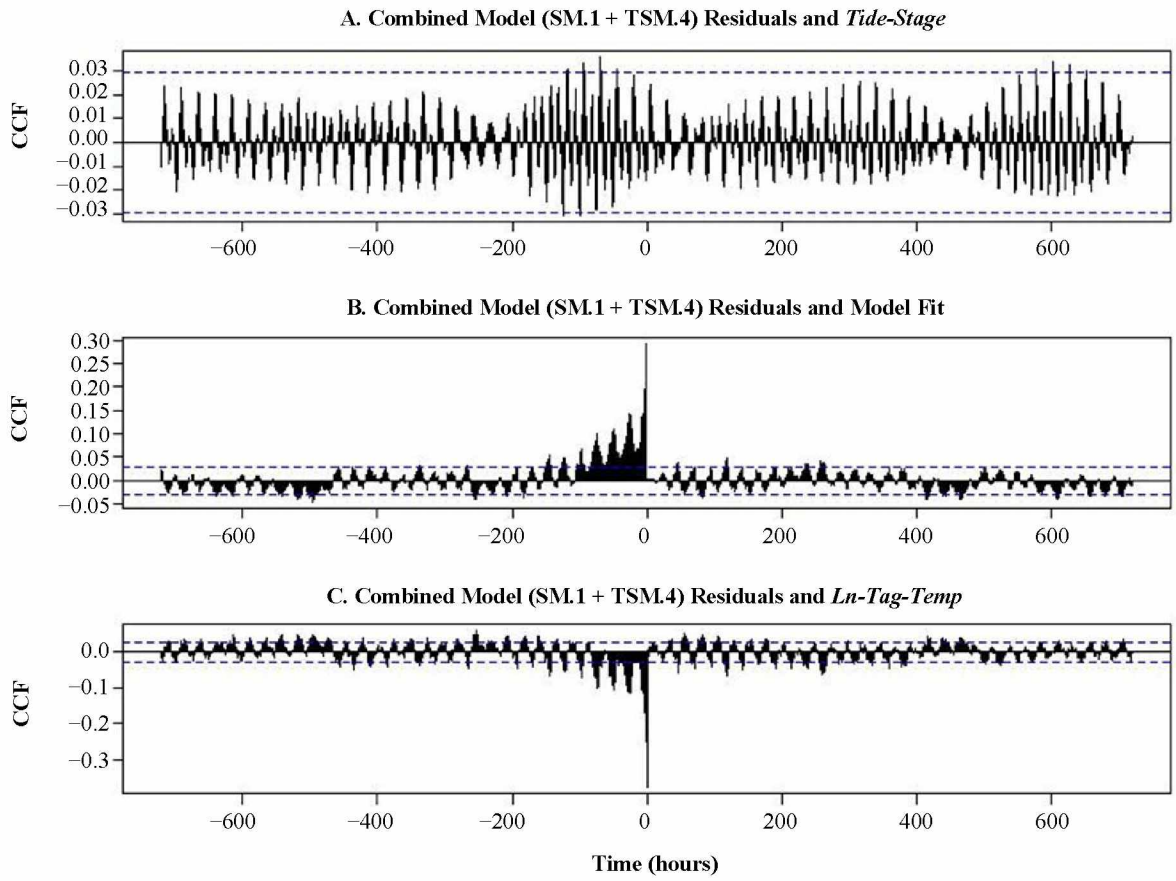

Figure 4.S.A.11: Cross correlation function of SM.1 + TSM.4 lagged residuals (c. 1 month).
Cross correlation function (CCF) of lagged residuals (moving to the left from zero) of the combined model (SM.1 + TSM.4) after 100 iterations plotted against lagged (moving to the right from zero) *Tide-Stage* (Panel A), model fit (Panel B), and *Ln-Tag-Temp* (Panel C) for lags of up to 720 hours (c. 1 month); the stippled lines represent the approximate 95% confidence intervals for lagged AR processes.

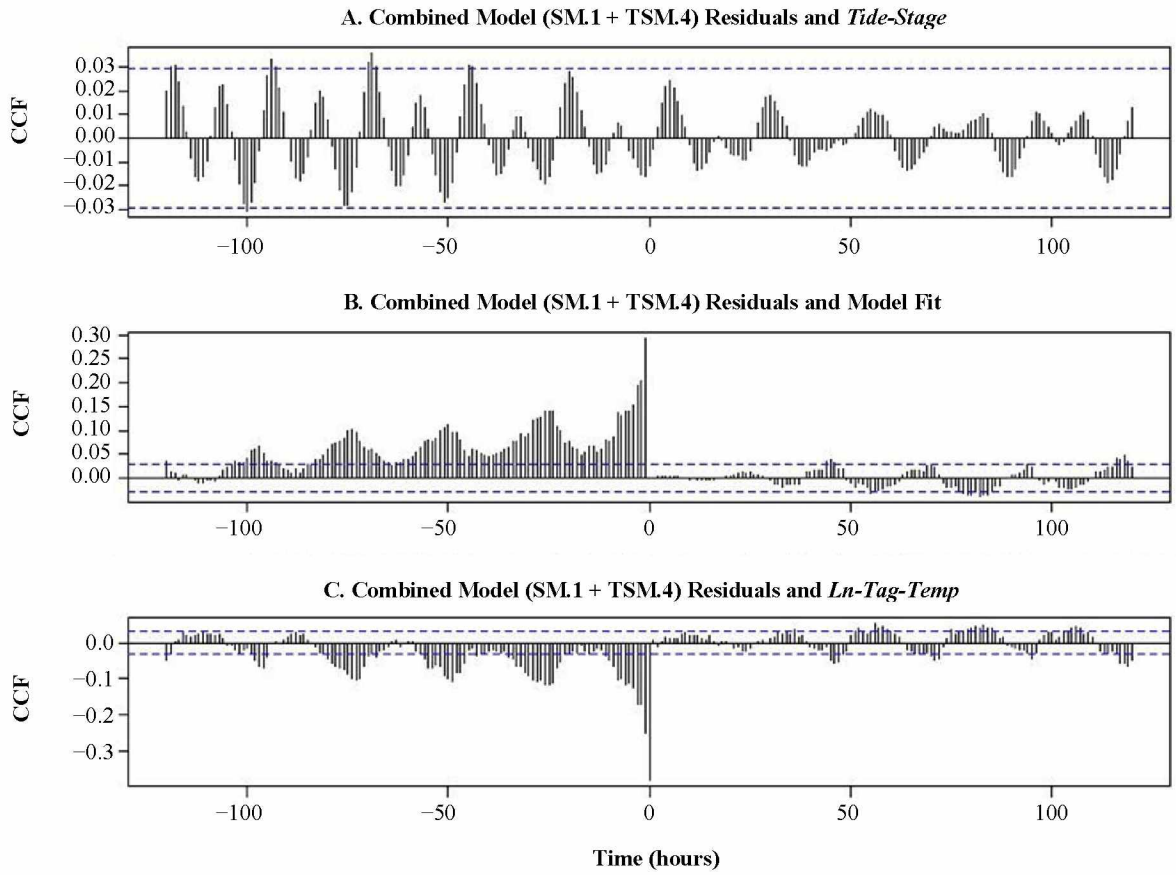

Figure 4.S.A.12: Cross correlation function of SM.1 + TSM.4 lagged residuals (5 days).
Cross correlation function (CCF) of lagged residuals (moving to the left from zero) of the combined model (SM.1 + TSM.4) after 100 iterations plotted against lagged (moving to the right from zero) *Tide-Stage* (Panel A), model fit (Panel B), and *Ln-Tag-Temp* (Panel C) for lags of up to 120 hours (5 days); the stippled lines represent the approximate 95% confidence intervals for lagged AR processes.

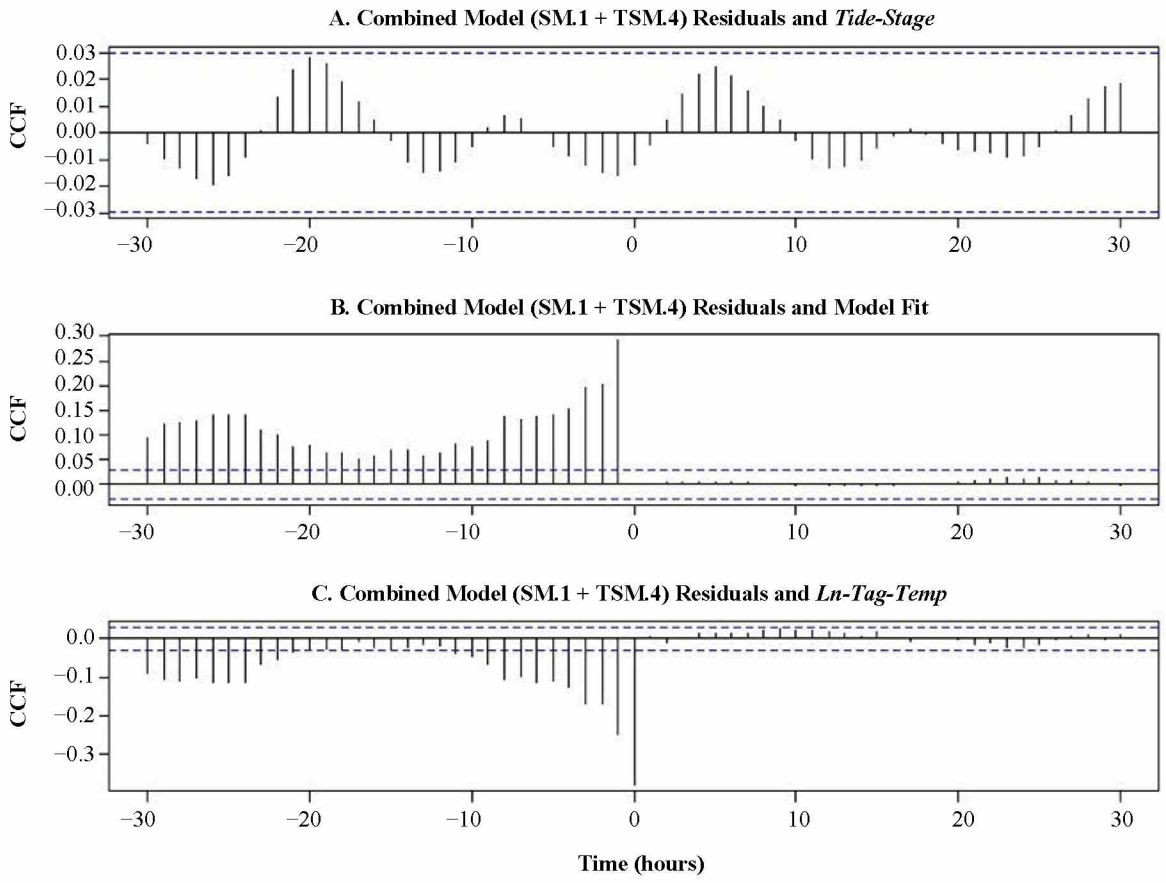

Figure 4.S.A.13: Cross correlation function of SM.1 + TSM.4 lagged residuals (c. 1 day).
Cross correlation function (CCF) of lagged residuals (moving to the left from zero) of the combined model (SM.1 + TSM.4) after 100 iterations plotted against lagged (moving to the right from zero) *Tide-Stage* (Panel A), model fit (Panel B), and *Ln-Tag-Temp* (Panel C) for lags of up to 30 hours (c. 1 day); the stippled lines represent the approximate 95% confidence intervals for lagged AR processes.

Conclusions

Chapter 1 identified a significant increase in Pacific sleeper shark relative abundance from sablefish longline surveys in the Gulf of Alaska during the years 1989–2003. This result was consistent with the CPUE of Pacific sleeper sharks captured incidentally in fishery independent bottom trawl surveys, which also increased significantly between the years 1984 and 1996 in the same region. Accurate relative abundance indices are needed for stock assessment. However, high inter-annual variability (probably resulting from low sample size) in Pacific sleeper shark CPUE obtained from sablefish longline surveys may reflect factors other than abundance. Consequently, it might be important to compare Pacific sleeper shark relative abundance trends obtained from sablefish longline surveys to those obtained from another fishery independent longline survey in the region conducted by the International Pacific Halibut Commission (IPHC) in order to verify the results.

In Chapter 2, forward projection with Monte Carlo simulation using a length-based age-structured model identified that the aggregate risk of Pacific sleeper shark incidental exploitation rates ending in an overfished condition in the Gulf of Alaska increased from 0% under a low exploitation rate scenario to 59% under a high exploitation rate scenario. This result is important for management because the low exploitation rate scenario was based on official catch estimates and all of the plausible scenario combinations explored using the low exploitation rate scenario were sustainable. In contrast, the high exploitation rate scenario was based on preliminary estimates of unreported incidental catch, and many of the plausible scenario combinations explored using the high exploitation rate scenario resulted in a high proportion of runs ending in an overfished condition. Consequently, a priority for management is to reduce the uncertainty in unreported Pacific sleeper shark incidental catch estimates in the Gulf of Alaska. An observer program is now in place to monitor the historically unobserved Pacific halibut fishery in the Gulf of Alaska, which will reduce this uncertainty.

In Chapter 3, analysis of stable isotope ratios of nitrogen ($\delta^{15}N$) and lipid normalized carbon ($\delta^{13}C'$) identified feeding in separate food webs in the EBS and GOA and increasing trophic position with length. Stable-isotope and stomach-content analysis results were consistent in suggesting that changes in Pacific sleeper shark abundance could have direct effects on relatively lower trophic level populations of fishes and squid in both the EBS and GOA. These results can be used in ecosystem models to predict ecosystem responses to changes in Pacific sleeper shark relative abundance.

In Chapter 4, time series analysis of Pacific sleeper shark electronic archival tag data demonstrated that statistical inference about habitat utilization can be drawn from an entire time series depth profile stored on electronic archival tags. A simple autoregressive relationship was identified governing Pacific sleeper shark short-term movements (at an hourly time step) and a structural model was

identified governing longer time period movement patterns (at a monthly time step). These results can be used to develop mathematical models of Pacific sleeper shark time at depth in order to identify possible interactions with commercial fisheries and with other species in the northeast Pacific Ocean.

References

Baum, J. K., and B. Worm. 2009. Cascading top-down effects of changing oceanic predator abundances. Journal of Animal Ecology 78:699–714.

Benz, G. W., R. Hocking, A. Kowunna Sr., S. A. Bullard, and J. C. George. 2004. A second species of Arctic shark: Pacific sleeper shark *Somniosus pacificus* from Point Hope, Alaska. Polar Biology 27:250–252.

Borets, L. A. 1986. Ichthyofauna of the Northwestern and Hawaiian submarine ranges. Journal of Ichthyology 26:1–13.

Bright, H. B. 1959. The occurrence and food of the sleeper shark, *Somniosus pacificus*, in a central Alaska bay. Copeia 1:76–77.

Caut, S., E. Angulo, and F. Courchamp. 2009. Variation in discrimination factors ($\Delta^{15}N$ and $\Delta^{13}C$): the effect of diet isotopic values and applications for diet reconstruction. Journal of Applied Ecology 46:443–453.

Chikaraishi, Y., N. O. Ogawa, Y. Kashiyama, Y. Takano, H. Suga, A. Tomitani, H. Miyashita, H. Kitazato, and N. Ohkouchi. 2009. Determination of aquatic food-web structure based on compound-specific nitrogen isotopic composition of amino acids. Limnology and Oceanography-Methods 7:740–750.

Compagno, L. J. V. 1984. FAO species catalogue. Vol. 4. Sharks of the world. An annotated and illustrated catalogue of shark species known to date, part 1 - hexanchiformes to lamniformes. FAO Fisheries Synopsis 125:1–249.

Cortés 1999, E. 1999. Standardized diet compositions and trophic levels of sharks. ICES Journal of Marine Science 56:707–717.

Courtney, D., C. Tribuzio, and K. J. Goldman. 2006a. Section 18, BSAI sharks. Pages 1083–1132 *in* Stock assessment and fishery evaluation report for the groundfish resources of the Bering Sea and Aleutian Islands for 2007. North Pacific Fishery Management Council, Anchorage, Alaska.

Courtney, D., C. Tribuzio, K. J. Goldman, and J. Rice. 2006b. Appendix E, GOA sharks. Pages 481–562 *in* Stock assessment and fishery evaluation report for the groundfish resources of the Gulf of Alaska for 2007. North Pacific Fishery Management Council, Anchorage, Alaska.

Dale, J. J., N. J. Wallsgrove, B. N. Popp, and K. N. Holland. 2011. Nursery habitat use and foraging ecology of the brown stingray *Dasyatis lata* determined from stomach contents, bulk and amino acid stable isotopes. Marine Ecology Progress Series 433:221–236.

DeNiro, M. J., and S. Epstein. 1978. Influence of diet on distribution of carbon isotopes in animals. Geochimica et Cosmochimica Acta 42:495–506.

DeNiro, M. J., and S. Epstein. 1981. Influence of diet on the distribution of nitrogen isotopes in animals. Geochimica et Cosmochimica Acta 45:341–351.

Ebert, D. A., L. J. V. Compagno, and L. J. Natanson. 1987. Biological notes on the Pacific sleeper shark, *Somniosus pacificus* (chondrichthyes: squalidae). California Fish and Game 73:117–123.

Ebert, D. A., and M. V. Winton. 2010. Chondrichthyans of high latitude seas. Pages 115–158 *in* J. C. Carrier, J. A. Musick, and M. R. Heithaus, editors. Sharks and their relatives II; biodiversity, adaptive physiology, and conservation. CRC Press, Boca Raton, FL.

Forrest, R. E., and C. J. Walters. 2009. Estimating thresholds to optimal harvest rate for long-lived, low-fecundity sharks accounting for selectivity and density dependence in recruitment. Canadian Journal of Fisheries and Aquatic Sciences 66:2062–2080.

Frid, A., G. G. Baker, and L. M. Dill. 2008. Do shark declines create fear-released systems? Oikos 117:191–201.

Frid, A., J. Burns, G. G. Baker, and R. E. Thorne. 2009. Predicting synergistic effects of resources and predators on foraging decisions by juvenile Steller sea lions. Oecologia 158:775–786.

Frid, A., L. M. Dill, R. E. Thorne, and G. M. Blundell. 2007. Inferring prey perception of relative danger in large-scale marine systems. Evolutionary Ecology Research 9:635–649.

Gotshall, D. W., and T. Jow. 1965. Sleeper sharks (*Somniosus pacificus*) off Trinidad, California, with life history notes. California Fish and Game 51:294 –298.

Hansen, P. M. 1963. Tagging experiments with the Greenland shark (*Somniosus microcephalus* (Bloch and Schneider)) in Subarea 1. International Commission Northwest Atlantic Fisheries Special Publication 4:172–175.

Heithaus, M. R., A. Frid, J. J. Vaudo, B. Worm, and A. J. Wirsing. 2010. Unraveling the ecological importance of elasmobranchs. Pages 611–638 *in* J. C. Carrier, J. A. Musick, and M. R. Heithaus, editors. Sharks and their relatives II; biodiversity, adaptive physiology, and conservation. CRC Press, Boca Raton, FL.

Heithaus, M. R., A. Frid, A. J. Wirsing, and B. Worm. 2008. Predicting ecological consequences of marine top predator declines. Trends in Ecology and Evolution 23:202–210.

Hollowed, A. B., and W. S. Wooster. 1995. Decadal-scale variations in the eastern subarctic Pacific: II. Response of northeast Pacific fish stocks. Pages 373–385 *in* R. J. Beamish, editor. Climate change and northern fish populations. Canadian Special Publication in Fisheries and Aquatic Science 121.

Horning, M., and J. A. E. Mellish. 2014. In cold blood: evidence of Pacific sleeper shark (*Somniosus pacificus*) predation on Steller sea lions (*Eumetopias jubatus*) in the Gulf of Alaska. Fishery Bulletin 112:297–310.

Hulbert, L. B., M. F. Sigler, and C. R. Lunsford. 2006. Depth and movement behaviour of the Pacific Sleeper Shark in the northeast Pacific Ocean. Journal of Fish Biology 69:406–425.

Hussey, N. E., J. Brush, I. D. McCarthy, and A. T. Fisk. 2010a. $\delta^{15}N$ and $\delta^{13}C$ diet-tissue discrimination factors for large sharks under semi-controlled conditions. Comparative Biochemistry and Physiology A 155:445–453.

Hussey, N. E., A. Cosandey-Godin, R. P. Walter, K. J. Hedges, M. VanGerwen-Toyne, A. N. Barkley, S. T. Kessel, and A. T. Fisk. 2015. Juvenile Greenland sharks *Somniosus microcephalus* (Bloch & Schneider, 1801) in the Canadian Arctic. Polar Biology 38:493–504.

Hussey, N. E., S. F. J. Dudley, I. D. McCarthy, G. Cliff, and A. T. Fisk. 2011. Stable isotope profiles of large marine predators: viable indicators of trophic position, diet, and movement in sharks? Canadian Journal of Fisheries and Aquatic Sciences 68:2029–2045.

Hussey, N. E., M. A. MacNeil, and A. T. Fisk. 2010b. The requirement for accurate diet tissue discrimination factors for interpreting stable isotopes in sharks. Hydrobiologia 654:1–5.

Hussey, N. E., M. A. MacNeil, J. A. Olin, B. C. McMeans, M. J. Kinney, D. D. Chapman, and A. T. Fisk. 2012. Stable isotopes and elasmobranchs: tissue types, methods, applications and assumptions. Journal of Fish Biology 80:1449–1484.

Kim, S. L., and P. L. Koch. 2012. Methods to collect, preserve, and prepare elasmobranch tissues for stable isotope analysis. Environmental Biology of Fishes 95:53–63.

Kitchell, J. F., T. E. Essington, C. H. Boggs, D. E. Schindler, and C. J. Walters. 2002. The role of sharks and longline fisheries in a pelagic ecosystem of the central Pacific. Ecosystems 5:202–216.

Kyne, P. M., and C. A. Simpfendorfer. 2010. Deepwater chondrichthyans. Pages 37–113 *in* J. C. Carrier, J. A. Musick, and M. R. Heithaus, editors. Sharks and their relatives II: biodiversity, adaptive physiology, and conservation. CRC Press, Boca Raton, Florida.

Logan, J. M. and M. E. Lutcavage. 2010a. Stable isotope dynamics in elasmobranch fishes. Hydrobiologia 644:231–244.

Logan, J. M. and M. E. Lutcavage. 2010b. Reply to Hussey et al.: The requirement for accurate diet-tissue discrimination factors for interpreting stable isotopes in sharks. Hydrobiologia 654:7–12.

Marsh, J. M., N. Hillgruber, and R. J. Foy. 2012. Temporal and ontogenetic variability in trophic role of four groundfish species—walleye pollock, pacific cod, arrowtooth flounder, and Pacific halibut—around Kodiak Island in the Gulf of Alaska. Transactions of the American Fisheries Society 141:468–486.

Martínez del Rio, C., N. Wolf, S. A. Carleton, and L. Z. Gannes. 2009. Isotopic ecology ten years after a call for more laboratory experiments. Biological Reviews 84:91–111.

Maunder, M. N., and A. E. Punt. 2004. Standardizing catch and effort data: a review of recent approaches. Fisheries Research 70:141–159.

McMeans, B. C., J. Svavarsson, S. Dennard, and A. T. Fisk. 2010. Diet and resource use among Greenland sharks (*Somniosus microcephalus*) and teleosts sampled in Icelandic waters, using $\delta^{13}C$, $\delta^{15}N$, and mercury. Canadian Journal of Fisheries and Aquatic Sciences 67:1428–1438.

Mecklenburg, C. W., T. A., Mecklenburg, and L. K. Thorsteinson. 2002. Fishes of Alaska. American Fisheries Society, Bethesda, MD.

Menon, M. M. 2004. Spatiotemporal modeling of Pacific Sleeper Shark (*Somniosus pacificus*) and Spiny Dogfish (*Squalus acanthias*) bycatch in the northeast Pacific Ocean. Master's thesis. University of Washington, Seattle.

Menon, M. M., V. F. Gallucci, and L. L. Conquest. 2005. Sampling designs for the estimation of longline bycatch. Pages 851–870 *in* G. H. Kruse, V. F. Gallucci, D. E. Hay, R. I. Perry, R. M. Peterman, T. C. Shirley, P. D. Spencer, B. Wilson, and D. Woodby, editors. Fisheries assessment and management in data-limited situations. Alaska Sea Grant College Program, AK-SG-05-02, University of Alaska, Fairbanks.

Minagawa, M., and E. Wada. 1984. Stepwise enrichment of ^{15}N along food chains: further evidence and the relation between ^{15}N and animal age. Geochimica et Cosmochimica Acta 48:1135–1140.

MSRA (Magnuson–Stevens Fishery Conservation and Management Reauthorization Act of 2006). 2006. U.S. Public Law 109-479, 120 Statute 3575.

Mueter, F. J., and B. L. Norcross. 2002. Spatial and temporal patterns in the demersal fish community on the shelf and upper slope regions of the Gulf of Alaska. Fishery Bulletin 100:559–581.

Murray, B. W., J. Y. Wang, S.-C. Yang, J. D. Stevens, A. Fisk, and J. Svavarsson. 2008. Mitochondrial cytochrome b variation in sleeper sharks (Squaliformes: Somniosidae). Marine Biology 153:1015–1022.

Myers, R. A., J. K. Baum, T. D. Shepherd, S. P. Powers, and C. H. Peterson. 2007. Cascading effects of the loss of apex predatory sharks from a coastal ocean. Science 315:1846–1850.

Nielsen, J., R. B. Hedeholm, J. Heinemeier, P. G. Bushnell, J. S. Christiansen, J. Olsen, C. B. Ramsey, R. W. Brill, M. Simon, K. F. Steffensen, and J. F. Steffensen. 2016. Eye lens radiocarbon reveals centuries of longevity in the Greenland shark (*Somniosus microcephalus*). Science 353:702–704.

O'Brien, S. M., V. F. Gallucci, and L. Hauser. 2013. Effects of species biology on the historical demography of sharks and their implications for likely consequences of contemporary climate change. Conservation Genetics 14:125–144.

Orlov, A. M. 1999. Capture of especially large sleeper shark *Somniosus pacificus* (Squalidae) with some notes on its ecology in northwestern Pacific. Journal of Ichthyology 39:548–553.

Orlov, A. M., and A. A. Baitalyuk. 2014. Spatial distribution and features of biology of Pacific sleeper shark *Somniosus pacificus* in the North Pacific. Journal of Ichthyology 54:526–546.

Orlov, A. M., and S. I. Moiseev. 1999a. New data on the biology of the Pacific sleeper shark, *Somniosus pacificus* (Squalidae) in the northwestern Pacific Ocean. Pages 177–186 *in* D. MacKinlay, K. Howard, and J. Cech Jr., editors. Fish performance studies. Department of Fisheries and Oceans, Vancouver, BC.

Orlov, A. M., and S. I. Moiseev. 1999b. Some biological features of Pacific sleeper shark, *Somniosus pacificus* (Bigelow et Schroeder 1944) (Squalidae) in the northwestern Pacific Ocean. Oceanological Studies 28:3–16.

Pikitch, E. K., C. Santora, E. A. Babcock, A. Bakun, R. Bonfil, D. O. Conover, P. Dayton, P., Doukakis, D. Fluharty, B. Heneman, E. D. Houde, J. Link, P. A. Livingston, M. Mangel, M. K. McAllister, J. Pope, and K. J. Sainsbury. 2004. Ecosystem based fishery management. Science 305:346–347.

Post, D. M. 2002. Using stable isotopes to estimate trophic position: models, methods, and assumptions. Ecology 83:703–718.

Rodgveller, C. J., C. R. Lunsford, and J. T. Fujioka. 2008. Evidence of hook competition in longline surveys. Fishery Bulletin 106:364–374.

Schaufler, L., R. Heintz, M. Sigler, and L. B. Hulbert. 2005. Fatty acid composition of sleeper shark (*Somniosus pacificus*) liver and muscle reveals nutritional dependence on planktivores. ICES CM 2005/N:05. Available at http://www.ices.dk/products/CMdocs/2005/N/N0505.pdf/ (accessed 1 June 2011).

Sigler, M. F., and J. T. Fujioka. 1988. Evaluation of variability in sablefish, *Anoplopoma fimbria*, abundance indices in the Gulf of Alaska using the bootstrap method. Fishery Bulletin 86:445–452.

Sigler, M. F., L. B. Hulbert, C. R. Lunsford, N. H. Thompson, K. Burek, G. O'Corry-Crowe, and A. C. Hirons. 2006. Diet of Pacific sleeper sharks, a potential Steller sea lion predator, in the northeast Pacific Ocean. Journal of Fish Biology 69:392– 405.

Smith, C. R., and A. R. Baco. 2003. Ecology of whale falls at the deep-sea floor. Oceanography and Marine Biology: an Annual Review 41:311–354.

Smith, S. E., D. W. Au, and C. Show. 1998. Intrinsic rebound potentials of 26 species of Pacific sharks. Marine and Freshwater Research 49:663–678.

Taggart, S. J., A. G. Andrews, J. Mondragon, and E. A. Mathews. 2005. Co-occurrence of Pacific sleeper sharks *Somniosus pacificus* and harbor seals *Phoca vitulina* in Glacier Bay. Alaska Fishery Research Bulletin 11:113–117.

Taylor, I. G., V. Gertseva, R. D. Methot Jr., and M. N. Maunder. 2013. A stock–recruitment relationship based on pre-recruit survival, illustrated with application to spiny dogfish shark. Fisheries Research 142:15–21.

Then, A. Y., J. M. Hoenig, N. G. Hall, and D. A. Hewitt. 2015. Evaluating the predictive performance of empirical estimators of natural mortality rate using information on over 200 fish species. ICES Journal of Marine Science 72:82–92.

Tribuzio, C. A., K. Echave, C. Rodgveller, and P.-J. Hulson. 2012. Section 20: assessment of the shark stock complex in the Bering Sea and Aleutian Islands. Pages 1771–1848 *in* Stock assessment and fishery evaluation report for the groundfish resources of the Bering Sea and Aleutian Islands for 2013. North Pacific Fishery Management Council, Anchorage, Alaska.

Tribuzio, C. A., K. Echave, C. Rodgveller, P.-J. Hulson, and K. J. Goldman. 2011. Chapter 20: assessment of the shark stock complex in the Gulf of Alaska. Pages 1393–1446 *in* Stock assessment and fishery evaluation report for the groundfish resources of the Gulf of Alaska for 2012. North Pacific Fishery Management Council, Anchorage, Alaska.

Vander Zanden, M. J., G. Cabana, and J. B. Rasmussen. 1997. Comparing trophic position of freshwater fish calculated using stable nitrogen isotope ratios ($\delta^{15}N$) and literature dietary data. Canadian Journal of Fisheries and Aquatic Sciences 54:1142–1158.

Vander Zanden, M. J. and J. B. Rasmussen. 2001. Variation in $\delta^{15}N$ and $\delta^{13}C$ trophic fractionation: implications for aquatic food web studies. Limnology and Oceanography 46:2061–2066.

Vanderklift, M. A. and S. Ponsard. 2003. Sources of variation in consumer-diet $\delta^{15}N$ enrichment: a meta-analysis. Oecologia 136:169–182.

Walter, R. P., D. Roy, N. E. Hussey, B. Stelbrink, K. M. Kovacs, C. Lydersen, B. C. McMeans, J. Svavarsson, S. T. Kessel, S. Biton Porsmoguer, S. Wildes, C. A. Tribuzio, S. E. Campana, S. D. Petersen, R. D. Grubbs, D. D. Heath, K. J. Hedges, and A. T. Fisk. 2017. Origins of the Greenland shark (*Somniosus microcephalus*): Impacts of ice-olation and introgression. Ecology and Evolution. DOI: 10.1002/ece3.3325.

Wang, J. Y. and S.-C. Yang. 2004. First records of Pacific sleeper sharks (*Somniosus pacificus* Bigelow and Schroeder, 1944) in the subtropical waters of eastern Taiwan. Bulletin of Marine Science 74:229–235.

Wetherbee, B. M., and E. Cortés. 2004. Food consumption and feeding habits. Pages 225–246 *in* J. C. Carrier, J. A. Musick, and M. R. Heithaus, editors. Biology of Sharks and their Relatives. CRC Press, Boca Raton, FL.

Wolf, N., S. A. Carleton, and C. M. Martínez del Rio. 2009. Ten years of experimental animal isotopic ecology. Functional Ecology 23:17–26.

Yang, M.-S., and B. N. Page. 1999. Diet of Pacific sleeper shark, *Somniosus pacificus*, in the Gulf of Alaska. Fishery Bulletin 97:406–409.

Yano, K., J. D. Stevens, and L. J. V. Compagno. 2004. A review of the systematics of the sleeper shark genus *Somniosus* with redescriptions of *Somniosus (Somniosus) antarcticus* and *Somniosus (Rhinoscymnus) longus* (Squaliformes: Somniosidae). Ichthyological Research 51:360–373.

Yano, K., J. D. Stevens, and L. J. V. Compagno. 2007. Distribution, reproduction and feeding of the Greenland shark *Somniosus (Somniosus) microcephalus*, with notes on two other sleeper sharks, *Somniosus (Somniosus) pacificus* and *Somniosus (Somniosus) antarcticus*. Journal of Fish Biology 70:374–390.

Yeh, J. and J. C. Drazen. 2009. Depth zonation and bathymetric trends of deep-sea megafaunal scavengers of the Hawaiian Islands. Deep Sea Research I 56:251–266.